AD-A185 535 COMPUTER-AIDED STRUCTURAL ENGINEERING (CASE) PROJECT FINITE ELEMENT STUDI..(U) ARMY ENGINEER WATERWAYS EXPERIMENT STATION VICKSBURG MS INNOR.. 1/2

UNCLASSIFIED J P HARTMAN ET AL. AUG 87 WES/TR/ITL-87-4 F/G 9/1 NL

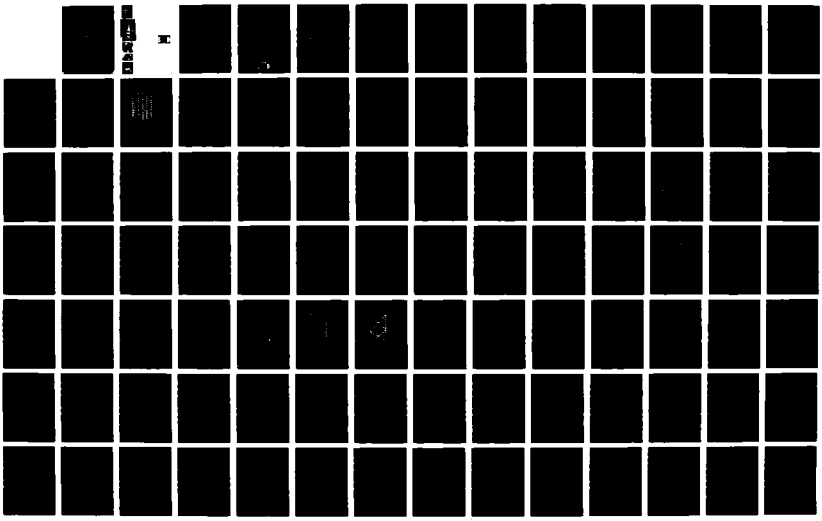

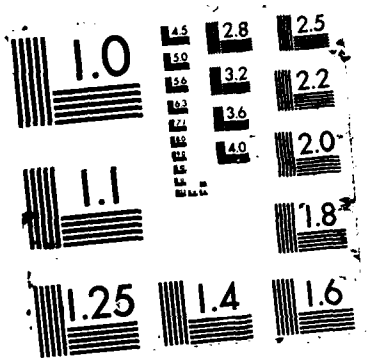
1.0
2.8
2.5
3.2
2.2
3.6
2.0
4.0
1.1
1.8
1.25
1.4
1.6

Destroy this report when no longer needed. Do not return it to the originator.

The findings in this report are not to be construed as an official Department of the Army position unless so designated by other authorized documents.

This program is furnished by the Government and is accepted and used by the recipient with the express understanding that the United States Government makes no warranties, expressed or implied, concerning the accuracy, completeness, reliability, usability, or suitability for any particular purpose of the information and data contained in this program or furnished in connection therewith, and the United States shall be under no liability whatsoever to any person by reason of any use made thereof. The program belongs to the Government. Therefore, the recipient further agrees not to assert any proprietary rights therein or to represent this program to anyone as other than a Government program.

The contents of this report are not to be used for advertising, publication, or promotional purposes. Citation of trade names does not constitute an official endorsement or approval of the use of such commercial products.

(12)

ADA185535

Unclassified
SECURITY CLASSIFICATION OF THIS PAGE

REPORT DOCUMENTATION PAGE

Form Approved
OMB No 0704-0188
Exp Date Jun 30, 1986

1a. REPORT SECURITY CLASSIFICATION Unclassified	1b. RESTRICTIVE MARKINGS
2a. SECURITY CLASSIFICATION AUTHORITY	3. DISTRIBUTION/AVAILABILITY OF REPORT Approved for public release; distribution unlimited
2b. DECLASSIFICATION/DOWNGRADING SCHEDULE	
4. PERFORMING ORGANIZATION REPORT NUMBER(S)	5. MONITORING ORGANIZATION REPORT NUMBER(S) Technical Report ITL-87-4
6a. NAME OF PERFORMING ORGANIZATION See reverse 6b. OFFICE SYMBOL (If applicable)	7a. NAME OF MONITORING ORGANIZATION USAEWES Information Technology Laboratory
6c. ADDRESS (City, State, and ZIP Code)	7b. ADDRESS (City, State, and ZIP Code) PO Box 631 Vicksburg, MS 39180-0631
8a. NAME OF FUNDING/SPONSORING ORGANIZATION See reverse 8b. OFFICE SYMBOL (If applicable)	9. PROCUREMENT INSTRUMENT IDENTIFICATION NUMBER
8c. ADDRESS (City, State, and ZIP Code) PO Box 1000 Washington, DC 20314-1000	10. SOURCE OF FUNDING NUMBERS PROGRAM ELEMENT NO. / PROJECT NO. / TASK NO / WORK UNIT ACCESSION NO

11. TITLE (Include Security Classification)

Finite Element Studies of a Horizontally Framed Miter Gate; Application and Summary

12. PERSONAL AUTHOR(S)
Hartman, Joseph P., Gibson, James D., Nelson, Michael D.

13a. TYPE OF REPORT	13b. TIME COVERED	14. DATE OF REPORT (Year, Month, Day)	15. PAGE COUNT
Report 7 of a series	FROM 1983 TO 1985	August 1987	170

16. SUPPLEMENTARY NOTATION
Available from National Technical Information Service, 5285 Port Royal Road, Springfield, VA 22161. This report was prepared under the Computer-Aided Structural (Continued)

17 COSATI CODES			18. SUBJECT TERMS (Continue on reverse if necessary and identify by block number)
FIELD	GROUP	SUB-GROUP	

19. ABSTRACT (Continue on reverse if necessary and identify by block number)

This volume presents an overview of a series of reports dealing with horizontally framed miter gates and their performance. The John Hollis Bankhead Lower Miter Gate on the Black Warrior River, Alabama, a typical and representative structure, was the subject of this in-depth study.

Parts II, III, and IV include commentaries on the separate reports addressing conventional horizontally framed gates, elastic buckling of girders, alternate gate configurations, and different methods of controlling the torsional stiffness of a gate leaf.

Appendix A is composed of the introductions and conclusions of the six separate reports. These reports are the basis for much of the information presented in Parts II, III, and IV.

(Continued)

20. DISTRIBUTION/AVAILABILITY OF ABSTRACT ☒ UNCLASSIFIED/UNLIMITED ☐ SAME AS RPT ☐ DTIC USERS	21. ABSTRACT SECURITY CLASSIFICATION Unclassified
22a. NAME OF RESPONSIBLE INDIVIDUAL	22b. TELEPHONE (Include Area Code) / 22c. OFFICE SYMBOL

DD FORM 1473, 84 MAR — 83 APR edition may be used until exhausted. All other editions are obsolete

SECURITY CLASSIFICATION OF THIS PAGE
Unclassified

DTIC
ELECTE
OCT 5 1987
S D
B

87 9

6a. NAME OF PERFORMING ORGANIZATION (Continued).

Computer-Aided Structural Engineering (CASE) Project Task Group on Miter Gates

8a. NAME OF FUNDING/SPONSORING ORGANIZATION (Continued).

US Army Corps of Engineers, Engineering and Construction Directorate

16. SUPPLEMENTARY NOTATION (Continued).

(CASE) Project. A list of published CASE reports is printed inside the back cover.

19. ABSTRACT (Continued).

The authors of Parts II, III, and IV are associated with the US Army Corps of Engineer Districts, Mobile and Seattle, and the Southwestern Division. The six reports included in Appendix A were written by three members of the faculty of the Georgia Institute of Technology.

A-1

PREFACE

Six separate finite element studies of horizontally framed miter gates were completed during the period 1981-1984 to interpret the basic behavior of conventional gates and to investigate several alternate miter gate configurations. The studies of the John Hollis Bankhead Lower Miter Gate on the Black Warrior River, Alabama, were conducted by Drs. L. Z. Emkin, K. M. Will, and B. J. Goodno of the Georgia Institute of Technology under the direction of the Computer-Aided Structural Engineering (CASE) Project managed by the Information Technology Laboratory (ITL), formerly the Automation Technology Center, US Army Engineer Waterways Experiment Station (WES). Funds for the CASE project were provided by the Engineering and Construction Directorate of the Office, Chief of Engineers (OCE).

A seventh report was written by Messrs. Joseph P. Hartman, James D. Gibson, and Michael D. Nelson of the CASE Project Task Group on Miter Gates. This report summarizes and comments on the six finite element studies and relates the studies to conventional design practices. An appendix to the report includes a summary of the introduction and conclusions of each of the finite element study reports. This report was designed as an overview of and a commentary on the six separate studies to reach a broad span of readers, thereby introducing and creating interest in the specific reports.

The summary and the following complete finite element studies are being published separately under the series title Finite Element Studies of a Horizontally Framed Miter Gate (Technical Report ITL-87-4). The six reports describing the research and its commentary are listed. For clarity in referencing these studies in the summary and finite element study reports, they are functionally numbered as shown and referred to accordingly.

Report 1. Initial and Refined Finite Element Models (Phases A, B, C).

Report 2. Simplified Frame Model (Phase D).

Report 3. Alternate Configuration Miter Gate Finite Element Studies -- Open Sections.

Report 4. Alternate Configuration Miter Gate Finite Element Studies -- Closed Sections.

Report 5. Alternate Configuration Miter Gate Finite Element Studies -- Additional Closed Sections.

Report 6. Elastic Buckling of Girders in Horizontally Framed Miter Gates.

Report 1 presents Phases A, B, and C of the initial and refined element series of the studies. These investigations used both member and plate finite elements to represent one gate leaf. Section A relates the Phase A studies as a coarse mesh model formulated and used to predict dead load deflections. The same model formulation was used to predict member forces and element stresses for a variety of additional loading and support states. When the model proved to be too flexible under dead load, a fine mesh model of two girders from the gate leaf was prepared to study the torsional stiffness of the structure. An analysis sequence was then formulated to represent the jacking and prestressing operation required to bring the leaf to an initial plumb position.

Report 1 continues with an account of the Phase B work reported in Section B. A fine mesh verification model was prepared to resolve torsional stiffness discrepancies between the Phase A coarse mesh model and measured field displacements. In addition, the analysis superposition procedure was revised to permit specification of the measured prestress values in the diagonals. Stress contour plots of a representative girder and force free-body diagrams in the gudgeon and pintle areas were prepared for comparison with hand-based analysis values used for design.

Section C describes the continuation of Phase B studies, identified as Phase C. When a more refined model of the diagonal connection plates was added to the Phase B coarse mesh model, Phase C was developed. Its influence on prestressing operations, gate plumbness, and flow of forces near gudgeon and pintle regions was determined and gate motions caused by differential temperature effects were examined.

Report 2 explains the Phase D (simplified frame version of the Phase B model) study of Report 1 and describes simplified frame models S1 and S2. In these models, space frame member elements replaced all plate finite elements in the gate leaf (except for the diagonal and strut arm connection regions). Based on the knowledge of gate behavior gained from the plate finite element models of Report 1, the simpler frame models appeared to be more economical to generate and analyze as well as more useful in providing member force values to be used in design. This report presents a comparison of gross force values for the frame models and the plate models and makes recommendations with respect to use of simplified models in design.

Reports 3 and 4 describe the alternate configuration miter gate finite element models for both open and closed sections, respectively. The influence

of a partial skin plate and a variety of frameworks added to the downstream side of the miter gate leaf was studied. Torsional stiffness of the gate was altered, and structure responses to dead, operational, and environmental loadings were changed by addition of elements to the downstream side of the gate.

Report 5 describes the behavior of additional closed section alternate configuration miter gate finite element models. Two of the torque-tube models studied in Report 4 were modified for further study in the final report. In one model, the torque tubes along the top and bottom of the gate were enlarged to enclose the two spaces between both the top three and bottom three horizontal girders. In the second model, torque tubes were positioned along the sides of the gate leaf but were reduced in size compared to earlier models. An extra set of vertical diaphragms was added between end and first interior diaphragms to complete the vertical torque tubes. Report 5 describes these two models in detail and presents the results of dead load, torsional stiffness, prestressing, and hydrostatic and temporal loading comparisons with previous models. Similar results are presented for a revised model II of the Phase B Series (see Report 1) in which the cross-sectional areas of the prestressing diagonals were doubled in size.

Report 6 concerns the elastic buckling of girders in horizontally framed miter gates. Both weak and strong axis buckling of one girder in the gate leaf was studied in depth for symmetric modes only. Detailed finite element models were prepared and buckled modal displacement patterns were studied and compared with those assumed in current design procedures.

Members of the CASE Task Group on Miter Gates and their Corps of Engineers affiliations are:

Mr. Joseph P. Hartman, Southwestern Division (Chairman)
Mr. Eugene Ardine, Ohio River Division
Mr. Joseph Bozzay, Huntington District
Mr. James D. Gibson, Mobile District
Mr. Clifton C. Hamby, Vicksburg District
Mr. Carl Johnson, Rock Island District
Mr. Michael D. Nelson, Seattle District
Mr. William A. Price, III, Waterways Experiment Station
Dr. N. Radhakrishnan, Waterways Experiment Station
Mr. Robert Smith, Office, Chief of Engineers

The work involved in this project was done under the direction of Dr. N. Radhakrishnan, CASE Project Manager and Acting Chief, ITL. Mr. William Price, ITL, was the technical coordinator. Mr. Robert Smith,

Chief, Structures Branch, OCE, was the OCE Point of Contact. Editing was done by Ms. Gilda Miller, Information Products Division, ITL, WES.

COL Allen F. Grum, USA, was the previous Director of WES. COL Dwayne G. Lee is the present Commander and Director. Dr. Robert W. Whalin is Technical Director.

CONTENTS

	Page
PREFACE	1
PART I: GENERAL OVERVIEW	6
PART II: INTERPRETATION OF FINITE ELEMENT STUDIES OF A HORIZONTALLY FRAMED MITER GATE	7
Evaluation of Study Results	7
Basis for Study	7
Gate and Model Geometry	8
Boundary and Loading Conditions	10
Gate Torsion	13
Temperature Stresses	14
Horizontal Girder Stresses	14
Diaphragm Stresses	16
Force Distribution Data	19
Force Distribution Around Gusset Plates	19
Force Distribution Around Pintle	27
Force Distribution Around Hinge	30
Force Distribution Around Operating Strut	31
Force Distribution Verification	33
Strain Gage Data	37
Conclusions	37
Recommendations	39
PART III: ELASTIC BUCKLING OF GIRDERS	40
Preview	40
Typical Girder Selected	40
Minor Axis Buckling	40
Major Axis Buckling	41
Summary	42
Conclusions	43
PART IV: STRUCTURAL BEHAVIOR OF ALTERNATE CONFIGURATIONS OF MITER GATES	44
Introduction	44
Background	44
Gate and Model Geometry	46
Loading Conditions	48
Gate Torsion and Stiffness	52
Prestressing Behavior	72
Hydrostatic and Temporal Loading Behavior	76
Vertical Torque-Tube Design Considerations	104
Comparative Analysis of Gallipolis Gate	108
Conclusions	124
Discussion	126
Recommendations	130
APPENDIX A: SUMMARIES-FINITE ELEMENT STUDIES OF A HORIZONTALLY FRAMED MITER GATE	A-1

FINITE ELEMENT STUDIES OF A HORIZONTALLY FRAMED MITER GATE

APPLICATION AND SUMMARY

PART I: GENERAL OVERVIEW

1. Observations and conclusions in this report are based on six finite element (FE) studies of a configuration of the John Hollis Bankhead Lower Miter Gate, Black Warrior River, Ala. These studies are listed in the Preface in order of sequence and title. Since the results are based on investigations of a single miter gate, these results should be used with caution in designing other miter gates with quite different configurations. Appendix A includes the introductions, summaries, and conclusions of the six separate miter gate studies.

2. The following Parts II, III, and IV were prepared by members Joseph P. Hartman, James D. Gibson, and Michael D. Nelson, respectively, of the Computer-Aided Structural Engineering (CASE) Task Group on Miter Gates for use by design engineers. This material includes input from the entire CASE Task Group. Part II presents an interpretation of results of the FE studies of a conventional, horizontally framed miter gate. It is concerned with distribution of applied loads into the gate structure and goes further to compare the FE results with traditional design assumptions.

3. Part III approaches elastic buckling behavior of a typical girder of the miter gate. These accepted suppositions are compared with results of a detailed FE study of a single girder.

4. Part IV offers a detailed evaluation of several types of structural modifications which might increase the torsional stiffness of a gate leaf. Typical modifications include: varying the size of diagonal members, additions of fixed bracing on the downstream face, full downstream skin plate, and different torque-tube sizes (partial downstream skin plate). Each of these configurations was investigated through an FE analysis.

PART II: INTERPRETATION OF FINITE ELEMENT STUDIES OF A HORIZONTALLY FRAMED MITER GATE*

Evaluation of Study Results

5. Part II of this report summarizes and evaluates results of Reports 1 and 2, FE studies ("Initial and Refined Finite Element Models (Phases A, B, C)" and "Simplified Frame Model (Phase D)") of a conventional miter gate at John Hollis Bankhead Lock and Dam. These examinations were performed under sponsorship of the Task Group on Miter Gates, as part of the Corps of Engineers' Computer-Aided Structural Engineering (CASE) Project. This part of the summary presents the study results and their interpretation in a form convenient for use by design engineers. These findings relate to overall miter gate behavior in the mitered and unmitered positions and to a general distribution of internal stresses and forces in various gate components.

Basis for Study

6. Design criteria for miter gates are currently provided in Engineer Manual 1110-2-2703,** and the basic structural standards can be summarized as follows. The horizontal girders, each acting as a leg of a three-hinged arch, are the main load-carrying members of a gate. Hydrostatic loads are applied to the girders by the tributary area method, and skin plate and intercostals are used to transfer these loads to the girders. Accordingly, girders must be designed to resist the horizontal component of the diagonal tensioning force. Vertical diaphragms should be able to resist localized machinery, jacking, and diagonal tensioning forces, and be capable of transferring shear forces between girders to equalize loads and deflections. Diagonals are used to allow plumb alignment of the miter blocks and to add torsional stiffness to a gate, while a quoin post is provided to transfer gate dead weight to the pintle. Each of these members is assumed to experience a straight-line distribution of stress and strain over its cross section.

---

* Joseph P. Hartman. 1985. US Army Engineer Division, Southwestern.

** Headquarters, Department of the Army. 1984. "Lock Gates and Operating Equipment," Engineer Manual 1110-2-2703, Washington, DC.

7. Shortcomings of these criteria are related to the highly indeterminate configuration of the gate leaf. The only statically fixed behaviors of the gate are the external reactions in the unmitered position and the action as a three-hinged arch while mitered. Concentrated loads at the hinge, pintle, operating strut, and diagonal connections are distributed among the main members of the gate in an indeterminate manner. Due to the grid-type configuration of the gate leaf, distributed loads must also be transferred randomly through the gate members.

8. The referenced FE studies were performed in the hope of measuring the importance of this indeterminate behavior. The studies were expected to provide sufficient data to develop general design criteria for distribution of concentrated loads and for internal redistribution of hydrostatic loads.

Gate and Model Geometry

9. The lower miter gate for John Hollis Bankhead Lock and Dam, Black Warrior River, Ala., provided the gate geometry needed for these studies. Each gate leaf is approximately 89 ft high and 62 ft wide. The gate has the conventional, horizontally framed configuration, using 18 horizontal girders as the main, load-carrying members. A single set of diagonals is used between the four corners of each leaf.

10. The GTSTRUDL program was instrumental in modeling this gate geometry. Attempts to adequately represent gate behavior resulted in the use of three different models: coarse mesh model (CM), fine mesh model (FM), and simplified model (SM). These models are illustrated in Figures 1 through 3. In the CM (581 joints, 886 members, and 844 elements) and FM (1,350 joints, 2,441 members, and 1,605 elements) models, hybrid membrane and plate FE's were used for the skin plate, for webs of girders and diaphragms, and for various other components. Space frame members (beams) were used for flanges of girders and diaphragms, as well as for diagonals, intercostals, and other components. GTSTRUDL's capability to represent end joint sizes and member eccentricities was utilized to obtain the best possible correlation between behaviors of the real gate and the models. The SM (707 joints, 1,646 members, and 22 elements) differed from the CM and FM in the representation of the skin plate and the webs of girders and diaphragms in that these components were

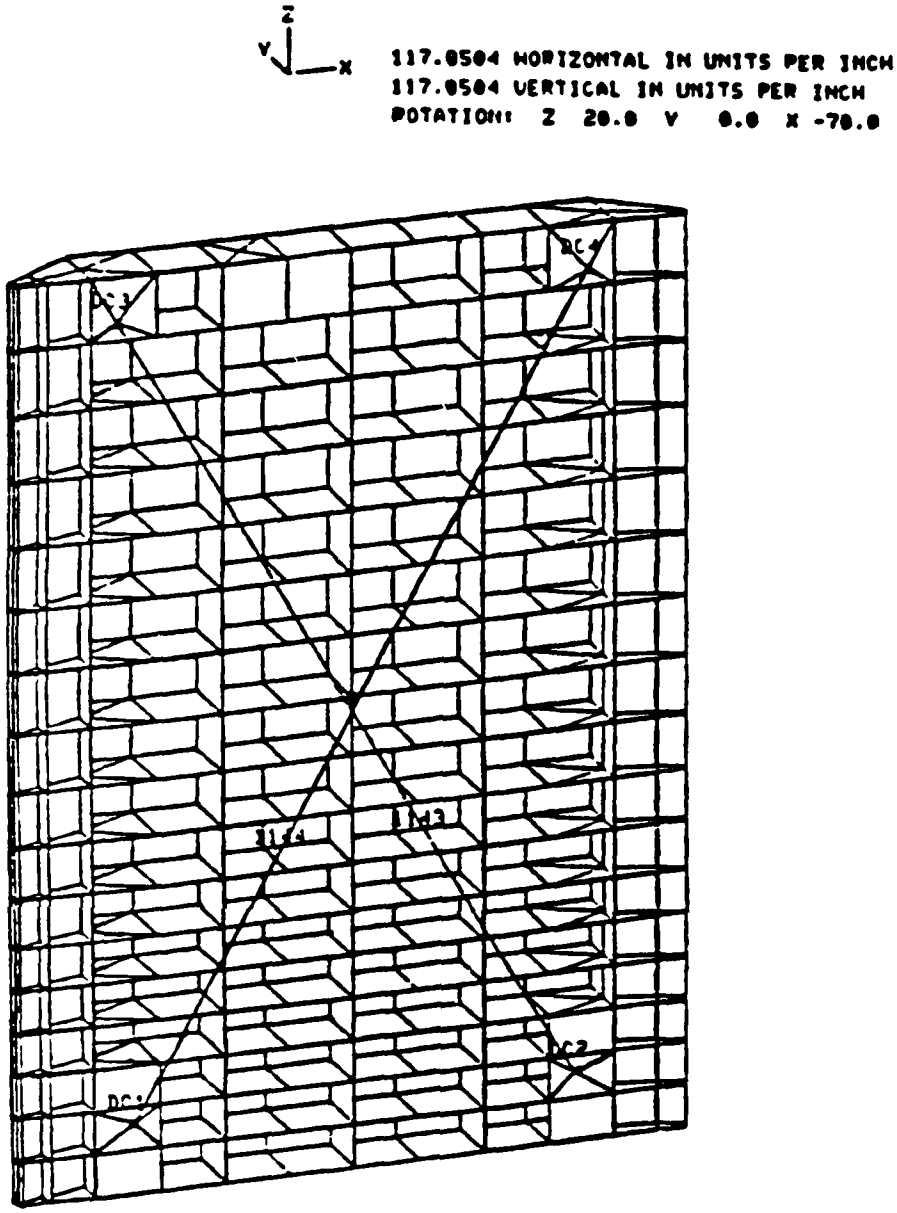

Figure 1. Coarse mesh model (CM)

represented by space frame members. FE's were used only around the connection points for the operating strut and the diagonals.

11. Several reasons led to the use of three separate models in the studies. Verification of results from one model by comparison with another required separate models. Three models were also necessary since each was expected to be best suited for a particular type result, e.g., the FM produced the most realistic stress distribution in the girder webs, while the SM made it easier to determine overall load paths through the gate structure. Evaluation of model behavior is presented in the following paragraphs.

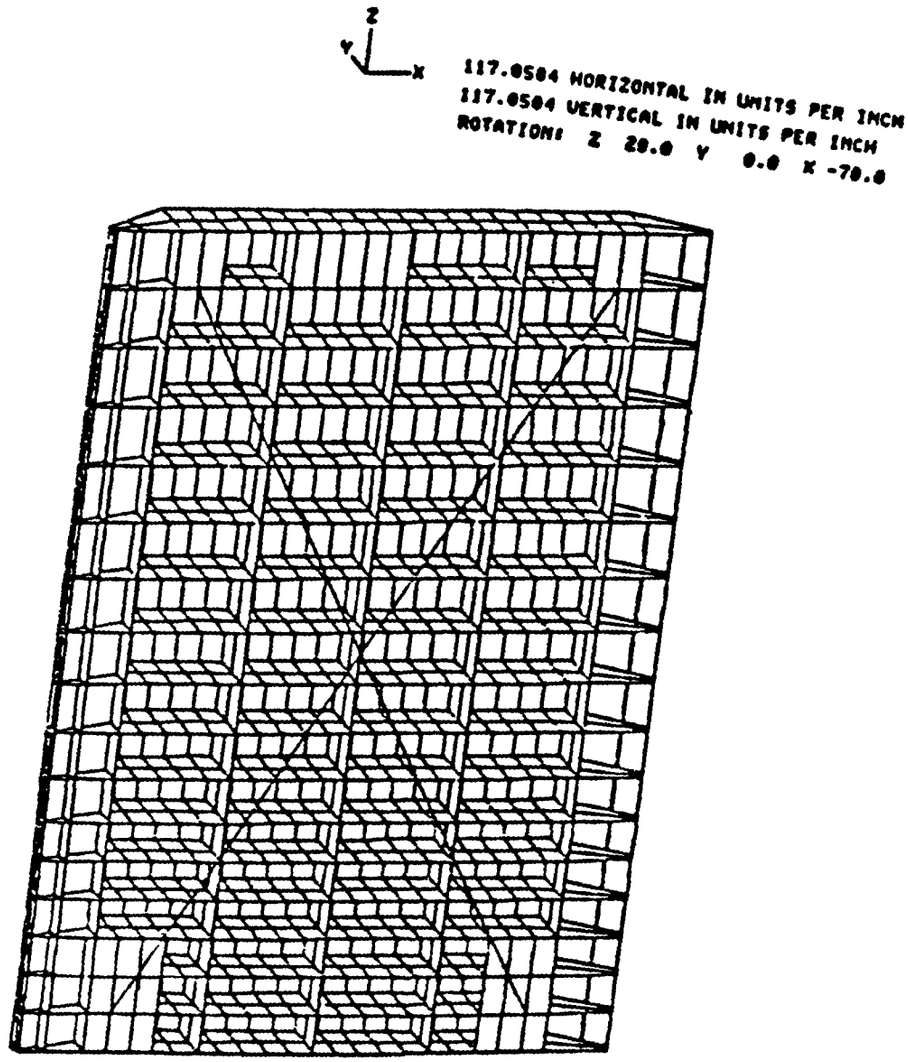

Figure 2. Fine mesh model (FM)

Boundary and Loading Conditions

12. The following paragraphs discuss related boundary conditions used in evaluations of gate behavior. Several load cases are illustrated in Figure 4.

13. The gate has two sets of boundary conditions. The first condition represents the gate in the mitered position, and acts as part of a three-hinged arch. Reactions are provided at each girder at the quoin and miter

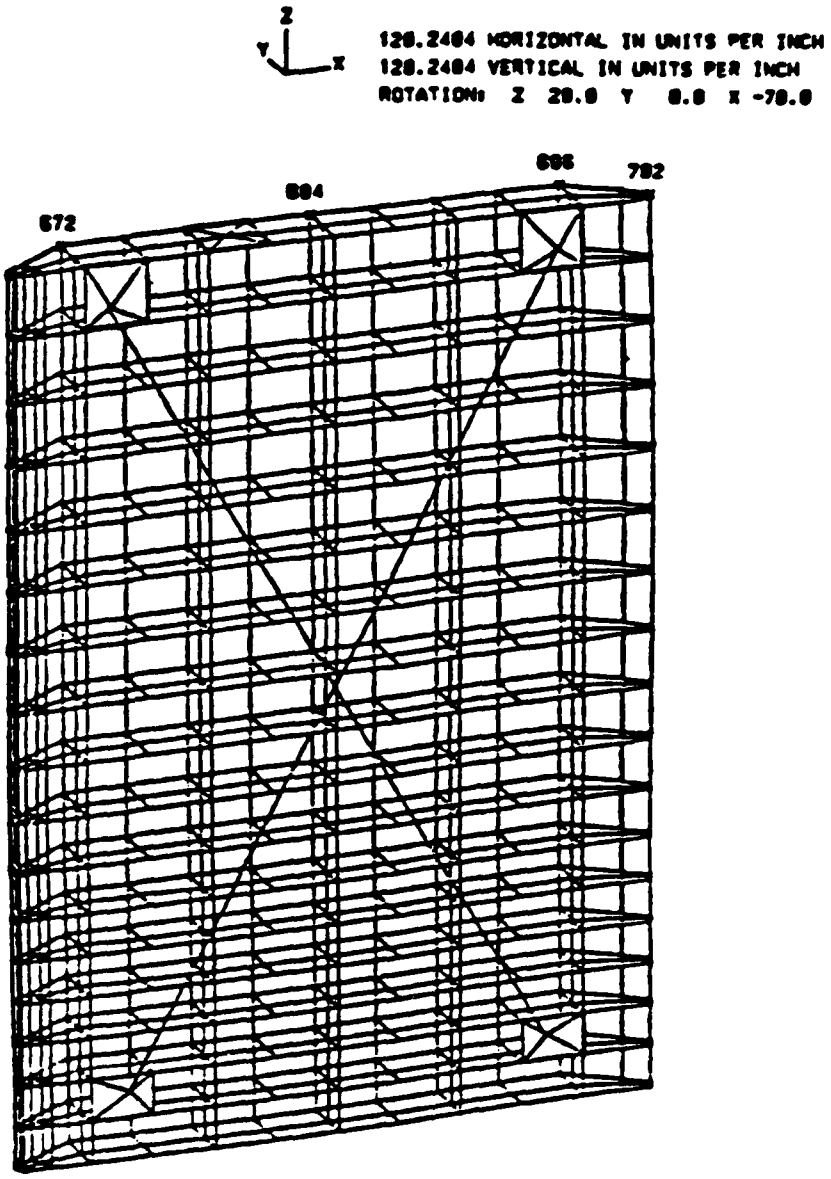

Figure 3. Simplified model (SM)

bearings, parallel to thrust diaphragms. In this configuration, the hinge (gudgeon pin) and pintle remain active as reaction points. Note that this differs from conventional manual analysis-assumptions which ignore the effects of hinge and pintle reactions in the mitered configuration. The other set of boundary conditions represents a gate in the unmitered position. The hinge and pintle provide the main reactions, with the operating strut preventing rotation about the hinge line. The strut was assumed to be oriented at an angle of 48 deg from normal to the gate, and provided a reaction force only in that direction.

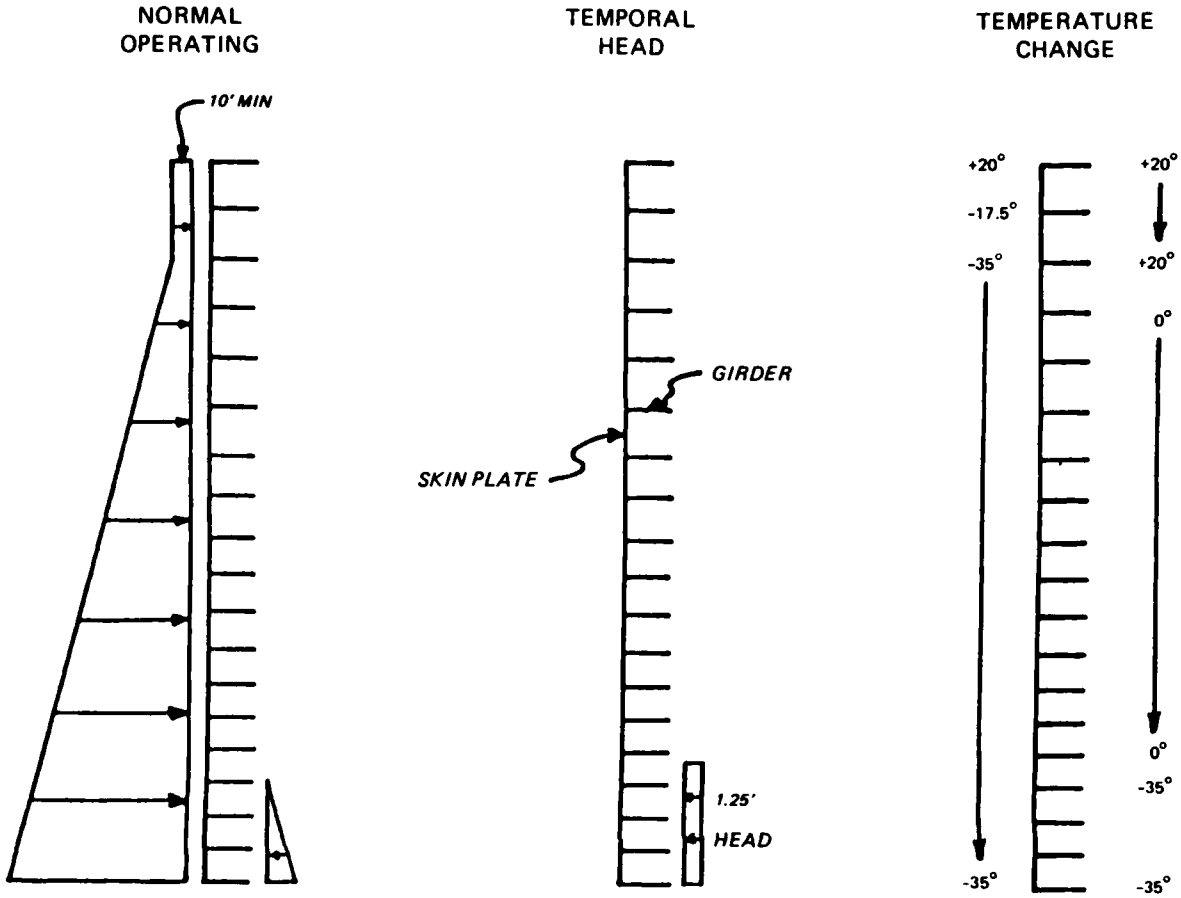

Figure 4. Gate loads

14. Loads applied to the gate in the mitered configuration represented hydrostatic loads due to normal differential head and thermal loads due to an assumed temperature distribution. The hydrostatic loads represented the effects of an upper pool at elevation (el) 255,* 3 ft below girder 1, and a lower pool at el 186. A 10-ft minimum head was applied to the upper part of the gate. The temperature distribution used for analysis assumed the following changes from baseline temperature. Temperatures of the upstream sides of girders 3 through 18 were -35° F, temperatures of the upstream sides of girders 1 and 2 were +20° F and -17.5° F, respectively. Temperatures of the downstream sides of girders 15 through 18 were -35° F, those of the downstream sides of girders 1 through 3 were +20° F, and those of the downstream sides of

---

* All elevations (el) cited herein are in feet referred to the National Geodetic Vertical Datum (NGVD).

the remaining girders were 0° F. This distribution was intended to represent a thermal loading concurrent with the hydrostatic load condition. Temperatures of submerged parts of the gate were -35° F, and the temperature of the upper part of the gate exposed to the sun was +20° F.

15. Loads applied to the unmitered gate consisted of dead loads, diagonal prestressing forces, and temporal head loading. Dead loads represented the actual dead weight of gate materials. Applied forces in the gate diagonals were 599 and 278 kips in the positive and negative diagonals, respectively. These are the actual field measured values for this gate. The temporal head loading was a differential head of 1.25 ft acting upstream. This load was applied over the lower 15 ft of the gate.

Gate Torsion

16. Torsional behavior of the gate was studied in some detail. This part contains only a brief summary of the main findings for torsion of a conventional gate. Further discussion of gate torsion is included in Part IV. The complete list of reports involved in the miter gate study can be found on page 1 of the preface.

17. Before diagonals are installed, miter gates are very flexible in torsion. Observed gate behavior and FE results are consistent on this point, although the model results never matched the measured torsional deflection of the installed gate. Stiffness of a gate leaf without diagonals is due to thin-member torsional behavior of the various plates and flanges comprising the structure. Despite painstaking efforts to correctly model this behavior, FE results always indicated greater flexibility than measured values. The reasons for this discrepancy have not been determined. It may be due to undiscovered modeling inadequacies or due to extra stiffness imparted by gate construction details.

18. Behavior of a gate with diagonals is not significantly influenced by thin-member torsion. Therefore, the above mentioned discrepancy between modeled and measured stiffness was not interpreted as a serious model deficiency which would affect other types of gate behavior. With diagonals installed, model results verify that the gate is much stiffer, due to its behavior as a closed section. Stresses in the diagonals are the result of initial prestressing and to resistance to torsional loads applied to the gate.

Temperature Stresses

19. Applied thermal loads are described in paragraph 14. Due to the nonuniform temperature distribution, warping of the gate should be expected. With the gate mitered and hydrostatically loaded, such warping might induce higher stresses at undesirable locations.

20. Results indicated that stresses due to temperature warping were relatively small. The maximum skin plate stress was less than 3 ksi. In the horizontal girders the maximum temperature stress was about 5 ksi, but this was highly localized around the pintle, in the bottom girder. Stresses at other girder locations were significantly smaller. The warping causes a redistribution of reaction forces along the quoin and miter blocks. The maximum change in miter reaction force at any girder is 40 kips which is a small percentage of the maximum normal operating reaction of approximately 1,500 kips.

21. The conclusion to be drawn from this investigation is that temperature-induced stresses are localized and fairly small. They may be safely ignored during the usual miter gate design process.

Horizontal Girder Stresses

22. The behavior of the girders acting as the main structure of a three-hinged arch is addressed in the following three paragraphs. It includes the effects of the skin plate that serves as part of the girder upstream flange.

23. Hydrostatic loads from the normal operating condition are usually assumed to be distributed to the girders by tributary areas. The analysis of the full gate structure verifies this as a reasonable method. Figure 5 shows the quoin and miter reaction forces for each girder, as predicted by the finite element model (FEM). These are compared with the manually calculated reactions, usually with only a few percentage differences. However, this analysis shows that the bottom girder (at the miter end) carries a slightly higher load than the manual analysis indicates, and, in conjunction, the loads in the adjacent girders are reduced somewhat. One interesting result is the difference in quoin and miter reactions near the top and bottom of the leaf. The hinge and pintle help resist part of the hydrostatic load, thus significantly reducing the girder reactions at the quoin end. Note that this result is

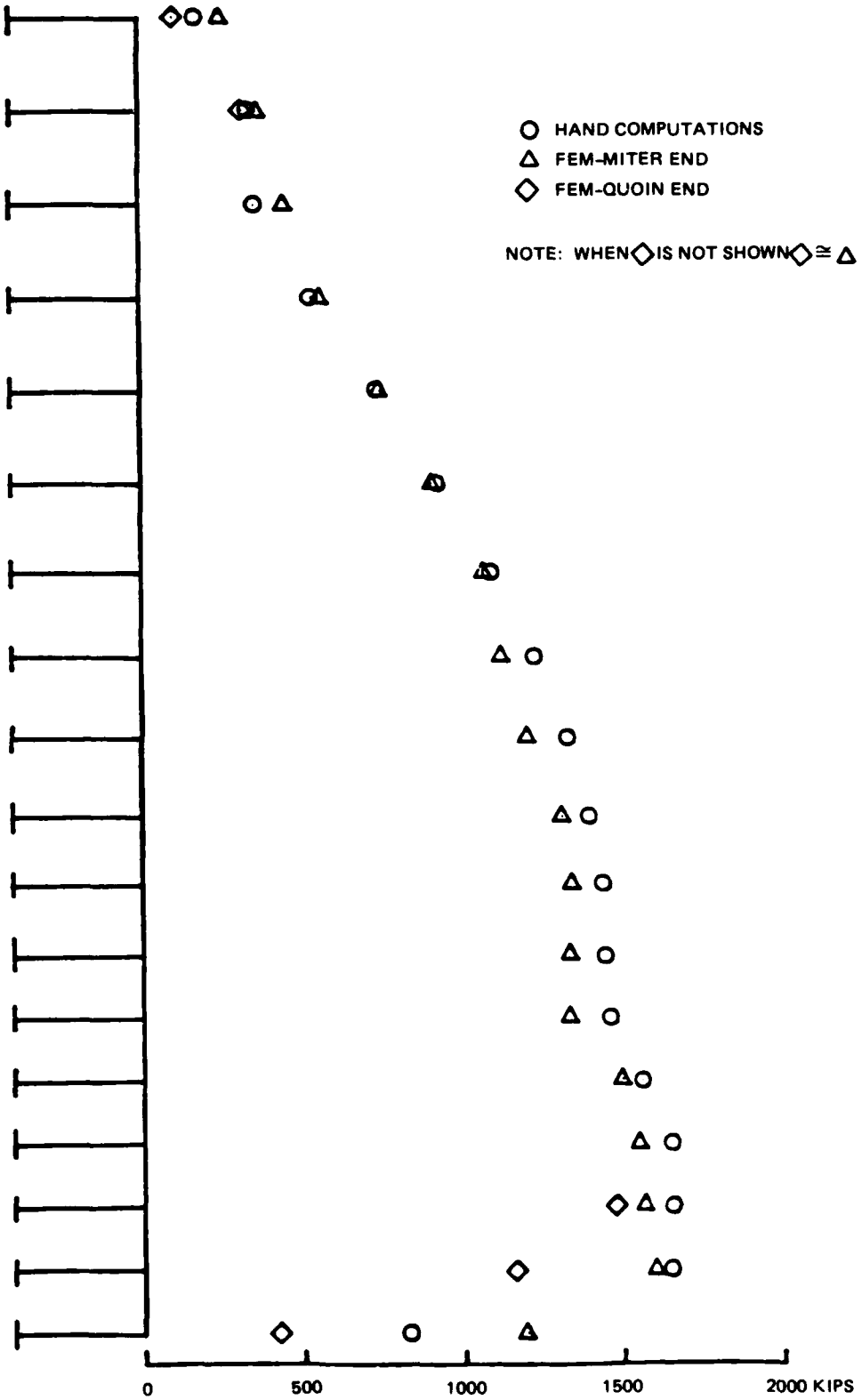

Figure 5. Girder end reactions

dependent on the modeling assumption that the quoin, hinge, and pintle are all rigid supports.

24. The applied load is carried by each girder as bending plus axial load. The skin plate experiences compressive stresses since it is part of the girder upstream flange. Skin plate stress contours for this behavior are shown in Figure 6. This plot conforms well with the manual analysis results which predict a fairly uniform maximum stress at the bottom few girders and a reduced stress toward the top of the gate. Stress contours in the girder web were also plotted. These are shown in Figure 7 for girder 10. Near the center of the gate the stresses vary linearly from the upstream to the downstream edge of the girder in a pattern corresponding to manual analysis assumptions. However, model stresses are slightly lower since the full skin plate width is effective in bending. Nearer the ends, the girder stress distribution is more erratic. Concentrations exist due to discontinuous members and changing cross section. Though the FE mesh was not fine enough for a highly accurate stress distribution, it is obvious that a localized high stress occurs just past the end of the thrust diaphragm. The model predicted approximately 21-ksi compression stress at this point. Net section forces are equal between the model and manual analyses, since the model also shows a lower stress at the upstream and downstream flanges.

25. The localized high web stress should be kept in mind when detailing gates. The girder web should be stiffened at this point or a thicker web section extended further past the end diaphragm. The FEM distribution of girder reactions indicates that the manual analysis is adequate with the exception that the top and bottom girders may carry a somewhat higher load than that shown by hand analysis.

Diaphragm Stresses

26. Interior diaphragms join the various horizontal girders. These diaphragms experience stresses due to redistribution of girder loads and to general warping of the gate structure. However, in all cases such stresses were found to be quite low (less than 6 ksi). Evidently, the current practice of providing minimum size web and flange members for these diaphragms is acceptable.

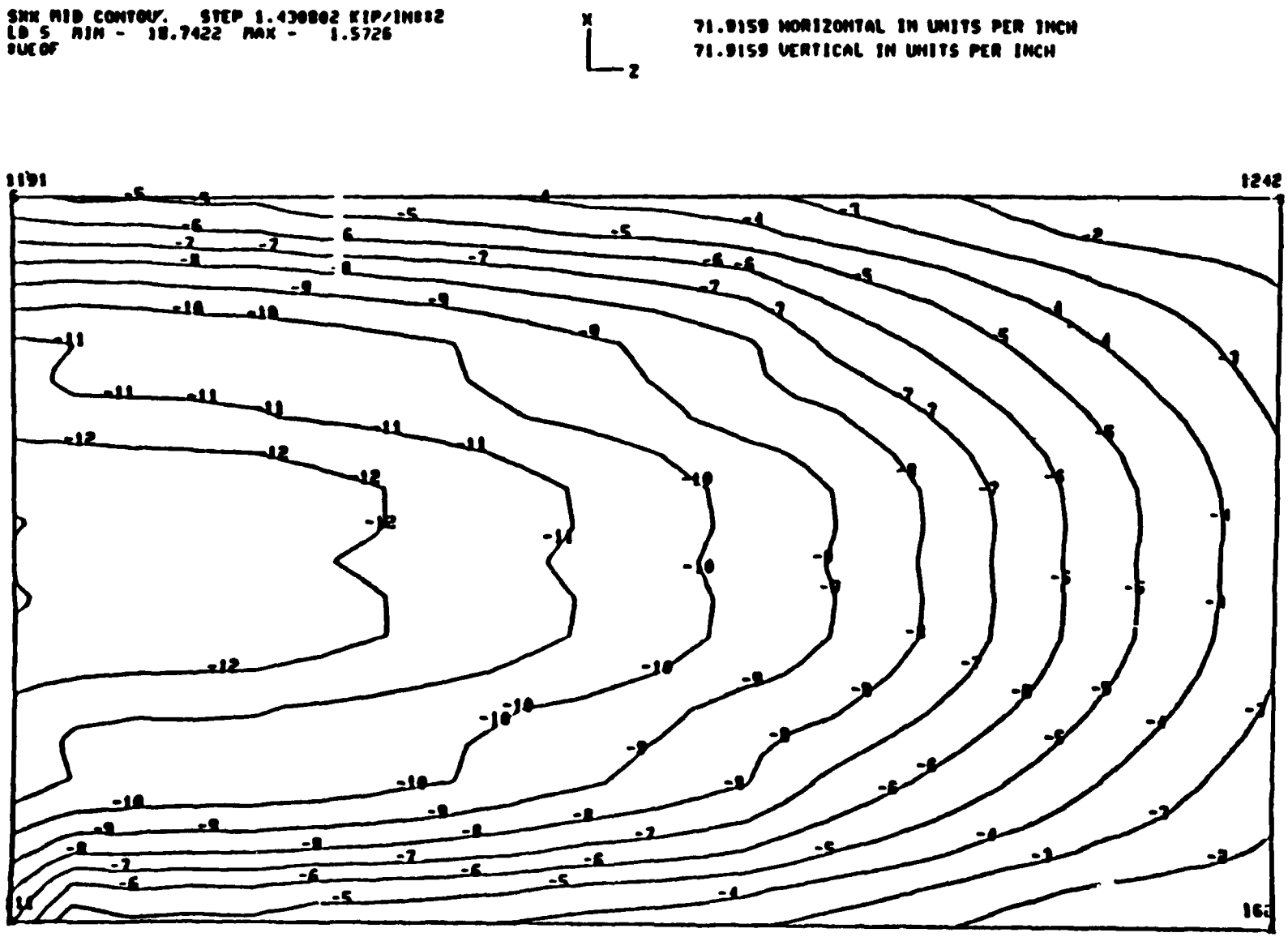

Figure 6. Fine-mesh SXX contour on skin plate for hydrostatic loading

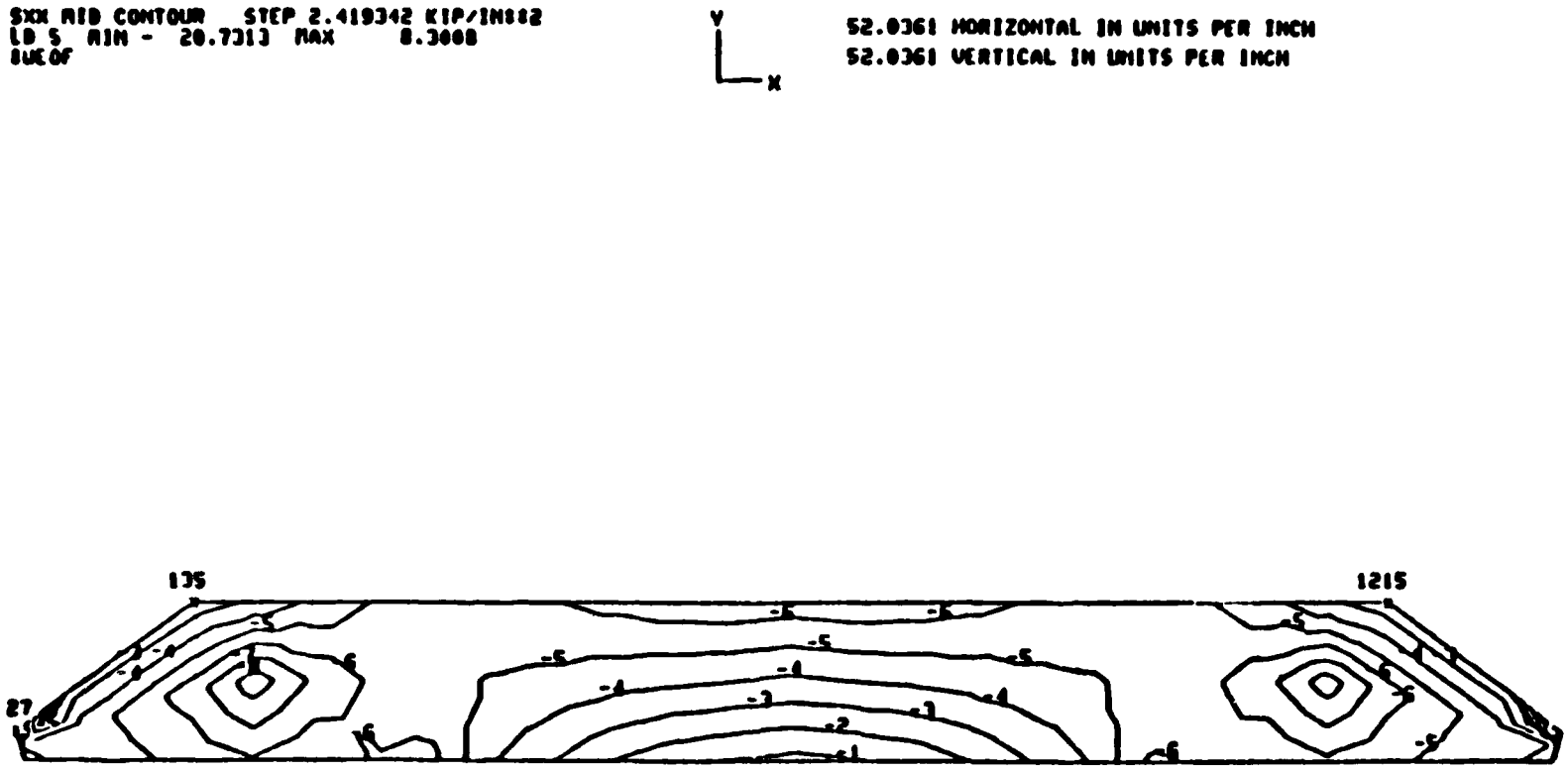

Figure 7. Fine-mesh SXX stress in girder 10 for hydrostatic loading

27. End diaphragms act the same as interior diaphragms but experience additional stresses due to various load concentrations in the gate structure. These additional stresses are the result of certain internal load distributions as described in the following sections, and generally these stresses are fairly small. However, the jacking condition, with its severe jack loads and diagonal stresses, can cause locally high stresses in the adjacent diaphragms. Therefore, at the application points of such loads, the diaphragms should be reinforced. It is not possible, based on FE results, to recommend a general design procedure for this condition.

Force Distribution Data

28. The following paragraphs present a summary of study results concerning distribution of forces around various load concentration points in the gate. Note that "force distribution" is not the same as "stress distribution," but rather a summary of the total force carried through a certain gate component. For example, what portion of the hinge reaction is carried as axial load in girder 2, and what portion is carried as shear in the thrust diaphragm?

29. Force distribution results are taken from two FEM's, the CM and the SM. The CM probably better represents the true behavior of the gate structure. However, interpretation of its results as forces may be inaccurate due to the presence of many plate and membrane elements which provide a variety of load paths. The SM probably provides a less accurate initial solution for gate behavior but interpretation of results is simpler since all member data are output as forces. It is not yet certain which model provides the most accurate representation of force distribution in the gate. Results from the CM and SM often differ in magnitude; however, the distribution patterns are similar for both analyses. Therefore, the results from either model may be suitable for further insights into complex gate behavior, even though they may not be suitable for developing a specific method or formula for design.

Force Distribution Around Gusset Plates

30. Gusset plates are used to distribute large forces from the diagonals into the surrounding gate members. The geometry of the gussets for this

gate is shown in Figures 8 and 9, with identical gussets at the quoin and miter ends. The lower gussets are connected to the bottom four girders and to the end diaphragm, leaving one edge free. The upper gusset plates are similar but are attached only to the top two girders. Note that the intersections of the end diaphragms with the top and bottom girders are used to determine the center line of the diagonals.

31. To determine distribution of forces from the lower gusset plate, the corner of the gate near the pintle was isolated as a free body as shown in

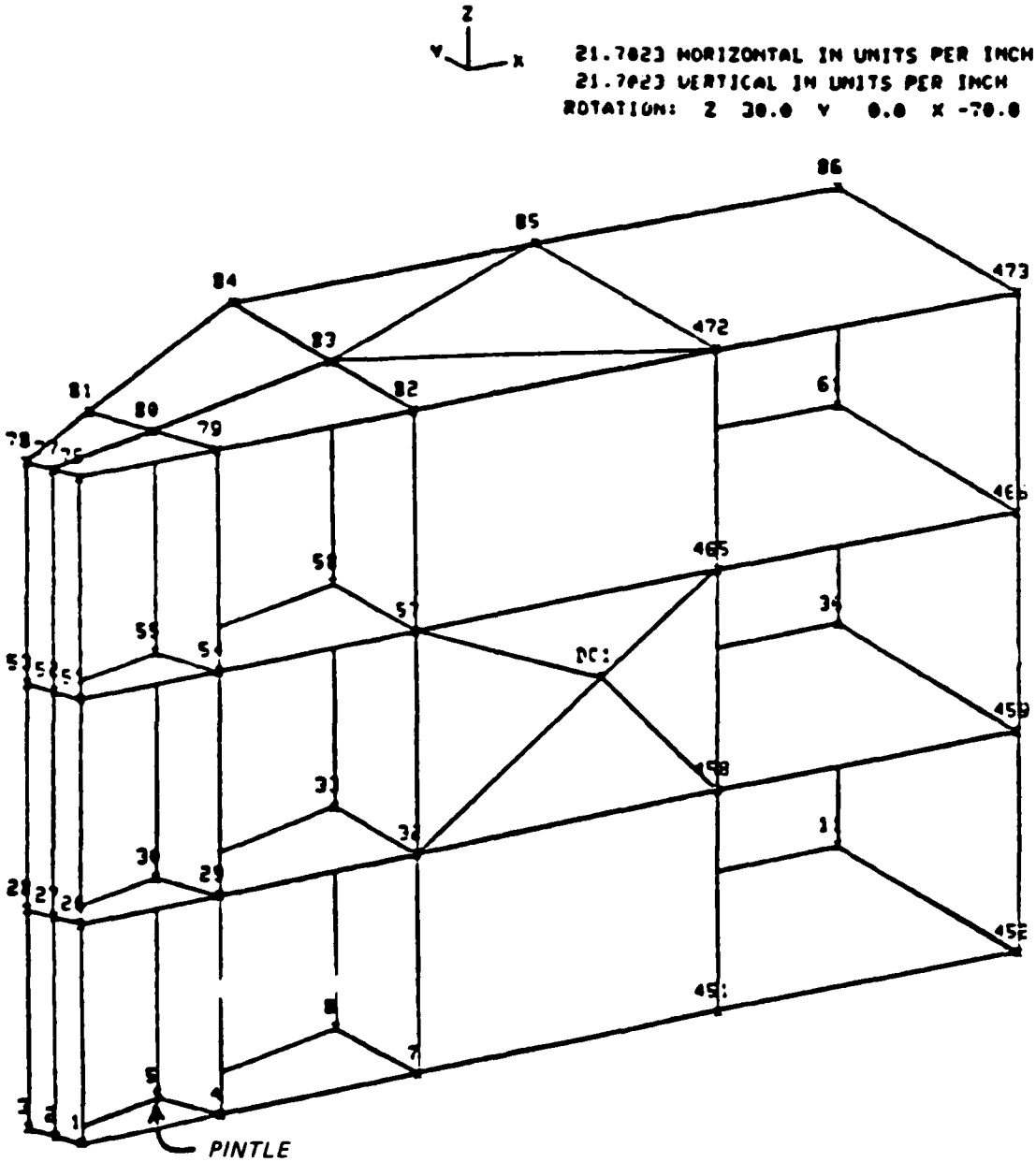

Figure 8. Free body in region of the pintle

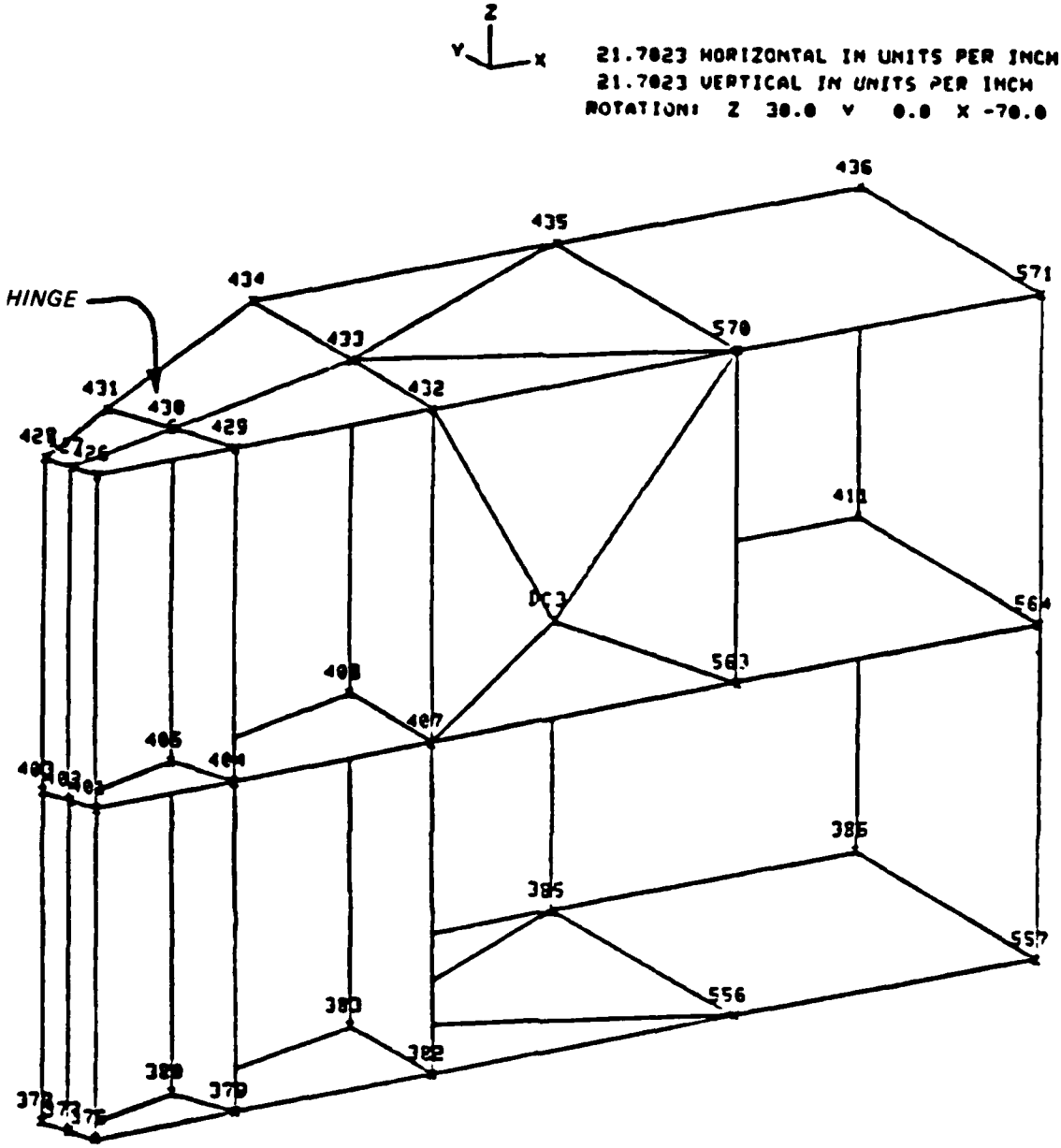

Figure 9. Free body region of the gudgeon pin

Figure 8. The loading condition consisted only of diagonal prestress force, with no load acting at the pintle. This simplified loading was chosen in order to facilitate interpretation of the force distribution results. The diagonal load is 278 kips which provides a vertical component of 243 kips and a horizontal component of 136 kips.

32. Distribution of horizontal forces is shown in Table 1 and Figure 10. SM and CM results do not match. However, the pattern of distribution is similar; lower girders 17 and 18 carry high compression loads, girder 16

Table 1

Horizontal Force Distribution at Lower Gusset for Diagonal Prestress Loading

Member	Horizontal Force, kips CM	Horizontal Force, kips SM
Above girder 15	118 (0.87)	142 (1.04)
Girder 15	78 (0.57)	33 (0.24)
Girder 16	-44 (-0.32)	-30 (-0.22)
Girder 17	-106 (-0.78)	-147 (-1.08)
Girder 18	-182 (-1.34)	-134 (-0.99)
Total	-136 (-1.00)	-136 (-1.00)

Note: The numbers in parentheses are the tabulated load divided by the horizontal component of the diagonal force (136 kips). Negative values indicate compression.

has much lower compression, and girder 15 has a tension force. Because of modeling details, the CM results are probably more accurate and will be used for the following discussion. The results are surprising; rather than a sharing of the total force among the girders, the bottom girder alone actually carries more than the total applied load. This distribution can be partially explained by considering the member geometry and visualizing probable load paths. The center line of the diagonal passes through the intersection of girder 18 and the end diaphragm. The vertical component of the diagonal force is reacted as shown in Figure 11, largely by the quoin post and end diaphragm with this reaction being eccentric to point A and inducing a moment. This moment, and the horizontal component of the diagonal force, must be reacted by the girders. Additional resistance is provided by horizontal shears (V_H) in the skin plate and quoin post just above girder 15. To satisfy static equilibrium, the girder force pattern must resemble that predicted by the FE analysis. This is illustrated in Figure 12, and is explained further in paragraph 35 for the upper gusset plate.

33. Since the diagonal is eccentric to the centroids of the girders (in the downstream direction), it induces strong axis moments in each gate

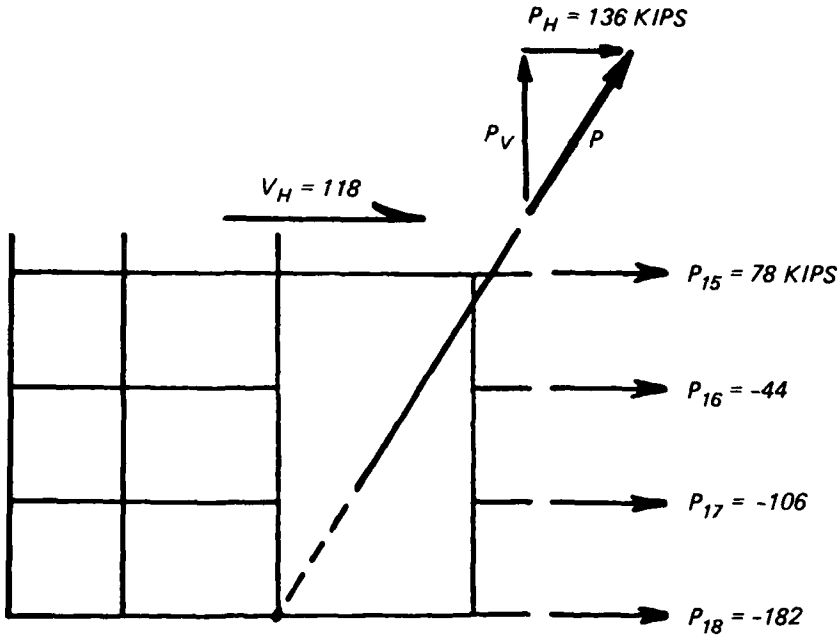

P_H = horizontal component of diagonal force
P_{15} = reaction force in girder 15
P_{16} = reaction force in girder 16
P_{17} = reaction force in girder 17
P_{18} = reaction force in girder 18
V_H = reaction force in all members above girder 15

Figure 10. Horizontal force distribution at lower gusset for diagonal prestress loading

component. These moments are shown in Table 2, the distribution is similar to horizontal force distribution.

34. The vertical component of the diagonal force is distributed to various gate elements of the CM as shown in Table 3 and Figure 11. As for the horizontal component, the distribution is surprisingly variable. The end diaphragm carries a force almost equal to the entire applied load, and the quoin post load is approximately 60 percent as large. Since these two reactions are greater than the applied vertical component, the remaining gate elements must satisfy static equilibrium with an upward reaction force about half as large as the applied force. This last reaction is provided mainly by tensions and shear in the skin plate and first interior diaphragm. Significant strong axis bending occurs in the quion post and end diaphragm, with calculated eccentricity of 58 and 60 in., respectively, from the plane of the skin plate.

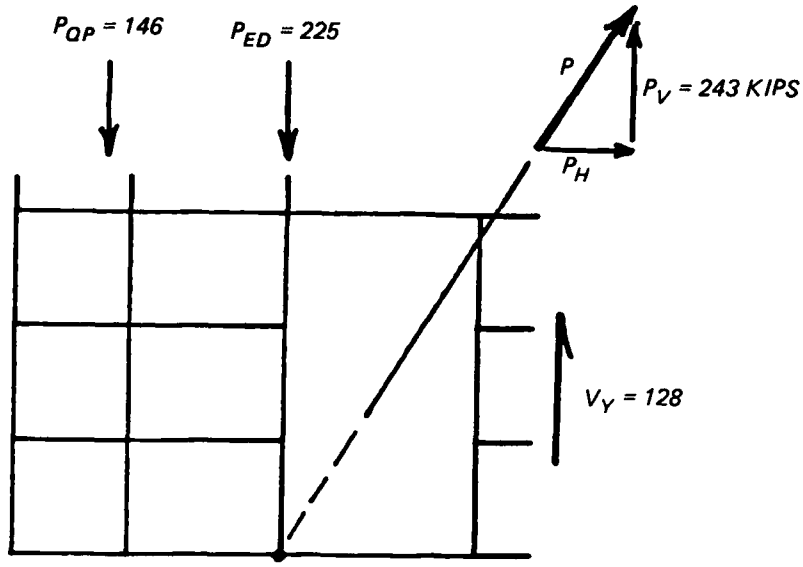

P_V = vertical component of diagonal force

P_{ED} = reaction force in end diaphragm, includes forces in adjacent portions of of skin plate and thrust diaphragm

P_{QP} = reaction force in quoin post components

V_V = reaction force in girders and remaining portion of skin plate

Figure 11. Vertical force distribution at lower gusset for diagonal prestress loading

35. Distribution of forces around the upper gusset plate has been similarly investigated. A free body was isolated as shown in Figure 9, the gusset being connected only to the top two girders. The diagonal prestress loading was investigated; the diagonal load was 599 kips, with a horizontal component of 293 kips and a vertical component of 523 kips. Reaction forces to this load are shown in Table 4. The CM results are judged to be more reliable since much of the load transfer must be carried by shear in various plates, and the simplified model may not represent this load path very well. Interpretation of the force distribution is similar to that for the lower gusset plate. The line of action of the diagonal force passes through the intersection of the end diaphragm and the top girder, labeled point B in Figure 13. The vertical reactions are mainly provided by the quoin post and end diaphragm, and are eccentric to point B by 13.0 in., as shown in Figure 13. The horizontal reactions are eccentric to point B by 23.3 in. (above the top girder). The intersection of the vertical and horizontal reactions is labeled

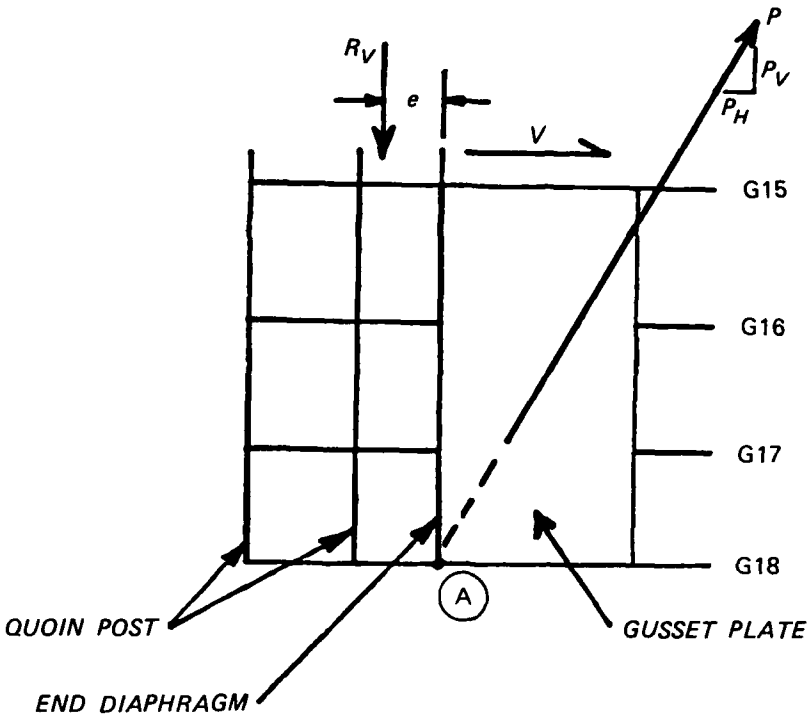

$$\Sigma F_V = 0 : P_V = R_V$$
$$\Sigma F_H = 0 : P_H = R_{18} + R_{17} + R_{16} + R_{15} + V$$
$$\Sigma M_A = 0 : eR_V = h_{17}R_{17} + h_{16}R_{16} + h_{15}(R_{15} + V)$$

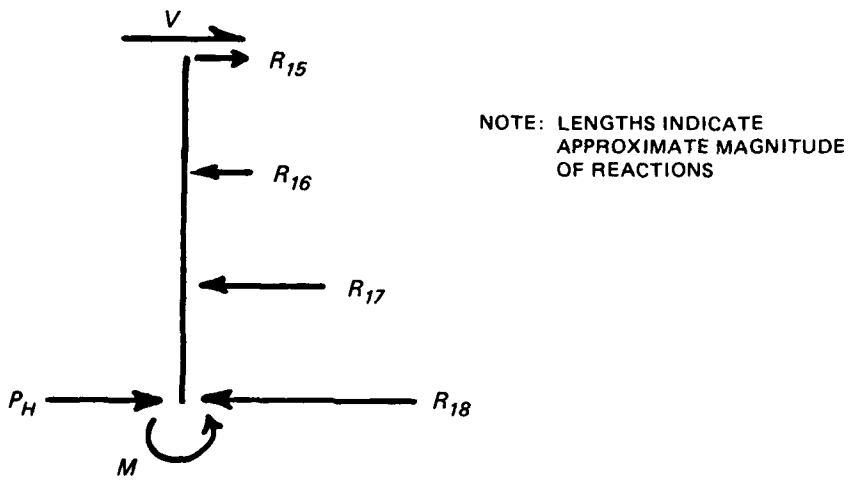

Figure 12. Static equilibrium at lower gusset plate

point B'. To satisfy static equilibrium the line of action of the diagonal must also pass through B', and this would occur if e_H = 23.2 in., very close to the calculated value of 23.3 in. Thus, the unexpected distribution of horizontal reactions in the girders is simply whatever is necessary to satisfy equilibrium conditions.

Table 2

Moment Distribution to Lower Girders

for Diagonal Prestress Loading

Member	Axial Force, kips	Moment, in.-kips	Eccentricity, in.
Girder 15	78	4,334	56
Girder 16	-44	-3,766	86
Girder 17	-106	-8,618	81
Girder 18	-182	-14,076	77
Diagonal	--	--	75

Note: Moments are calculated about the plane of the skin plate.

Table 3

Vertical Force Distribution at Lower Gusset

for Diagonal Prestress Loading

Member	Vertical Force, kips
Quoin post	-146 (-0.60)
End diaphragm	-225 (-0.93)
At interior diaphragm	128 (0.53)
Total	-243 (-1.00)

Note: The numbers in parentheses are the tabulated load divided by the vertical component of the diagonal force (243 kips). Negative values indicate compression.

Table 4

Force Distribution at Upper Gusset from Diagonal Prestress Loading

Member	Horizontal Forces, kips CM	SM
Girder 1	-439 (-1.50)	-179
Girder 2	178 (0.61)	-102
Girder 3	-26 (-0.09)	-30
Below girder 3	-6 (-0.02)	18
Total	-293 (-1.00)	-293
	Vertical Forces, kips	
	CM	**SM**
Quoin post	-198 (-0.38)	-121
End diaphragm	-281 (-0.54)	-315
At interior diaphragm	-44 (-0.08)	-87
Total	-523 (-1.00)	-523

Note: The numbers in parentheses are the tabulated load divided by the vertical component of the diagonal force (243 kips). Negative values indicate compression.

Force Distribution Around Pintle

36. This section presents the distribution of pintle forces into the surrounding gate elements. The free body used to evaluate the distribution is the same as for the lower gusset plate and is shown in Figure 8. Applied loads consisted only of the gate dead loads (no diagonal prestressing) and resulted in pintle forces of 595 kips vertically and 198 kips horizontally. These applied loads showed a negligible force of 13 kips perpendicular to the plane of the gate. Distribution of internal forces in the gate elements is based on CM results and is shown in Figure 14.

37. Vertical forces are largely carried by the quoin post elements. However, within three girder spaces the quoin post force is just half the total pintle reaction. The pintle vertical force, evidently, is rapidly distributed to other elements of the gate structure, such as the end diaphragm, skin plate, and interior diaphragms. This would indicate that it is not necessary to use the full pintle load or the full height of the quoin post to design the post for buckling.

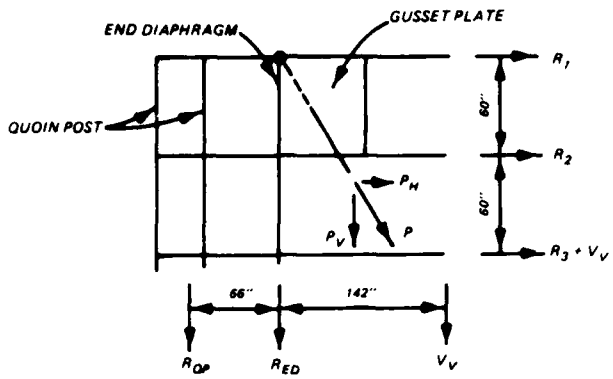

ECCENTRICITY OF REACTIONS (FROM FINITE ELEMENT RESULTS)

$e_V = -(66\,R_{QP} - 142\,V_V) \div P_V = 13.0''$

$e_H = (60\,R_2 + 120\,(R_3 + V_H)) \div P_H = 23.3''$

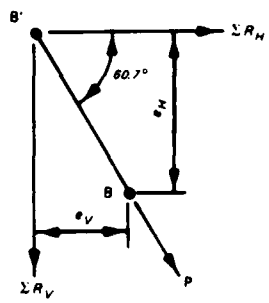

ECCENTRICITY TO SATISFY EQUILIBRIUM ($\Sigma M_B = 0$)

$e_H = e_V \text{ TAN } 60.7° = 23.2'' \geq 23.3''$

Figure 13. Static equilibrium at upper gusset plate

38. Distribution of horizontal forces is more complicated. It might be expected that the bottom few girders would carry most of the horizontal force. However, the FE results show that these girders carry only a small portion of the pintle horizontal force, with the majority of the force taken in girder 15 and in the elements above this girder. The reason for this distribution is that the large vertical pintle reaction tends to rotate the corner of the gate clockwise (in relation to Figure 14). The horizontal girders contribute reaction forces resisting such rotation. These reactions must necessarily be tensile forces in the lower girders, with the upper girders in compression. These forces are superimposed with the girder forces necessary to react the

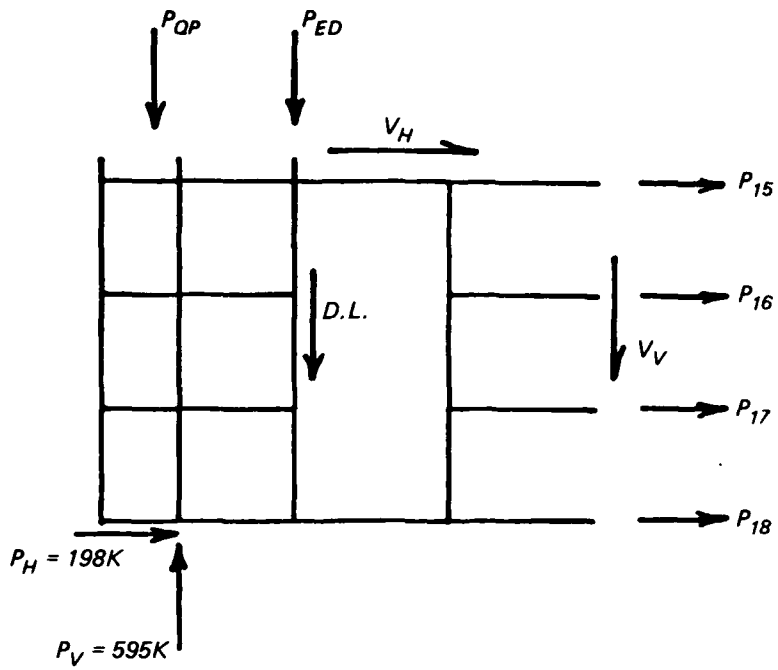

Vertical Forces, kips		Horizontal Forces, kips	
P_{QP}	= 297	V_H	= -83
P_{ED}	= 120	P_{15}	= -72
V_V	= 126	P_{16}	= -27
D.L.	= 52	P_{17}	= -23
		P_{18}	= 7
	595		-198

D.L. = dead weight of material within free body

V_V = vertical force in elements inside end diaphragm

V_H = horizontal force in elements above girder 15

Figure 14. Distribution of forces around pintle

horizontal component of the pintle force, thus producing the net horizontal force distribution shown in Figure 14. This pattern of forces is also consistent with the eccentricity calculations used to satisfy static equilibrium, as presented in Figure 13.

Force Distribution Around Hinge

39. This section presents the distribution of reaction forces from the hinge into surrounding gate elements. The free body used to evaluate the distribution is identical to that for the upper gusset plate and is shown in Figure 9. Applied forces consist only of gate dead load (no diagonal prestressing), and result in a hinge reaction of 198 kips horizontally, no vertical reaction, and a negligible force of 13 kips perpendicular to the plane of the gate. Figure 15 illustrates distribution of internal forces in the gate elements based on CM results.

40. These results indicate that the top girder carries a force almost equal to the hinge reactions. Loads in the other horizontal and vertical

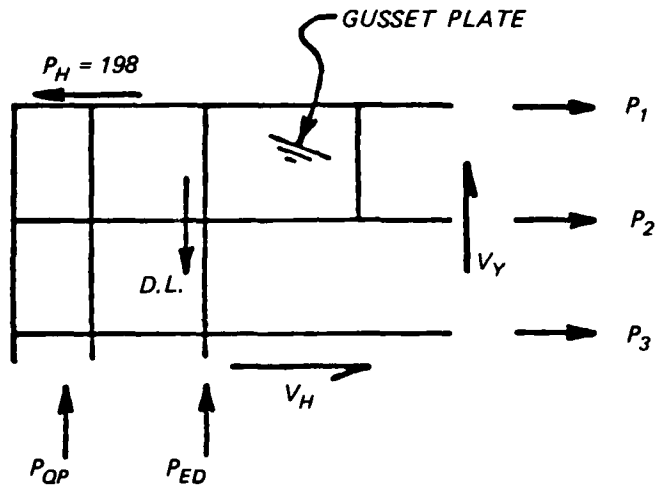

Vertical Forces, kips		Horizontal Forces, kips	
P_{QP} =	67	P_1 =	190
P_{ED} =	4	P_2 =	-109
V_V =	-42	P_3 =	37
D.L. =	-29	V_H =	80
	0		198

D.L. = dead weight of material within free body

V_V = vertical force in elements inside end diaphragm

V_H = horizontal force in elements below girder 3

Figure 15. Distribution of forces around hinge

members are again affected by a rotational deformation of the corner of the gate. Vertical forces are compression in the quoin post, near zero in the end diaphragm, and change to tension beyond the end diaphragm. The second girder carries a surprisingly high compression load because of this corner deformation. The reason for the severe difference in forces between the top two girders must be related to the gusset plate, which spans just between these girders. A larger gusset would probably result in a more gradual change in girder forces, similar to the force distribution around the pintle.

Force Distribution Around Operating Strut

41. This section presents the distribution of operating strut forces into the surrounding gate elements. The free body used to evaluate the distribution is shown in Figure 16. Applied loads consist of a temporal head

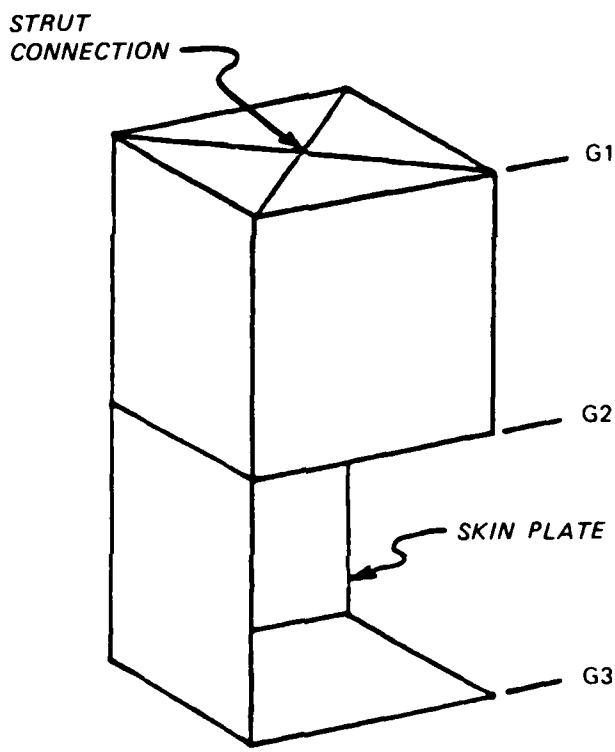

Figure 16. Free body at strut

acting on the lower portion of the gate. The balancing strut reaction is a horizontal force, 122 kips parallel and 110 kips perpendicular to the gate. Distribution of internal forces in gate elements, based on CM results, is shown in Figure 17.

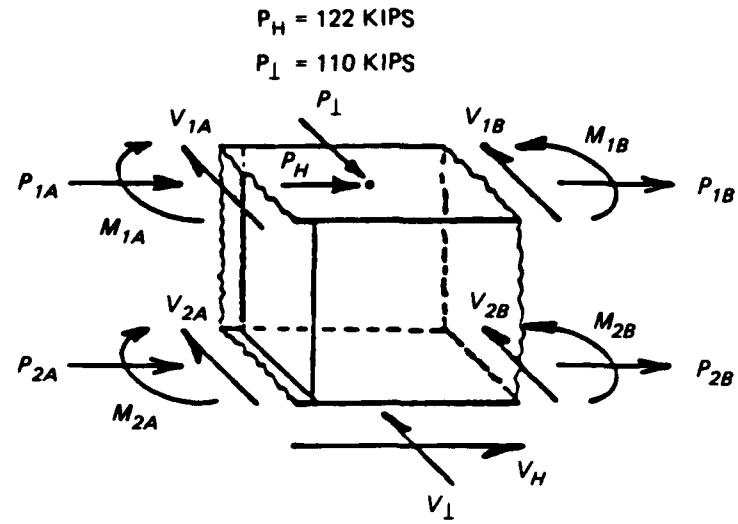

Parallel Forces, kips	Perpendicular Forces, kips	Moments, in.-k
P_{1A} = -178	V_{1A} = 80	M_{1A} = 11,060
P_{1B} = 3	V_{1B} = 6	M_{1B} = 7,880
P_{2A} = 66	V_{2A} = -3	M_{2A} = 4,250
P_{2B} = 14	V_{2B} = 56	M_{2B} = 5,550
V_H = -27	$V_\perp$ = -29	
-122	110	

V_H = forces parallel to gate, carried by members below girder 2

$V_\perp$ = forces perpendicular to gate, carried by members below girder 2

Figure 17. Distribution of forces around operating strut

42. The results show that most strut forces are carried by the top girder, on the hinge side of the strut connection. The top girder also has a significant bending moment near the strut. Forces in members below the top girder are significantly smaller.

43. An examination of the hinge reaction forces for this load case helps to explain the load distribution. The reactions at the hinge are 118 kips parallel and 103 kips perpendicular to the gate. Both these forces are in the direction opposite that of the strut reaction forces. Thus, the strut force component parallel to the gate causes an axial load in the top girder and is reacted entirely at the hinge. The strut and hinge forces perpendicular to the gate form a reaction couple to resist forces applied to the top girder through various elements of the gate. The elements mainly affected

are the vertical diaphragms. This concept is illustrated in Figure 18.

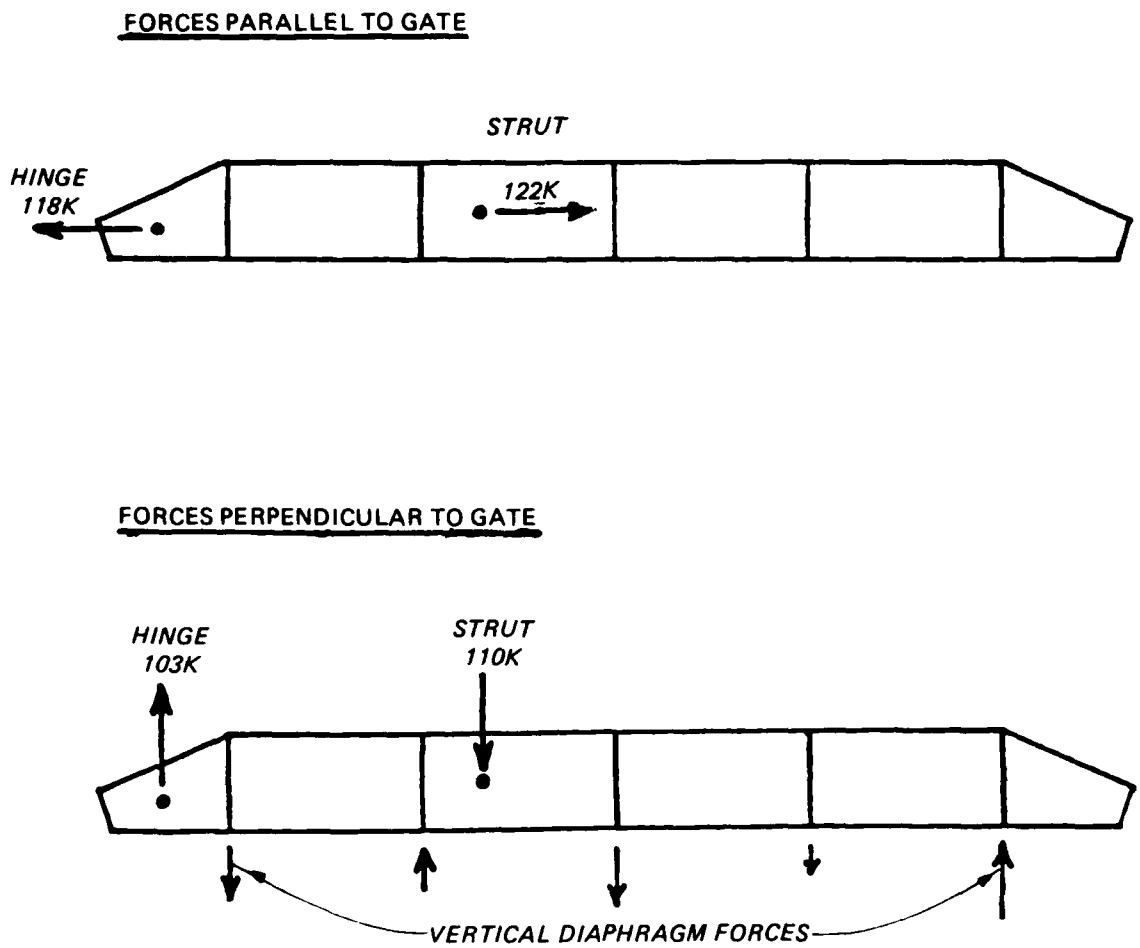

Figure 18. Strut and hinge reactions on girder 1

Force Distribution Verification

44. After the analyses of the Bankhead gates, another model was developed and based on the geometry of the miter gates at Gallipolis Lock and Dam. This model, shown in Figure 19, is similar to the Bankhead coarse mesh model. The Gallipolis model was used to verify force distribution patterns around the gusset plates with results presented in the following paragraphs.

45. A free body of the lower gusset area is shown in Figure 20, with the lower gusset plate extending over only three girders. The diagonal prestress loading was 524 kips, the horizontal component was 336 kips, and the vertical component was 403 kips. Distributions of horizontal and vertical

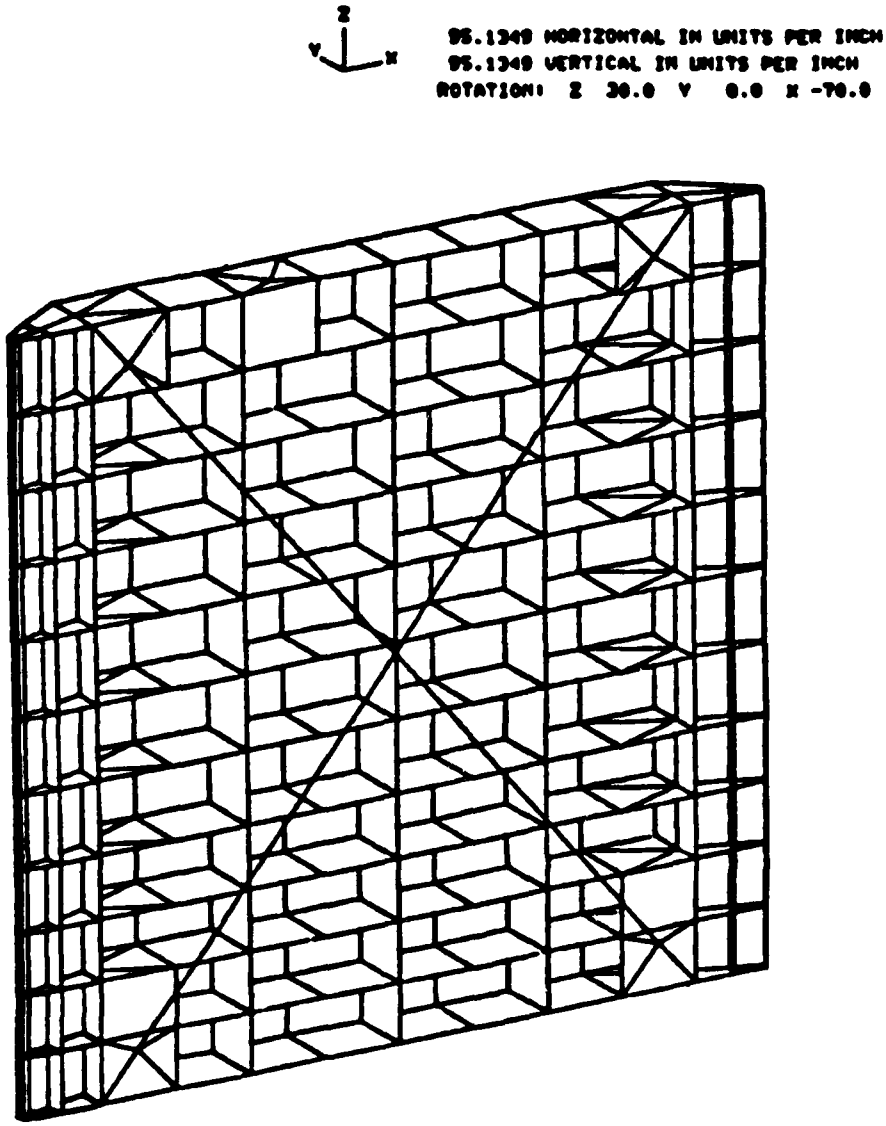

Figure 19. Model of Gallipolis Miter Gate

forces are shown in Table 5, and distribution of girder moments is shown in Table 6. The Gallipolis verification studies resulted in a pattern similar to the Bankhead results. Girder 12 carries a load greater than the horizontal component of the diagonal prestress, while girder 10 is actually in tension. This may be compared to Bankhead gate values in Table 1. The calculated distribution of moments due to diagonal eccentricity matches the distribution of axial load in the two lower girders, similar to Bankhead (Table 2). The moment in girder 10 breaks the pattern; however, the load and moment in girder 10 are not of significant magnitude. The distribution of vertical forces is mainly to the quoin post and end diaphragm, though the percentage

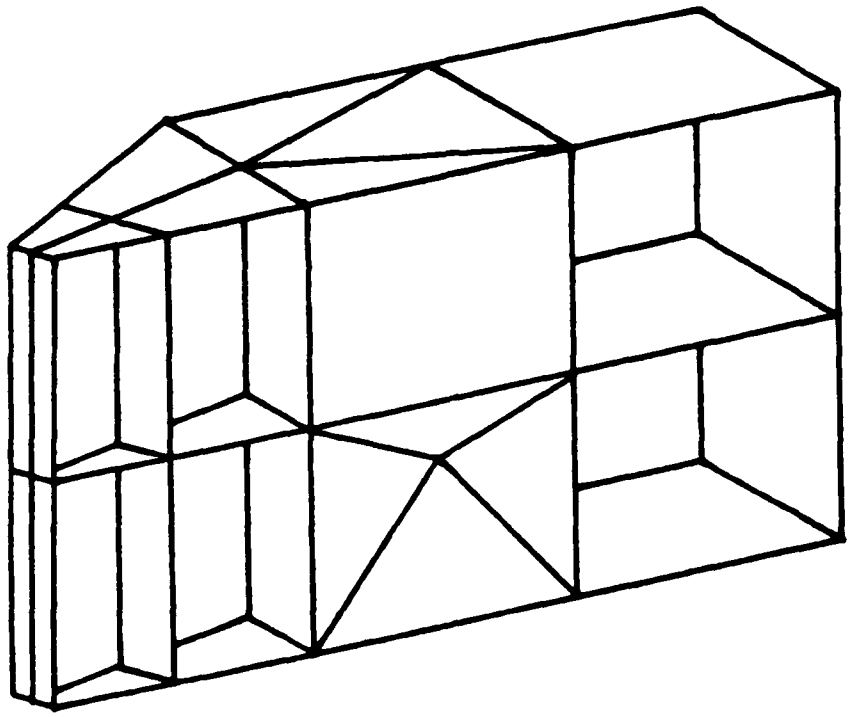

Figure 20. Free body at pintle, Gallipolis

distribution does not fully agree with the Bankhead results (compare to Table 3).

46. A free body of the upper gusset area is similar to that shown in Figure 9. The diagonal prestress loading was 632 kips; 405 kips horizontal and 485 kips vertical. Distributions of horizontal and vertical forces are shown in Table 7. The percentage distribution of vertical forces shows excellent agreement with results from the Bankhead gate (compare to Table 4). However, distribution of horizontal forces is different from Bankhead. One reason for this is the flatter slope of the diagonals on the Gallipolis gate, a 40-deg slope compared to a 60-deg slope for Bankhead. By a calculation similar to Figure 13, the required eccentricity of horizontal forces, to satisfy equilibrium, is 14.3 in. Based on forces from Table 7, the actual eccentricity is 14.1 in. Again, there is excellent agreement between these values, thereby proving the validity of this calculation.

47. The general distribution of reaction forces around the gusset plates in the Gallipolis gate is consistent with distribution patterns for the Bankhead gate. The explanations for these distributions apply to both gates equally well. Therefore, the Gallipolis results verify the previous Bankhead results.

Table 5

Force Distribution at Lower Gusset for Diagonal Prestress Loading (Gallipolis)

Member	Horizontal Force, kips
Above girder 10	146 (0.43)
Girder 10	39 (0.12)
Girder 11	-174 (-0.52)
Girder 12	-347 (-1.03)
Total	-336 (-1.00)
	Vertical Force, kips
Quoin post	-164 (-0.41)
End diaphragm	-285 (-0.71)
At interior diaphragm	46 (0.12)
Total	-403 (-1.00)

Note: The numbers in parentheses are the tabulated load divided by the total horizontal or vertical component of the diagonal force. Negative values indicate compression.

Table 6

Moment Distribution to Lower Girders for Diagonal Prestress Loading (Gallipolis)

Member	Axial Force, kips	Moment, in.-kips	Eccentricity, in.
Girder 10	39	-222	-6
Girder 11	-174	-10,616	61
Girder 12	-347	-19,287	56
Diagonal	--	--	67

Note: Moments are calculated about the plane of the skin plate.

Table 7

Force Distribution at Upper Gusset for Diagonal Prestress Loading (Gallipolis)

Member	Horizontal Force, kips
Girder 1	-392 (-0.97)
Girder 2	-110 (-0.27)
Girder 3	-5 (-0.01)
Below girder 3	102 (0.25)
Total	-405 (-1.00)
	Vertical Force, kips
Quoin post	-197 (-0.41)
End diaphragm	-255 (-0.52)
At interior diaphragm	-33 (-0.07)
Total	-485 (-1.00)

Note: The numbers in parentheses are the tabulated load divided by the vertical component of the diagonal force (243 kips). Negative values indicate compression.

Strain Gage Data

48. Limited strain gage data were available for the gate. This instrumentation was not done in a programmed manner. The gage readings do not agree with the FE predictions of internal force distribution. Due to the limited nature of both the strain gate and the FE data, it is not yet possible to make definite conclusions in this project.

Conclusions

49. The conclusions drawn in this report are based mainly on analyses of one gate, with another gate analysis for partial verification. Therefore, strict design criteria cannot be recommended based solely upon these studies. However, the studies do provide a better understanding of the pattern of gate behavior. They verify the conventional assumption of gate behavior as a three-hinged arch. They further indicate that force distributions are quite complex in areas near concentrated loads.

Summary of findings

50. All portions of these studies which evaluated the overall behavior of a miter gate tended to verify conventional design assumptions. Torsional behavior of a gate leaf is dictated by the presence of diagonals, which permit closed-section torsion of the gate rather than thin-member torsion. Forces in the diagonals are due to prestressing and applied torsional loads, and not due to gate dead loads except as they affect the calculated torque.

51. Temperature variations do cause warping and load redistribution in the gate. However, temperature-induced stresses are small and localized and may be safely ignored.

52. The studies duplicated the behavior of horizontal girders as segments of a three-hinged arch. At the top and bottom of the gate, girder loads differ somewhat from the assumed tributary area loading. The vertical diaphragms evidently redistribute loads more evenly among the girders. Also, quoin reactions near the top and bottom might be reduced due to hinge and pintle support. Internal stresses in the girders were found to match hand-calculated values except for a local high stress just beyond the end of the thrust diaphragm. Because of this local high stress, designers should ensure that girder webs are adequately stiffened or are made slightly thicker in this area.

53. Stresses in vertical diaphragms were found to be small for all usual loadings. Therefore, designers may safely continue the current practice of providing minimum size members for webs and flanges of the diaphragms. The only exception to this is in the area of an applied jacking force, which often coincides with a high force in the diagonal. This combination may produce high local stresses in the affected diaphragm, and should be kept in mind when detailing this area of the gate structure.

Internal force distribution

54. The results reflect only the specific geometry and loadings used in these studies. They provide a basis for predicting similar behavior in other gates, however the limited amount of pertinent strain gage data, as mentioned previously, does not corroborate the FE results. Force distributions are irregular and components in any given member were shown to be of unexpected magnitude and even in opposite direction to that expected. This distribution can be partially explained by considering the static equilibrium of applied forces and their reactions (paragraph 35).

55. The extent of the gusset plate seems to have a significant effect on force distribution to surrounding members. This is evident from the difference in distributions around the top and bottom gussets, which are connected between two and four girders, respectively. Extending gusset plates over additional girders may lead to more uniform distribution of forces to those girders. The location of the diagonal center line (through the end diaphragm intersections with the top and bottom girders) also may have a significant effect on force distribution. Changing this line of action may result in a more uniform distribution. Forces in gate members due to pintle, hinge, or diagonal loads are often additive with member forces due to hydrostatic loading. Therefore, force distributions for any new gate design should be estimated and considered concurrent with hydrostatic loads to ensure an adequate gate design. The results presented herein should be used as a guide for estimating this force distribution.

Recommendations

56. The FE studies of miter gates, as summarized in this report, can help provide a better understanding of gate behavior. Therefore, gate designers should be familiar with this report and should attempt to apply its findings to future gate designs.

57. The original FE studies do not provide sufficient information to develop specific design criteria, especially given the lack of consistency between FE results and limited strain-gage data. Therefore, further FE studies should be performed to verify and refine the results of the original studies. These additional investigations should attempt to determine the influence of various modeling techniques and differences in gate size and configuration.

58. More extensive instrumentation is necessary to verify FE results. Therefore, new gates should be instrumented to determine the actual internal force distribution around areas of concentrated loads.

59. A final recommendation is for a thorough investigation of a selected gate. This would involve fully documenting the conventional design computations, thoroughly investigating the gate by the FE method, and fully instrumenting the gate to verify the results of the conventional and FE analyses. This three-step investigation of a single gate is essential for determining the adequacy of current design procedures.

PART III: ELASTIC BUCKLING OF GIRDERS*

Preview

60. Two methods are conventionally used to investigate buckling of horizontal girders in miter gates. One method is based on diaphragm spacing and minor axis section properties and the other is based on the full length of the gate leaf and major axis properties. To gain a better understanding of the girder's buckling behavior, FE studies were performed on a representative girder. These studies, presented as Report 6, "Elastic Buckling of Girders in Horizontally Framed Miter Gates," are interpreted in this part.

Typical Girder Selected

61. Girder 10 of the Bankhead lower gate was selected as a typical girder and models were developed for one half of the symmetrical girder. Timber fenders and intercostals were not included in the models but transverse and longitudinal stiffeners were represented in the FEM for minor axis buckling studies. In the major axis study, longitudinal and transverse stiffeners were not modeled explicitly but other girder elements were represented by FE's.

62. All structural elements were assumed to have a yield point of 46,000 psi, and the 8th Edition of American Institute of Steel Construction** was used to select effective width of unstiffened elements in compression.

Minor Axis Buckling

63. Minor axis buckling was investigated by using an FE computer program entitled BASP. Two types of displacement boundary conditions were utilized: initially, in-plane displacements at the quoin and center line of the girder were taken from previous FE studies of the gate leaf; and secondly, a propped cantilever model was used and considered more consistent with

---

* James D. Gibson. 1985, US Army Engineer District, Mobile.

** American Institute of Steel Construction. 1978 (Nov). "Specification for the Design, Fabrication, and Erection of Structural Steel for Buildings," 8th ed.

current hand-based design. The following discussion is based on the latter model.

64. The results of the minor axis buckling indicated a safety factor, or lambda value, of 2.08 as a minimum for the girder with one row of stiffeners before local web buckling occurred. The investigation also revealed that apparently both transverse and longitudinal web stiffeners are significantly effective in controlling localized web buckling. Lambda values increased as the number of horizontal stiffeners increased.

65. Local buckling studies with the BASP model also revealed an overall buckling mode normal to the plane of the web involving beam-column behavior of the downstream flange. Stresses associated with this mode, however, were well into the plastic range and, therefore, not consistent with the assumption of linear elastic buckling.

66. There were no buckling modes that involved the upstream flange.

Major Axis Buckling

67. In the investigation of strong or major axis buckling, a new FEM model of one half of girder 10 was developed and a different computer program called BUCKLE was used to determine critical buckling loads and mode shapes. All major axis studies used the propped cantilever conditions utilized for the minor axis study, with results of the study limited to linear elastic buckling.

68. Web stiffeners were accounted for in the model by restraining the translational displacement normal to the web at selected nodes. This was considered realistic due to the virtual absence of transverse web displacement along stiffener lines in the BASP runs made previously in the minor axis study.

69. The factor of safety, or lambda value, for the major axis study for one longitudinal stiffener was 1.786, or 14 percent lower than the lambda value for minor axis buckling, although there is some question as to the effect of the omission of web stiffeners. (These factors are related to localized web buckling, not buckling of the entire girder.) Again, the lambda values increased as the number of longitudinal stiffeners increased. Local web buckling, coupled with a rotational instability of the downstream flange

between diaphragms, appears to be the first and principal form of strong axis buckling.

70. All indicated buckling modes were related to local buckling of the web with instability of the downstream flange. None of the fundamental buckling modes for the strong axis case corresponds to an overall buckling failure of the girder, pinned at the quoin and miter points.

Summary

71. A comparison of available information from strain gages, FE analysis stresses, and hand calculations indicated reasonably good agreement for overall girder behavior. This suggests that the FE models adequately represent the prebuckled behavior of the girder and that hand calculations are a realistic representation of normal loading and stress distribution.

72. The study of both minor and major axis buckling was restricted to linear elastic buckling of an isolated girder. The restraining effect of the skin plate and vertical diaphragms was accounted for only in the effective width computations of girder components. Boundary conditions consistent with current hand design methods were employed throughout much of the study, even though these boundary conditions were not completely consistent with results of the FE analysis of the entire gate. Due to these slight inconsistencies, it is possible that the girder may exhibit other buckling modes. Also, the leaf as a whole might possess some overall forms of instability which were not detected by this investigation. Within the above noted restrictions, the principal finding of this study was that girder buckling behavior is much more localized than current hand procedures reflect.

73. Since the safety factor relative to buckling is essentially 2.0 or greater, this appears consistent with or greater than the safety factor used for other allowable stresses. Since the buckling lambda value is based on localized buckling, the actual factor of safety relative to overall buckling would be much greater than 2.0.

74. In a paper by Cherng, Phang, and Chang,* it was concluded, relative to girder buckling, that

---

* M. D. Cherng, M. K. Phang, and C. H. Chang. 1983 (Oct). "Miter-Type Navigation Lock Gates," Journal, Structural Engineering, American Society of Civil Engineers, Vol 109, No. 10.

> The unique solution on the load-deflecti · curves indicates that there is no other type of buckling mode than snap-through when the mitered angle is very large. For mitered angle not so large, the failure mode is governed by the flexural yield stress at the center of the gate girder. The result is compared with AISC beam-column formula upon which the current design is based. Good agreement is reached if the failure mode is governed by the maximum flexural stress, and thus the beam-column treatment is justified for practical purposes.

The mitered angle is the angle between the center-line axis of the lock and the work line of the leaf. The mitered angle for the normal 4-on-12 leaf slope is approximately 71.23 deg and the large angle is defined as over 84 deg. It does not appear that an angle over 84 deg would be used for conventional miter gates, and therefore snap-through buckling would not be a critical factor.

75. Both minor and major axis buckling results point to the effectiveness of transverse and longitudinal web stiffeners in controlling localized web instability. Therefore, horizontal web stiffeners should usually be selected so that the entire web is effective in column action for most gates. Gates with lesser head may require only partial web area, particularly if conditions are such that the girder is acting more as a plate girder than as a column. However, if the entire web is made effective by stiffeners, studies indicate that the current design method gives results that are slightly conservative.

76. Studies thus far have not resulted in an absolute means of predicting critical buckling modes or forces. Further studies would involve the more complex inelastic buckling of horizontal girders. This is considerably more tedious and expensive and does not appear to be warranted at this time.

Conclusions

77. These studies of a selected girder indicate that initial buckling will be due to local instability of the web or flange. Overall buckling of the girder about either axis would occur only at lambda values (factors of safety) well above 2.0. Therefore, even though current hand methods may not accurately account for buckling behavior, they will produce a conservative design, provided there are adequate stiffeners to prevent premature web or flange buckling.

PART IV: STRUCTURAL BEHAVIOR OF ALTERNATE CONFIGURATIONS OF MITER GATES*

Introduction

78. In the course of studying conventionally framed miter gates, Reports 1 and 2, it became evident that control of torsional deflection is a significant problem because of the inherent lack of rigidity of the open framing. While this lack of rigidity is compensated for by the use of diagonals, the tensioning of diagonals is an indeterminant process and the diagonals themselves are susceptible to damage. It was therefore decided to study alternate, closed sections with downstream skin plates over portions of the gate leaf to see if these alternate configurations would add enough stiffness to be effective and practical. A summary of the various models investigated is shown in Table 8.

Background

79. The John Hollis Bankhead Lock and Dam lower miter gate described in the finite element studies, Reports 1 and 2, was used as a benchmark conventional gate. The study began with variations on the conventional open sections with skin plate on the upstream side only in Report 3, "Alternate Configuration Miter Gate Finite Element Studies - Open Sections." Closed sections were then studied in the work described in the miter gate studies, Reports 4 and 5, "Alternate Configuration Miter Gate Finite Element Studies -- Closed Sections" and "Alternate Configuration Miter Gate Finite Element Studies -- Additional Closed Sections."

80. The complete study of closed-section alternate gate configurations included four basic types with variations of the more promising types. The more significant results are summarized in this part; their geometry configurations are listed on the following page.

---

* Michael D. Nelson, P.E. 1985. US Army Engineer District, Seattle.

Table 8

Summary of Model Configurations

Model	Description
	Conventional gate with a set of diagonals (John Hollis Bankhead Lock & Dam, lower gate, see Figure 21)
	Conventional gate with larger diagonals
	Double skinplate (conventional gate plus a full downstream skinplate, Figure 23)
1	Gate with horizontal torque tubes (Figure 24)
1L	Gate with larger horizontal torque tubes (Figure 25)
2	Gate with horizontal and vertical torque tubes (Figure 26)
3	Gate with vertical torque tubes (Figure 27)
3H	Same as model 3 but with access holes through the girder webs (Figure 28)
3S	Gate with smaller vertical torque tubes (Figure 29)
3SP	Same as model 3S but with a positive diagonal only, no negative diagonal
4	Gate with "K" bracing on downstream face (Figure 30)
4R	Same as model 4 but with reduced bracing size
5	Gate with cross bracing on downstream face (Figure 31)
5R	Same as model 5 but with reduced bracing size
ORH	Conventional gate (Gallipolis Lock and Dam, Figure 70)
ORHT	Same as model ORH but with vertical torque tubes (Figure 71)
ORHT1	Same as model ORHT but with a positive diagonal only, no negative diagonal

Note: Results from many of the above models are presented for models both with and without diagonals.

Gate and Model Geometry

81. Each lower miter gate leaf for the Bankhead Lock is approximately 89 ft high and 62 ft wide. The gate has a conventional horizontally framed configuration, using 18 horizontal girders as the main load-carrying members. Between the four corners of each leaf is a single set of diagonals located on the downstream face.

82. The as-built geometry was modeled by using the GTSTRUDL program. CM models (581 joints, 886 members, and 844 elements) of gates with and without diagonals are illustrated in Figures 21 and 22, respectively. In the models, hydrid membrane and plate FE's were used for the skin plate, the webs of girders and diaphragms, and for various other components. Space frame members (beams) were used for flanges of girders and diaphragms and for diagonals, intercostals, and other components. The capability of GTSTRUDL to represent end joint sizes and member eccentricities was utilized to obtain the best possible correlation behaviors of the real gate and the models.

83. A double-skin plate model of the gate had a 5/8-in.-thick-steel plate added to the downstream face between the two end diaphragms. The downstream flanges on the horizontal girders and vertical diaphragms between the end diaphragms were deleted due to the presence of the downstream skin plate. The double-skin plate model is illustrated in Figure 23.

84. Seven partial double-skin plate or "torque-tube" models, referred to as models 1, 1L, 2, 3, 3H,* 3S, and 3SP, are illustrated in Figures 24, 25, 26, 27, 28, and 29, respectively. In all cases, each model was produced by selectively inactivating portions of the 5/8-in. downstream skin plate in the double-skin plate model. At the same time, the horizontal girder and vertical diaphragm flange plates which were not covered by skin plate were reactivated. In all models, gusset plates at points of attachment of diagonals and downstream plates in the strut-arm region at the top of the gate were left unaltered and as-built plate thicknesses were used in these areas.

85. Four alternate configuration models, 4, 4R, 5, and 5R, are illustrated in Figures 30 and 31, respectively. Detailed information on the models (4, 4R, 5, and 5R), one of each pair of models with vertical and diagonal bracing of the entire downstream face and the other with two panels of

---

* Model 3H is model 3 with access holes added in the web.

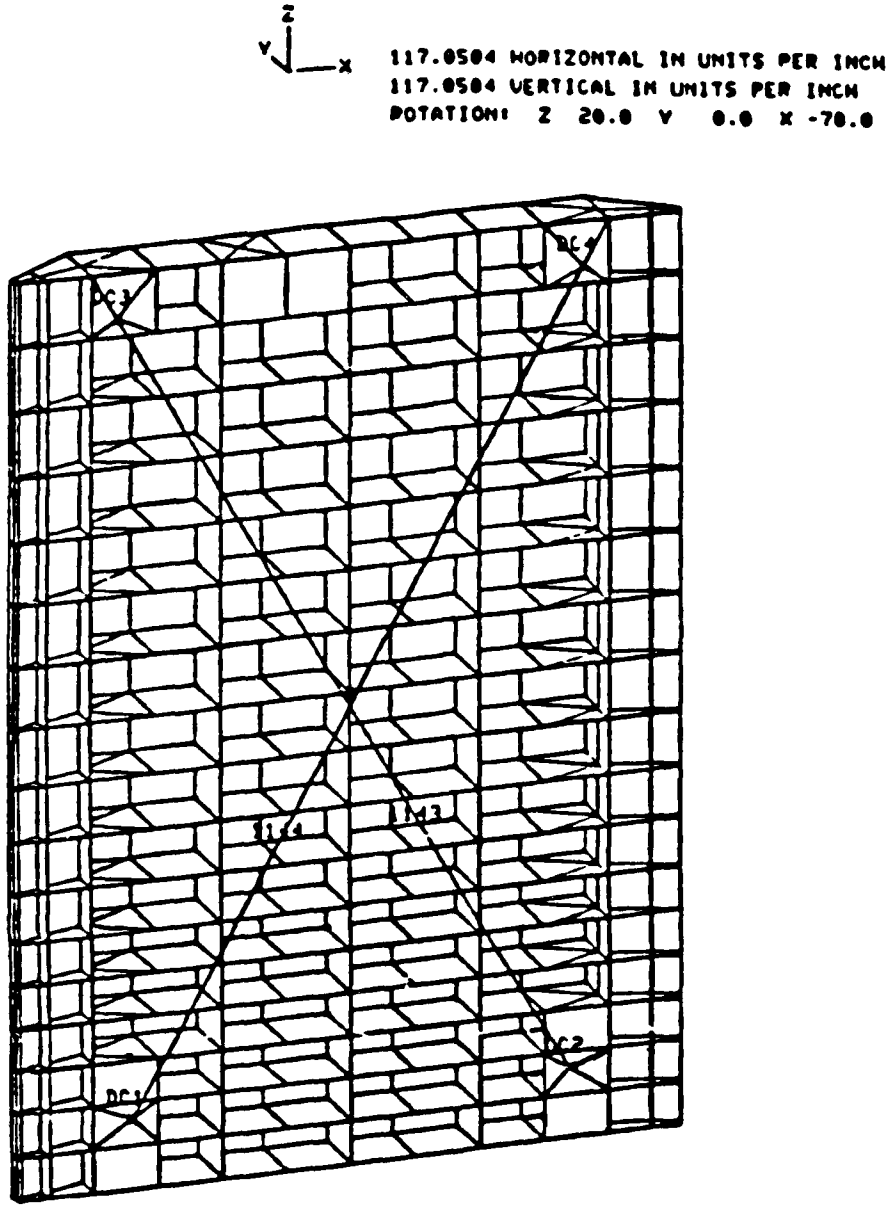

Figure 21. Finite element model, conventional gate, with diagonals

crossbracing over the downstream face, can be found in the miter gate study, Report 2. In these models, different arrangements of diagonal bracing were employed on the downstream side in an attempt to achieve the same performance improvements offered by the torque-tube models. This, at the same time, permitted ready access to all regions of the gate leaf for inspection and maintenance purposes.

86. As a final step, the conventional miter gate leaf model was modified to consider the influence of doubling the cross-sectional area of the

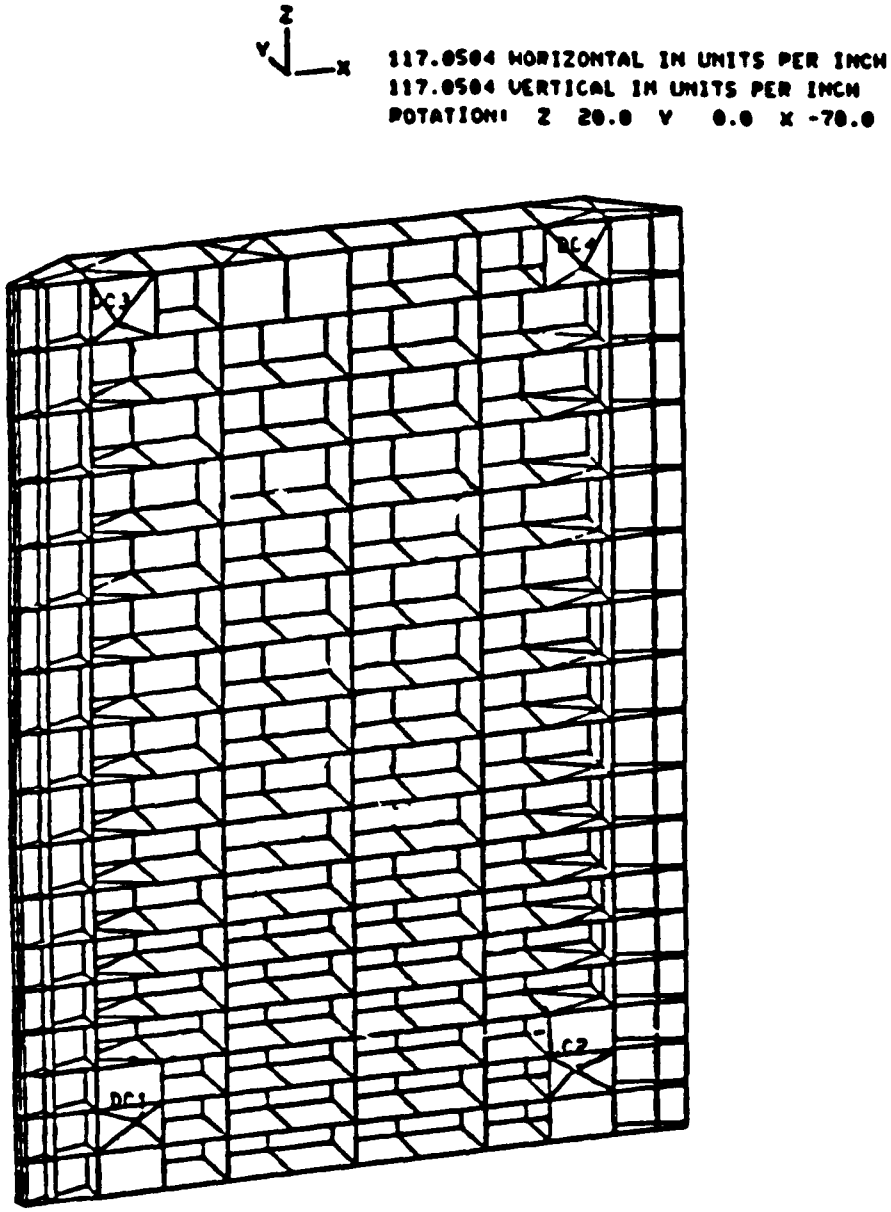

Figure 22. Finite element model, conventional gate without diagonals

diagonals. Only the cross-sectional areas of diagonal members 1143 and 1144 in Figure 21 were changed.

Loading Conditions

87. The following paragraphs provide a description of the models' applied loads and related boundary conditions used in gate behavior evaluations.

88. The gate has two different sets of boundary conditions. The first

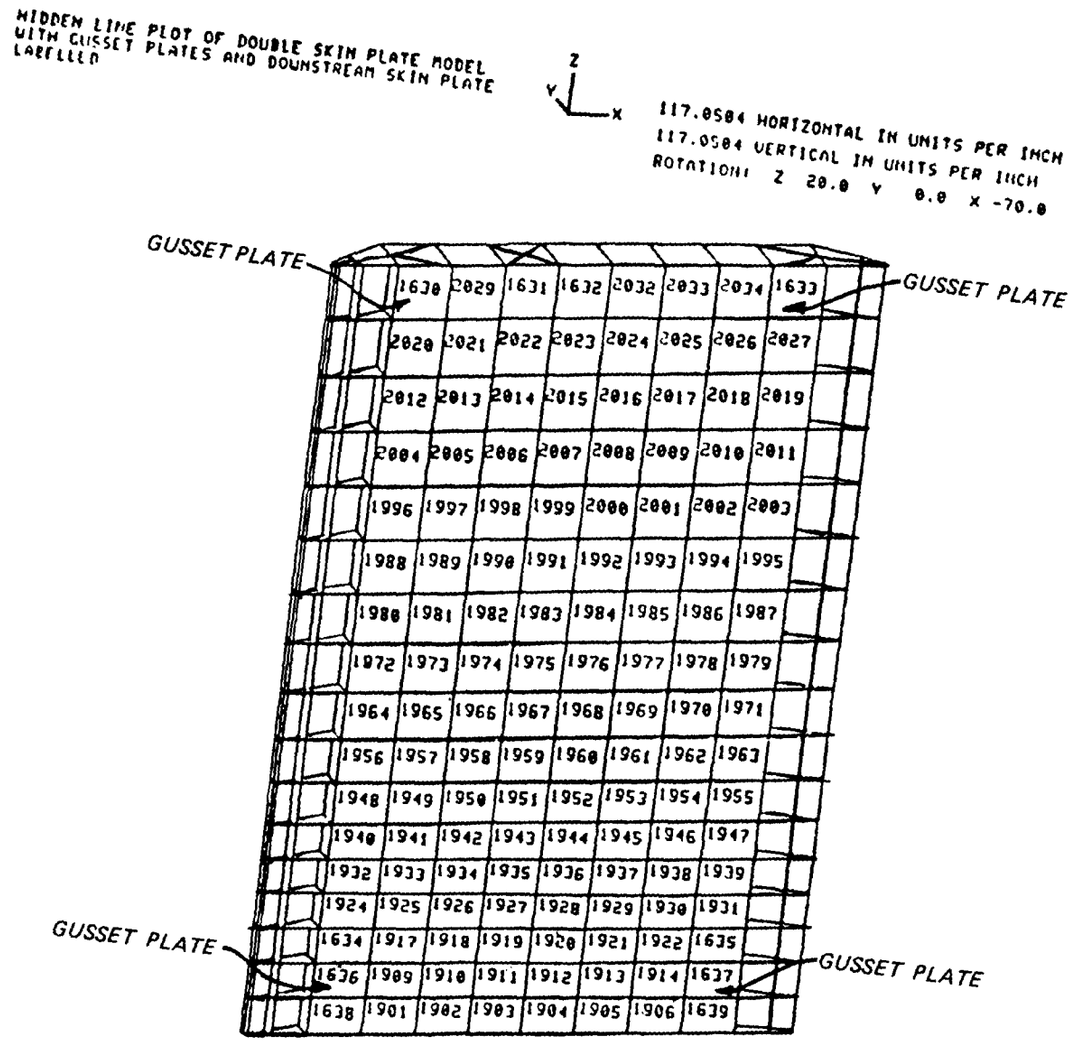

Figure 23. Double-skin plate model

set represents a gate in the unmitered position. The hinge (gudgeon pin) and pintle provide the main reactions, with the operating strut controlling rotation about the hinge line. The strut was assumed to be oriented at an angle of 48 deg from normal to the gate, and provides a reaction force in that one direction. The second set of conditions represents the gate in the mitered position and acts as part of a three-hinged arch. Reactions are provided at each girder at the quoin and miter bearings, and the direction of these reactions is parallel to the thrust diaphragms. In this configuration, the hinge and pintle remain active as reaction points. Note that this differs

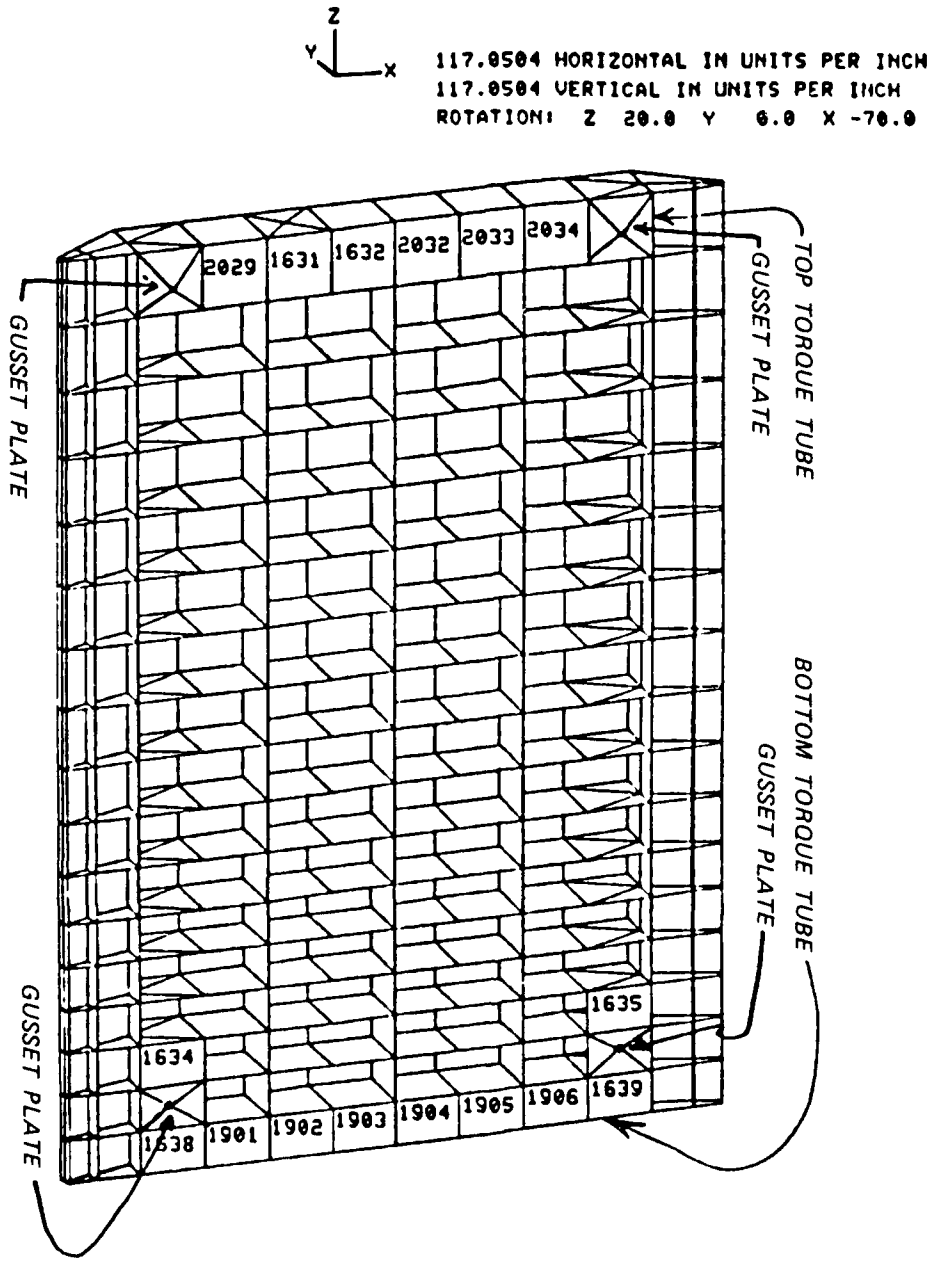

Figure 24. Torque-tube model 1

from conventional hand analysis assumptions which ignore the effects of hinge and pintle reactions in the mitered configuration.

89. Loads applied to the unmitered gate consisted of dead loads, diagonal prestressing forces, and normal operating hydrostatic or temporal hydrostatic head loading. Dead loads represented the actual dead weight of gate materials. Forces in the gate diagonals are the amount required to plumb the gate and resist temporal hydrostatic head loading. The temporal loading was a

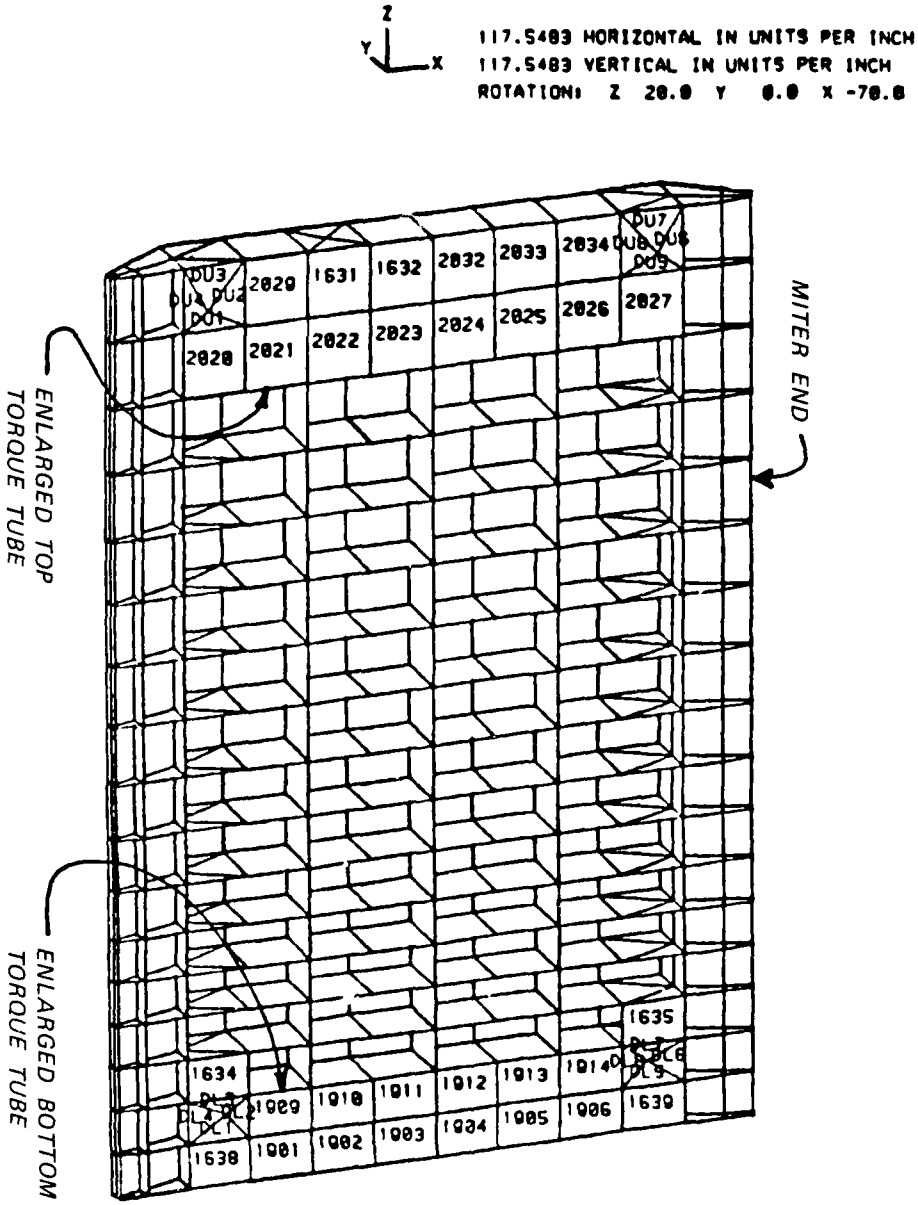

Figure 25. Torque-tube model 1L

differential hydrostatic head of 1.25 ft acting upstream. This load was applied over the lower 15 ft of the gate.

90. Load applied to the gate in the mitered configuration represented hydrostatic loads due to normal differential head. The hydrostatic loads represented the effects of an upper pool at el 255 ft, 3 ft below girder 1, and a lower pool at el 186 ft. A 10-ft minimum head was applied to the upper part of the gate.

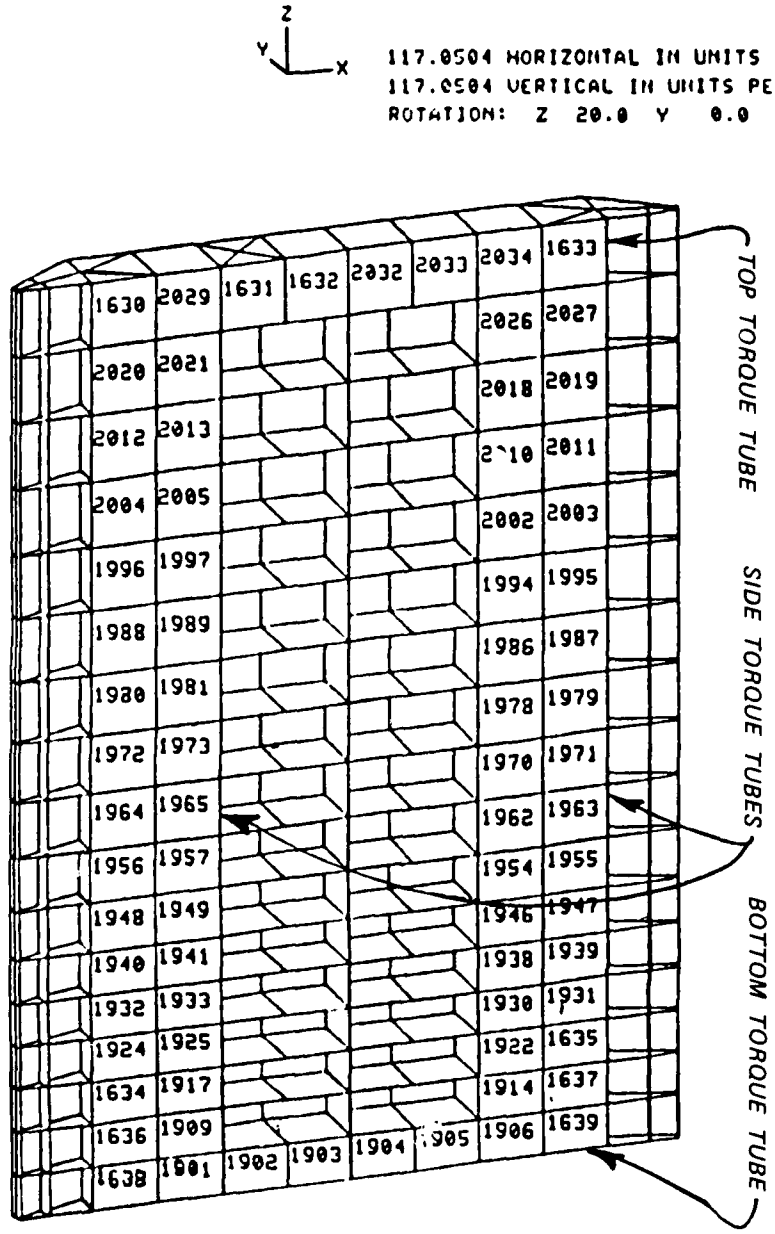

Figure 26. Torque-tube model 2

Gate Torsion and Stiffness

91. Torsional behavior of various gate models was studied in some detail and this report contains a summary of the main findings for torsion of these models. Further information on gate torsion can be found in Report 1 of the miter gate studies.

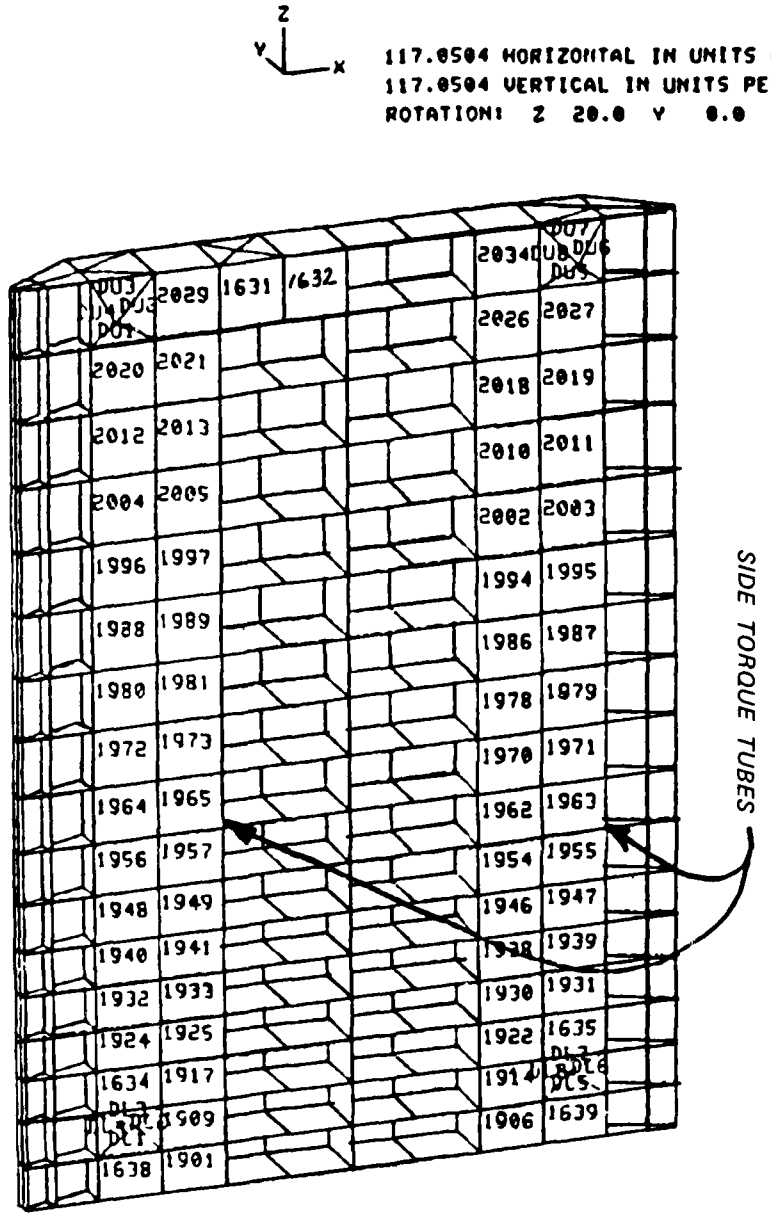

Figure 27. Torque-tube model 3

92. Before installation of the diagonals, miter gates are very flexible in torsion. Observed gate behavior and FE results are consistent on this point, although the model results were never able to match the measured torsional deflection of the installed Bankhead lower gate. Stiffness or dead load displacement of a gate leaf without diagonals is due to thin member torsional behavior of all the various plates and flanges comprising the structure. FE modeling results always indicated greater flexibility than field

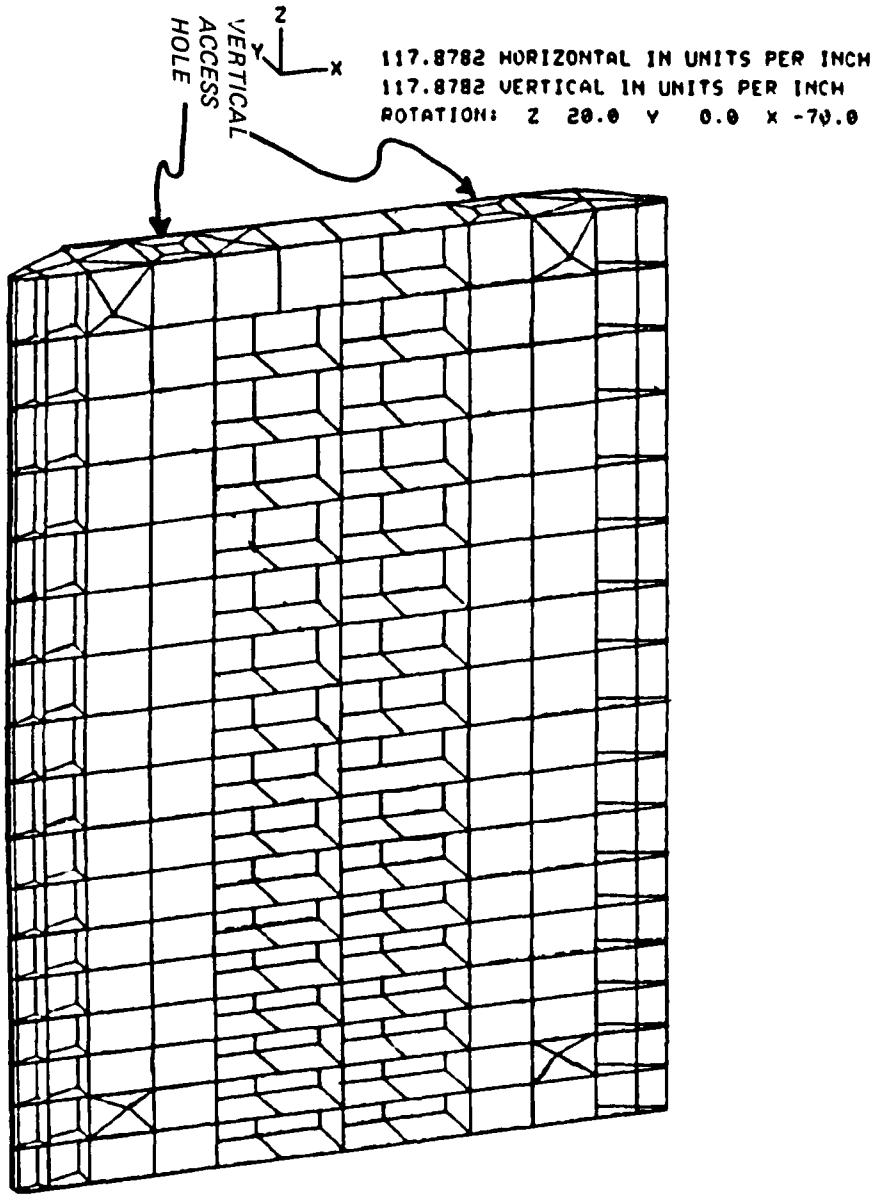

Figure 28. Torque-tube model 3H with vertical access holes

measured values with the reasons for this discrepancy yet undetermined. Possibilities are undiscovered modeling inaccuracies or extra stiffness imparted by gate fabrication details. However, behavior of a gate with diagonals installed is not significantly influenced by thin member torsion. This discrepancy between modeled and measured stiffness was therefore not considered as a serious model deficiency that would affect other types of gate behavior. With diagonals installed, model results verify that the gate is much stiffer.

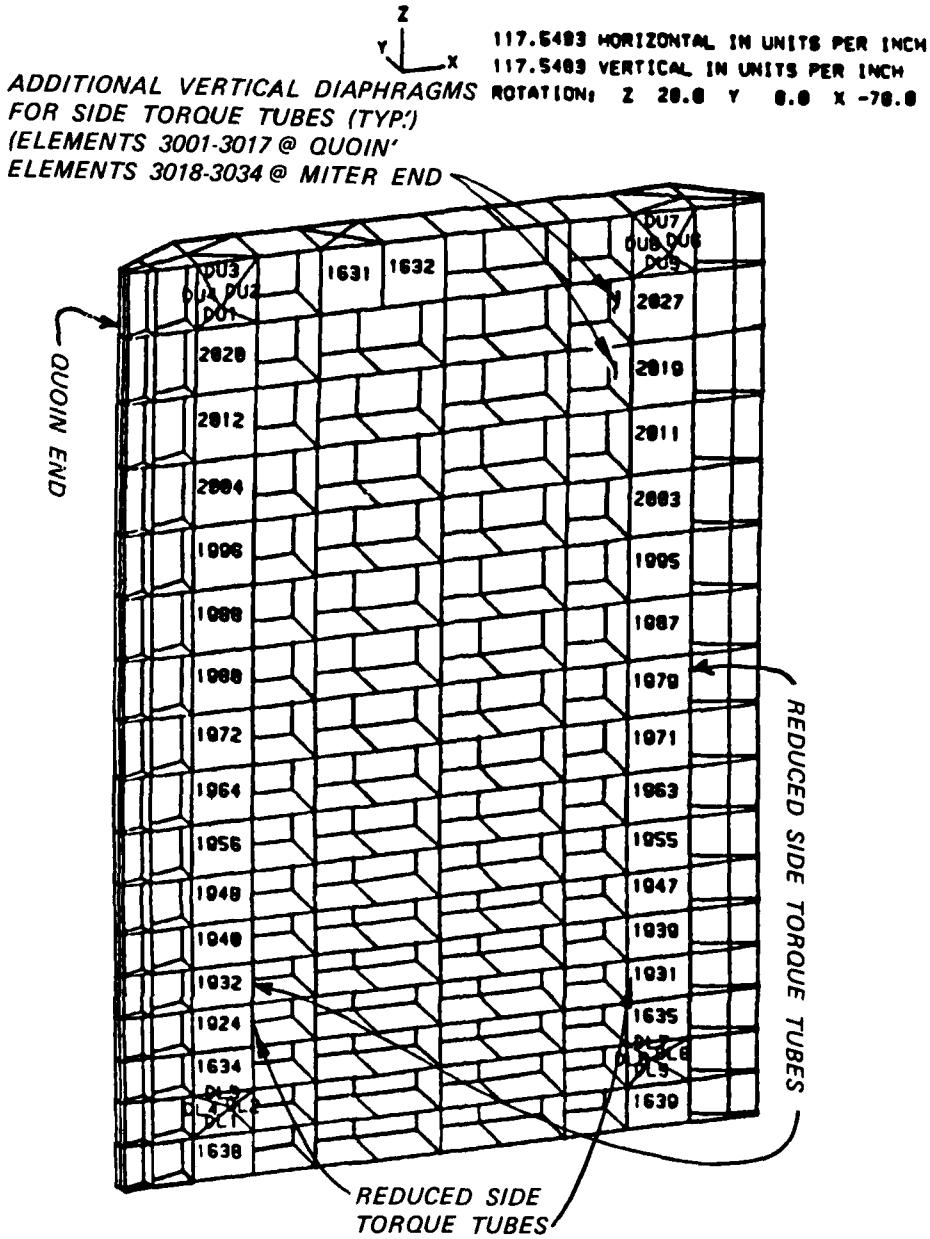

Figure 29. Torque-tube models 3S and 3SP

93. A dead load analysis of each model was performed to determine the dead weight of the gate leaf (i.e., reaction force R_z at joint 5 in Figure 32) and the out-of-plumb displacement at the miter end (i.e., at joint 449 in Figure 32) due to dead weight of gate leaf. Results of dead load analyses are shown in Figures 32-42 and summarized in Table 9. Note that the weight of the unprestressed diagonal bracing elements was included in the analysis of all alternate configuration models so that the designer could use diagonals for plumbing the gates.

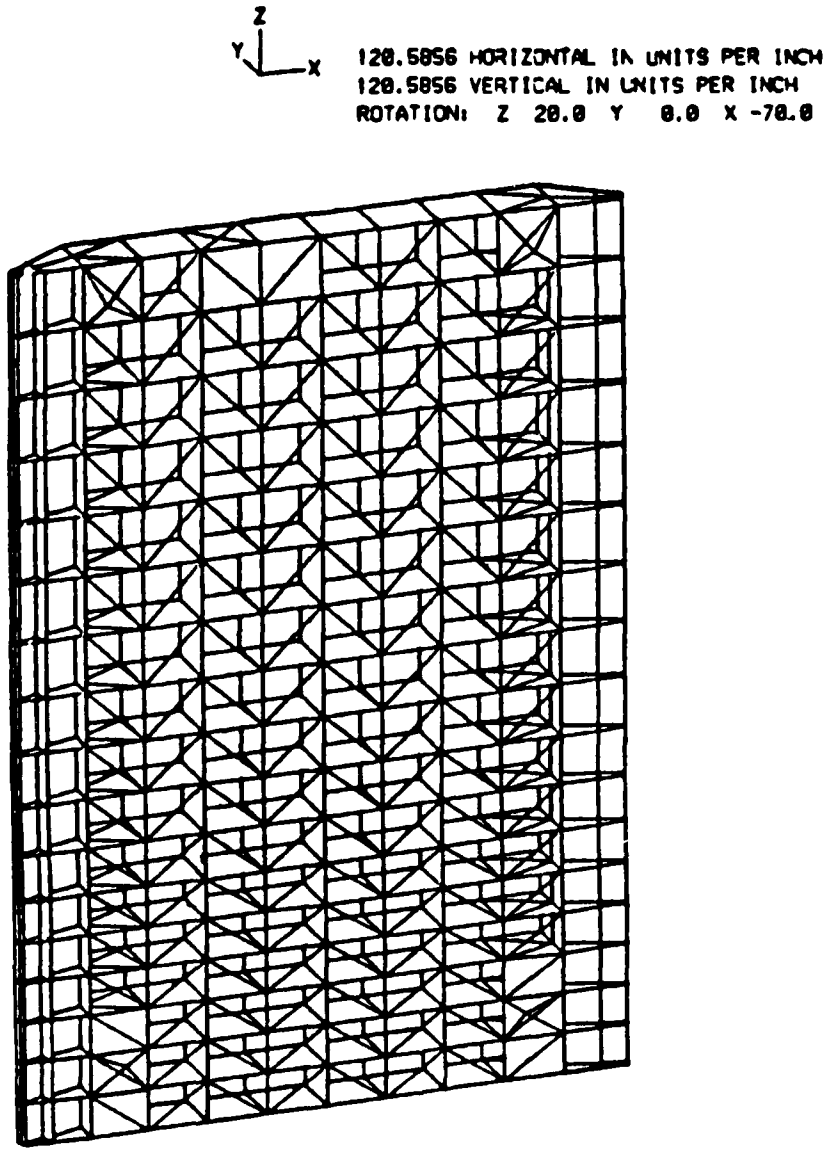

Figure 30. Alternate configuration models 4 and 4R

94. The torsional stiffness of the models was determined and compared with that of the conventional gate, both in its initial state with no diagonals, and in its final state with both prestressing diagonals in place. In all cases, the relative torsional stiffness of the gate model was assumed to be described by the value of the Y reaction required at joint 17 to impose a unit Y-displacement of the gate leaf with the gate tied back at joint 442 (Figure 43d). For all cases with diagonals, except one, the diagonals were assumed to have the same cross-sectional areas as in the conventional gate model. For the case of the conventional gate model with enlarged diagonals,

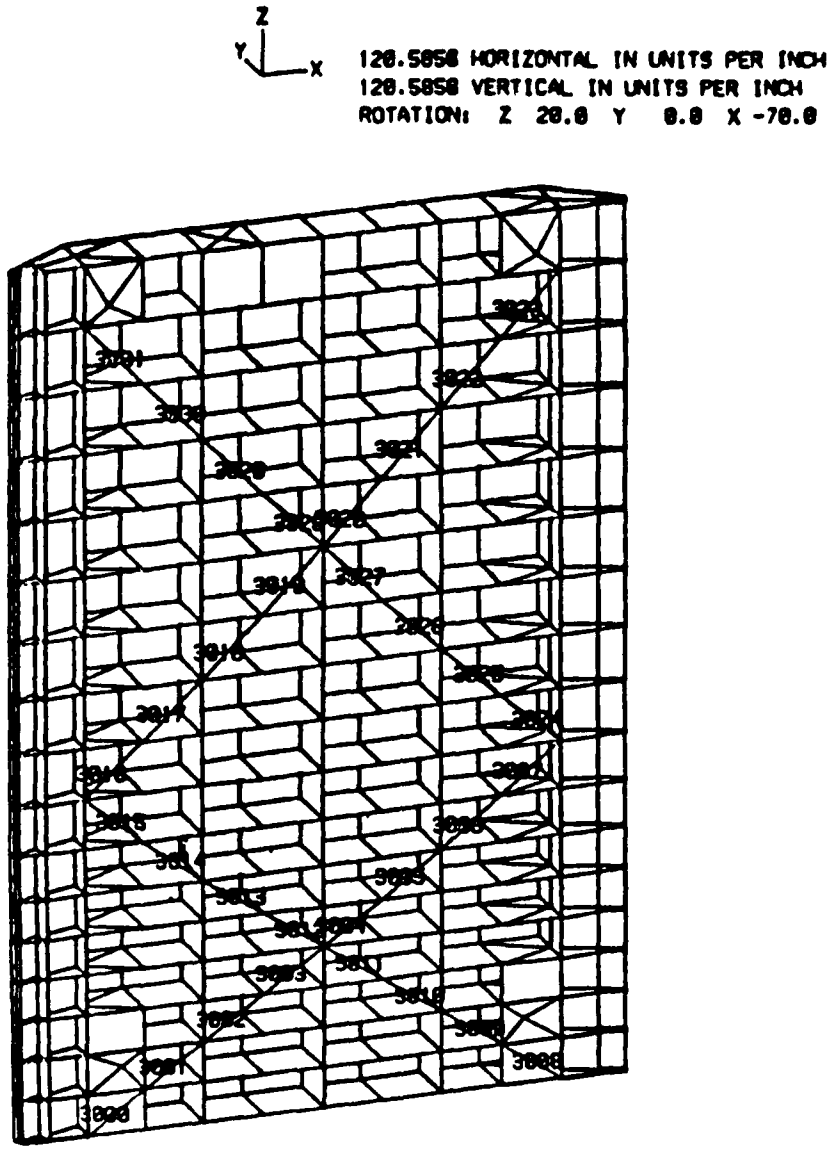

Figure 31. Alternate configuration models 5 and 5R

the cross-sectional areas of the diagonal elements in the original model were doubled in size, as noted earlier. The resulting reactions for all cases (shown as R_3 at joint 17 in Figure 43d) are presented in Table 10.

95. Forces in the diagonals are due to initial prestressing and to resistance to torsional loads applied to the gate. The stiffness, or torsional resistance, of the gates is one of the major factors involved in controlling the gates as they approach and are placed and held in the mitered position. The magnitudes of hydrostatic load and temporal heads, or surge, during gate operation make it necessary to place and hold the gate leaves in proper miter until a positive head can be placed on the gate.

JOINT	5	430	17
Rx	190.536	-190.536	0
Ry	12.981	-12.987	0
Rz	571.864	0	0
Mx	0	-27.932	0
My	0	-9.504	0

UNITS: KIPS, INCHES

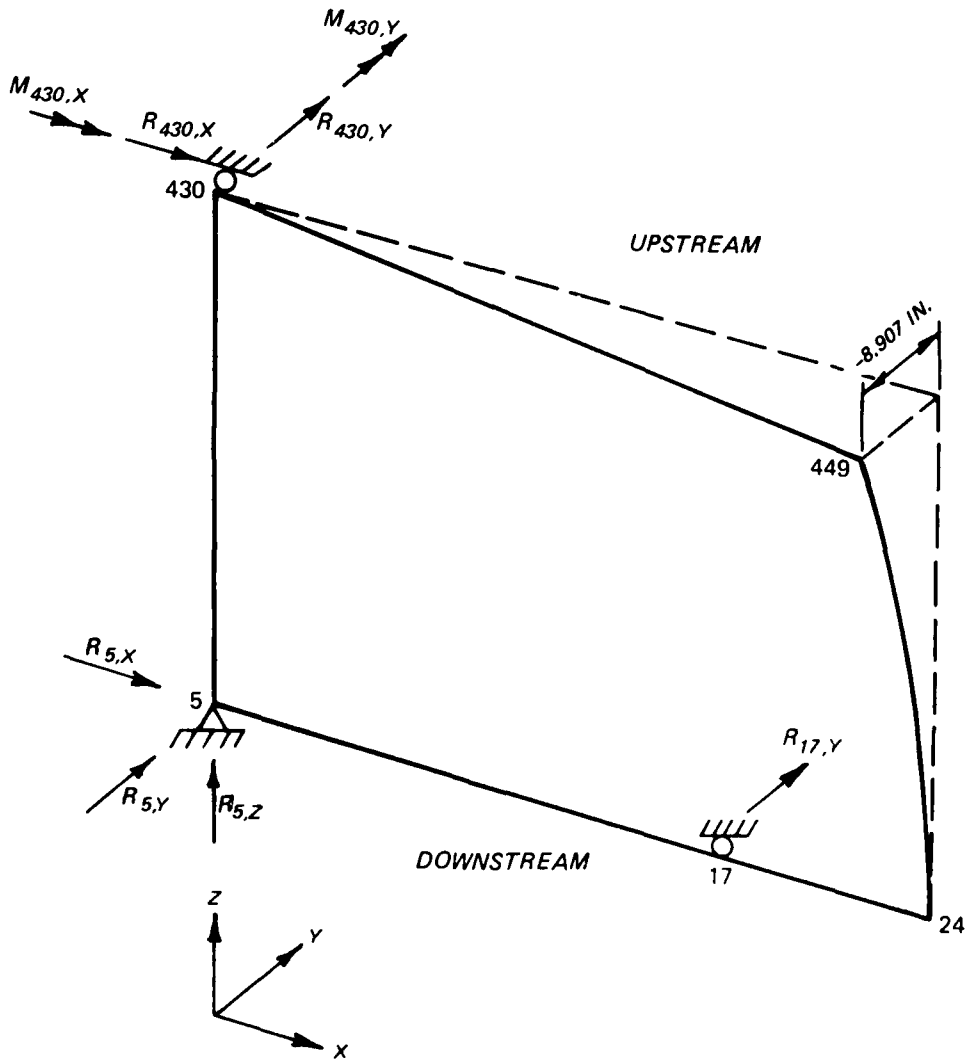

Figure 32. Conventional gate model dead load reactions and out-of-plumb displacements

JOINT	5	430	17
Rx	196.53	-196.53	0
Ry	12.695	-12.701	0
Rz	589.956	0	0
Mx	0	-30.11	0
My	0	-10.44	0

UNITS: KIPS, INCHES

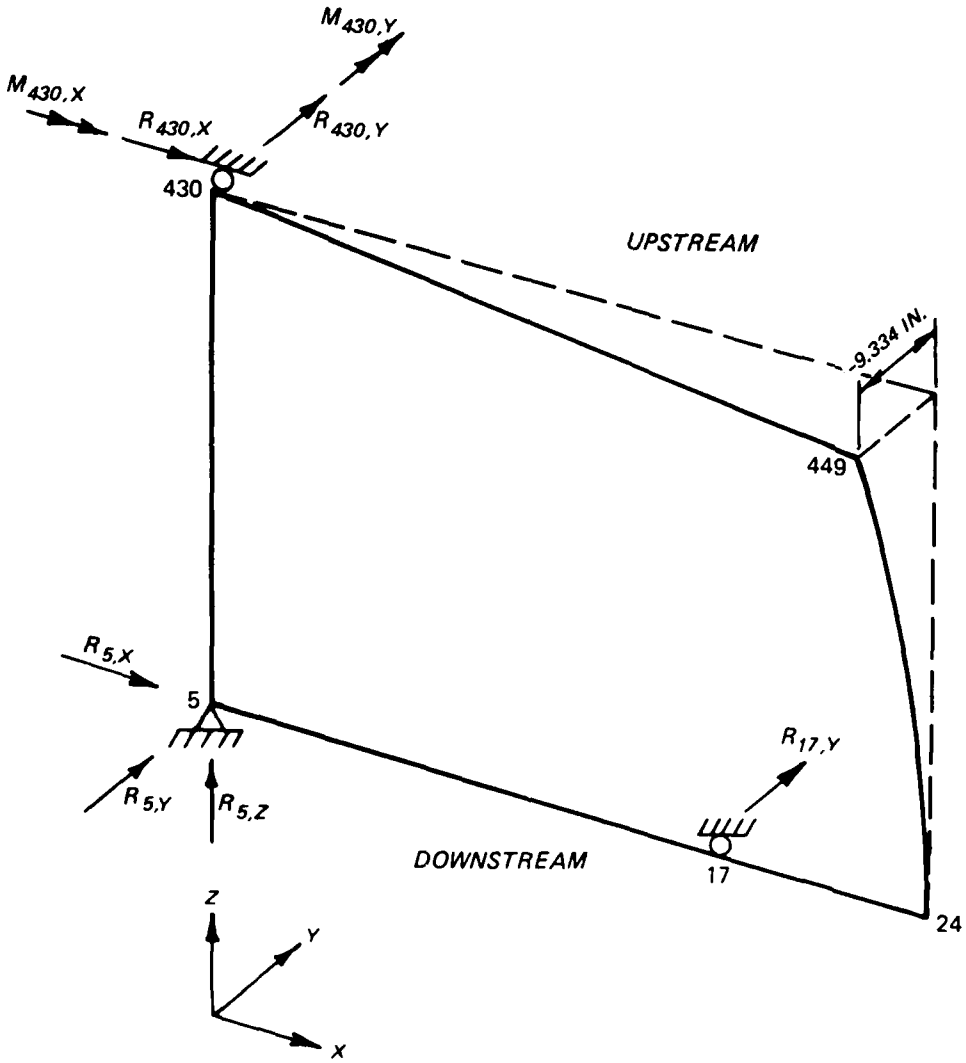

Figure 33. Conventional gate with enlarged diagonals, dead load reactions, and out-of-plumb displacements

JOINT	5	430	17
Rx	209.83	-209.83	0
Ry	11.98	-11.98	0.60
Rz	630.75	0	0
Mx	0	3.05	0
My	0	4.40	0

UNITS: KIPS, INCHES

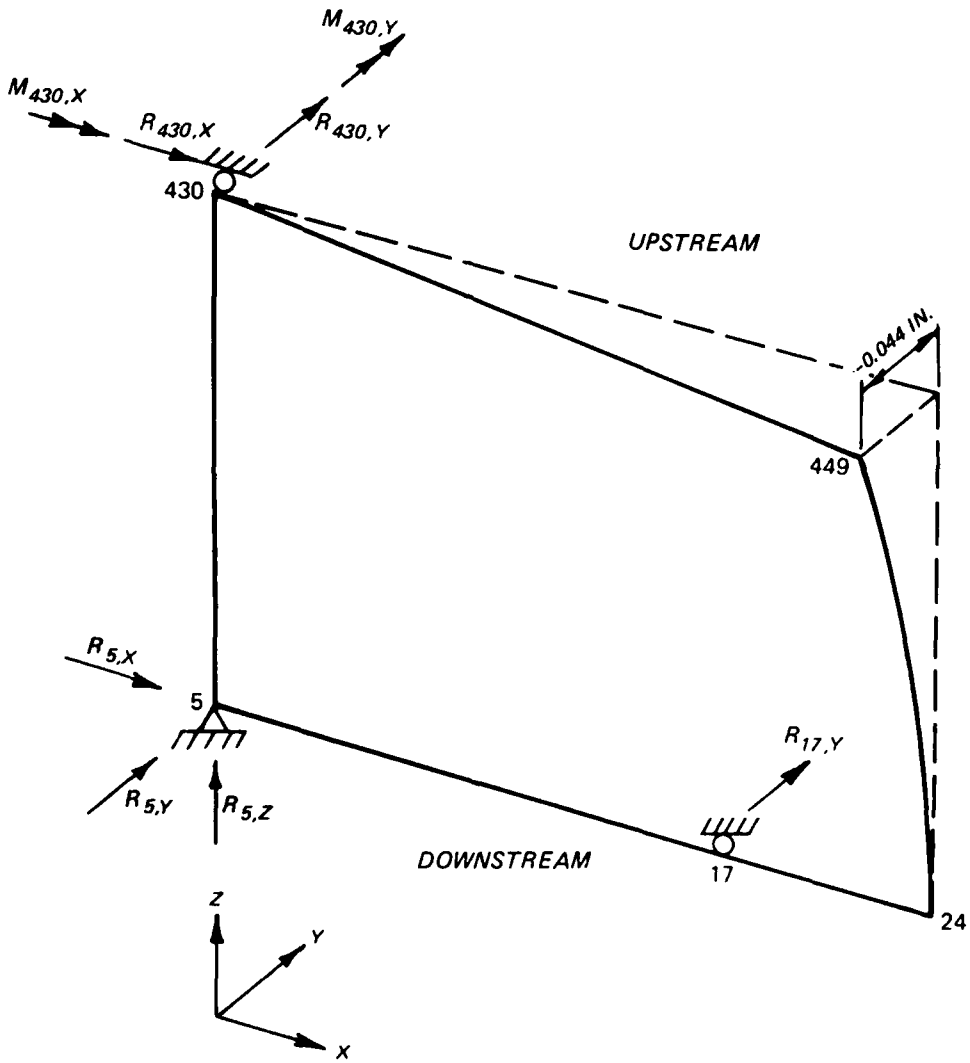

Figure 34. Double-skin plate model dead load reactions and out-of-plumb displacements

JOINT	5	430	17
Rx	192.47	-192.47	0
Ry	12.96	-12.96	0
Rz	572.55	0	0
Mx	0	-28.32	0
My	0	-10.16	0

UNITS: KIPS, INCHES

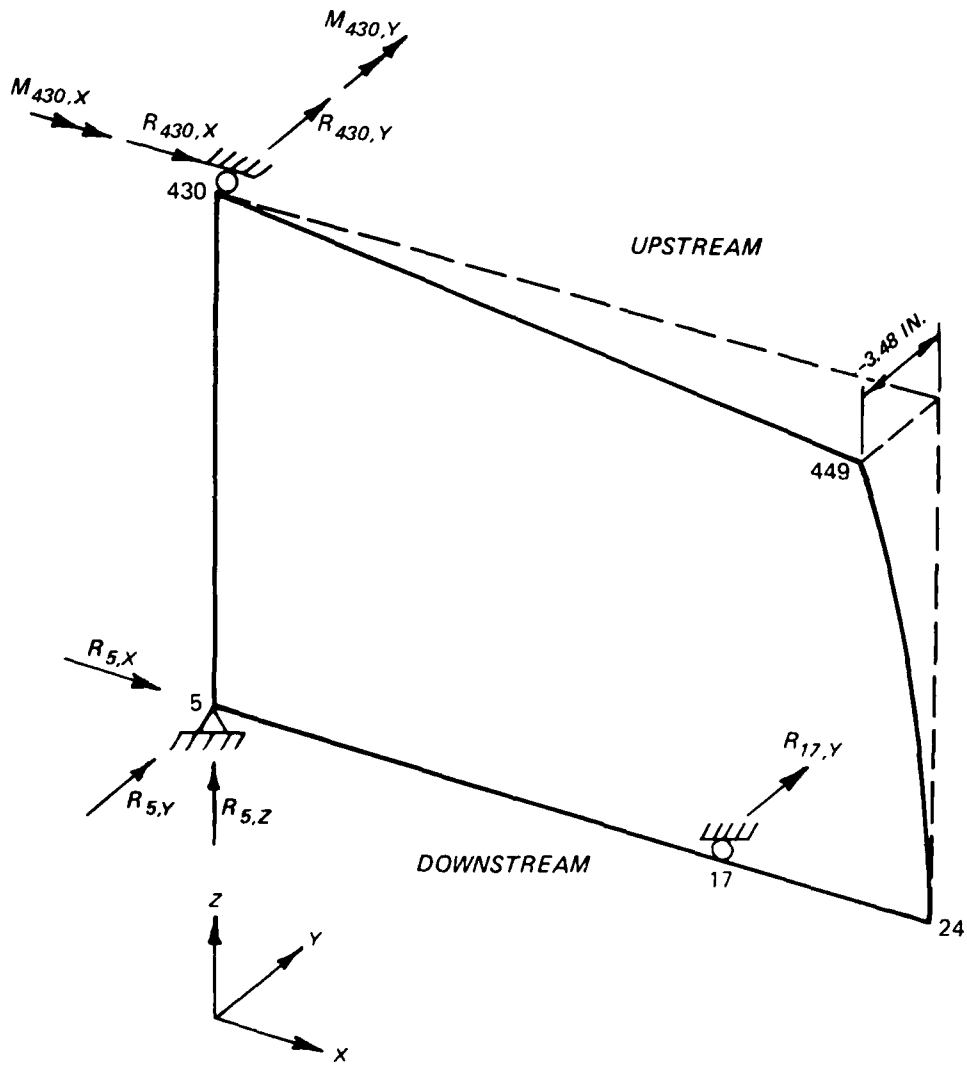

Figure 35. Torque-tube model 1 dead load reactions and out-of-plumb displacements

JOINT	5	430	17
Rx	195.24	-195.24	0
Ry	12.84	-12.84	0
Rz	579.45	0	0
Mx	0	-27.02	0
My	0	-8.54	0

UNITS: KIPS, INCHES

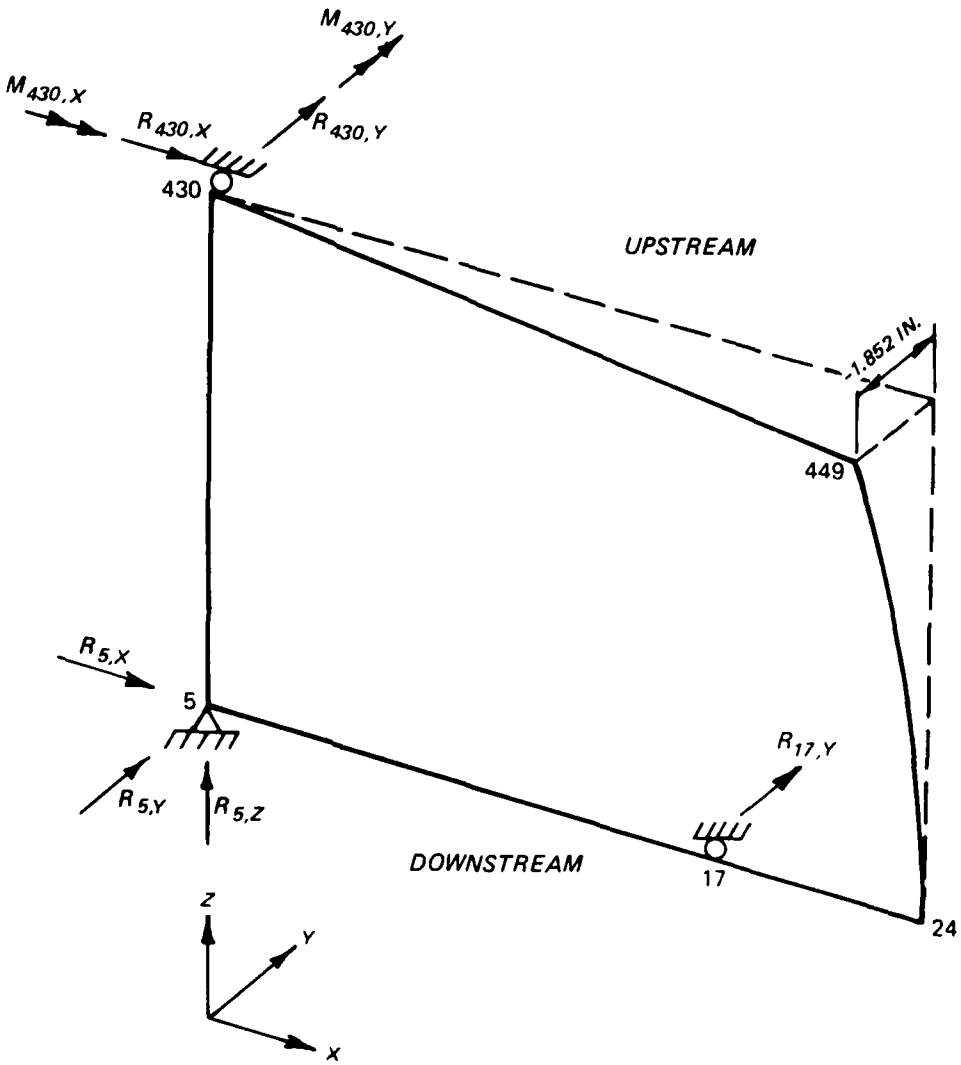

Figure 36. Torque-tube model 1L dead load reactions and out-of-plumb displacements

JOINT	5	430	17
Rx	198.08	-198.08	0
Ry	12.56	-12.56	0
Rz	595.10	0	0
Mx	0	0.38	0
My	0	3.65	0

UNITS: KIPS, INCHES

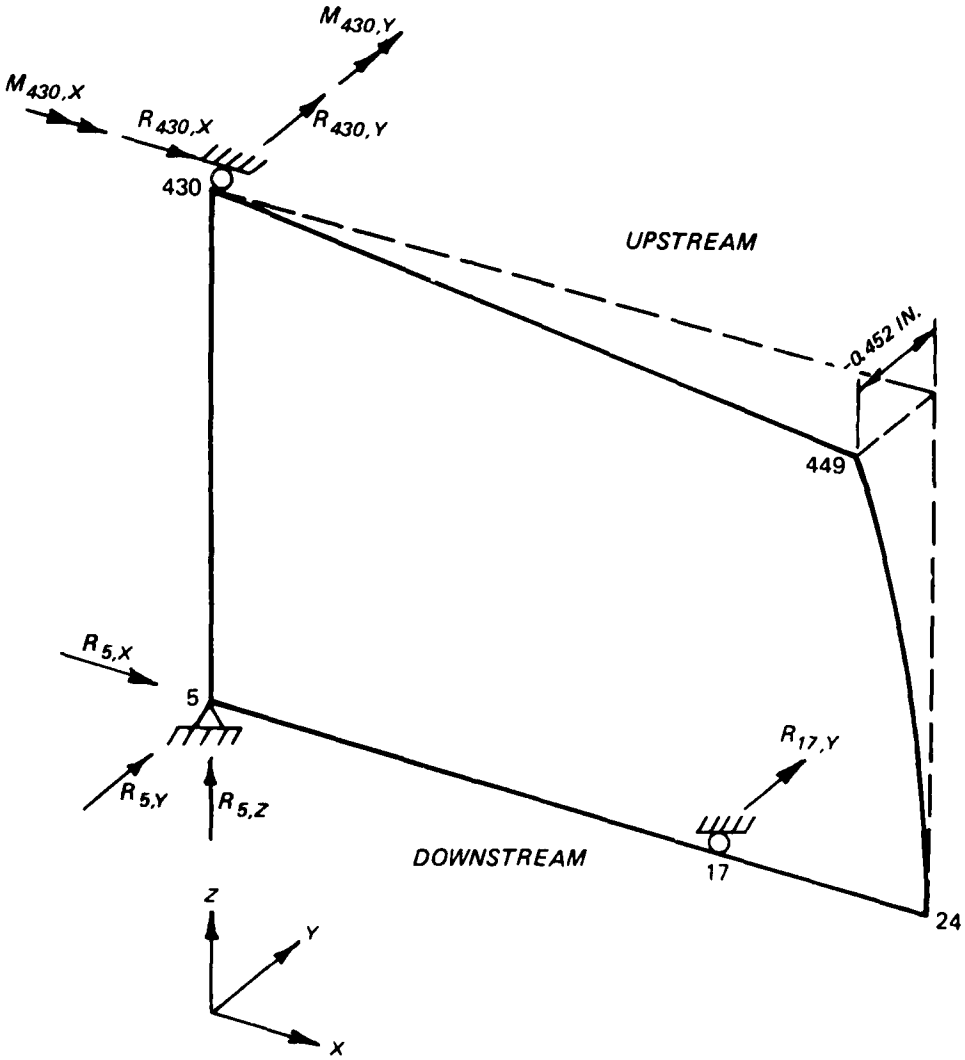

Figure 37. Torque-tube model 2 dead load reactions and out-of-plumb displacements

JOINT	5	430	17
Rx	197.20	-197.20	0
Ry	12.59	-12.59	0
Rz	593.32	0	0
Mx	0	0.36	0
My	0	3.56	0

UNITS: KIPS, INCHES

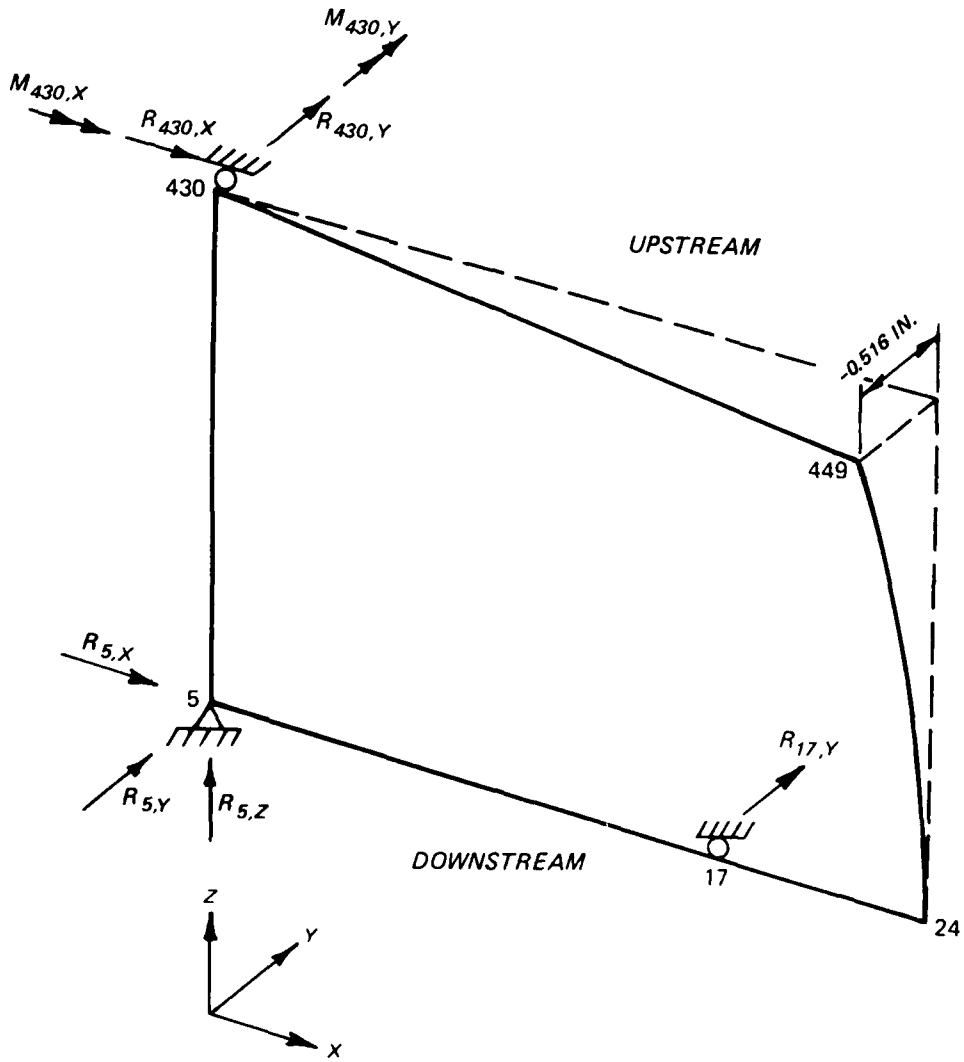

Figure 38. Torque-tube model 3 dead load reactions and out-of-plumb displacements

JOINT	5	430	17
Rx	191.30	-191.30	0
Ry	12.64	-12.64	0
Rz	576.22	0	0
Mx	0	-1.57	0
My	0	2.80	0

UNITS: KIPS, INCHES

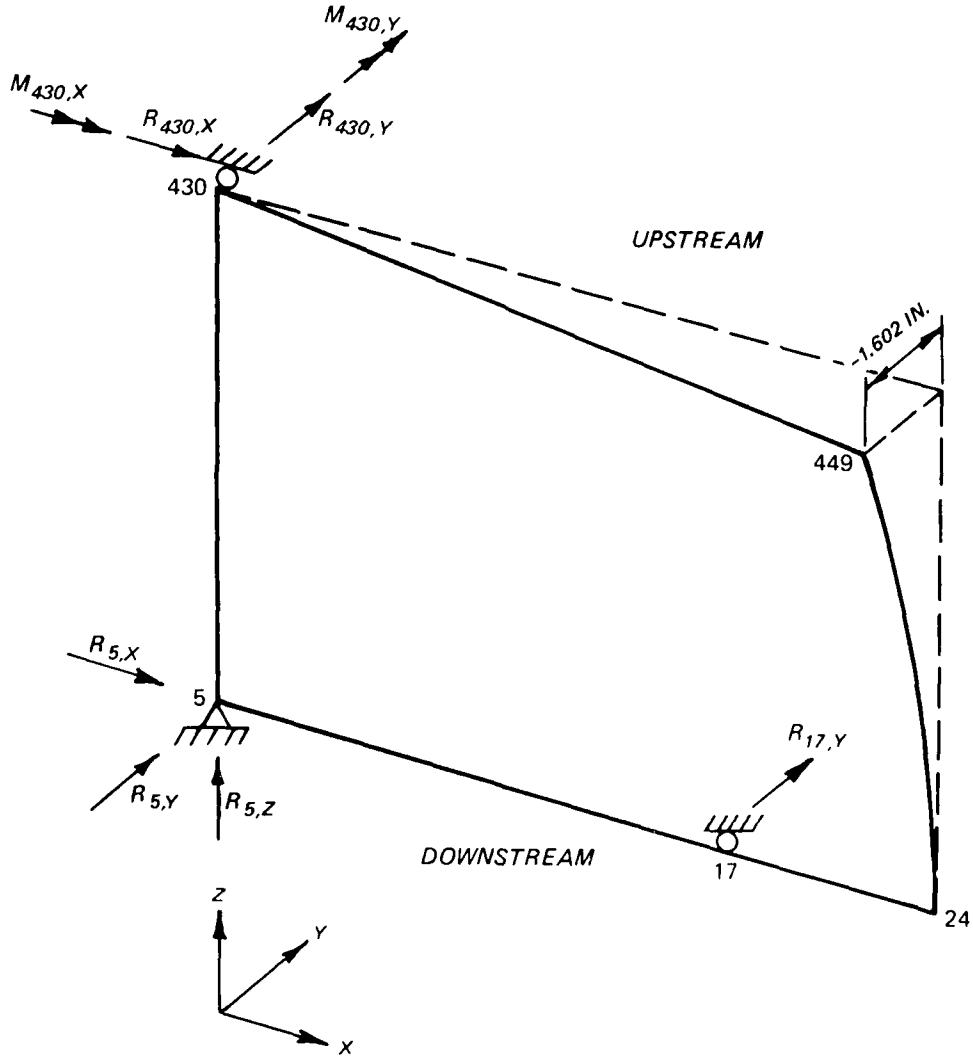

Figure 39. Torque-tube model 3S dead load reactions and out-of-plumb displacements

JOINT	5	430	17
Rx	188.52	-188.52	0
Ry	12.78	-12.78	0
Rz	568.00	0	0
Mx	0	-1.72	0
My	0	2.71	0

UNITS: KIPS, INCHES

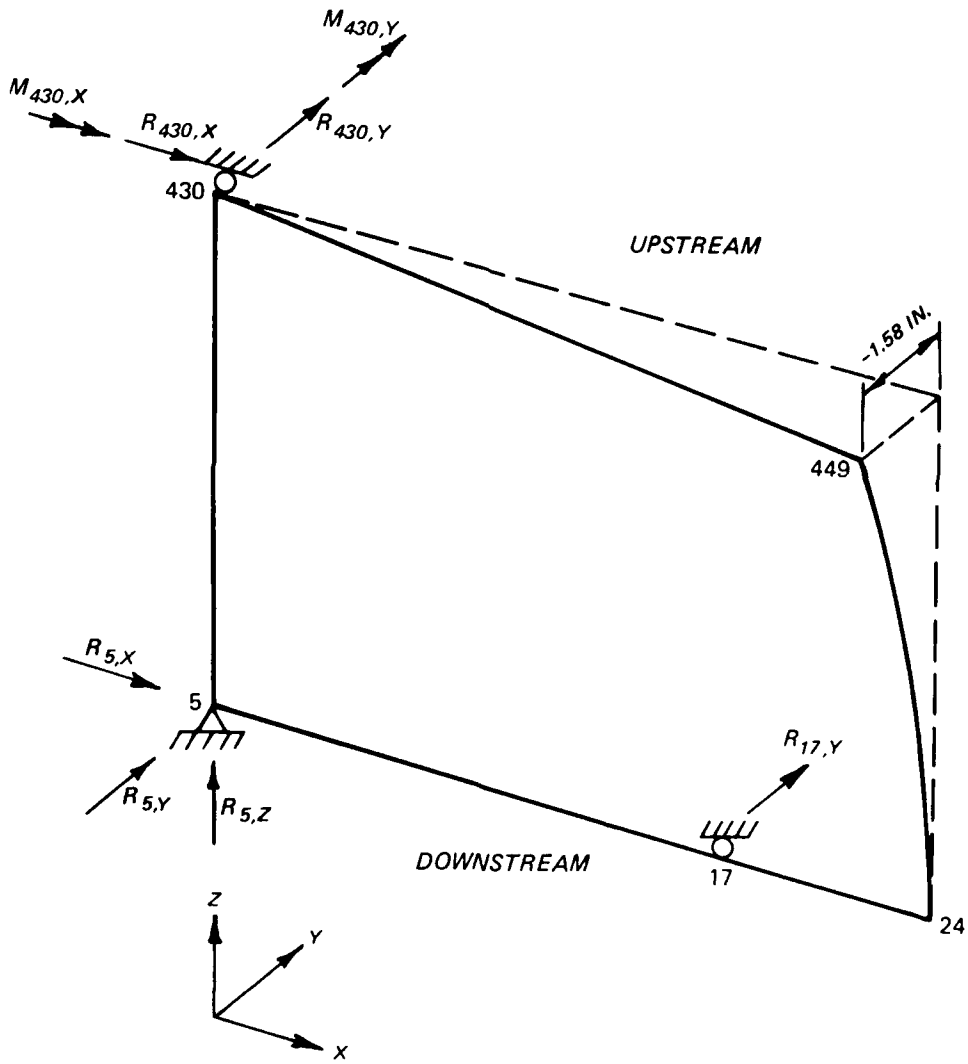

Figure 40. Torque-tube model 3SP dead load reactions and out-of-plumb displacements

MODEL 4			MODEL 4R			
JOINT	5	430	JOINT	5	430	17
Rx	205.90	-205.90	Rx	205.91	-205.91	0
Ry	12.17	-12.17	Ry	12.175	-12.175	0
Rz	619.16	0	Rz	619.16	0	0
Mx	0	-1.79	Mx	0	-1.90	0
My	0	3.01	My	0	2.95	0

UNITS: KIPS, INCHES

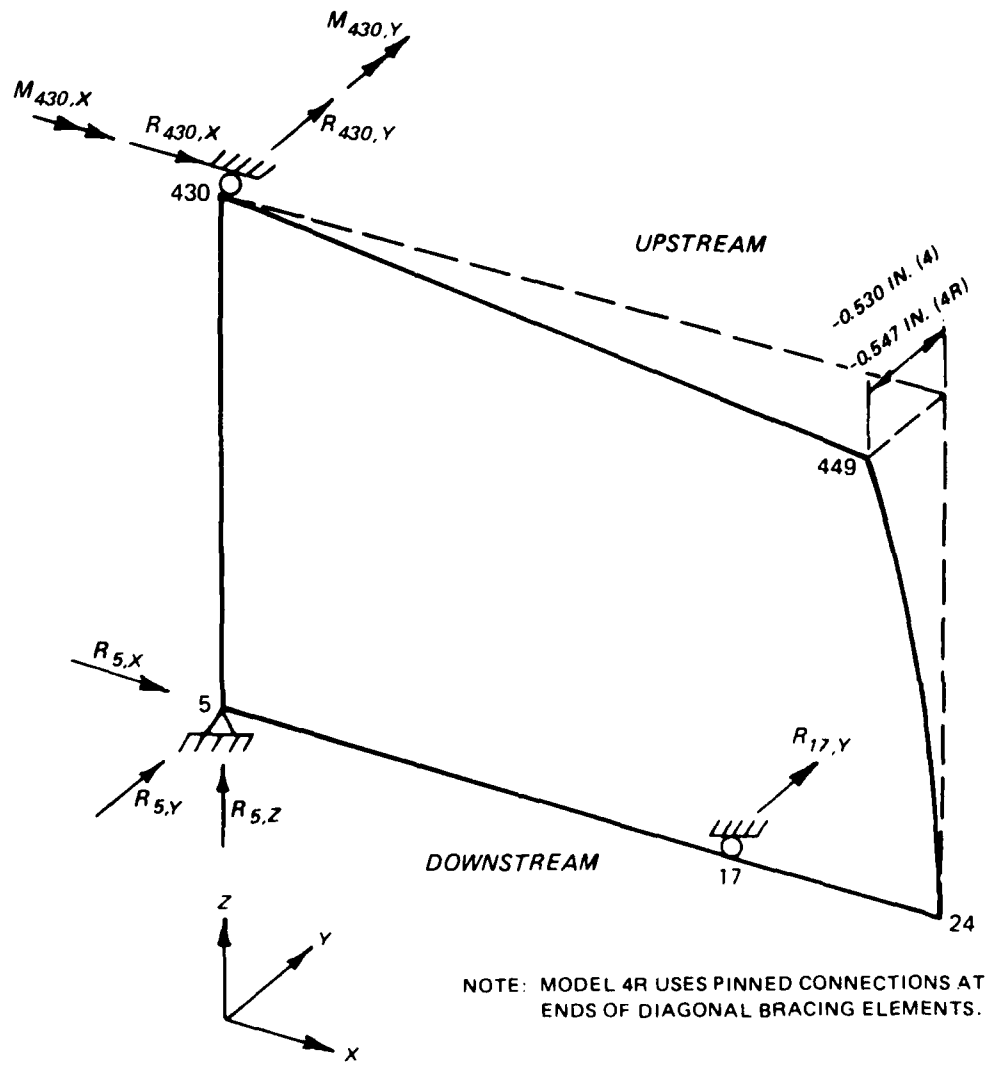

Figure 41. Alternate configuration models 4 and 4R dead load reactions and out-of-plumb displacements (results from loading 1)

MODEL 5			MODEL 5 R			
JOINT	5	430	JOINT	5	430	17
Rx	192.82	-192.82	Rx	192.82	-192.82	0
Ry	12.80	-12.80	Ry	12.80	-12.80	0
Rz	580.25	0	Rz	580.25	0	0
Mx	0	-0.62	Mx	0	-0.67	0
My	0	3.06	My	0	3.04	0

UNITS. KIPS, INCHES

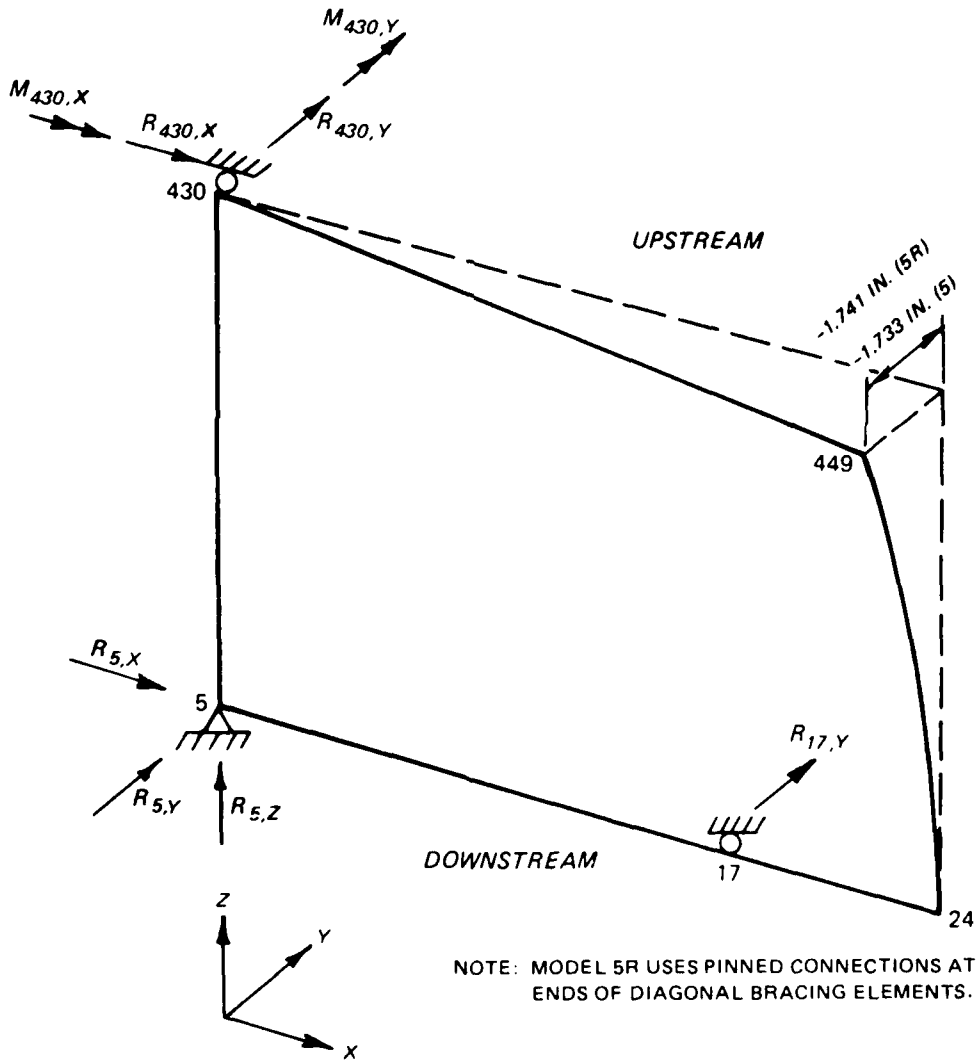

NOTE: MODEL 5R USES PINNED CONNECTIONS AT ENDS OF DIAGONAL BRACING ELEMENTS.

Figure 42. Alternate configuration models 5 and 5R dead load reactions and out-of-plumb displacements (results from loading 1)

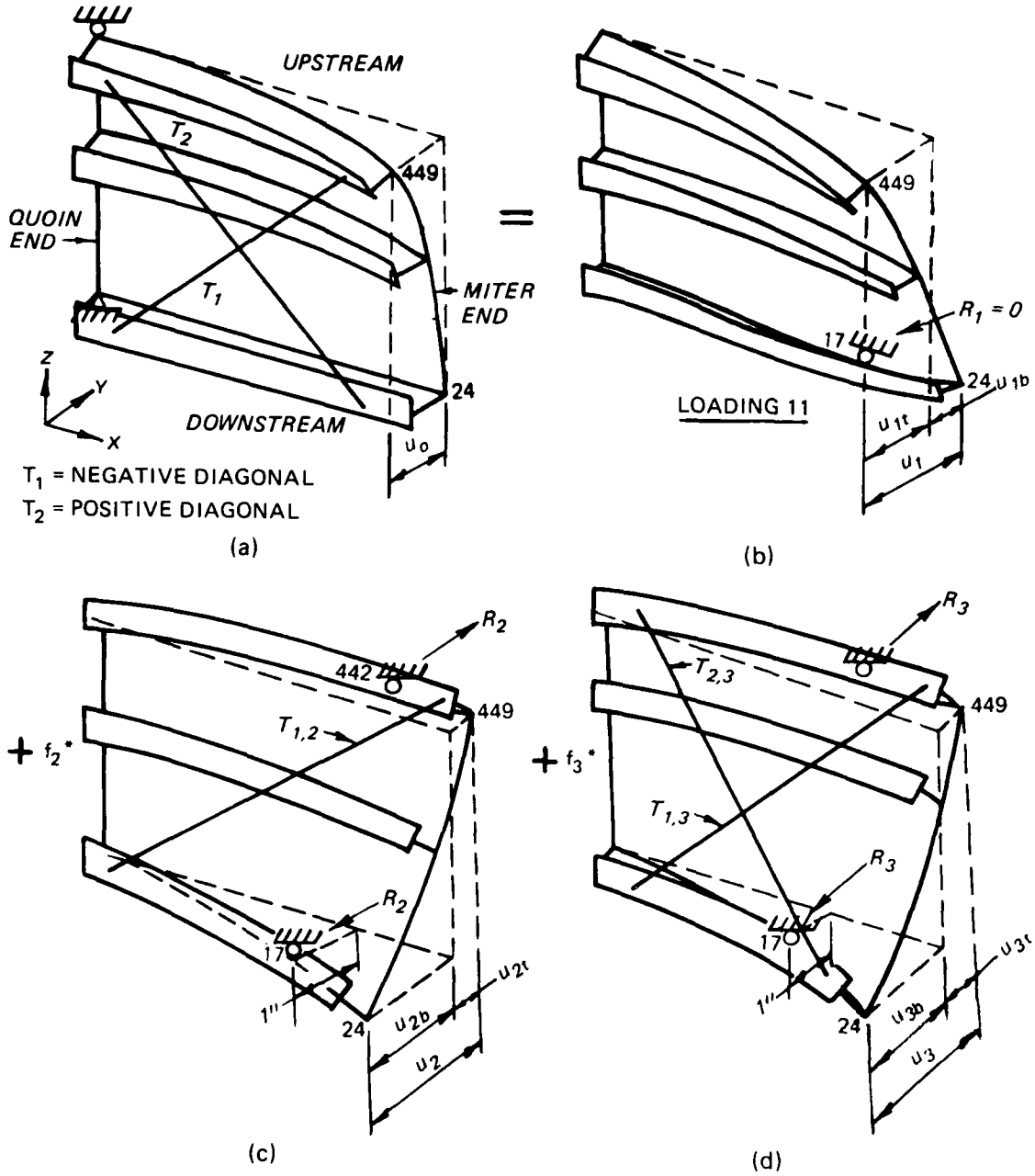

Figure 43. Gate torsional stiffness and diagonal prestressing superposition procedure

Table 9

Comparison of Gate Leaf Weights and Out-of-Plumb Displacement

Figure No.	Model	Dead Weight Weight kips*	Dead Weight Percent Increase**	Out-of-Plumb Displacement in.	Out-of-Plumb Displacement Ratio**
32	Conventional gate	571.864	--	8.907	1.0
33	Conventional gate with enlarged diagonals	589.956	+3.2	9.334	1.049
34	Double-skin plate	630.75	+10.3	0.044	0.005
35	Torque-tube model 1	572.55	+0.12	3.483	0.391
36	Torque-tube model 1L	579.45	+1.3	1.852	0.208
37	Torque-tube model 2	595.10	+4.1	0.452	0.051
38	Torque-tube model 3	593.32	+3.8	0.516	0.058
39	Torque-tube model 3S	576.22	+0.8	1.602	0.180
40	Torque-tube model 3SP	568.52	-0.7	1.580	0.177
41	Alternate configuration model 4	619.16	+8.2	0.530	0.059
41	Alternate configuration model 4R	619.16	+8.2	0.547	0.061
42	Alternate configuration model 5	580.25	+1.4	1.733	0.195
42	Alternate configuration model 5R	580.25	+1.4	1.741	0.195

* Includes weight of inactive diagonals but not of miscellaneous items such as rivets, weld material, etc.

** Relative to conventional gate.

96. Results of the torsional stiffness investigation indicate that when a double-skin plate is provided and diagonals are removed, the gate leaf is about 30 times as stiff as the Bankhead Lock gate without diagonals and about 10 times as stiff as the gate leaf with diagonals in place. Similarly, torque-tube models 1, 1L, 2, 3, 3S, 3SP, and alternate configuration models 4, 4R, 5, and 5R are about 2.4, 4.3, 12.7, 11.4, 4.7, 4.7, 12.3, 12.0, 4.6, and 4.6 times as stiff, respectively, as the conventional gate without diagonals. Models 1, 1L, 3, 3S, 3SP, 4, 4R, 5, and 5R are about 1.3, 1.8, 3.8, 2.0, 1.6, 4.1, 3.9, 2.0, and 1.9 times as stiff, respectively, as the conventional gate with diagonals. The addition of diagonals to models 1, 1L, 3, 3S, 3SP, 4, 4R, 5, and 5R provides increases in stiffness of about 1.8, 1.4, 1.1, 1.4, 1.2, 1.1, 1.1, 1.5, and 1.4 times, respectively, as those models without diagonals. The diagonals almost double the stiffness of model 1 and increase the stiffness of models 1L and 3S by approximately 40 percent, and only increase the stiffness of model 3 by approximately 10 percent. The addition of a positive diagonal to model 3SP increases the stiffness by approximately 20 percent. The diagonals increase the stiffness by 10 percent on models 4 and 4R and

Table 10

Torsional Stiffness Results, Bankhead Gate

Model	R_3 Y-Reaction at Joint 17, kips	Relative Torsional Stiffness
Conventional gate*	-2.875	1.0
Conventional gate with diagonals	-9.725	3.4
Conventional gate with enlarged diagonals	-11.219	3.9
Double-skin plate*	-84.736	29.5
Torque-tube model 1*	-6.927	2.4
Torque-tube model 1L*	-12.332	4.3
Torque-tube model 1 with diagonals	-12.639	4.4
Torque-tube model 1L with diagonals	-17.355	6.0
Torque-tube model 2*	-36.429	12.7
Torque-tube model 3*	-32.677	11.4
Torque-tube model 3S*	-13.55	4.7
Torque-tube model 3SP*	-13.55	4.7
Torque-tube model 3 with diagonals	-36.797	12.8
Torque-tube model 3S with diagonals	-19.210	6.7
Torque-tube model 3SP with positive diagonal only	-15.776	5.5
Alternate configuration, model 4*	-35.287	12.3
Alternate configuration, model 4R*	-34.611	12.0
Alternate configuration, model 4 with diagonals	-40.148	14.0
Alternate configuration, model 4R with diagonals	-38.528	13.4
Alternate configuration, model 5*	-13.253	4.6
Alternate configuration, model 5R*	-13.200	4.6
Alternate configuration, model 5 with diagonals	-19.457	6.8
Alternate configuration, model 5R with diagonals	-19.040	6.6

* No diagonals.

almost 50 percent on models 5 and 5R. There is a negligible change in stiffness of models 3, 3S, and 3SP when access holes are added to girder webs.

97. A conventional gate with enlarged diagonals experiences the 15 percent increase (from 3.4 to 3.9) in torsional stiffness compared with the conventional model with diagonals. Model 1L without diagonals is stiffened in torsion by 79 percent (from 2.4 to 4.3) compared with model 1 without diagonals, but only by 36 percent (from 4.4 to 6) when both models 1L and 1 contain diagonals; model 3S without diagonals decreases in stiffness by 59 percent (from 11.4 to 4.7) compared with model 3 without diagonals, and by 48 percent when both models 3S and 3 contain diagonals. Model 3SP without diagonals is the same stiffness as model 3S. Model 3SP with positive diagonal decreases in stiffness by 18 percent when compared to model 3S with diagonals. Models 4 and 4R with and without diagonals are approximately the same stiffness as model 3 with and without diagonals. The same is also true when comparing models 5 and 5R to model 1L.

Prestressing Behavior

98. One of the objectives of this study was to determine the behavior of the models during the prestressing of the gate diagonals. The models to be prestressed were models 1, 1L, 3, 3S, and 3SP. A conventional gate, with and without enlarged diagonals, was also investigated. The results of the dead load analysis and torsional stiffness study showed that model 3 is within 15 percent of both the dead load deflection and torsional stiffness of model 2. Therefore, model 2 will not be investigated any further. Also, gate performance improvements comparable to those of the torque-tube models could be achieved with alternate configuration models such as models 4, 4R, 5, and 5R, but the associated weight increase and fabrication problems made these models unacceptable. After investigating models 4, 4R, 5, and 5R and evaluating minimal increase in torsional stiffness as compared with the torque-tube models, the task group members recommended that these models not be considered for further study.

99. A prestressing superposition procedure was used and is illustrated in Figure 43 and presented in Report 4, "Alternate Configuration Miter Gate Finite Element Studies - Closed Sections." This procedure (summarized here) insures plumbness of the gate after the jacking and tensioning of the gate

diagonals are completed. It was initially used on the conventional gate model and was intended to make the diagonal braces on the model experience the actual field measured diagonal forces on the Bankhead Lock gates. The superposition procedure was established to make the negative diagonal force, T_1 in Figure 43, and the positive diagonal force, T_2 in Figure 43, equal their field measured values as follows:

$$\text{Diagonal force} = \text{area} \times (\text{average field measured stress})$$

$$\text{Negative diagonal force} = T_1 = 25.0 \text{ in.}^2 \times 11.12 \text{ ksi } T_1 = 278.0^k$$

$$\text{Positive diagonal force} = T_2 = 30.0 \text{ in.}^2 \times 19.97 \text{ ksi } T_2 = 599.18^k$$

100. The superposition procedure was conducted by considering the gate in its final position with prestressing diagonals in place, hanging freely under its dead load, and held only by the pintle and gudgeon pin supports as seen in Figure 43a. In this position, it is desired that the negative diagonal force T_1 equal 278.0^k and that the positive diagonal force T_2 equal 599.18^k, and that the resultant Y-direction reaction at joints 422 and 17, the temporary tieback and jacking points, equal 0.

101. In order to accomplish this state of diagonal forces, a superposition of three cases is performed as shown in Figure 43. The first superposition case (Figure 43b) consists of the gate hanging freely under its full dead load, but with no prestressing diagonals in place. A lateral support is provided in the Y-direction at joint 17 on the structure to prevent rigid body rotation. The Y-direction reaction at joint 17 is R_1, whose value is 0.0.

102. The second superposition case (Figure 43c) consists of the gate supported as in the second case (i.e., with a tieback support added at the top of the gate near the miter end at joint 442) and, in addition, the negative prestressing diagonal (T_1) is added prior to jacking. In this case, an unknown jacking force (R_2) is applied at joint 17 in the Y-direction downstream and is set equal to f_2R_2 where

R_2 = the virtual jacking force required to cause a unit displacement at joint 17 in the Y-direction with only the negative prestressing diagonal in place

f_2 = a superposition factor by which R_2 is multiplied in order to compute the actual jacking force

103. The virtual jacking force R_2 was computed as the Y-direction reaction at joint 17, due to a unit Y-direction support displacement at joint 17 and with only the negative prestressing diagonal in place.

104. The third, and last, superposition case (Figure 43d) consists of the gate supported in the identical way as the second case with the negative prestressing diagonal (T_1) in place and with the positive prestressing diagonal (T_2) put into place. This third superposition case is intended to model the effect of releasing the jacking force after the positive diagonal is attached.

105. The effect of releasing the jacking force applied in the second superposition case is modeled as a reaction force applied in the Y-direction (downstream), and set equal to f_3R_3 where

R_3 = the virtual jacking force required to cause a unit displacement at joint 17 in the Y-direction with both the negative and positive prestressing diagonals in place

f_3 = a superposition factor by which R_3 is multiplied in order to compute a force which is opposite in value to the actual joint 17 reaction force applied in the first and second superposition cases. This is required since the final Y-directional reaction at joint 17 must be equal to 0.0 as is the case in the real structure

106. The virtual force R_3 was computed as the Y-directional reaction at joint 17, due to a unit Y-directional support displacement at joint 17, and with both the negative and positive diagonals in place.

107. Referring again to Figure 43, the first, second, and third superposition cases must add up to the case of the actual gate in its final dead load state with both prestressing diagonals in place and at their field measured force values, with no reaction component at joints 17 and 442. The detailed computation of the proper superposition factors f_2 and f_3 required to accomplish this is presented in Report 4, the initial study of closed sections. Once the superposition factors were computed, loading combinations 11 (full dead load of gate), 12 (full dead load plus jacking force), and 13 (dead load plus final prestressing forces) were computed for all models. The required jacking and negative diagonal forces resulting from loading 12 are summarized in Table 11.

108. As expected, the jacking force is increased for model 1L compared with model 1 and decreased for models 3S and 3SP compared with model 3, as listed in Table 11, because of the corresponding changes in torsional stiffness in the torque-tube models (Table 10). Although the jacking force for model 3 is a factor of 2.03 times that of model 1, the resulting tensile force

Table 11

Summary of Jacking and Diagonal Force Results for Loadings 12 and 13

Model	Loading 12, kips		Loading 13, kips	
	Jacking	Negative Diagonal*	Negative Diagonal*	Positive Diagonal*
Conventional gate model	207.85	1,054.18	286.40	490.48
Conventional gate with enlarged diagonal	257.13	1,429.29	381.0	595.37
Model 1	185.88	592.36	103.06**	313.64**
Model 1L	224.53	466.93	51.51	270.57
Model 3	378.26	314.2	14.03**	193.77**
Model 3S	216.69	429.53	49.28	243.82
Model 3SP	139.50	0.0†	0.0	190.60

* Tension force.
** Taken from Report 2 of the miter gate study (Emkin, Goodno, and Will 1983b).
† Negative diagonal is deactivated.

in the negative diagonal for model 3 is almost one half that of model 1. Models 1L and 3S, however, have jacking and negative diagonal forces which differ by less than 10 percent. At the same time, doubling the size of the diagonals in the conventional gate model leads to a 24 percent increase in jacking force and a 36 percent increase in the negative diagonal force compared with the conventional gate model.

109. Review of loading 13 in Table 11 indicates a nearly consistent difference of about 200 kips between the negative and positive diagonal forces. Miter Gate Case Committee Chairman Joseph Hartman hypothesized that this difference in force may allow the negative diagonal force to be reduced to zero, and thereby reduce the jacking force required to plumb the gate. Furthermore, a negative diagonal with no force could lead to the possible elimination of the diagonal altogether. To evaluate the hypothesis, additional model studies were performed on torque-tube model 3S.

110. The new model, previously referred to as 3SP, was created by deactivating the negative diagonal on model 3S. The weights of the negative

diagonal and gusset plates were included in analysis. Except for deactivating of negative diagonal, model 3SP is the same as shown in Figure 29.

111. The dead load displacement, torsional stiffness, and prestressing behavior of model 3SP were studied by using the same procedures previously discussed. Results of the study are shown in Figure 40 and Tables 9, 10, and 11.

112. Results for loading 13 (dead load plus the final prestressing forces) on the models are presented in Figures 44 through 50. The forces in the positive and negative diagonals are also shown in these figures, but values for all models are summarized in Table 11. The final diagonal forces are increased 20 to 30 percent for a conventional gate model with double diagonals compared with the conventional gate model, but models 1L and 3S have diagonal forces which differ by less than 11 percent. However, a comparison of forces for models 1 and 1L and for models 3 and 3S, respectively, reveals considerable change in the final diagonal forces. Removal of the negative diagonal from model 3S resulted in a 36 percent reduction in the jacking force and a 22 percent reduction in the positive diagonal force. A comparison of forces for model 3SP and the conventional gate model reveals a 33 percent reduction in jacking force and a 61 percent reduction in positive diagonal force.

Hydrostatic and Temporal Loading Behavior

113. An investigation was performed to clarify the behavior of several of the models due to a hydrostatic high pool/low pool plus impact loading condition on a mitered gate configuration. A temporal hydrostatic head pressure loading, to simulate the resistance of the water on closing the gate, was also examined. Detailed descriptions of these loading conditions may be found in Report 4 of the miter gate studies which deals with closed sections. The models to be analyzed with these loadings were models 1, 1L, 3, 3S, and 3SP with diagonals and models 1L, 3, and 3S without diagonals. Model 3H with access holes and diagonals was also analyzed for hydrostatic high pool/low pool plus impact to determine if the access holes altered the behavior when compared with model 3 without access holes with diagonals. In addition to these models, the conventional gate with diagonals was analyzed.

114. The resulting reactions at the pintle and gugeon pin, as well as selected reactions along the miter and quoin ends due to hydrostatic high pool

JOINT	5	430
Rx	198.10	-198.10
Ry	13.51	-13.53
Rz	594.74	0
Mx	0	-75.25
My	0	-72.50

UNITS: (KIPS, INCH-KIPS)

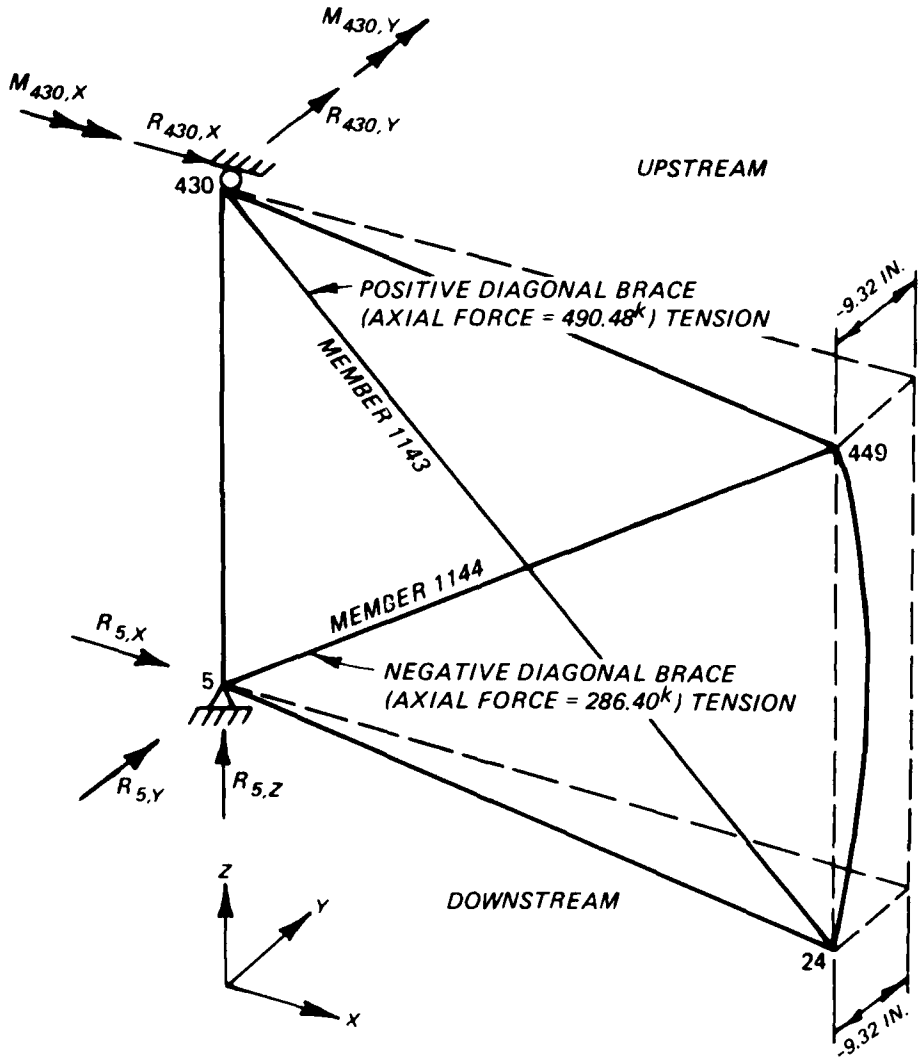

Figure 44. Reactions and joint displacements due to prestressing and dead load for conventional gate model

JOINT	5	430
R	204.33	-204.33
Ry	13.23	-13.24
Rz	613.55	0
Mx	0	-92.89
My	0	-89.22

UNITS: (KIPS, INCH-KIPS)

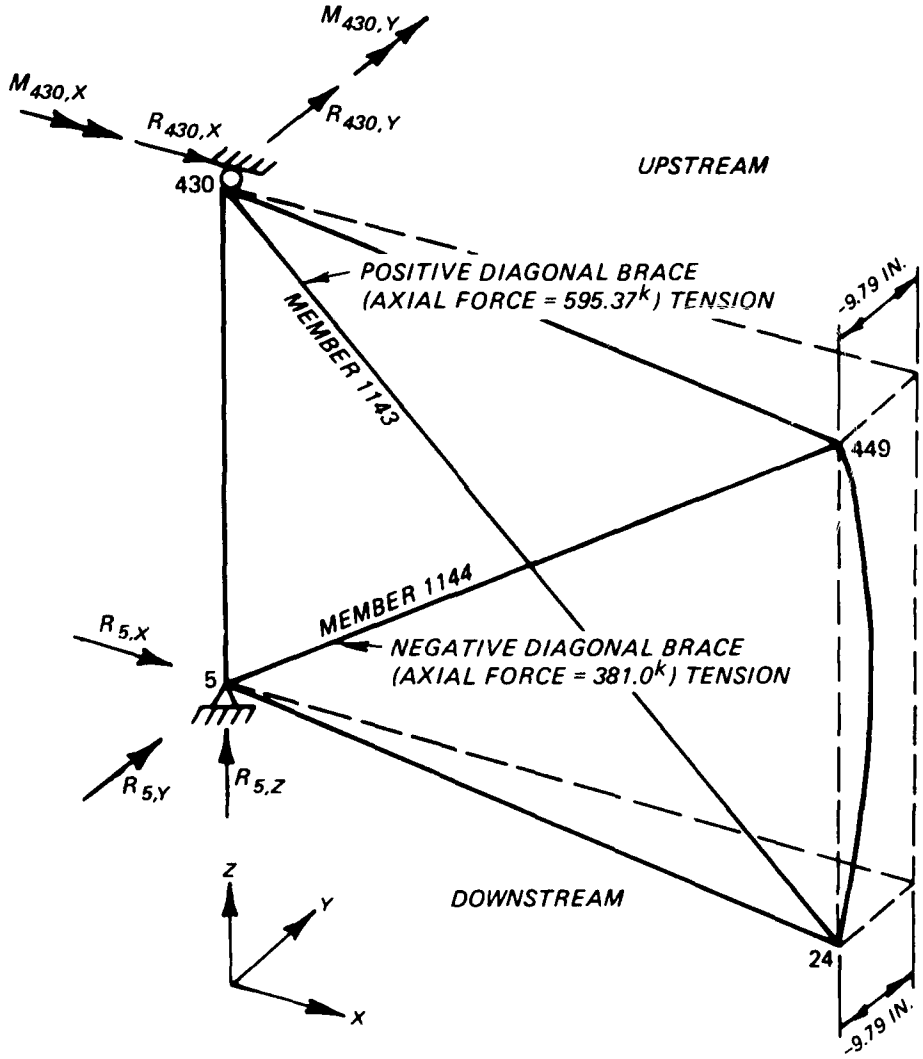

Figure 45. Reactions and joint displacements due to prestressing and dead load for conventional gate model with enlarged diagonals

JOINT	5	430
Rx	198.40	-198.40
Ry	13.46	-13.46
Rz	595.45	0
Mx	0	-24.00
My	0	-48.28

UNITS: (KIPS, INCH-KIPS)

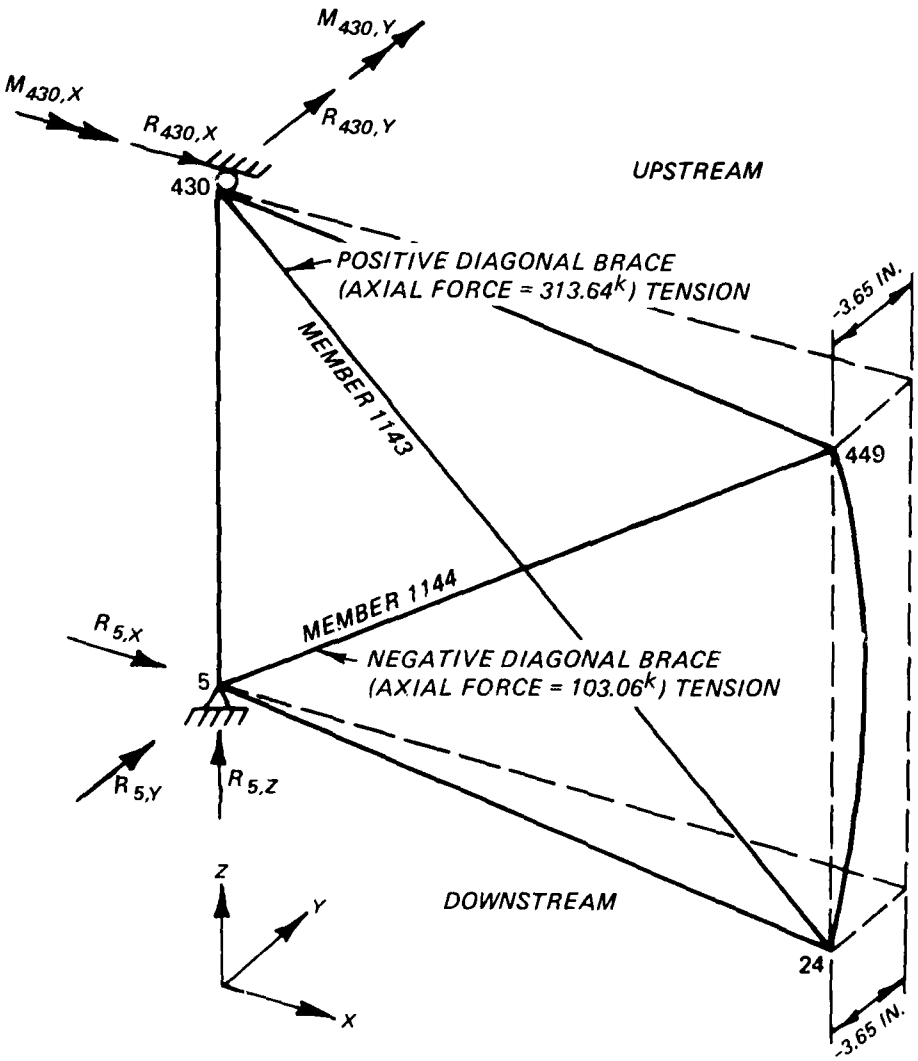

Figure 46. Reactions and joint displacements due to prestressing and dead load for model 1

JOINT	5	430
Rx	200.73	-200.73
Ry	13.33	-13.33
Rz	602.63	0
Mx	0	-13.26
My	0	-40.89

UNITS: (KIPS, INCH-KIPS)

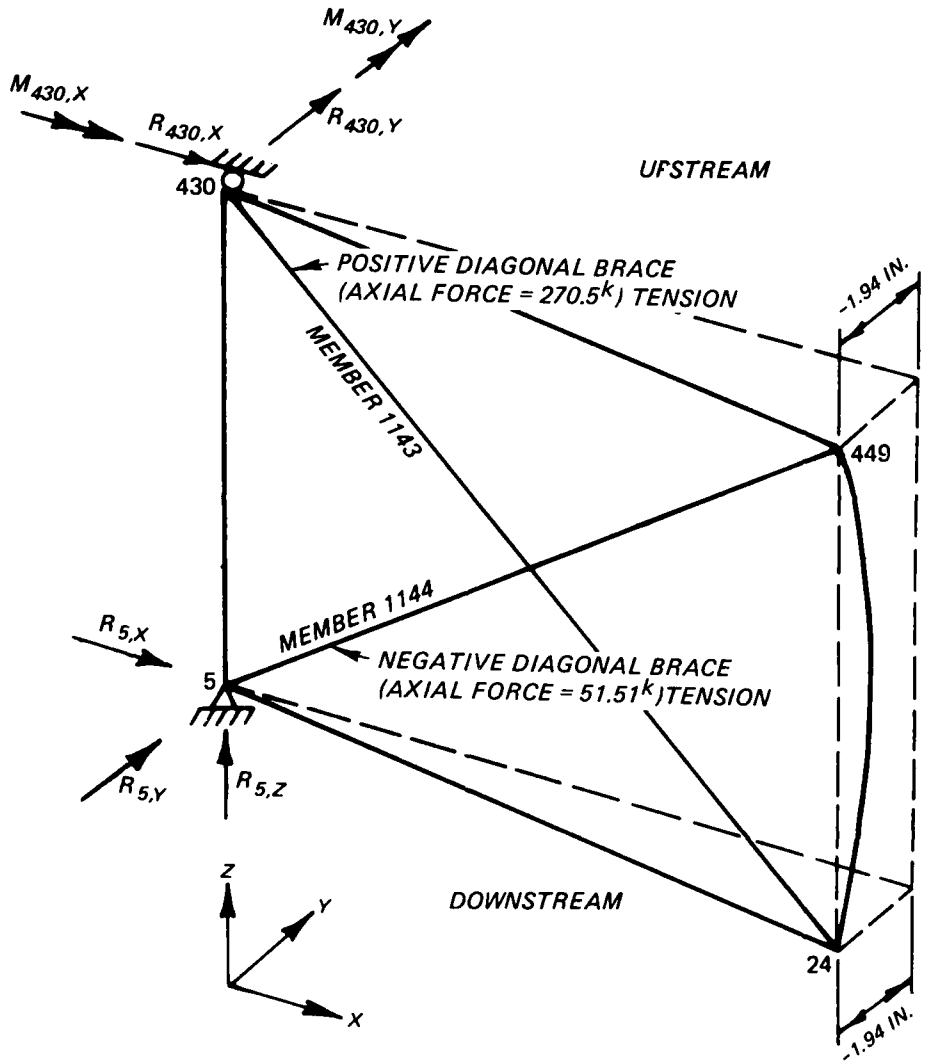

Figure 47. Reactions and joint displacements due to prestressing and dead load for model 1L

JOINT	5	430
Rx	205.12	-205.12
Ry	13.09	-13.09
Rz	617.05	0
Mx	0	0.88
My	0	-25.0

UNITS: (KIPS, INCH-KIPS)

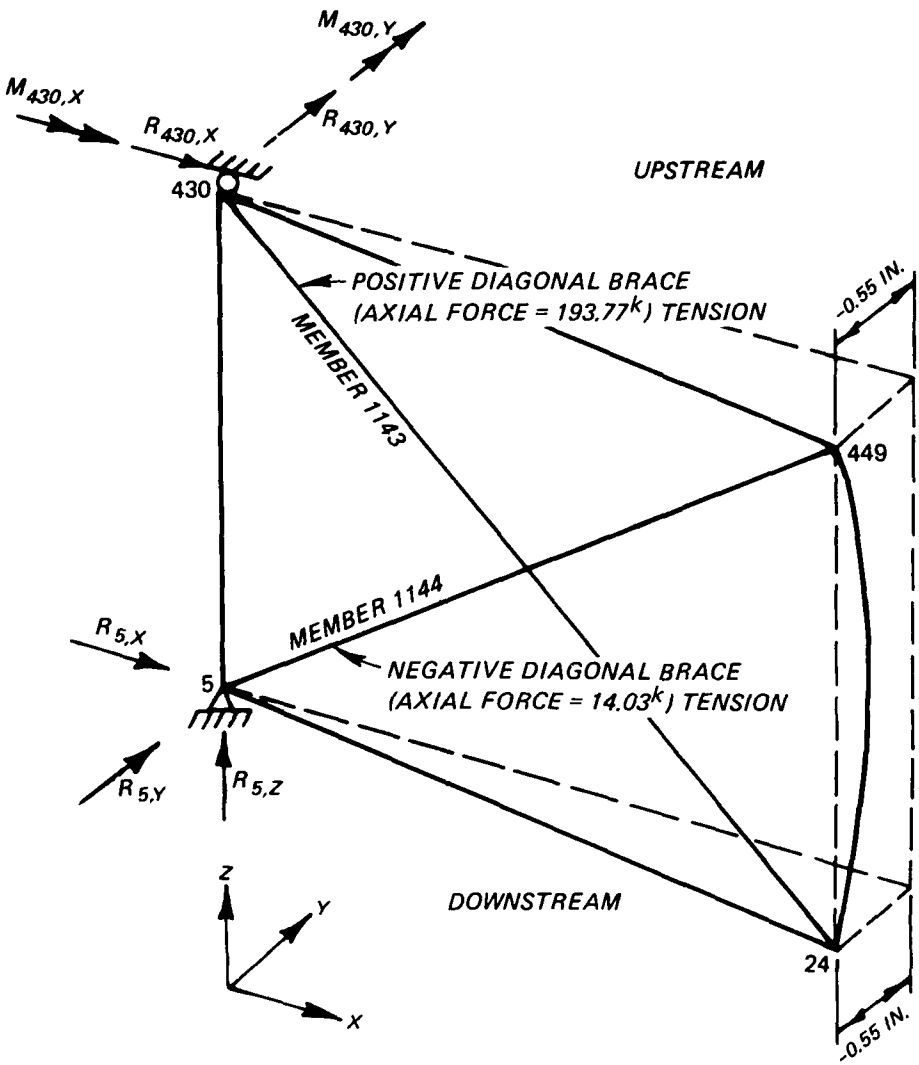

Figure 48. Reactions and joint displacements due to prestressing and dead load for model 3

JOINT	5	430
Rx	199.22	-199.22
Ry	13.15	-13.15
Rz	599.27	0
Mx	0	-2.94
My	0	-32.02

UNITS: (KIPS, INCH-KIPS)

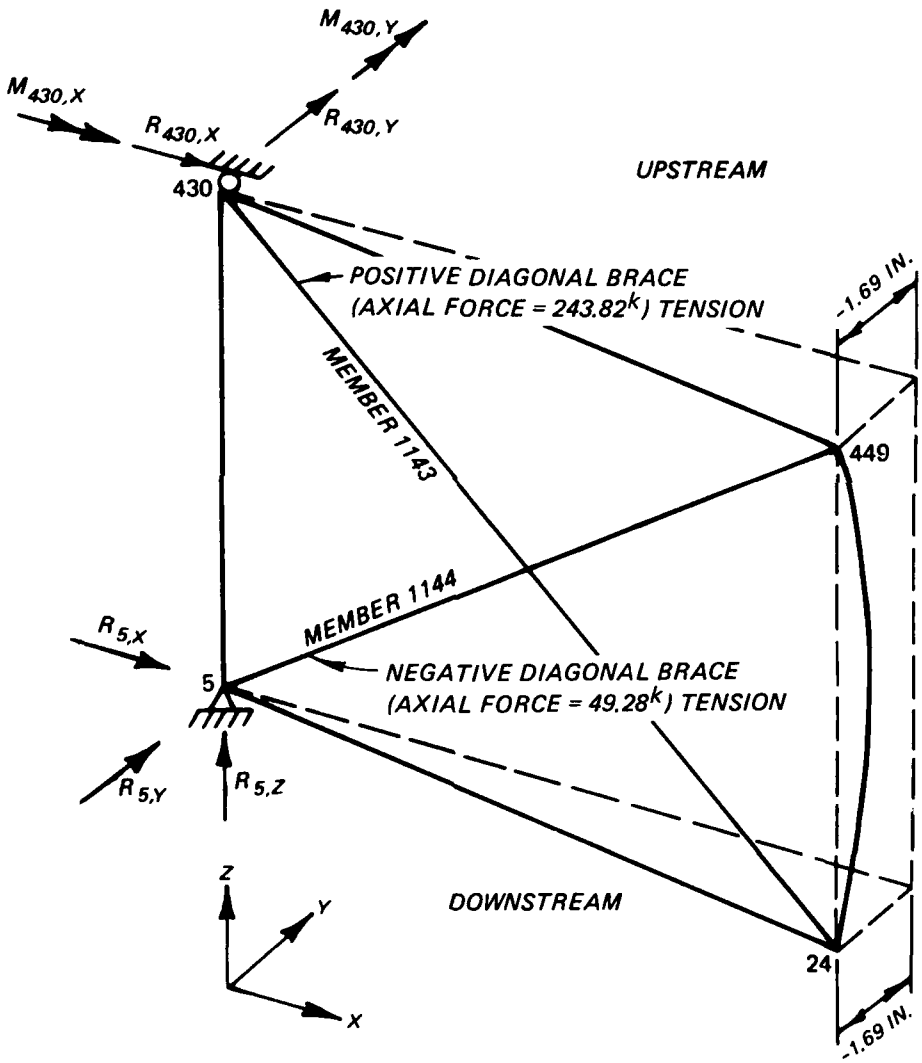

Figure 49. Reactions and joint displacements due to prestressing and dead load for model 3S

JOINT	5	357
Rx	196.31	-196.31
Ry	13.28	-13.28
Rz	590.72	0
Mx	0	-0.75
My	0	-23.89

UNITS: (KIPS, INCH-KIPS)

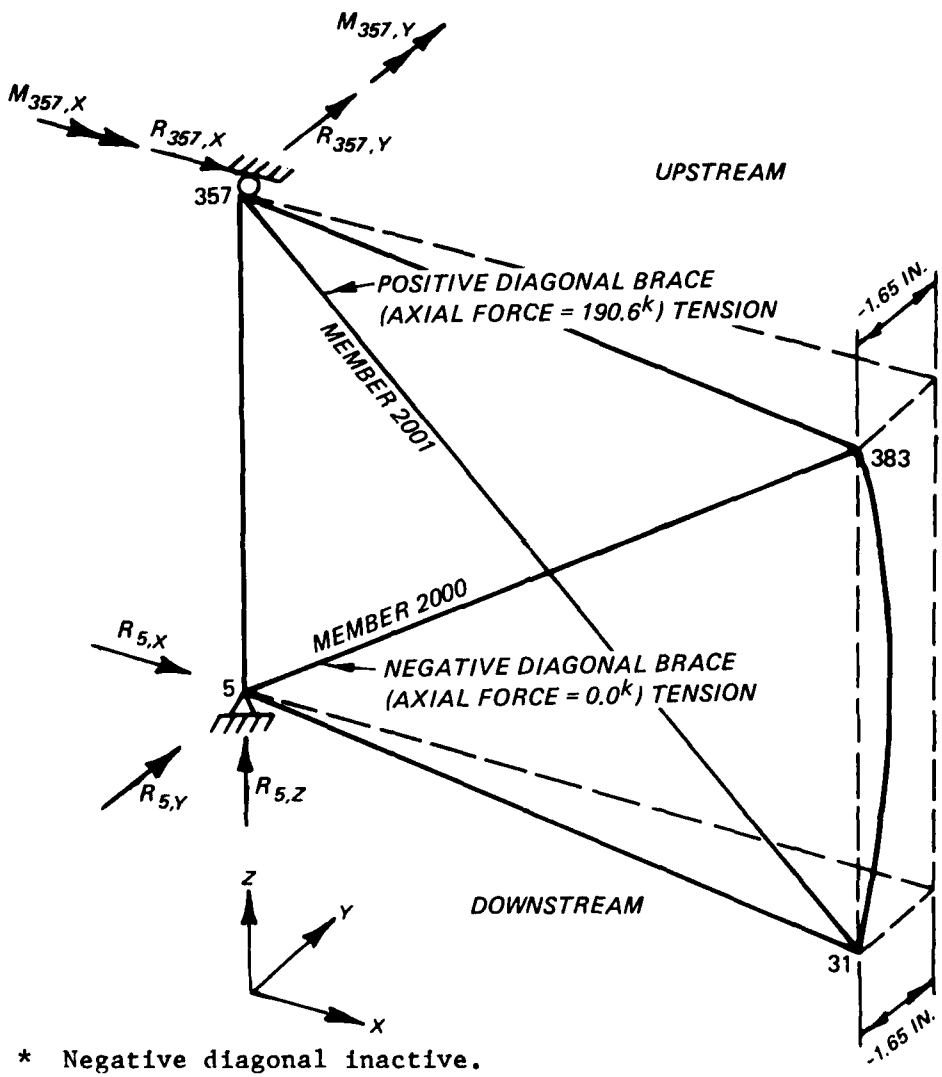

* Negative diagonal inactive.

Figure 50. Reactions and joint displacements due to prestressing and dead load for model 3SP (negative diagonal inactive)*

loading upstream and low pool loading downstream, are shown in Figures 51 through 59 for models 1, 1L, 3, and 3S with diagonals; models 1L, 3, and 3S without diagonals; and model 3H with diagonals, respectively. Reactions for model 3SP are similar to model 3S. In addition to these models, the same results for a conventional gate model are presented in Figure 59 for comparison. For all cases the reactions are close, indicating that the torque tubes have not significantly altered the distribution of the hydrostatic forces. The major differences in the gudgeon and pintle reactions are for the vertical component R_z . The conventional gate has 0.0 for the R_z reaction while model 1 has -36.12 kips, model 1L has -108.35 kips, all model 3 cases have -111.36 kips, and model 3S cases have -55.68 kips. These reactions are due to the buoyancy effects on the bottom torque tube of models 1 and 1L and the side torque tubes of models 3, 3H, 3S, and 3SP.

115. The reactions and miter end displacements due to the temporal hydrostatic loading are presented in Figures 60 through 67 for models 1, 1L, 3, 3S, and 3SP with diagonals and models 1L, 3, and 3S without diagonals, respectively. For comparison purposes, the reactions and miter end displacements for the conventional gate and conventional gate with enlarged diagonals are presented in Figures 68 and 69, respectively. Of particular interest are the values of twist of the gate to temporal loading. Measuring the twist as the difference in Y-displacements between joints 24 and 449 shown in Figures 60 through 69, the twist for the various models is shown below:

Model 1 with diagonals	3.43 in.
Model 1L with diagonals	2.38 in.
Model 3 with diagonals	1.03 in.
Model 3S with diagonals	2.00 in.
Model 1L without diagonals	3.36 in.
Model 3 without diagonals	1.16 in.
Model 3S without diagonals	2.85 in.
Model 3SP with positive diagonal	2.43 in.
Conventional gate with diagonals	4.67 in.
Conventional gate with enlarged diagonals	4.05 in.

116. The twist values listed above indicate that model 3 with and without diagonals has the highest level of stiffness under temporal loading while conventional gate with enlarged diagonals and model 1 are approximately three times as flexible as model 3. Model 1L with diagonals experiences only 70 percent of the twist displacement under temporal loading as model 1 with

JOINT	5	430
Rx	1192.70	209.95
Ry	411.15	56.41
Rz	36.12*	0
Mx	0	97.16
My	0	33.85

UNITS: (KIPS, INCH-KIPS)

* UPLIFT DUE TO BUOYANCY OF BOTTOM TORQUE TUBE

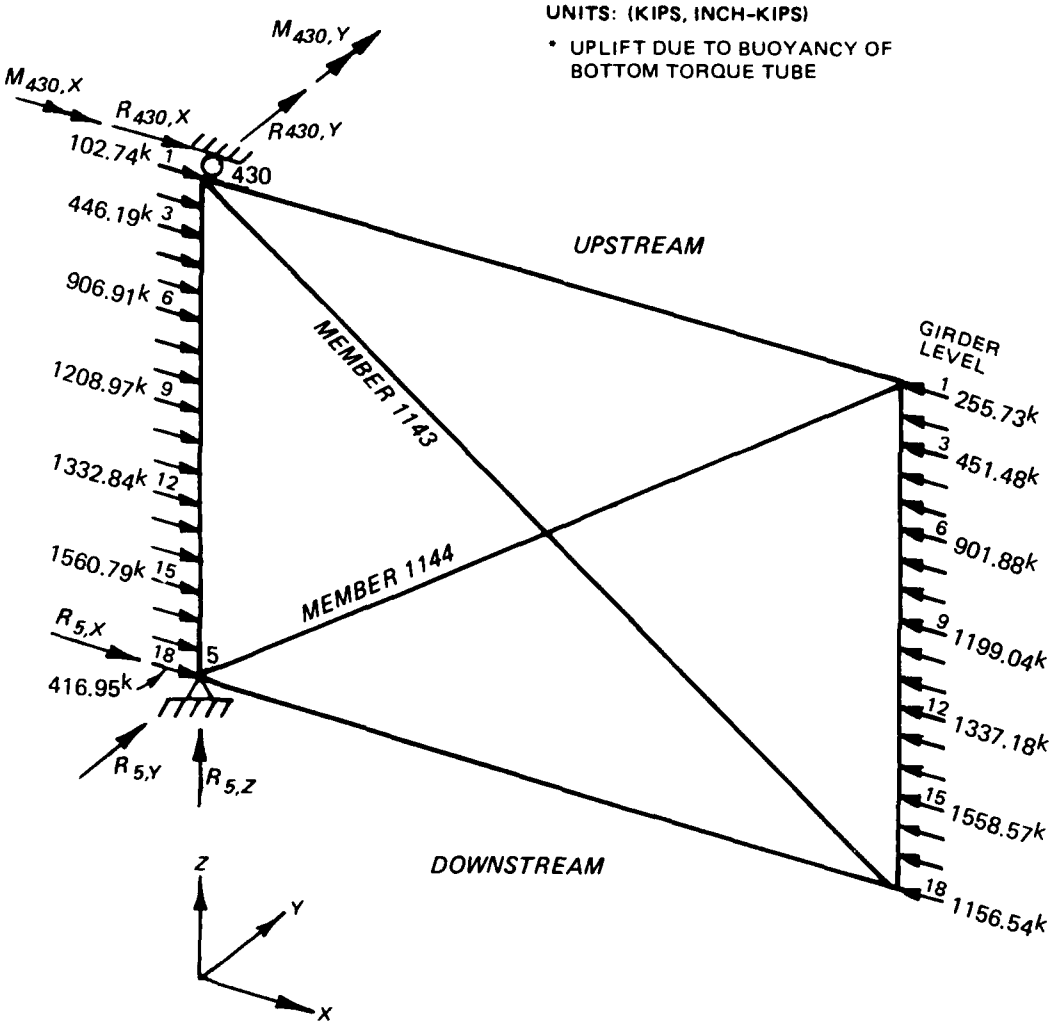

Figure 51. Reactions due to hydrostatic loading (high pool/ low pool) for model 1 with diagonals

JOINT	5	430
Rx	1154.71	206.40
Ry	405.17	48.53
Rz	-108.35*	0
Mx	0	98.73
My	0	34.18

UNITS: (KIPS, INCH-KIPS)

* UPLIFT DUE TO BUOYANCY OF BOTTOM TORQUE TUBE

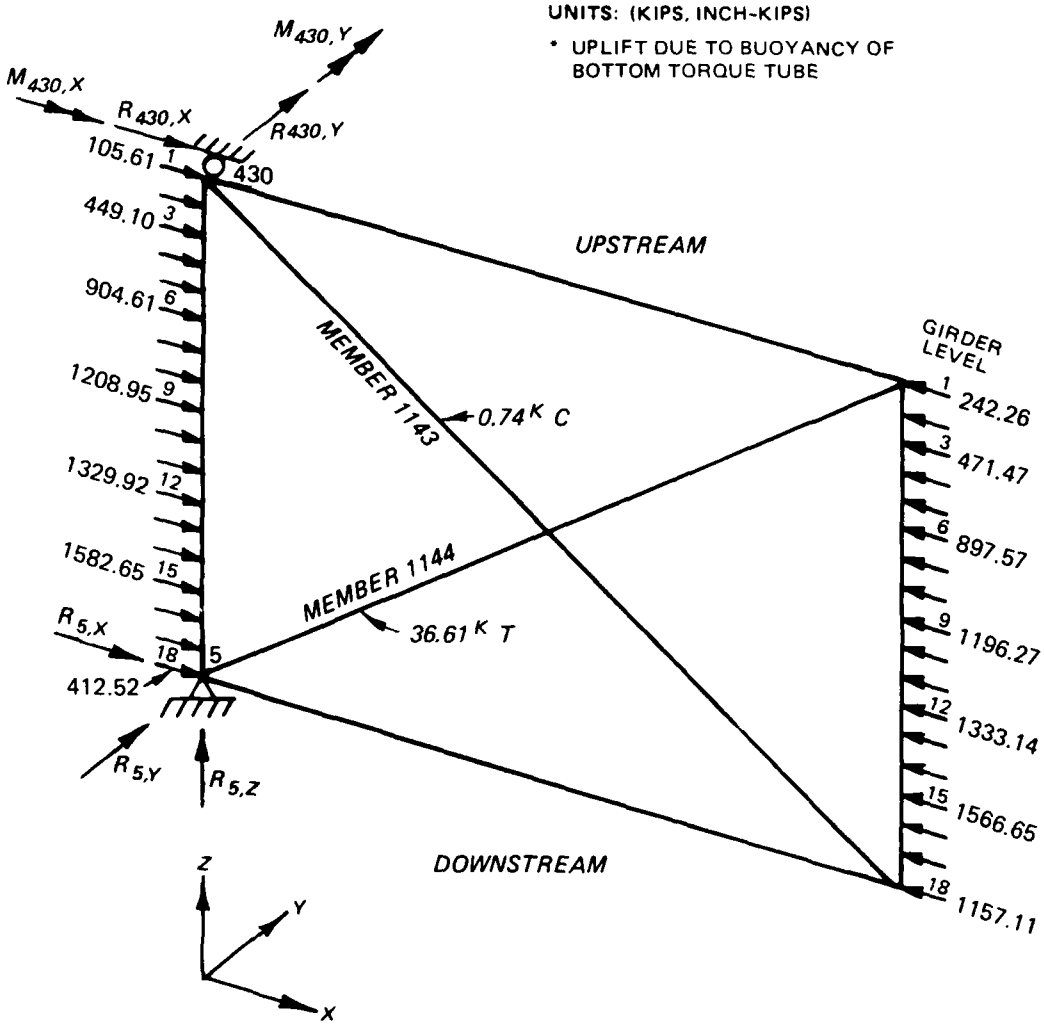

Figure 52. Reactions due to hydrostatic load (high pool/ low pool) for model 1L with diagonals

JOINT	5	430
Rx	1179.15	210.30
Ry	435.00	28.16
Rz	-111.36	0
Mx	0	77.54
My	0	26.64

UNITS: (KIPS, INCH-KIPS)

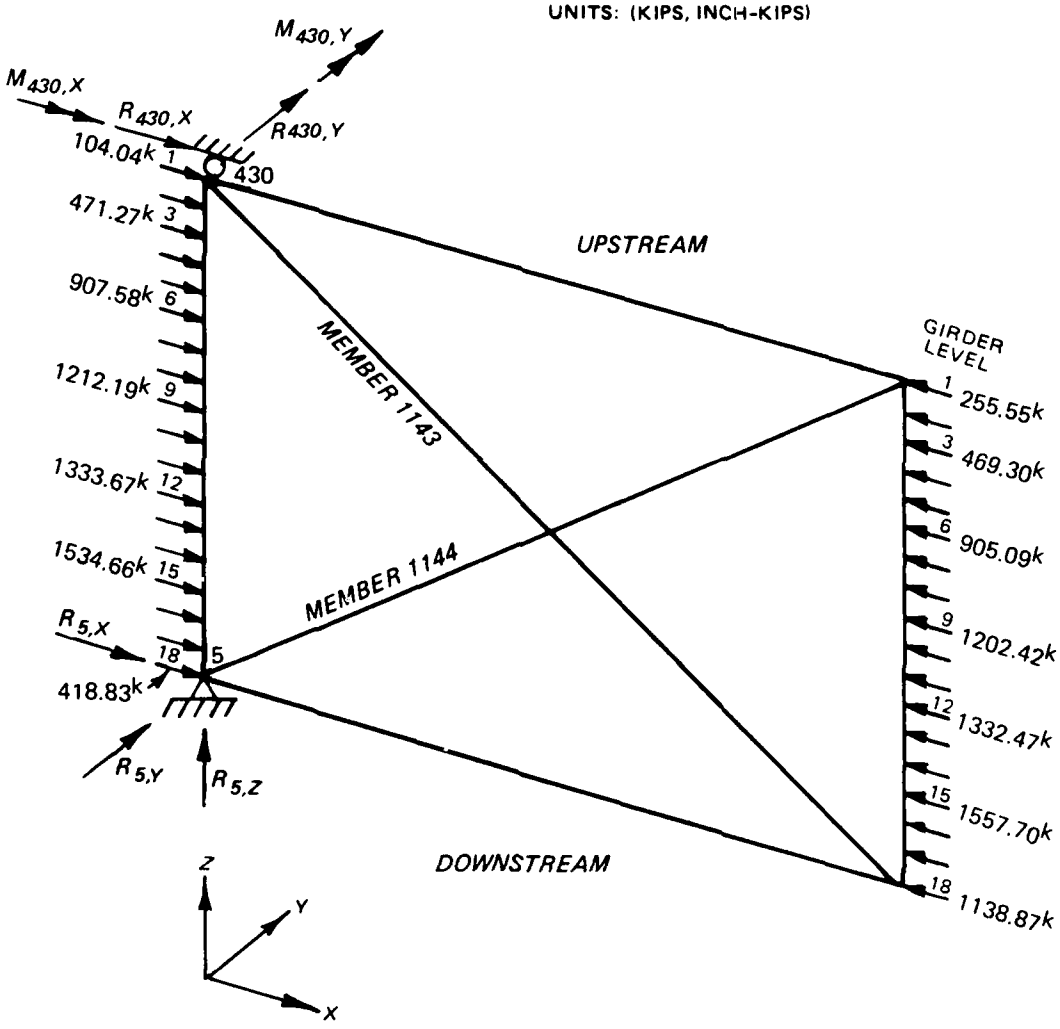

Figure 53. Reactions due to hydrostatic load (high pool/ low pool) for model 3 with diagonals

JOINT	5	430
Rx	1210.88	191.61
Ry	426.79	40.71
Rz	-55.68*	0
Mx	0	82.32
My	0	29.08

UNITS: (KIPS, INCH-KIPS)

* UPLIFT DUE TO BUOYANCY OF BOTTOM TORQUE TUBE

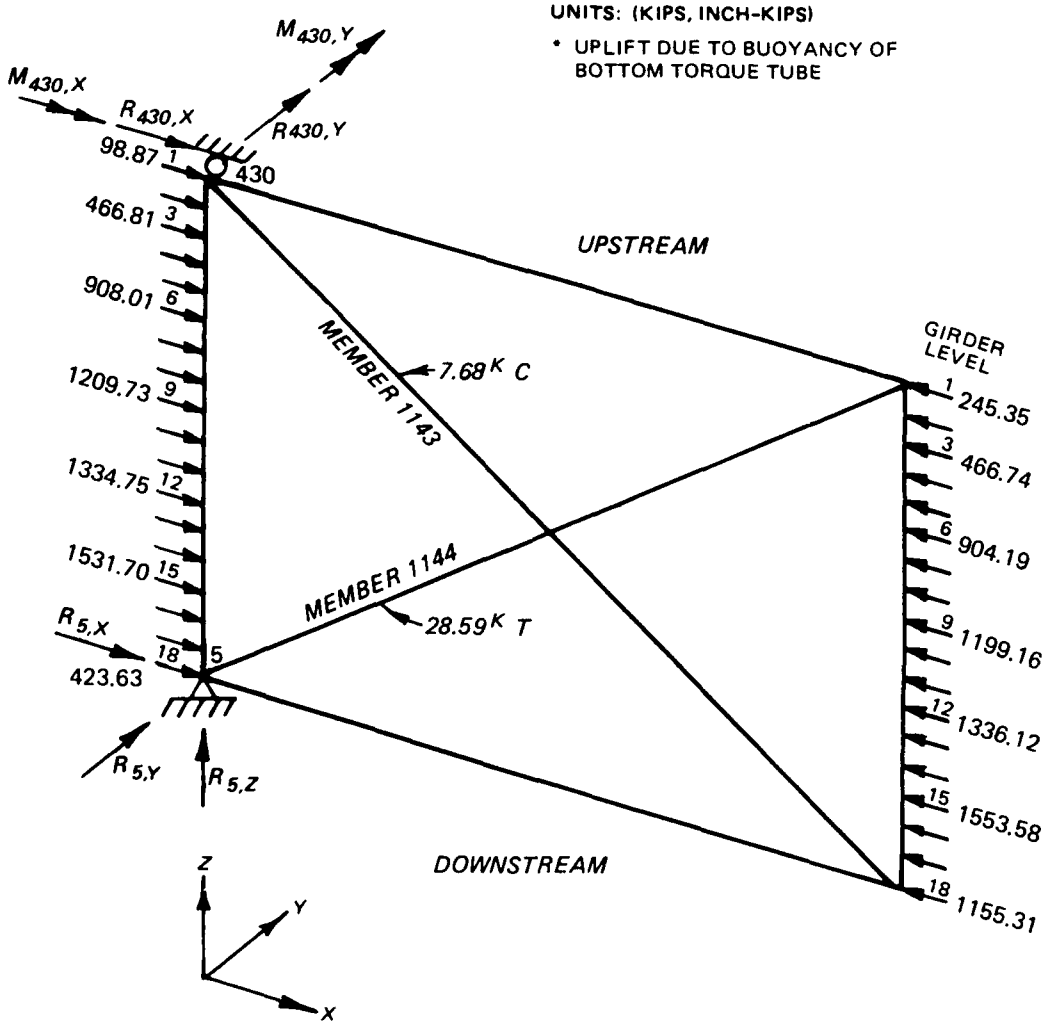

Figure 54. Reactions due to hydrostatic loading (high pool/ low pool) for model 3S with diagonals

JOINT	5	430
Rx	1152.35	200.60
Ry	398.30	52.69
Rz	-108.35*	0
Mx	0	100.81
My	0	34.86

UNITS: (KIPS, INCH-KIPS)

* UPLIFT DUE TO BUOYANCY OF BOTTOM TORQUE TUBE

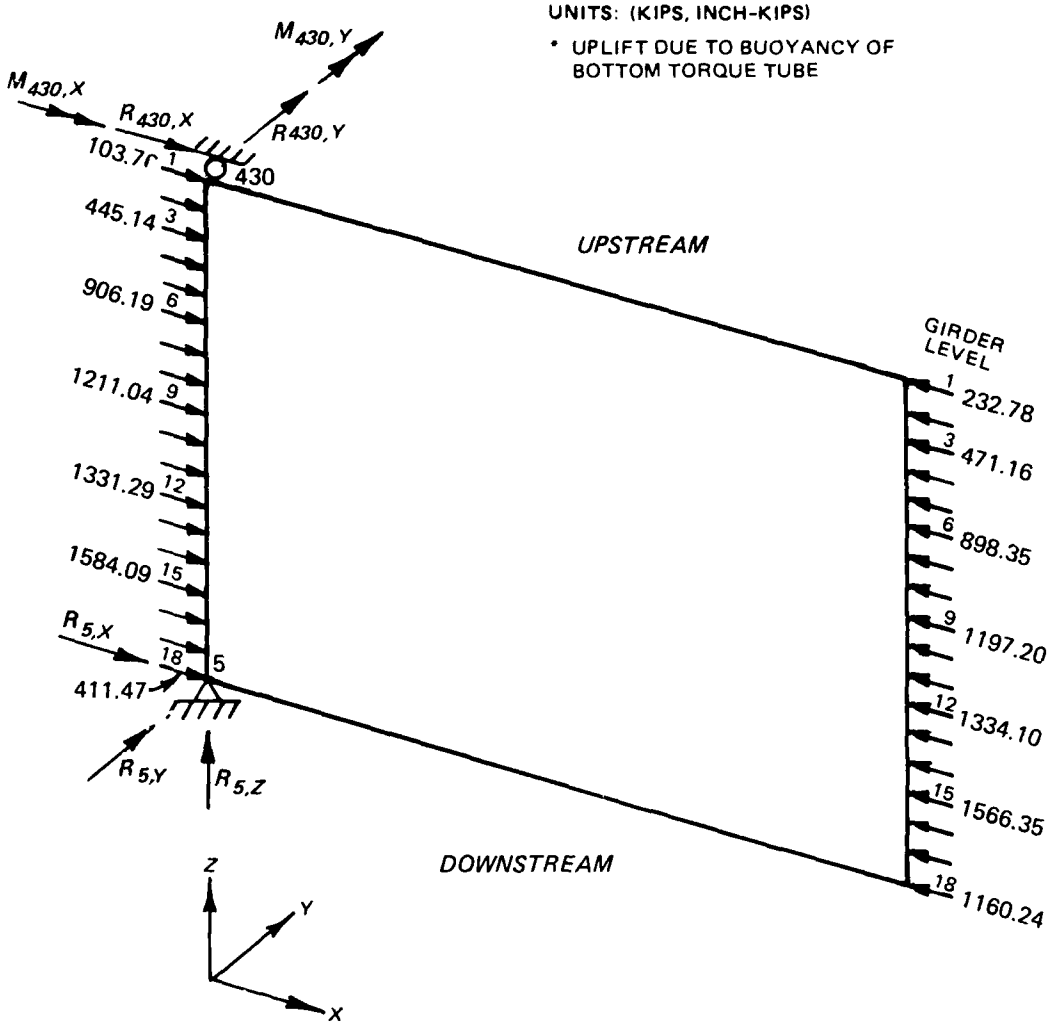

Figure 55. Reactions due to hydrostatic loading (high pool/ low pool) for model 1L without diagonals

JOINT	5	430
Rx	1178.86	206.12
Ry	430.37	31.30
Rz	-111.36*	0
Mx	0	78.78
My	0	26.76

UNITS: (KIPS, INCH-KIPS)

* UPLIFT DUE TO BUOYANCY OF BOTTOM TORQUE TUBE

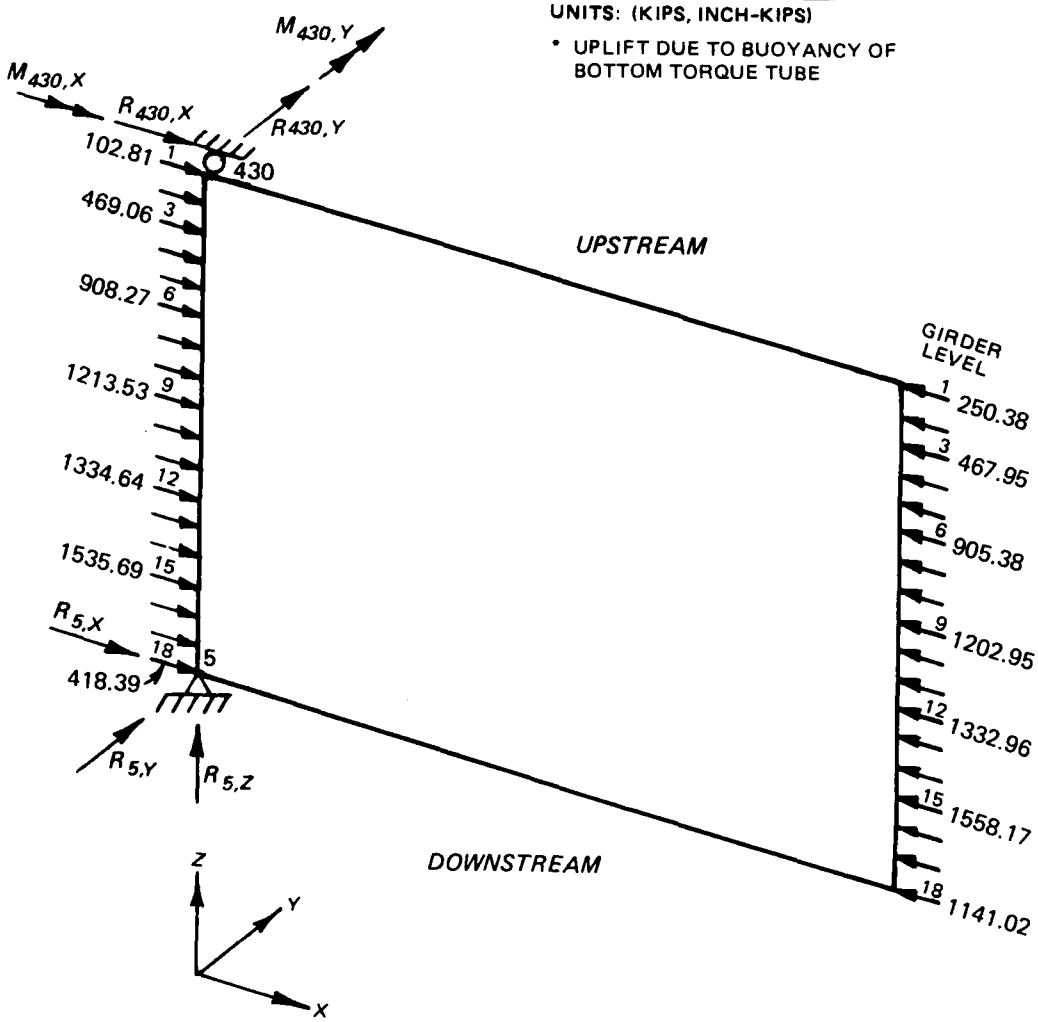

Figure 56. Reactions due to hydrostatic loading (high pool/ low pool) for model 3 without diagonals

JOINT	5	430
Rx	1212.02	186.40
Ry	420.74	45.40
Rz	-55.68*	0
Mx	0	83.99
My	0	28.53

UNITS: (KIPS, INCH-KIPS)

* UPLIFT DUE TO BUOYANCY OF BOTTOM TORQUE TUBE

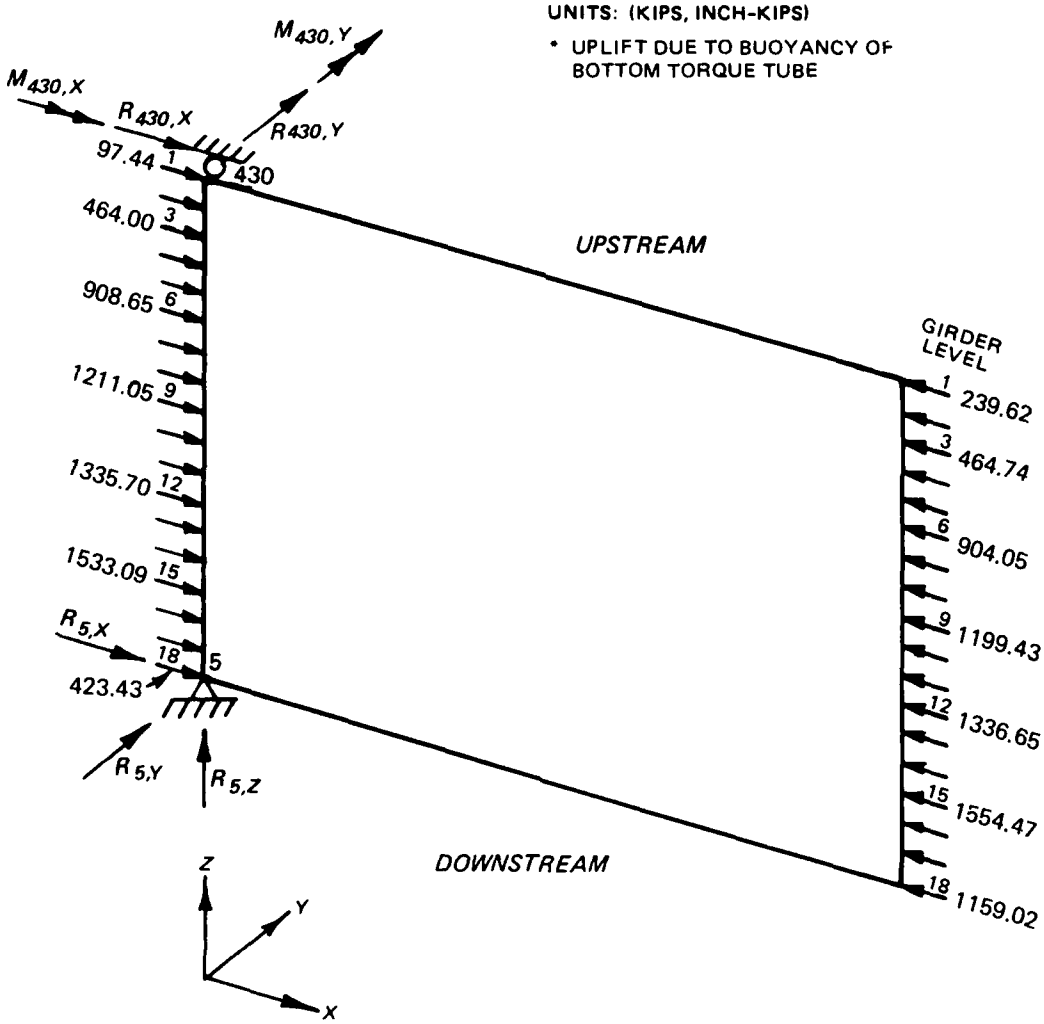

Figure 57. Reactions due to hydrostatic loading (high pool/ low pool) for model 3S without diagonals

JOINT	5	430
Rx	1198.11	210.08
Ry	441.81	27.59
Rz	-111.36*	0
Mx	0	77.88
My	0	26.85

UNITS: (KIPS, INCH-KIPS)

* UPLIFT DUE TO BUOYANCY OF BOTTOM TORQUE TUBE

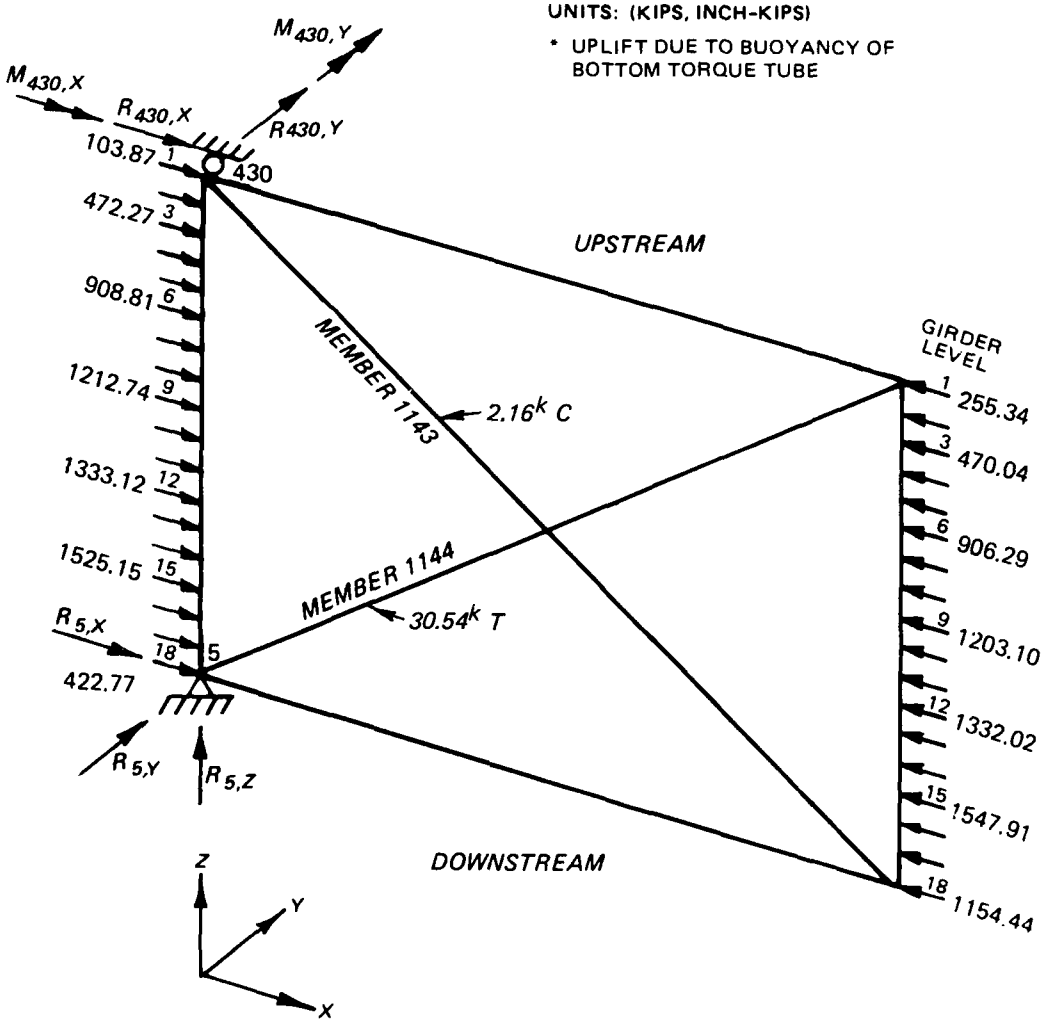

Figure 58. Reactions due to hydrostatic loading (high p[illegible] for model 3 with access holes and with diagon[illegible]

AD-A185 535 COMPUTER-AIDED STRUCTURAL ENGINEERING (CASE) PROJECT FINITE ELEMENT STUDI..(U) ARMY ENGINEER WATERWAYS EXPERIMENT STATION VICKSBURG MS INNOR.. 2/2

UNCLASSIFIED J P HARTMAN ET AL. AUG 87 WES/TR/ITL-87-4 F/G 9/1 NL

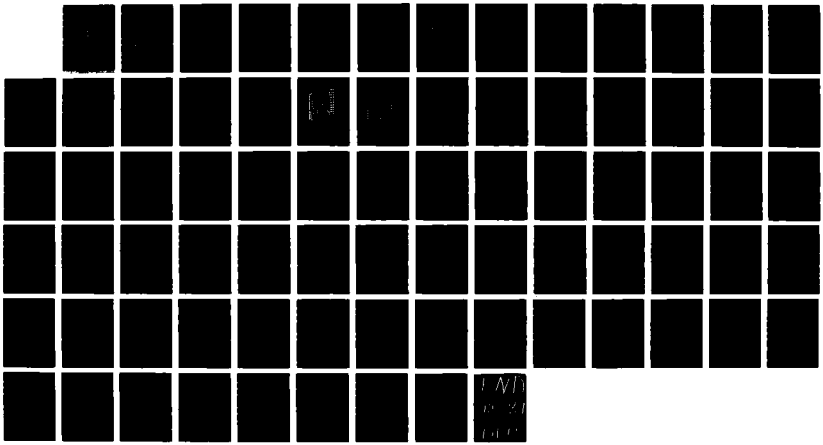

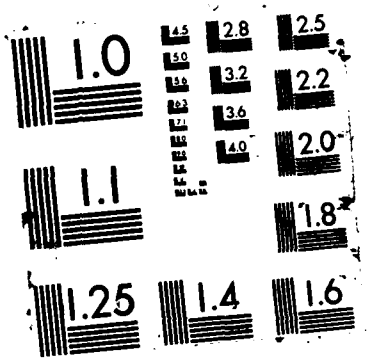
1.0
2.8
2.5
3.2
2.2
3.6
4.0
2.0
1.1
1.8
1.25
1.4
1.6

JOINT	5	430
Rx	1239.41	179.70
Ry	421.97	51.07
Rz	0	0
Mx	0	80.40
My	0	35.28

UNITS: (KIPS, INCH-KIPS)

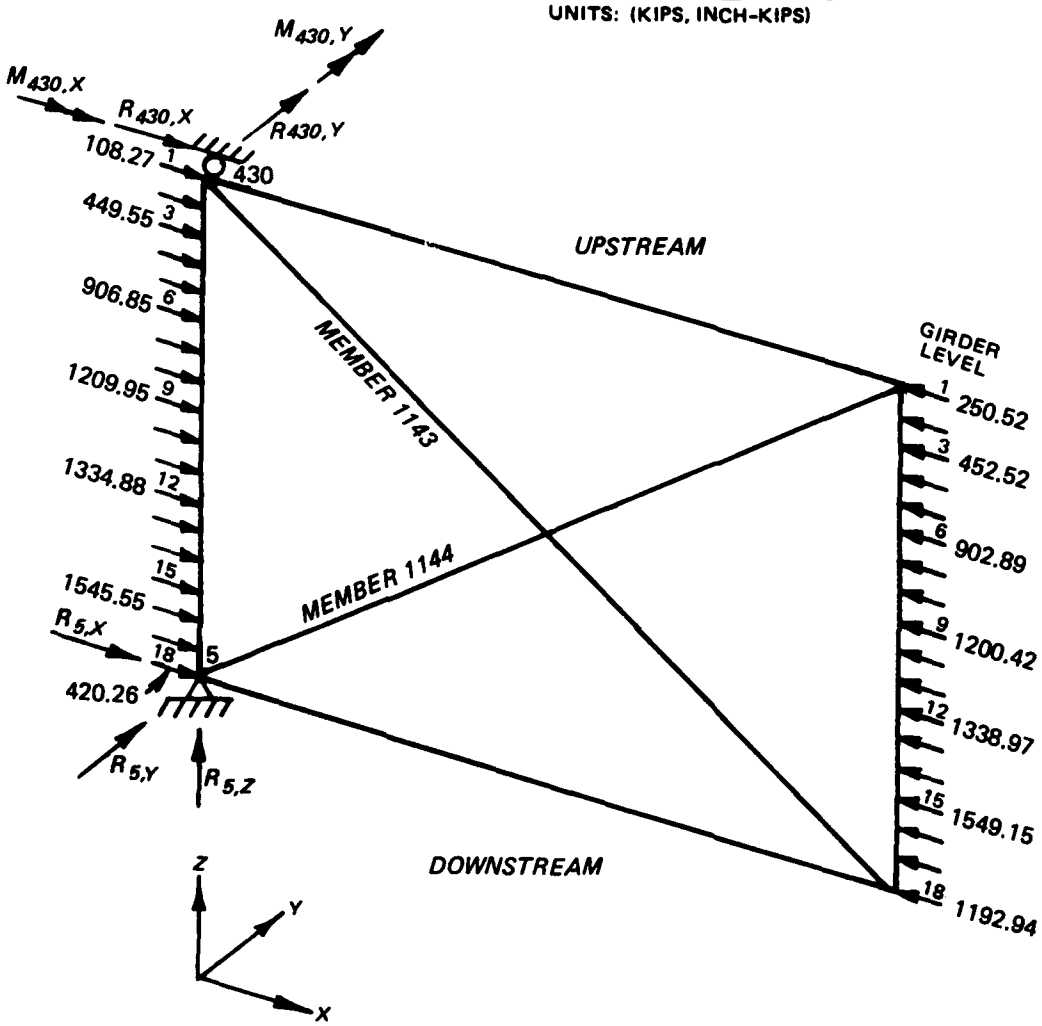

Figure 59. Reactions due to hydrostatic loading (high pool/low pool) for conventional gate model with diagonals

JOINT	5	430	577
Rx	-2.46	-114.11	116.50
Ry	-71.21	97.85	-104.9
Rz	0	0	0
Mx	0	-5.72	0
My	0	-15.98	0

UNITS: KIPS, INCHES

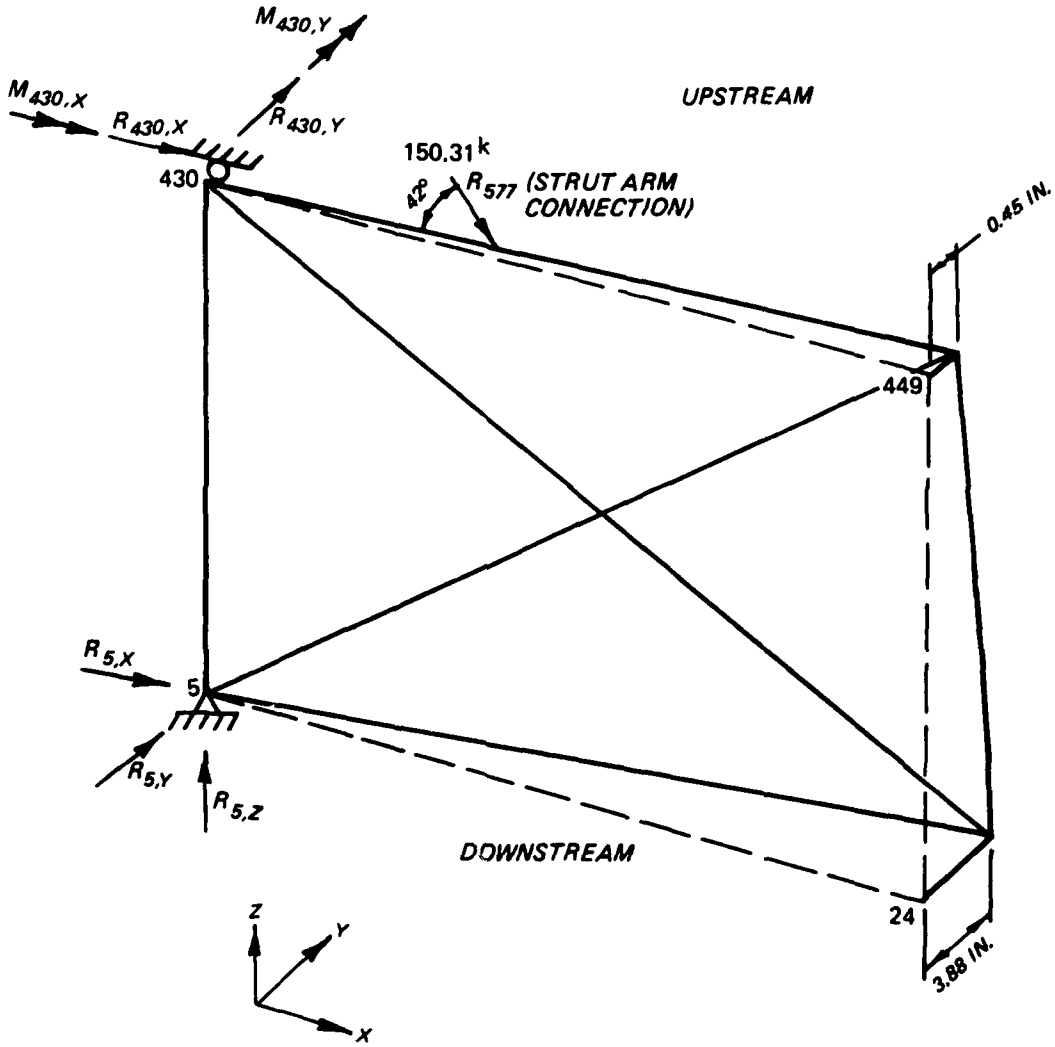

Figure 60. Reactions and displacements for model 1 with diagonals for temporal hydrostatic loading

JOINT	5	430	577
Rx	-1.51	-109.58	111.09
Ry	-67.78	93.18	-100.03
Rz	0	0	0
Mx	0	-8.97	0
My	0	-13.88	0

UNITS: KIPS, INCHES

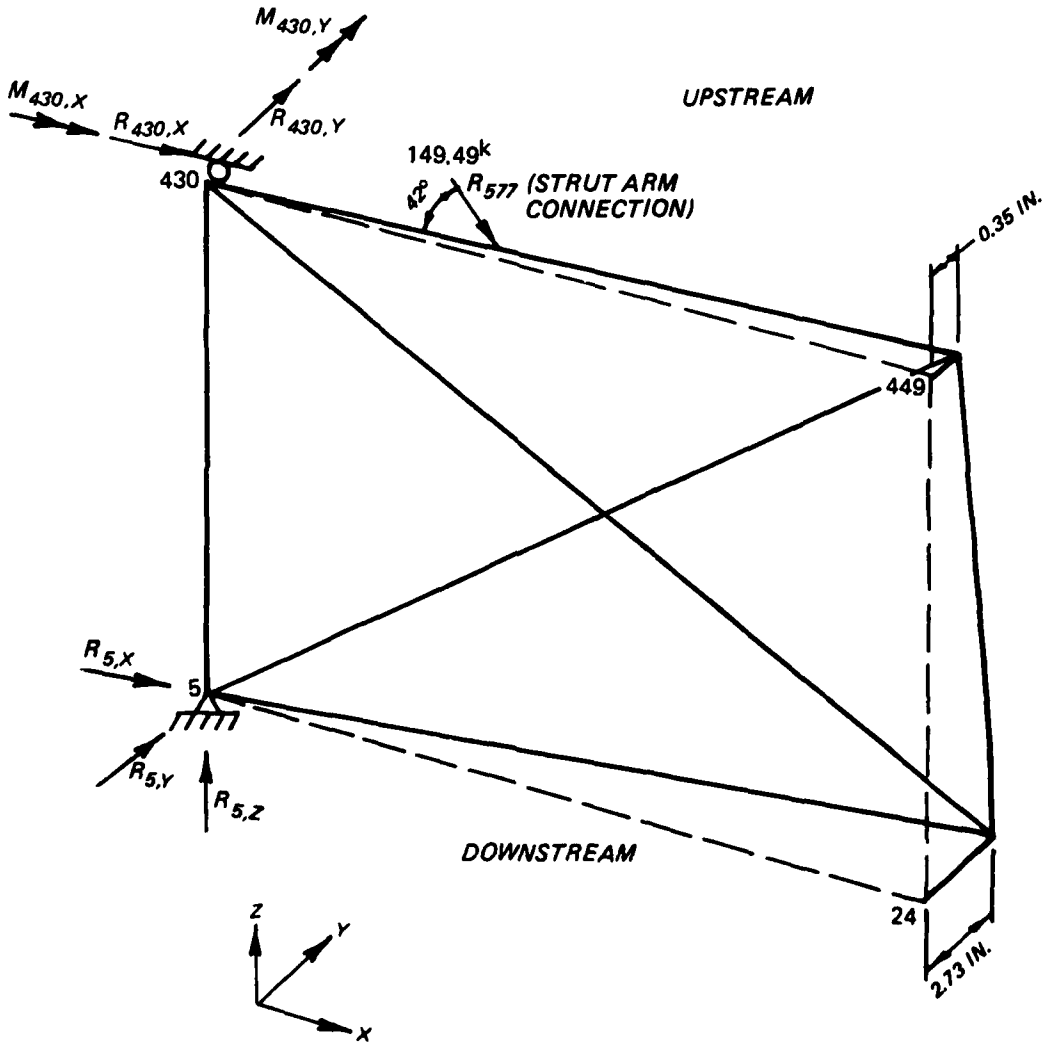

Figure 61. Reactions and displacements for model 1L with diagonals for temporal hydrostatic loading

JOINT	5	430	577
Rx	-4.17	-101.44	105.61
Ry	-64.56	88.70	-95.09
Rz	0	0	0
Mx	0	14.36	0
My	0	1.80	0

UNITS: KIPS, INCHES

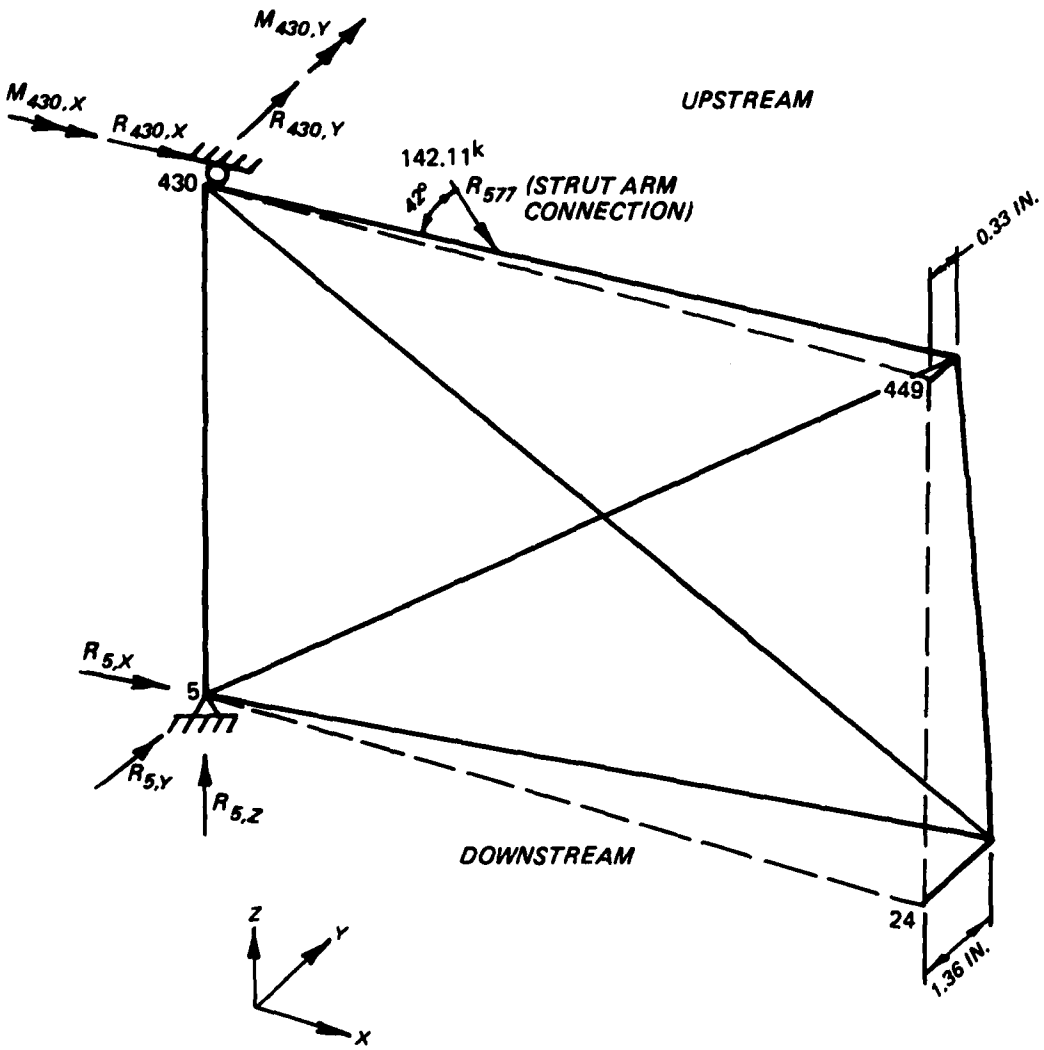

Figure 62. Reactions and displacements for model 3 with diagonals for temporal hydrostatic loading

JOINT	5	430	577
Rx	-4.19	-101.42	105.61
Ry	-64.56	88.70	-95.09
Rz	0	0	0
Mx	0	15.63	0
My	0	-0.77	0

UNITS: KIPS, INCHES

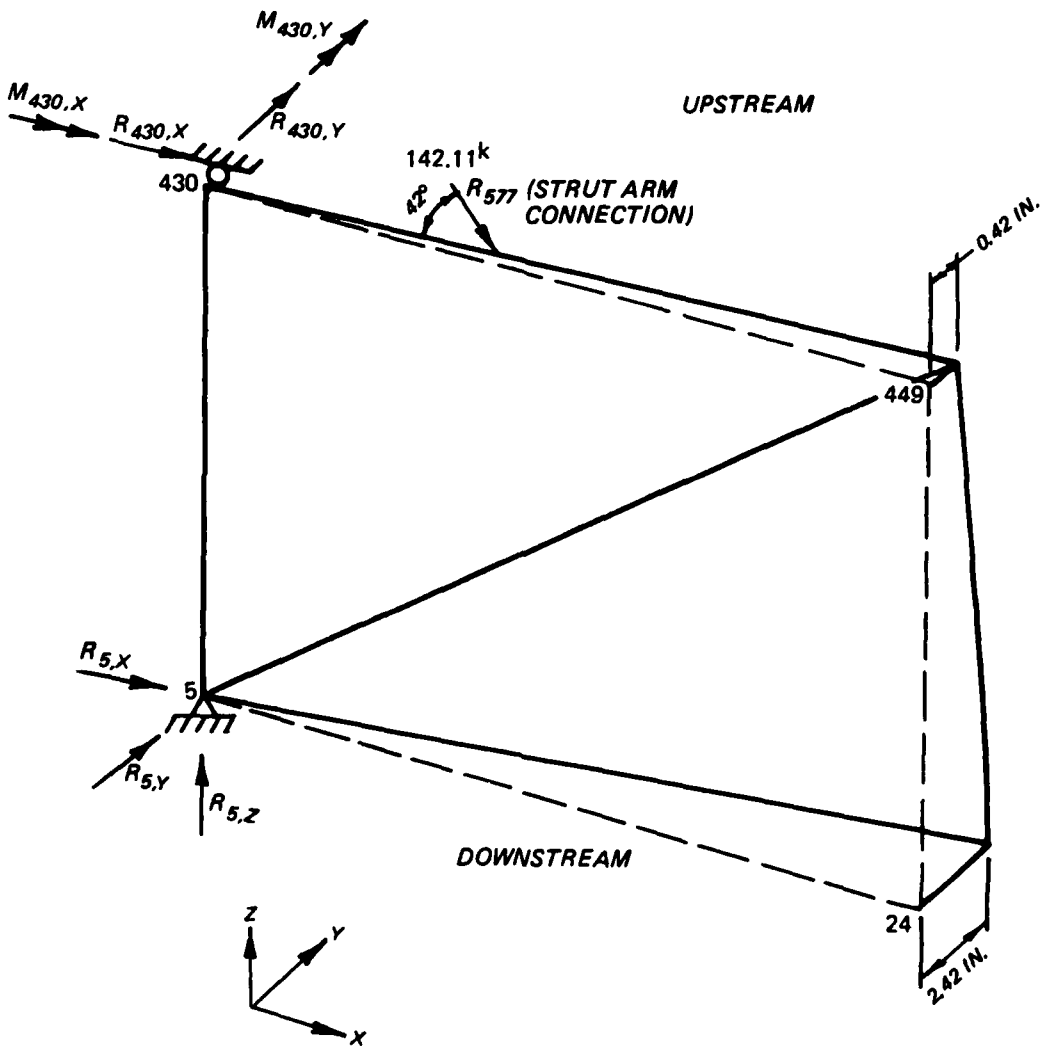

Figure 63. Reactions and displacements for model 3S with diagonals for temporal hydrostatic loading

JOINT	5	430	577
Rx	-4.25	-101.35	105.61
Ry	-64.56	88.70	-95.09
Rz	0	0	0
Mx	0	12.51	0
My	0	-2.82	0

UNITS: KIPS, INCHES

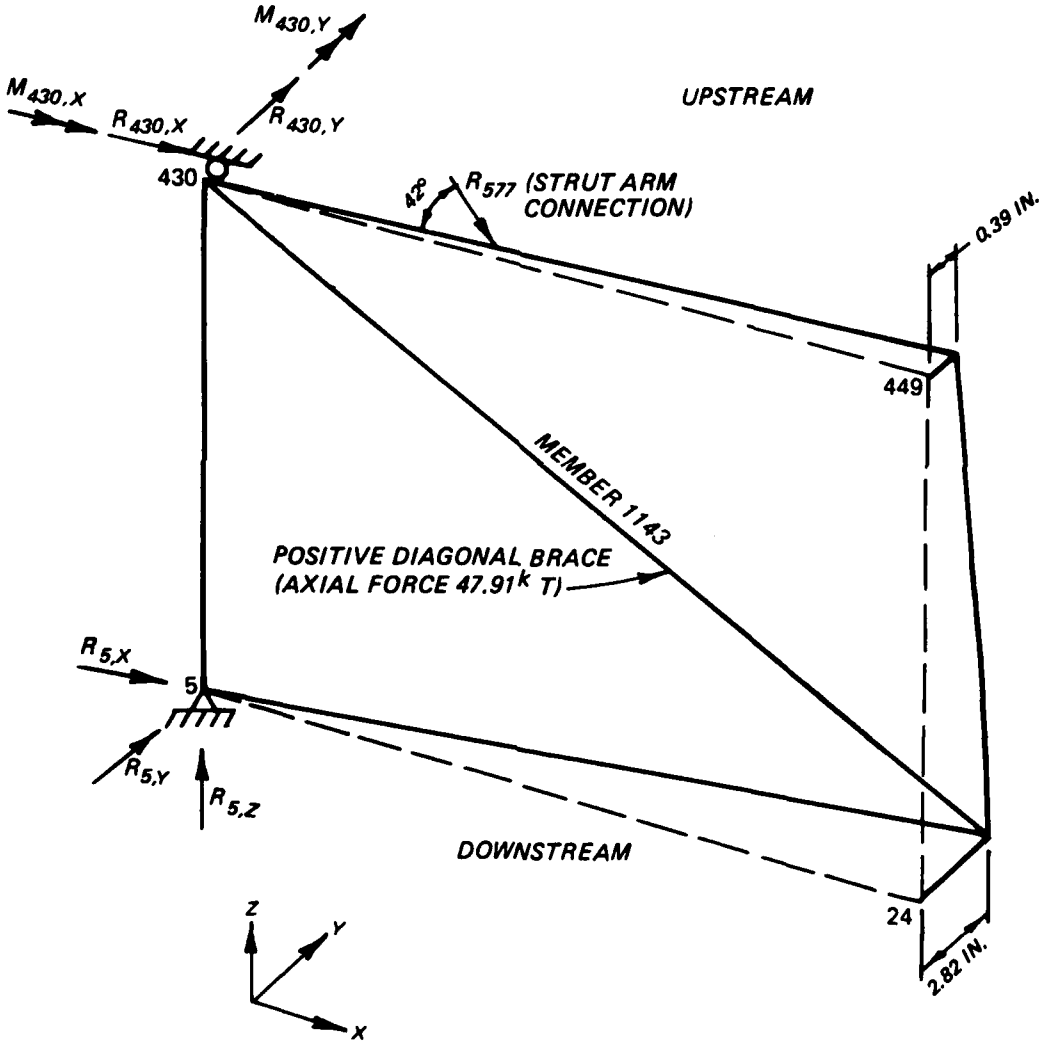

Figure 64. Reactions and displacements for model 3SP (inactive negative diagonal) for temporal hydrostatic loading

JOINT	5	430	577
Rx	-0.33	-110.76	111.09
Ry	-67.77	93.16	-100.03
Rz	0	0	0
Mx	0	-23.47	0
My	0	-13.36	0

UNITS: KIPS, INCHES

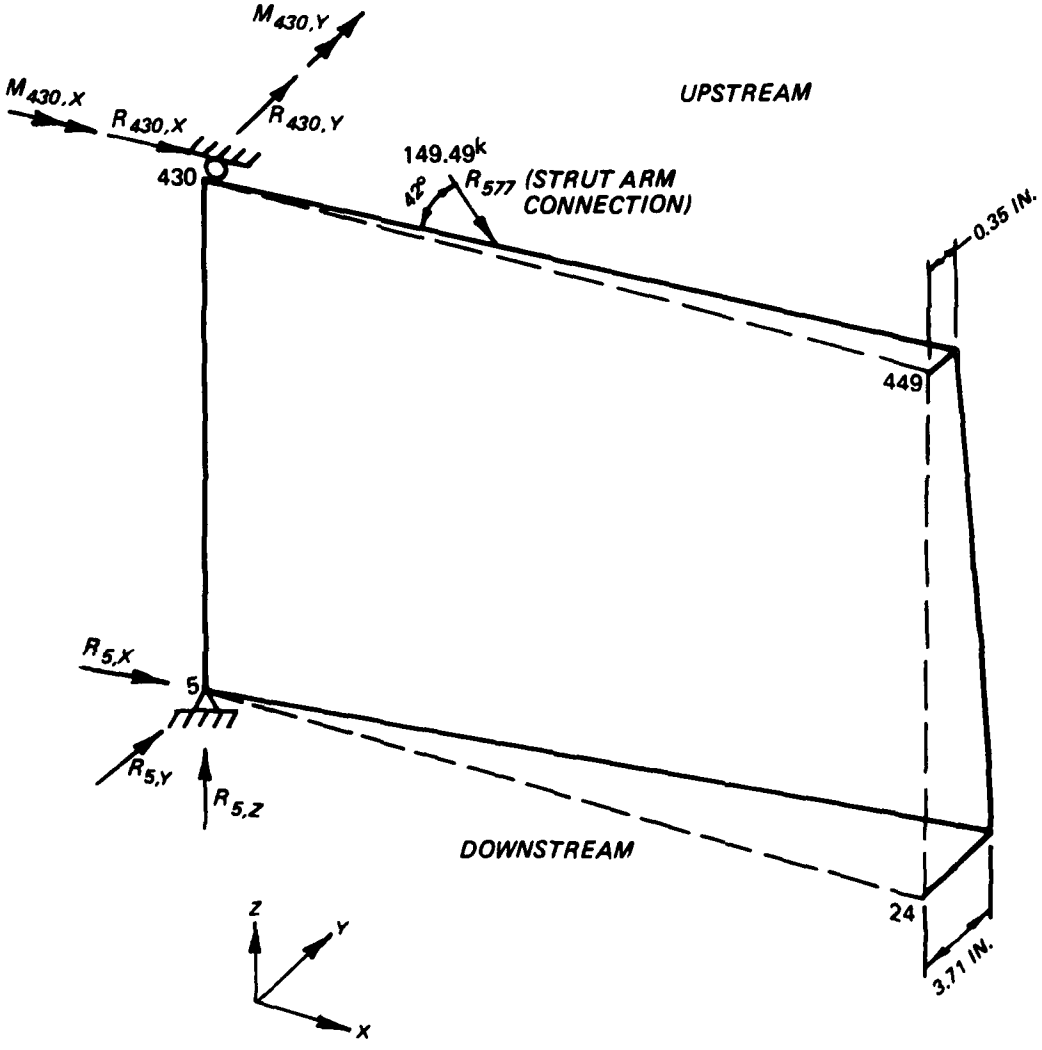

Figure 65. Reactions and displacements for model 1L without diagonals for temporal hydrostatic loading

JOINT	5	430	577
Rx	-4.17	-101.43	105.60
Ry	-64.56	88.70	-95.09
Rz	0	0	0
Mx	0	13.29	0
My	0	4.19	0

UNITS: KIPS, INCHES

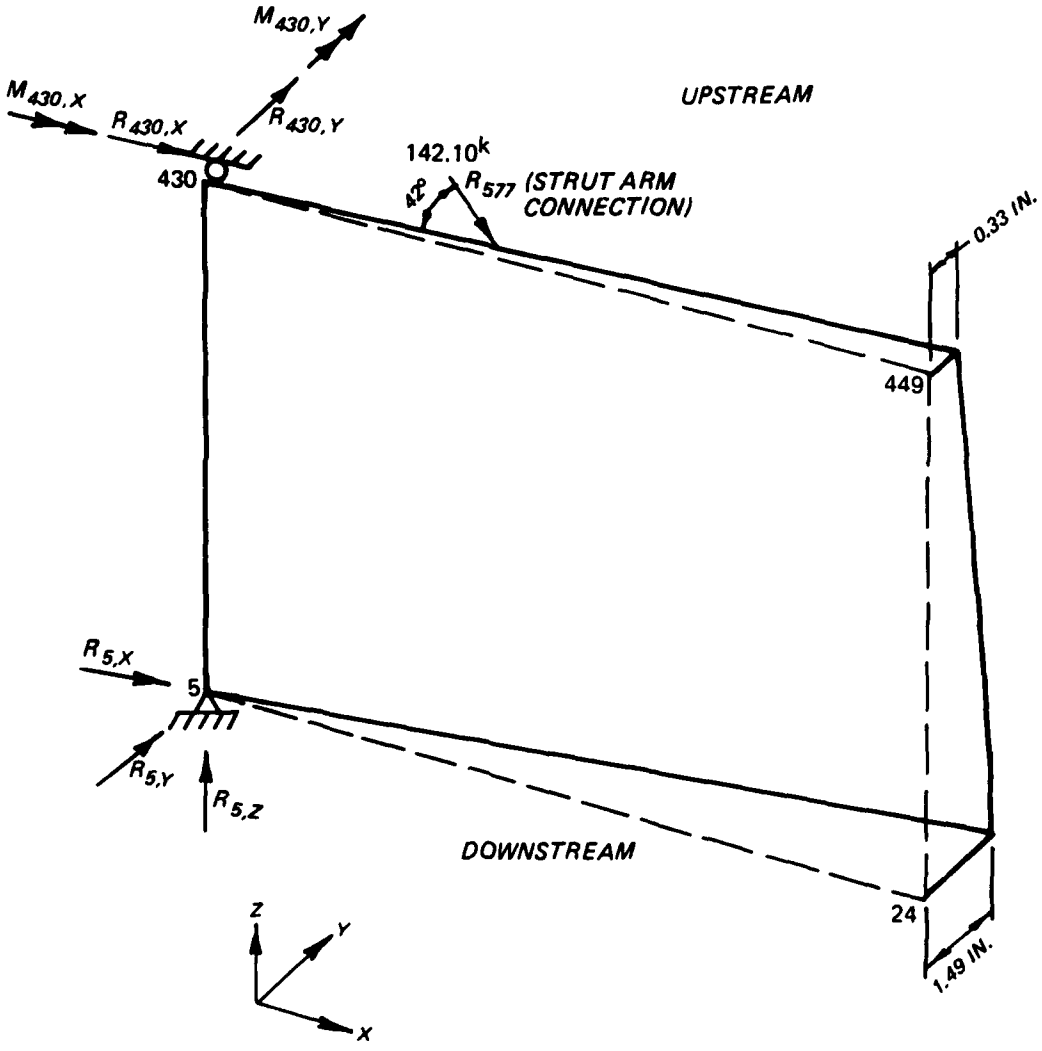

Figure 66. Reactions and displacements for model 3 without diagonals for temporal hydrostatic loading

JOINT	5	430	577
Rx	-4.32	-101.29	105.61
Ry	-64.56	88.70	-95.09
Rz	0	0	0
Mx	0	12.25	0
My	0	3.90	0

UNITS: KIPS, INCHES

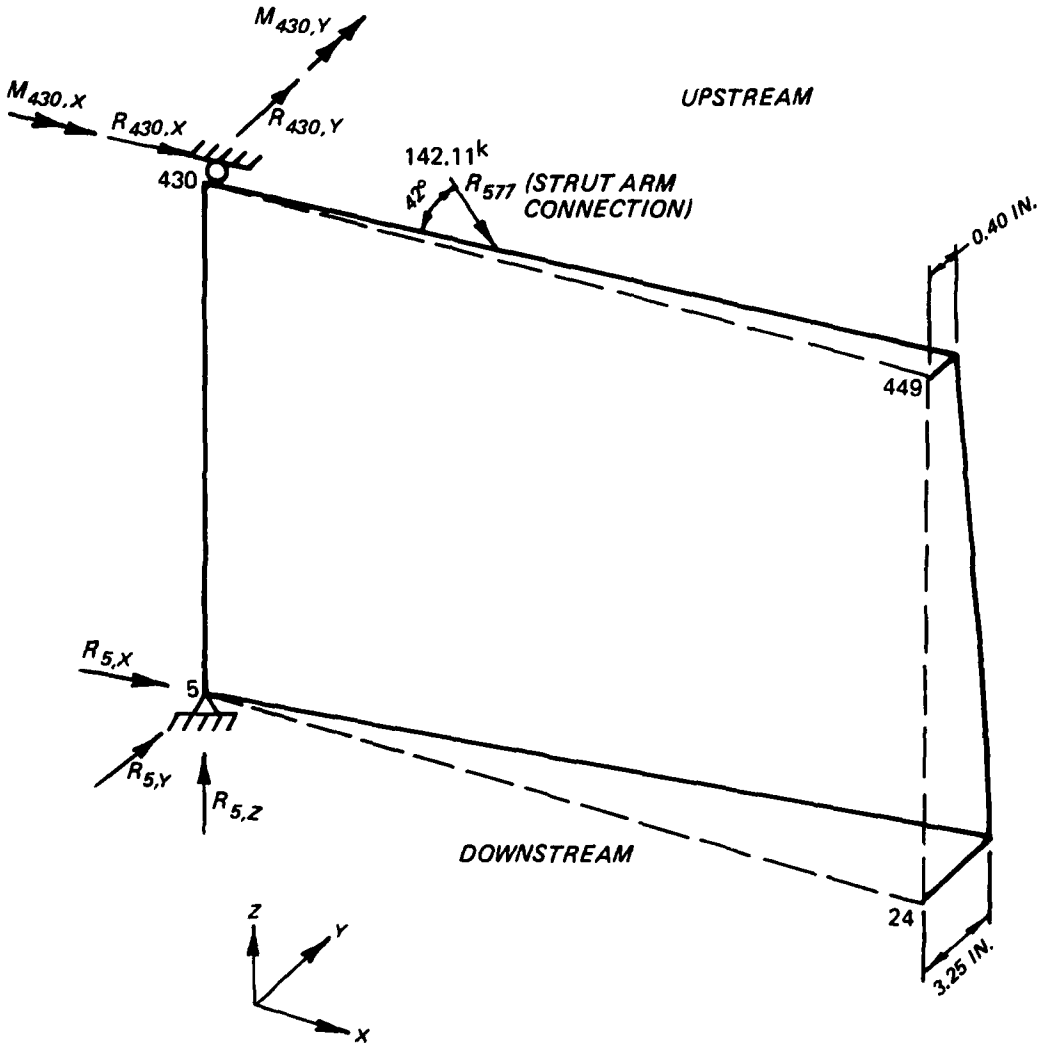

Figure 67. Reactions and displacements for model 3S without diagonals for temporal hydrostatic loading

JOINT	5	430	577
Rx	-3.83	-118.24	122.08
Ry	-74.81	102.72	-109.92
Rz	0	0	0
Mx	0	4.09	0
My	0	-10.33	0

UNITS: KIPS, INCHES

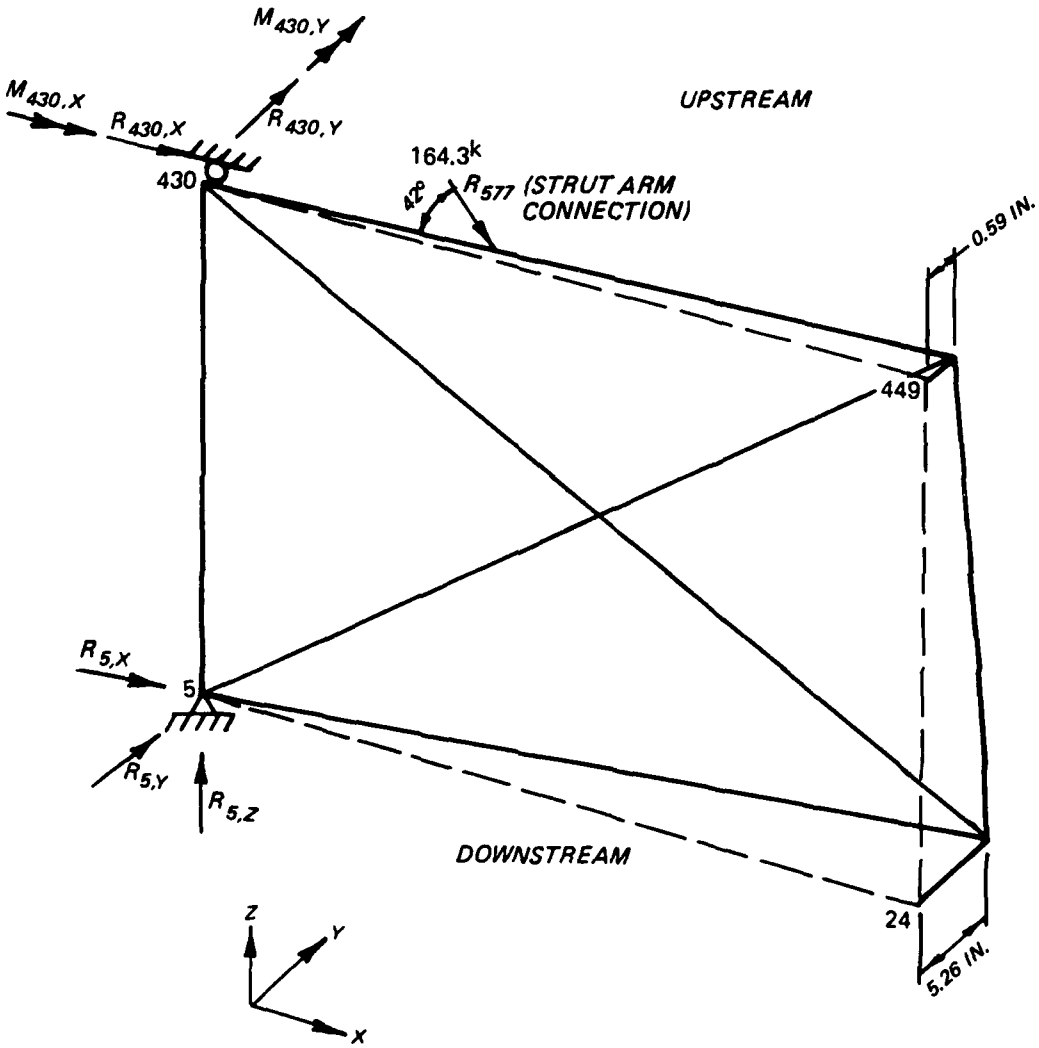

Figure 68. Reactions and displacements for conventional gate model for temporal hydrostatic loading

JOINT	5	430	577
Rx	-3.83	-118.25	122.0
Ry	-74.82	102.73	-109.0
Rz	0	0	0
Mx	0	6.74	0
My	0	-9.07	0

UNITS: KIPS, INCHES

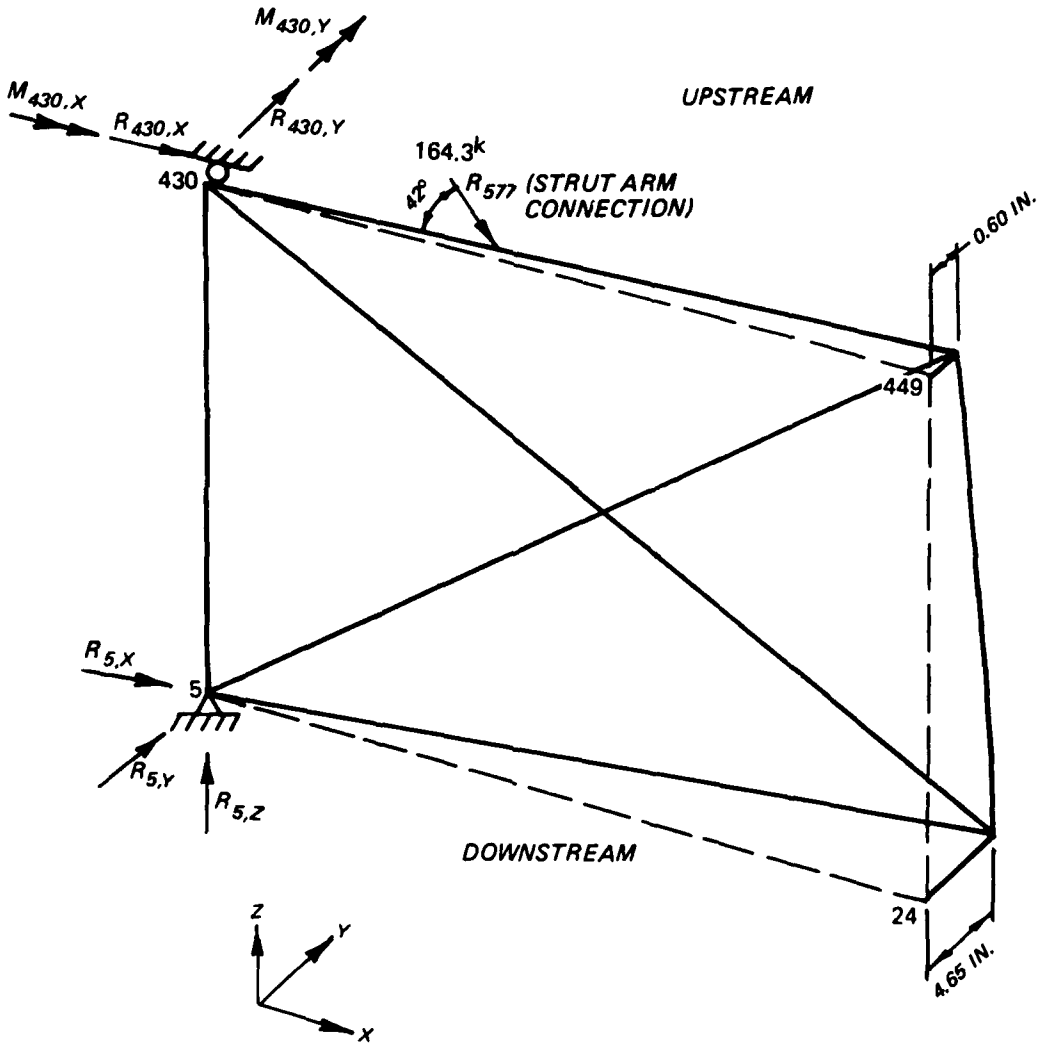

Figure 69. Reactions and displacements for conventional gate with enlarged diagonals for temporal hydrostatic loading

diagonals. Model 3S with diagonals undergoes almost twice the twist displacement of model 3 with diagonals, and model 3SP with positive diagonal only undergoes 2.4 times the twist displacement of model 3 with diagonals. Finally, models 1L and 3S (each with diagonals) are almost the same in level of twist displacement. All gate leaf twisting listed above is consistent with torsional stiffness values presented earlier in Table 10.

Vertical Torque-Tube Design Considerations

117. The contribution of the torque tubes to the action of the leaves as a three-hinged arch may be neglected. The torque tubes will increase the torsional stiffness of the leaves, and this added stiffness may reduce or eliminate the cross-sectional area required for the diagonals. Studies are ongoing to develop design methods to account for torque-tube stiffness. If the torque tubes are installed by welding as permanent components of the leaf, consideration may be given to respacing the intermediate diaphragms using three equal spaces between torque-tube diaphragm plates. This approach will influence, to some extent, the intercostal and skin-plate designs and may eliminate the option of operating the gate without torque tubes in the event of maintenance and repair problems. The vertical torque tubes are located at the quoin and miter ends of gate leaf seen in Figures 27 through 29 and described below:

a. Quoin end torque tube is made up of a vertical diaphragm plate equal in width to the horizontal girder web depth, the downstream plate approximately of the same width, the quoin diaphragm plate, and the skin plate. The torque tube is square in cross section, discontinuous between horizontal girders, and extends from bottom girder to top girder. Access holes are provided in the vertical torque-tube diaphragm plates to facilitate fabrication and maintenance. The torque tube may be of welded or bolted construction.

b. Miter end torque tube is the same as the quoin end torque tube, with its location on the miter end of the leaf.

c. Dimensions and details of torque-tube sections are listed below:

(1) Definitions

t (TD) = thickness, torque-tube diaphragm plate
w (TD) = width, torque-tube diaphragm plate
h (TD) = height, torque-tube diaphragm plate
t (TDS) = thickness, torque-tube downstream plate

w (TDS) = width, torque-tube downstream plate
h (TDS) = height, torque-tube downstream plate

(2) Component sizes

Minimum thickness: t (TD) = t (TDS) = 3/8 in.

Maximum thickness: t (TD) = t (TDS) = vertical leaf diaphragm thickness

w (TD) = horizontal girder web depth

w (TDS) = w (TD) - (1/2 × quoin or miter diaphragm flange width)

h (TD) = horizontal girder spacing less half of girder-web thickness above and below

h (TDS) = horizontal girder spacing less half of downstream girder flanges above and below

(3) The torque-tube diaphragm and downstream plates with the skin and quoin or miter diaphragm plates form a square, vertical tube section between two horizontal girders. Downstream flange splices, if any, should be located outside the torque tube toward the center line of the leaf to avoid weld concentrations. The downstream plate of the torque tube may be butt welded to the girder flange plates or fillet welded, overlapping the inside face of flange plates.

118. Hartman* has proposed a procedure for torsional design of miter gates with torque tubes based on information from EM 1110-2-2703 and Blodgett.**

a. The following formulas use nomenclature changed from that used in the references to the following:

E_S Modulus of elasticity for shear (12×10^6 psi)

J_V Torsional resistance of all vertical members (sum), in.^{4}

J_H Torsional resistance of all horizontal members (sum), in.^{4}

L_V Vertical distance between top and bottom girders, in.

L_H Horizontal distance from pintle to miter end, in.

T_Z Torque area: Torque (T) times distance (Z) between points of application and reaction, kip-in.^{2}

---

* Author of Part II.

** O. W. Blodgett. 1976. "Design of Welded Structures," The James F. Lincoln Arc Welding Foundation, Cleveland, Oh.

b. The following equation is taken from the publication by Blodgett and is identified as Equation 4 in the text of that publication.

Derivation

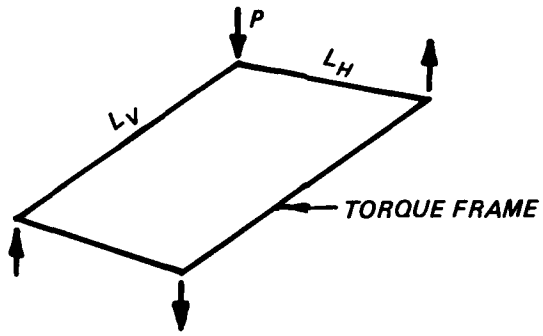

$$\Delta = \frac{PL_V L_H}{E_S}\left(\frac{1}{\frac{J_V}{L_H} + \frac{J_H}{L_V}}\right) \tag{1}$$

Since $T = P \times L_V$

Then $T_Z = (P \times L_V)L_H$

The above equation can be rewritten as

$$\Delta = \frac{T_Z}{E_S}\left(\frac{1}{\frac{J_V}{L_H} + \frac{J_H}{L_V}}\right) \tag{2}$$

c. The following two equations are taken from material in EM 1110-2-2703. They are identified as Equations 3-23 and 3-26 in the manual.

$$\Delta = \frac{T_Z}{Q_O + \Sigma Q} \tag{3}$$

where Q_O and ΣQ are elasticity constants of a leaf without diagonals, and of the diagonals, respectively. Since

$$Q_O = KE_S \left(\frac{J_V}{L_H} + \frac{J_H}{L_V} \right) \tag{4}$$

and since, for a leaf without diagonals, the following is true:

$$\Sigma Q = 0$$

$$\Delta = \frac{T_Z}{KE_S} \left(\frac{1}{\frac{J_V}{L_H} + \frac{J_H}{L_V}} \right) \tag{5}$$

119. Note the similarity of Equations 2 and 5, derived from the two different references. The only difference is the constant K which is assigned an empirical value to make values from Equation 5 conform to limited experimental results.

120. From Equations 2 and 3, it can be seen that the elasticity constant (stiffness) due to torque tubes should be

$$Q_T = E_S \left(\frac{J_{VT}}{L_H} + \frac{J_{HT}}{L_V} \right) \tag{6}$$

where J_{VT} and J_{HT} represent the sums of the torsional resistance of all vertical and horizontal torque tubes. Equation 3, found in EM 1110-2-2703 may then be modified to

$$\Delta = \frac{T_Z}{Q_O + Q_D + Q_T} \tag{7}$$

where Q_O , Q_D , and Q_T represent the elasticity constants due to thin-member torsion of gate components, addition of diagonals, and action of torque tubes, respectively. Equations 6 and 7 should be used as the basis for design of gates with torque tubes.

121. If torque tubes are not continuous the full height (or width) of

the gate, a modified torsional resistance (J_{EQ}) must be used in Equation 6. Consider the following example.

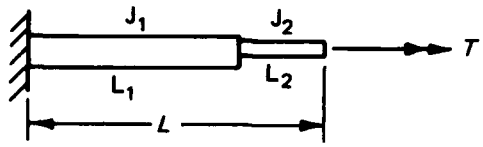

$$\theta = \frac{T}{E_S} \sum \frac{L}{J} = \frac{T}{E_S}\left(\frac{L_1}{J_1} + \frac{L_2}{J_2}\right)$$

$$Q = \frac{T}{\theta} = E_S\left(\frac{1}{\frac{L_1}{J_1} + \frac{L_2}{J_2}}\right) = E_S\left(\frac{J_1 J_2}{J_2 L_1 + J_1 L_2}\right)$$

Let $m = L_1/L$ and $n = L_2/L$, then

$$Q = E_S\left(\frac{J_1 J_2}{mJ_2 + nJ_1}\right)\frac{1}{L}$$

and if $Q = E_S(J_{EQ}/L)$ then

$$J_{EQ} = \frac{J_1 J_2}{mJ_2 + nJ_1}$$

It can be seen that the magnitude of J_{EQ} will be greatly reduced if the value of J_1 or J_2 is very small. This would be the case if the torque tubes were not full length.

Comparative Analysis of Gallipolis Gate

122. After the analysis of the Bankhead gates, another finite element model was developed based on the geometry of the lower miter gates of the main lock for Gallipolis Lock and Dam on the Ohio River. The Gallipolis gate was

selected in an attempt to verify the results obtained from the Bankhead analysis.

123. Each lower miter gate leaf for the Gallipolis main lock is approximately 58 ft high and 62 ft wide. The gate has a conventional, horizontally framed configuration with 12 horizontal girders. Between the four corners of each leaf are single sets of three diagonals located on the downstream face.

124. The gate geometry was modeled similar to the Bankhead gate by using the GTSTRUDL program. Three CM models of conventional and torque-tube configurations were developed to evaluate gate behavior for the various loading conditions previously discussed. The models, referred to as models ORH, ORHT and ORHT1, are illustrated in Figures 70 and 71. Notes: Model ORHT is model OHR with a vertical torque tube at each nod of the gate. Model ORHT1 is model ORHT without the negative diagonal.

125. Load cases used for the Bankhead gate model analysis were also used to analyze the Gallipolis models. Results of the analysis are shown on Figures 72 through 80 and summarized in Tables 12, 13, and 14. The tables also show a comparison between the Gallipolis conventional gate and torque-tube models ORHT and ORHT1, as well as the Bankhead conventional gate and torque-tube models 3S and 3SP.

126. Review of the tables indicates that although the Gallipolis gate is about one half the weight and about 30 ft shorter than the conventional Bankhead gate, the out-of-plumb displacement is almost fifty percent greater. However, the displacement for the torque-tube models is about the same. The Gallipolis torque-tube models gained a greater increase in torsional stiffness when compared to the Gallipolis conventional gate than did the Bankhead gate torque tubes.

127. Results of prestressing behavior analysis are shown in Table 14. Initial prestress jacking loads on Gallipolis gate models are consistent with Bankhead gate models. However, final prestressing loads show an average difference of approximately 110 kips between the negative and positive diagonal forces. Removal of the negative diagonal from model ORHT resulted in a 52 percent reduction in jacking force and a 36 percent reduction in positive diagonal force. A comparison of forces for model ORHT1 and conventional Gallipolis gate models reveals a 76 percent reduction in jacking force and an 83 percent reduction in positive diagonal force. Furthermore, eliminating the negative diagonal has reduced the force in the positive diagonal in agreement

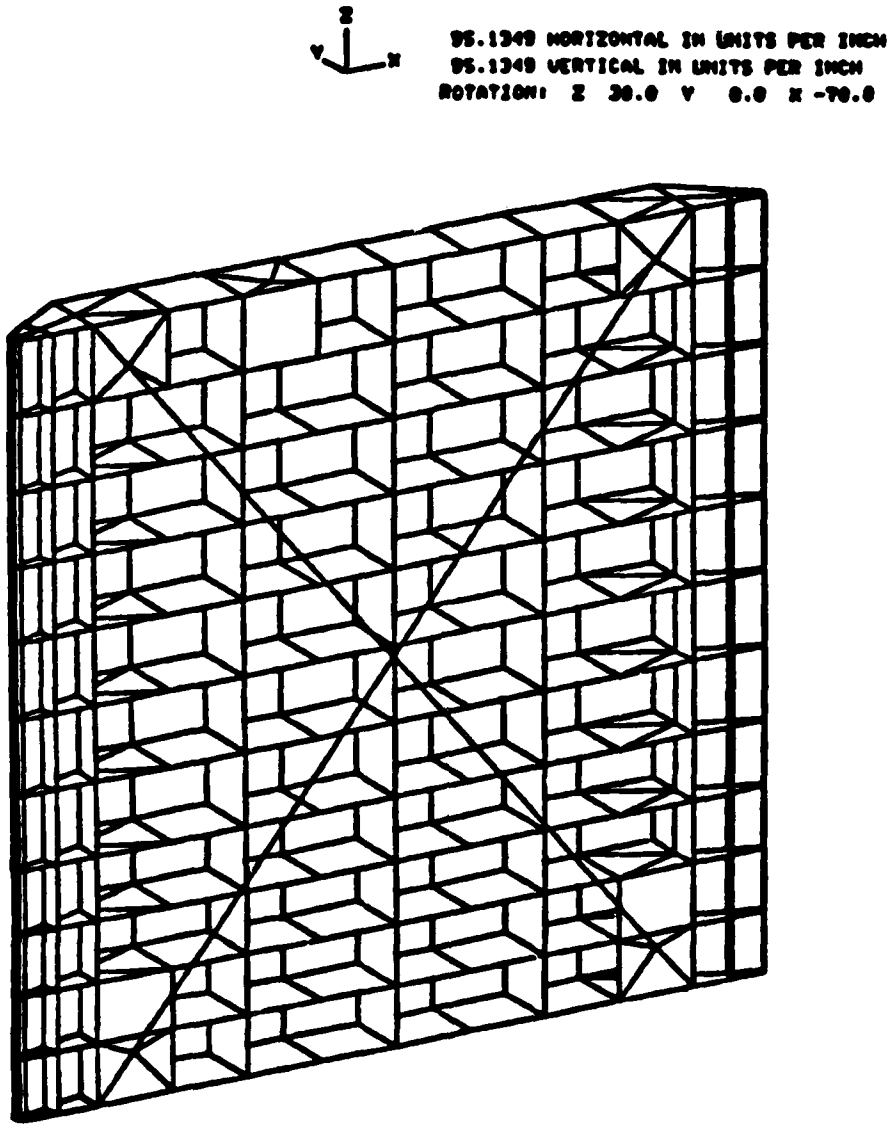

Figure 70. Finite element model, Gallipolis conventional gate model ORH

with Hartman's hypothesis previously discussed in paragraph 108.

128. Results of the hydrostatic and temporal head loading analysis are consistent with results of the Bankhead gate model studies. Reactions and displacements for temporal head loading behavior are shown in Figures 78, 79, and 80. The gate twist, due to temporal head loading, was measured as the difference in Y-displacement between joints 31 and 383. The twist for models with diagonals is shown on the following page:

Model ORH	3.40 in.
Model ORHT	2.09 in.
Model ORHT1	2.69 in.
Conventional Bankhead Gate	4.67 in.
Model 3S	2.00 in.
Model 3SP	2.43 in.

129. The twist values listed in paragraph 123 show a close agreement between the Bankhead and Gallipolis torque-tube models. This further verifies the results obtained from the Bankhead analysis.

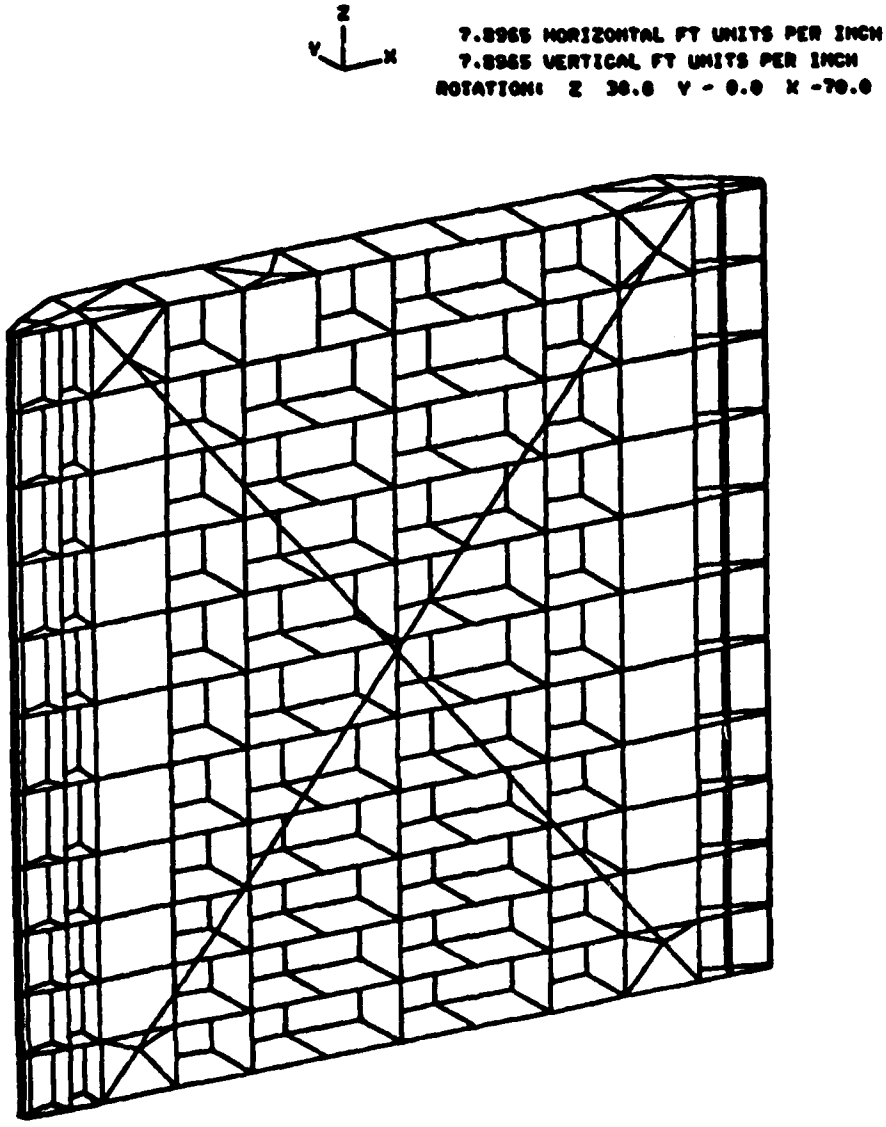

Figure 71. Hidden line plot of Gallipolis torque-tube models ORHT and ORHT1

JOINT	5	357	26
Rx	139.27	-139.27	0
Ry	8.09	-8.09	0
Rz	292.52	0	0
Mx	0	-0.53	0
My	0	-1.04	0

UNITS: KIPS, INCHES

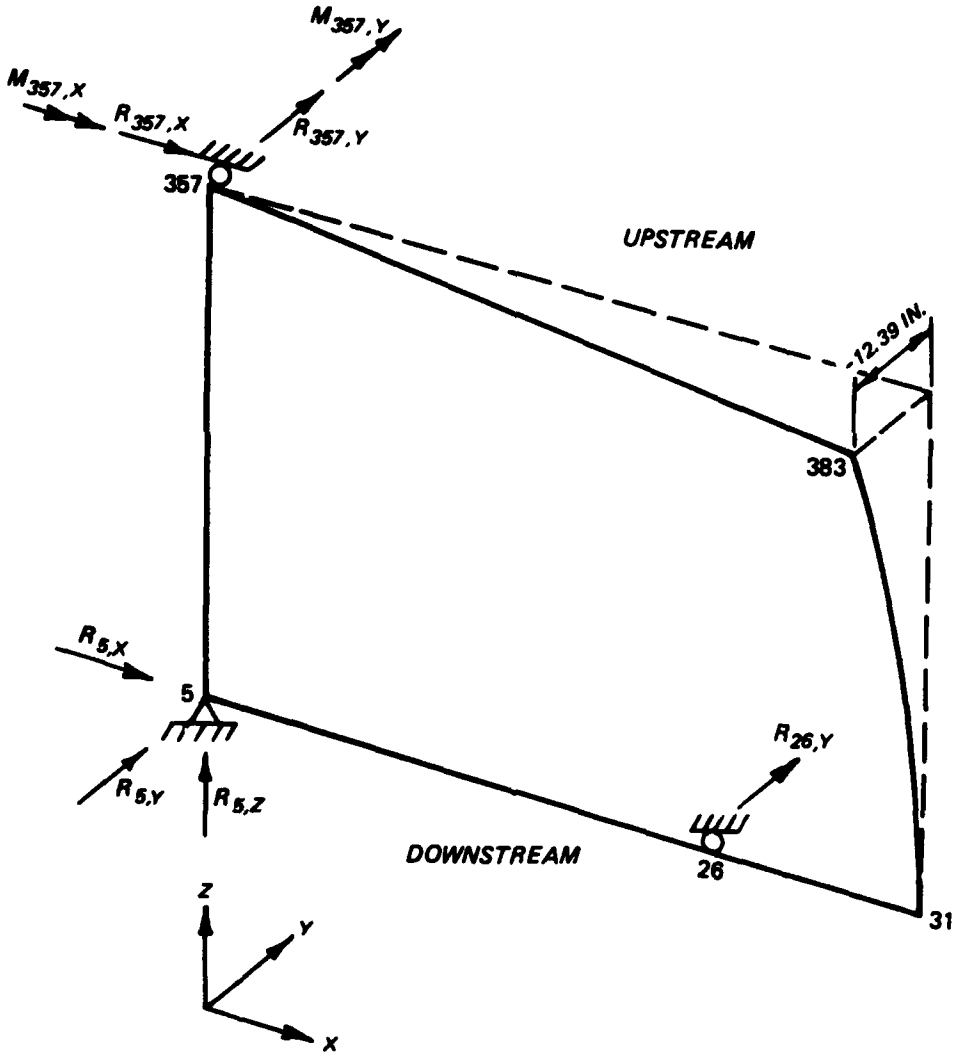

Figure 72. Conventional gate model ORH showing dead load displacements and out-of-plumb displacements

JOINT	5	357	26
Rx	147.09	-147.09	0
Ry	8.19	-8.19	0
Rz	308.81	0	0
Mx	0	0.25	0
My	0	0.29	0

UNITS: KIPS, INCHES

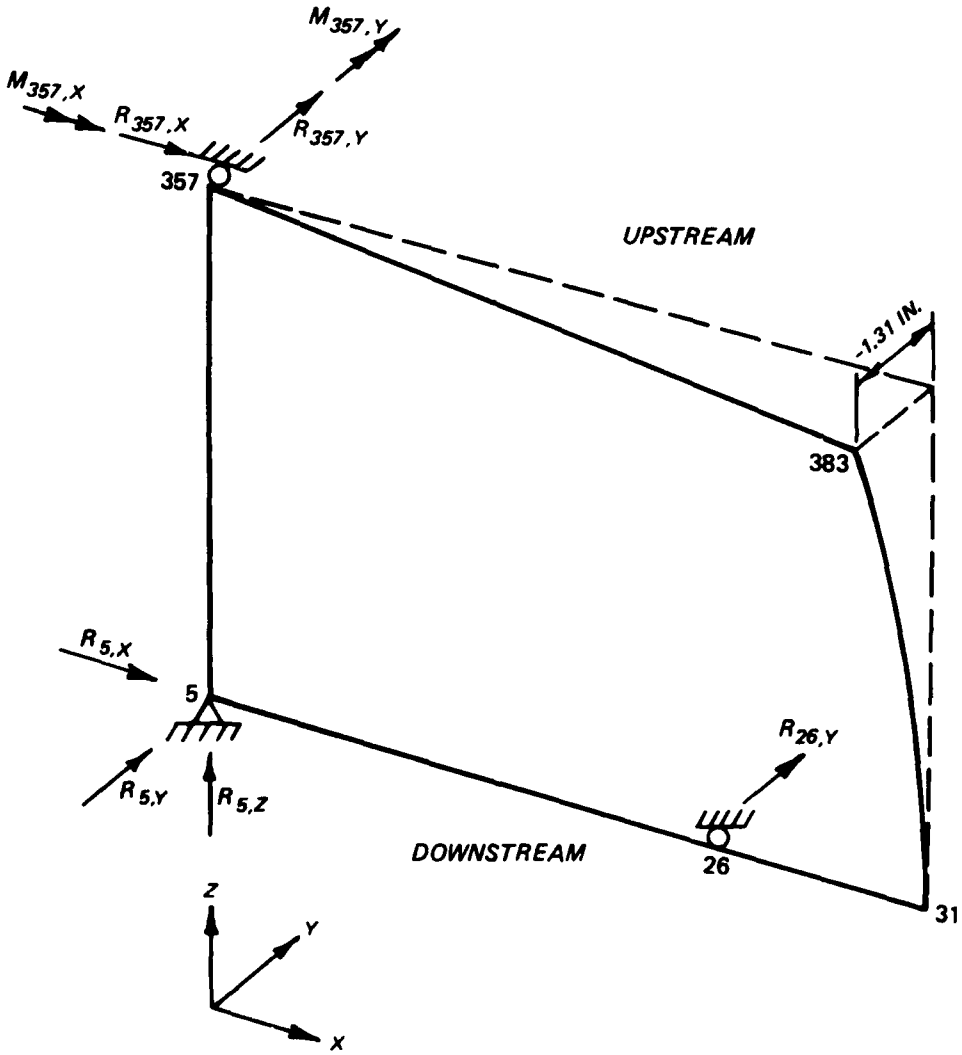

Figure 73. Torque-tube model ORHT showing dead load displacements and out-of-plumb displacements

JOINT	5	357	26
Rx	0	0	0
Ry	0	0	0
Rz	295.99	0	0
Mx	0	0	0
My	0	0	0

UNITS: KIPS, INCHES

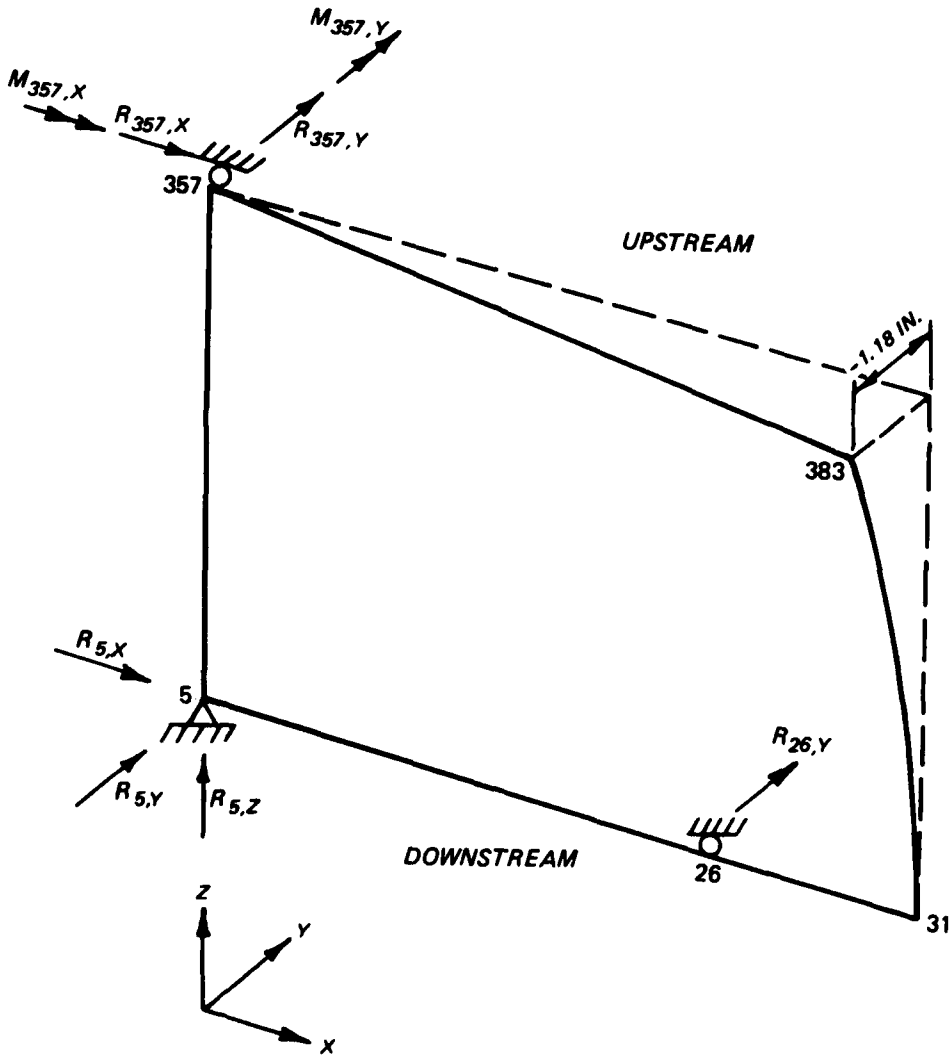

Figure 74. Torque-tube model ORHT1 showing dead load displacements and out-of-plumb displacements (positive diagonal only)

JOINT	5	357
Rx	144.76	-144.76
Ry	8.42	-8.42
Rz	304.22	0
Mx	0	-9.22
My	0	-57.65

UNITS: (KIPS, INCH-KIPS)

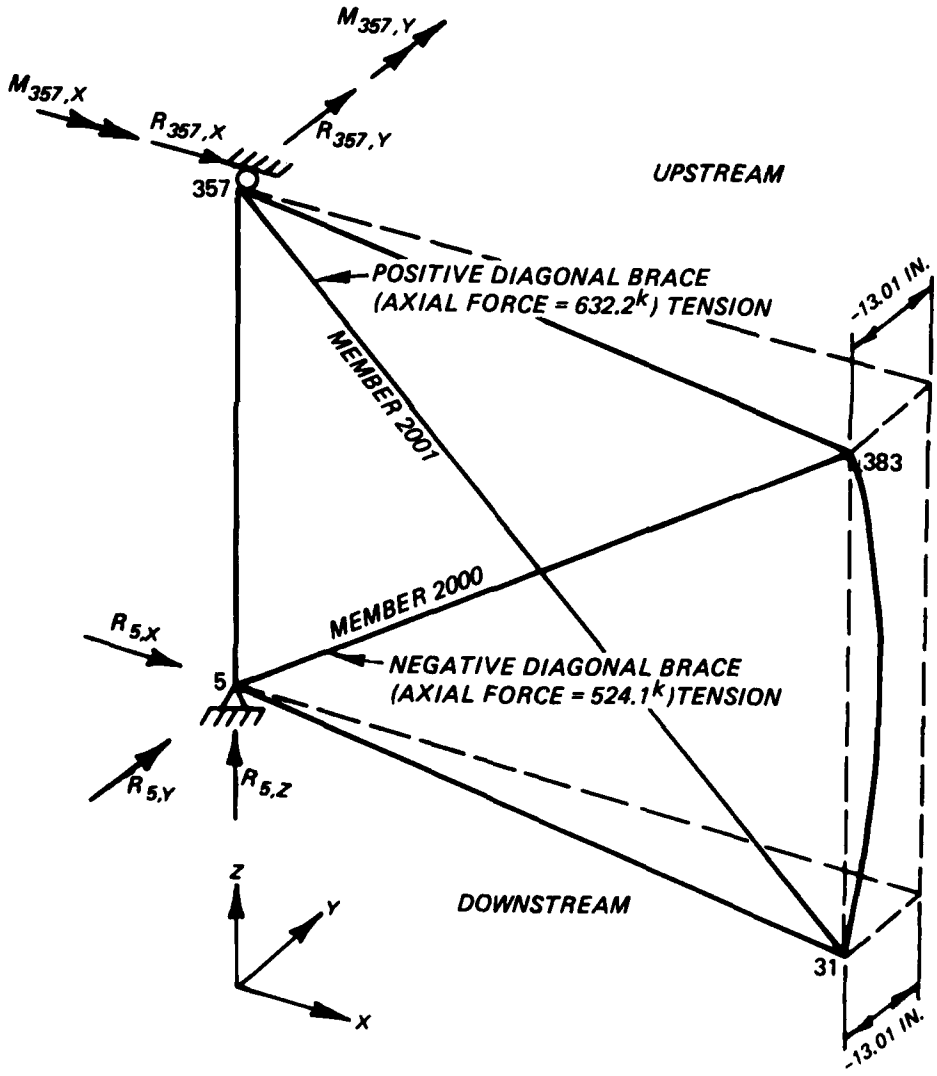

Figure 75. Reactions and joint displacements due to prestressing and dead load (load 13) for conventional gate model ORH

JOINT	5	357
Rx	152.95	-152.95
Ry	8.52	-8.52
Rz	321.16	0
Mx	0	0.52
My	0	-15.86

UNITS: (KIPS, INCH-KIPS)

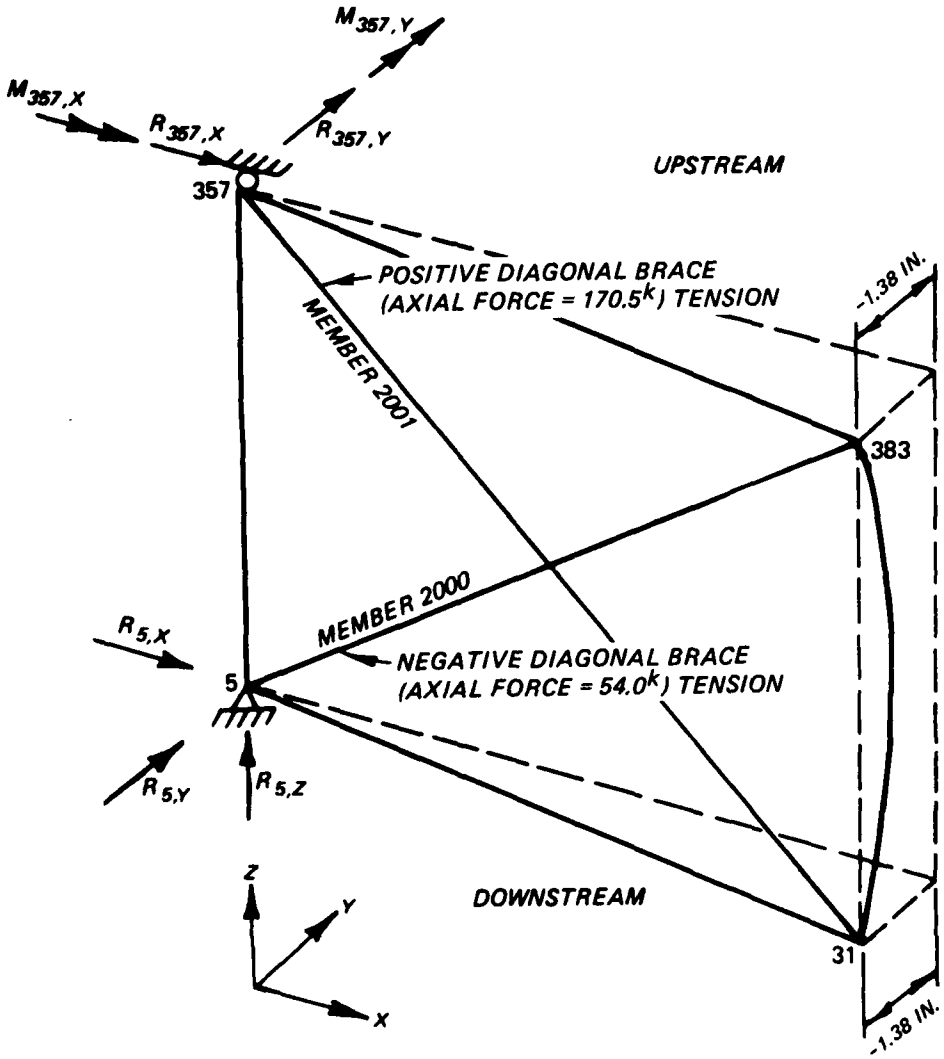

Figure 76. Reactions and joint displacements due to prestressing and dead load (load 13) for torque-tube model ORHT

JOINT	5	357
Rx	144.53	-144.53
Ry	7.54	-7.54
Rz	307.82	0
Mx	0	-1.42
My	0	-9.78

UNITS: (KIPS, INCH-KIPS)

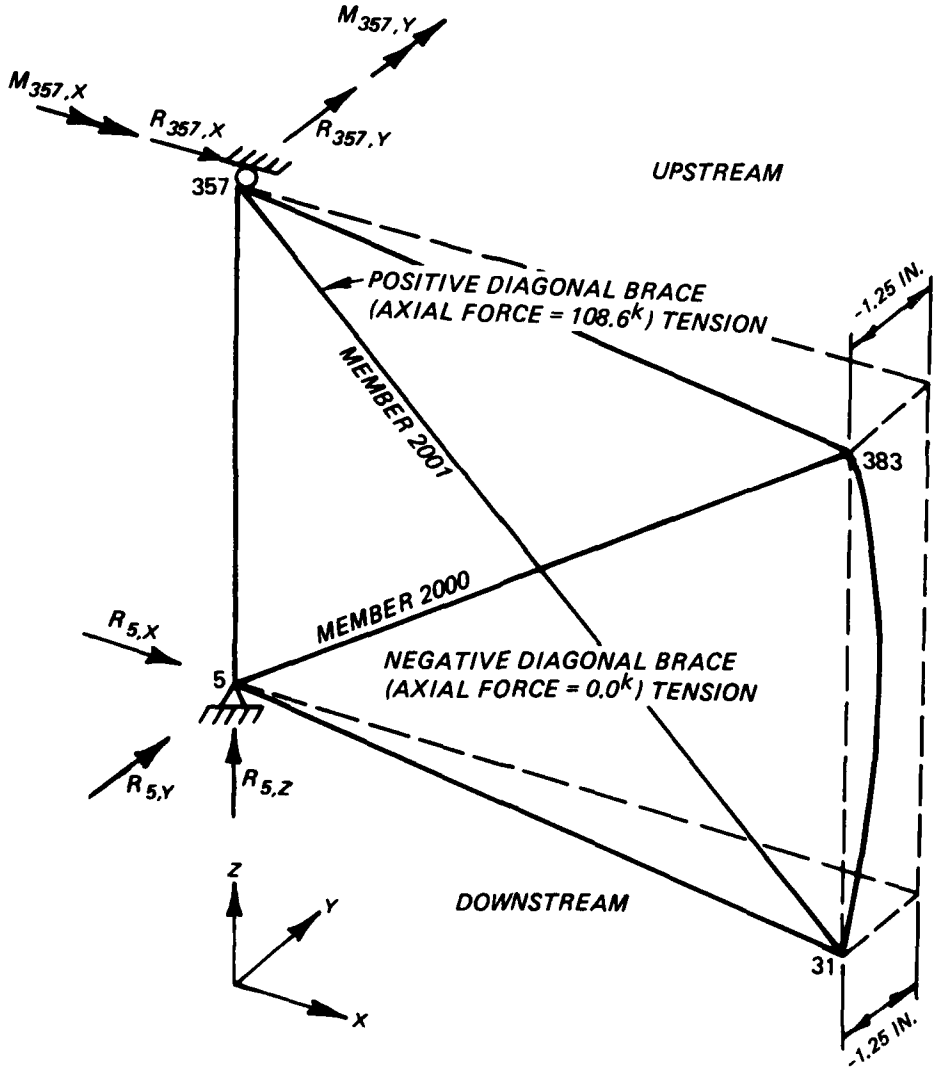

* Negative diagonal inactive.

Figure 77. Reactions and joint displacements due to prestressing and dead load (load 13) for torque-tube model ORHT1

JOINT	5	357	405
Rx	-0.01	-130.18	130.18
Ry	-69.99	107.21	-117.22
Rz	0	0	0
Mx	0	2.50	0
My	0	-7.19	0

UNITS: KIPS, INCHES

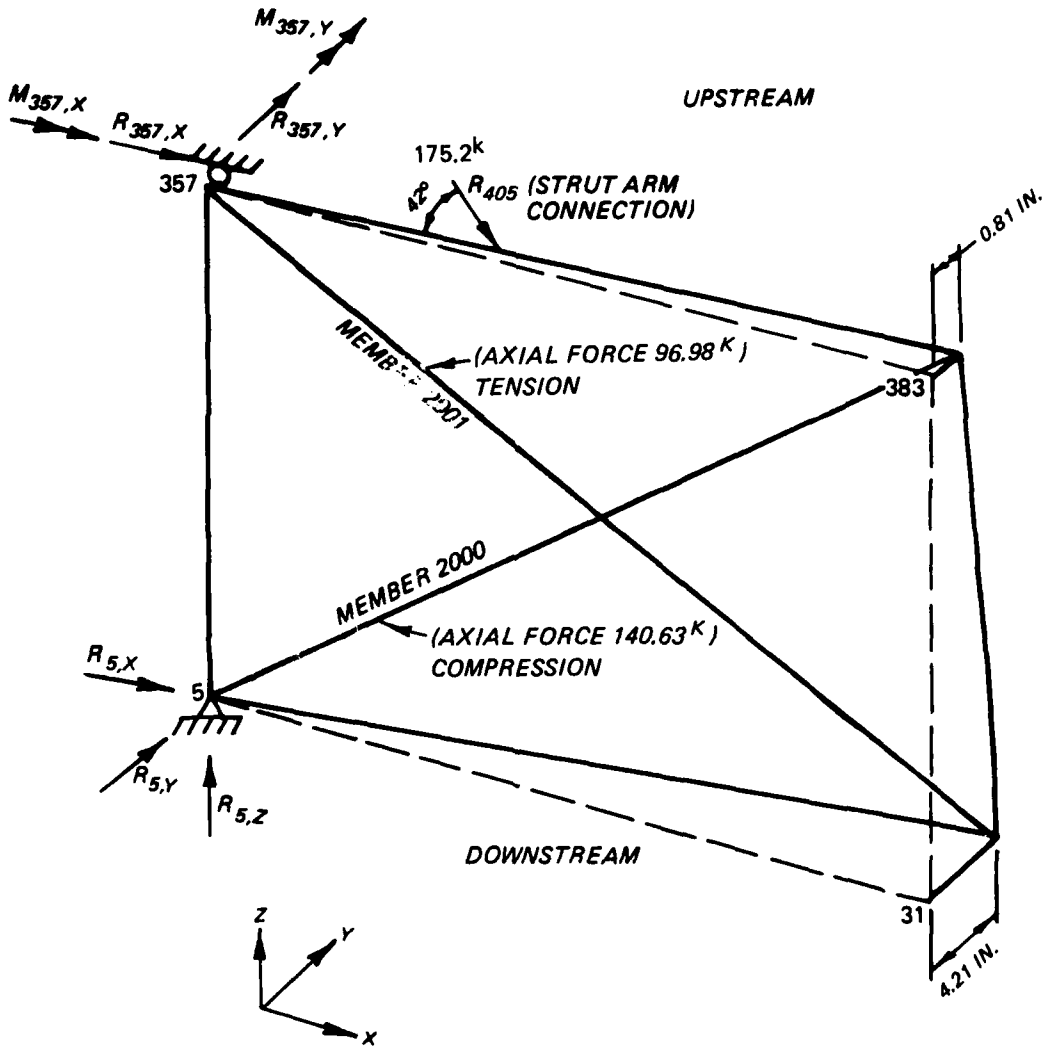

Figure 78. Reactions and displacements for conventional gate model ORH for temporal hydrostatic loading (load 4)

JOINT	5	357	405
Rx	0	-138.95	138.95
Ry	-74.22	113.95	-125.11
Rz	0	0	0
Mx	0	2.54	0
My	0	-3.76	0

UNITS: KIPS, INCHES

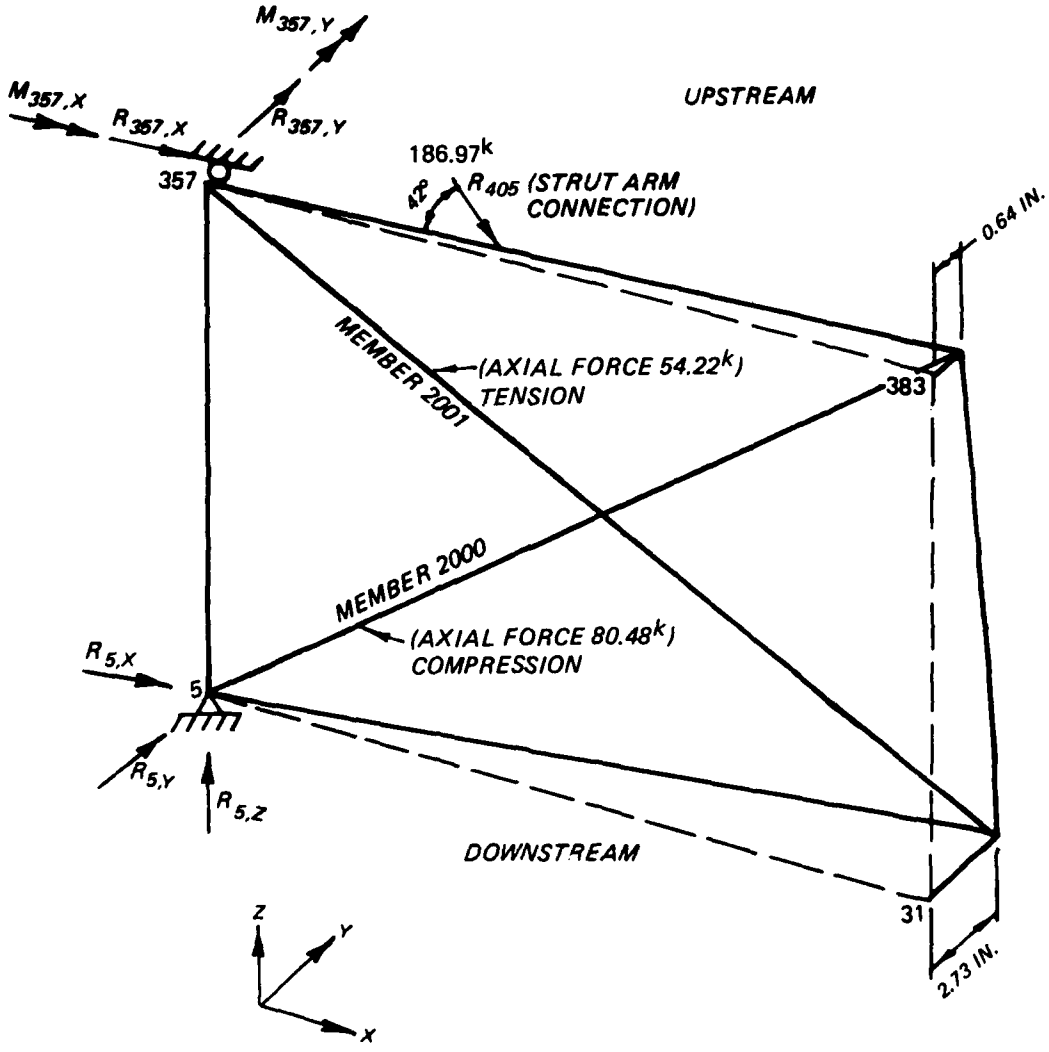

Figure 79. Reactions and displacements for torque-tube model ORHT for temporal hydrostatic loading (load 4)

JOINT	5	357	405
Rx	0	-141.83	141.83
Ry	-74.22	116.54	-127.71
Rz	0	0	0
Mx	0	0.52	0
My	0	-5.92	0

UNITS: KIPS, INCHES

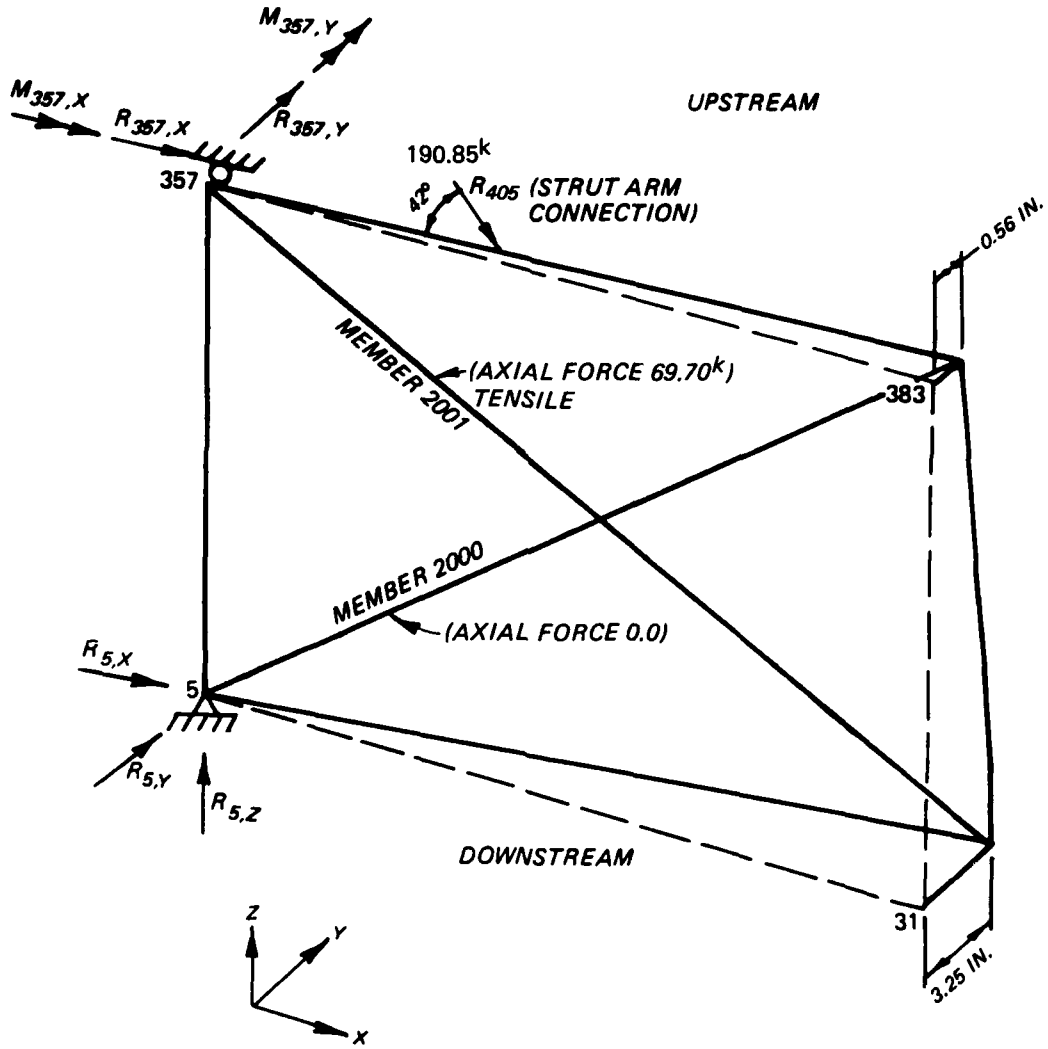

* Negative diagonal inactive.

Figure 80. Reactions and displacements for torque-tube model ORHT1 for temporal hydrostatic loading (load 4)

Table 12

Comparison of Gate Leaf Weights and Out-of-Plumb Displacements

Gallipolis Lower Miter Gate

Figure No.	Model	Weight kips*	Out-of-Plumb Displacement in.	Out-of-Plumb Displacement Ratio
32	Conventional Bankhead gate	571.86	8.91	1.0**
39	3S	576.22	1.60	0.180**
40	3SP	568.52	1.58	0.177**
72	ORH	292.52	12.42	1.0†
73	ORHT	308.81	1.30	0.105†
74	ORHT1	295.99	1.18	0.095†

* Includes weight of inactive diagonals but not of miscellaneous items such as rivets, weld material, etc.

** Relative to conventional Bankhead gate.

† Relative to conventional Gallipolis gate.

Table 13

Torsional Stiffness Comparisons

Model	Y-Reaction at Joint 26, kips	Relative Torsional Stiffness
ORH*	-1.38	1.0**
ORH with diagonals	-8.42	6.1**
ORHT	-20.32	14.7**
ORHT1	-15.40	11.2**
Conventional Bankhead gate	-2.88	1.0†
Conventional Bankhead gate	-9.725	3.4†
3S	-19.20	6.7†
3SP	-15.78	5.5†

* No diagonals.
** Conventional Gallipolis gate without diagonals taken as 1.0.
† Conventional Bankhead gate without diagonals taken as 1.0.

Table 14

Summary and Comparison of Jacking and Diagonal Force Results for Loadings 12 and 13, Gallipolis Gate

Model	Loading 12, kips		Loading 13, kips	
	Jacking	Negative Diagonal*	Negative Diagonal*	Positive Diagonal*
Conventional model ORH	254.49	1,515.5	524.1	632.2
Model ORHT	126.24	327.6	54.0	170.5
Model ORHT1	60.85	0.0**	0.0**	108.6
Conventional Bankhead gate	207.85	1,054.2	286.4	490.5
Model 3S	216.69	429.5	49.28	243.82
Model 3SP	139.5	0.0**	0.0**	190.6

* Tension force.
** Negative diagonal is deactivated.

130. Analysis of the various stress levels in the Gallipolis models showed all stresses to be well below the allowable limits. Similar to the Bankhead torque-tube studies, the Gallipolis torque-tube models offer a more uniform distribution of stress when compared to the conventional gate models.

Conclusions

131. Conclusions drawn in this study are based on analyses of selected gates. Therefore, strict design criteria based upon these studies cannot be recommended. However, the studies provide a better understanding of behavior of miter gate alternate configurations. Furthermore, analysis at the various Gallipolis gate models tends to verify the results obtained from the Bankhead gate analysis.

132. All portions of these studies which evaluated the overall behavior of a miter gate tended to verify conventional design assumptions. Torsional behavior of the conventional gate leaf is dictated by the presence of diagonals, which permit closed-section torsion of the gate rather than thin-member torsion.

133. Analyses of the gate models have focused on their performance characteristics, relative to conventional gate, in the following areas: (a) deadweight and out-of-plumb displacements (Tables 9 and 12), (b) torsional stiffness values (Tables 10 and 13), (c) jacking and diagonal forces due to prestressing (Tables 11 and 14), (d) response to hydrostatic and temporal loadings, and (e) reaction forces and stress states associated with hydrostatic, temporal, and jacking and prestressing loadings. The aforementioned tables present summary data to support the principal findings of the study and are discussed below.

134. The analyses indicate that the double-skin plate model is a considerably stiffer structure than the original Bankhead design. The dead load out-of-plumb deflection at the miter end was predicted to be 0.044 in. for the double-skin model as compared with 8.907 in. for the conventional gate model. This large reduction in the deflection is due to the fact that the shear center is much closer to the center of gravity and also that the torsional stiffness of a gate with closed cross section is much larger than that of the original Bankhead design with open cross sections. Although the double-skin plate model is stiffer than the original Bankhead model, there are several

disadvantages in using the double-skin plate: (a) increased amount of steel required (approximately 10 percent), (b) increased cost and/or difficulty in fabricating the closed sections, and (c) increased maintenance costs and difficulty of inspection of the enclosed regions.

135. Enlarging the diagonals to twice the cross-sectional area values used for the conventional Bankhead gate results in a weight increase of 3 percent and causes a 5 percent increase in dead load deflection. At the same time, the torsional stiffness of the gate is increased 15 percent by the larger diagonals yielding a 13 percent reduction in twist displacements because of temporal loading. For jacking and prestressing operations, a 24 percent (or 50 kips) increase in jacking force is required for the enlarged diagonal case, and the final diagonal forces are increased by 20 to 30 percent over corresponding values for the conventional gate. Overall, the conventional gate with enlarged diagonals appears to be a less economical and largely ineffective, yet very simple, approach to improved gate performance.

136. A comparison of torque-tube models 1 and 1L reveals that model 1L offers significant improvements over model 1 with dead load displacements reduced to one half of model 1 values. At the same time, deadweight of the leaf was increased by just 7 kips (1.2 percent) due to the increase in size of horizontal torque tubes. Model 1L shows a 37 percent improvement over model 1 in torsional stiffness and a 30 percent reduction in gate twist as a result of temporal loading. However, models 1 and 1L both produce areas of concentrated stresses in the quoin end diaphragm due to jacking. Finally, model 1L has the requirement for additional horizontal access holes for inspection of the enlarged top and bottom torque tubes.

137. Models 3, 3S, and 3SP offer a more uniform distribution of stiffness and stress than models 1 or 1L. Model 3 has greatly increased torsional stiffness and thus a small dead load deflective value. However, model 3 is 15 kips or more (approximately 3 percent) heavier than models 1, 1L, 3S, or 3SP and may be too stiff in that the required jacking force for model 3 exceeds that of the models 1L and 3S by roughly 160 kips and exceeds model 3SP by approximately 240 kips. On the other hand, models 3S and 3SP have the same uniformity of stress distribution as model 3. The prestressing jacking force for model 3S is approximately the same as the conventional gate. However, the jacking force for model 3SP is approximately 68 kips less than the conventional gate.

138. The access holes in girder web plates investigated in model 3 produced a negligible difference in the out-of-plumb displacement and torsional stiffness of model 3, 3S, or 3SP. In addition, the differences in the behavior due to the hydrostatic loading were also negligible. Therefore, the access holes have little effect on the gross behavior of models 3, 3S, or 3SP.

139. The Gallipolis gates are about two thirds the height of the Bankhead gates and both are the same width. As previously discussed, the model studies for both gates have demonstrated that improvement in gate performance can be achieved with torque-tube configurations.

140. These studies have also shown that torque-tube models offer several advantages over conventional gates as well as the double-skin plate model. The diagonals on torque-tube models were found to slightly alter the torsional stiffness and stress distributions due to hydrostatic and temporal loadings. The effect of the vertical access hole was also found to be negligible on the overall behavior of the gate. Therefore, torque-tube models appear to offer an excellent alternative to conventional gate design for the reasons noted above. A summary of the advantages and disadvantages of torque-tube models is shown in Table 15.

Discussion

141. All of the methods of increasing leaf stiffness were evaluated according to increase in leaf stiffness, added weight of gate leaves, complexity of fabrication, maintenance, and repair.

142. Since the top horizontal tube would not be subjected to submergence in the lower pool on a routine basis, inspection and maintenance for this section would be minimal. Inspection and maintenance on the bottom horizontal torque tube would also be easier and safer since the elevation above the sill is minimal. The vertical tubes with access through bolted cover plates or manholes in vertical diaphragms would require that inspection and maintenance workers enter at each girder level with some leaves being more than 100 ft in height.

143. The diagonal size used on Bankhead was not determined in relation to temporal load, since this was not a design consideration at that time. The significant point is that conventional diagonals of a larger size could have increased the torsional stiffness of the Bankhead leaves considerably, as much

Table 15

Evaluation of Torque-Tube Model Results

Model	Advantages	Disadvantages
1 Double-skin plate over entire gate leaf between end diaphragms	Enormous stiffness.	Judged too difficult to adjust for exact closure and too expensive to fabricate and difficult to maintain. Not pursued further.
Horizontal top and bottom torque tubes	Reasonable jacking force of 186 kips. Approximately same weight as original gate.	Too flexible, 3.5-in. dead load. Low torsional stiffness versus models 1L, 3, 3S. Higher stresses in diaphragms due to jacking than model 3 or 3S. Nonuniform distribution of stiffness.
1L Enlarged horizontal top and bottom torque tubes	Stiffer than model 1. Approximately same stiffness as model 3S. Approximately same weight as original gate. Jacking force still achievable.	Nonuniform distribution of stiffness. Higher stress in diaphragms than model 3 or 3S. More flexible than model 3S and especially model 3. Requires horizontal access holes for inspections.
Horizontal torque tubes between top two girders and between bottom two girders; vertical torque tubes between each end diaphragm and the adjacent first interior diaphragms; forming a continuous tube all around the gate leaf	Significant improvement in stiffness over model 1. It seemed promising enough to warrant modifying into model 3.	Judged too difficult to fabricate and too difficult to maintain.
3 Side torque tubes between end diaphragms and second interior diaphragms	Stiffest torque-tube model. Very little dead load deflection. Uniform distribution of stiffness.	Too stiff. Jacking force of 378 kips required if diagonals are used. Heaviest torque-tube model. Requires vertical access holes. If diagonals are used, one carries very little force.

(Continued)

Table 15 (Concluded)

Model	Advantages	Disadvantages
3S Reduced side torque tubes, between end diaphragm and first interior diagphragm	Dead load deflection and torsional stiffness approximately the same as model 1L. Jacking force approximately the same as model 1L. Weight approximately the same as model 1L. Uniform distribution of stiffness. Produces lower stresses than model 1L.	Not as stiff as model 3. Requires vertical access holes through all girders at both ends. Requires two additional diaphragms.
3SP Model 3S with positive diagonal only	Dead load deflection is same as model 3S and weight is the lowest of all models. Torsional stiffness is less than model 3S. Jacking and diagonal forces are considerably lower than all other models. Uniform distribution of stiffness and stresses.	Not as stiff as model 3. Requires vertical access holes through all girders at both ends. Requires two additional diaphragms.
ORHT Gallipolis gate with vertical side torque tubes	Large decrease in dead load deflection and increase in torsional stiffness compared to conventional gate. Jacking force is one half the conventional gate value. Diagonal forces are significantly reduced.	Heavier weight than conventional gate. Requires vertical or horizontal access holes through intermediate diaphragms or girders. Requires additional diaphragms.
ORHT1 Model ORHT with positive diagonals only	Lighter weight than model ORHT but a similar increase in torsional stiffness compared to conventional gate. Approximately same weight as conventional gate. Jacking force less than one quarter the conventional gate value. Positive diagonal force one sixth the conventional gate value.	Not as stiff as model ORHT. Same access hole requirements as model ORHT. Requires additional diaphragms.

as twice or more. This fact should be considered when comparing methods for increasing gate stiffness.

144. There are many areas of consideration to be evaluated on each gate. Conventional diagonals may be the acceptable choice for smaller gates not subject to unusual loadings. On the other edge of the spectrum, torque tubes have merit for larger gates with unusual loading conditions. The use of vertical, horizontal, or a combination of the two systems of torque tubes will also have to be selected on an individual gate basis. Experience indicates that diagonals may, in all probability, be required to align the miter ends of the leaves, due to fabrication tolerances and variation in gudgeon pin and pintle locations. However, if miter bar attachments, castings or weldments, could provide upstream or downstream adjustment of miter ends of torque-tube gates, there might no longer be a need for diagonal stiffeners.

145. Increased fabrication cost is to be expected where torque tubes are used, with the vertical tubes somewhat higher due to the greater number of compartments. Inspection and maintenance will also have an increased cost, again with the vertical tubes having an increase due to the number of compartments and travel distance from the surface for workmen with equipment. For some gates, the additional initial cost and increased maintenance may be outweighed by other benefits, thereby making torque tubes the better choice. Only actual fabrication and construction will determine if horizontal or vertical torque tubes are an acceptable and workable solution for increasing leaf stiffness.

146. There is also some indication at this point that an increase in stiffness may have detrimental side effects. Cracking of flange to gusset plate connections and loss of gate leaf ability to deflect slightly and achieve a reasonable bearing transfer position of the miter ends are among the undesirable effects. This occurs on a daily basis when the temperature changes and the leaves are not perfectly aligned vertically, with slight changes in diagonals which usually cause a small negative deflection.

147. Another significant factor is that the ratio of deflection to stiffness is nonlinear for conventional diagonals. The conventional gate leaves without diagonals require little torque to twist the leaves a small amount. While the diagonals increase the amount of torque required for the first inch away from the plumb, the ratio of torque to deflection is still similar to the leaf without diagonals. The leaves with torque tubes may

follow this same pattern, and possibly influence the need for diagonals in conjunction with torque tubes.

Recommendations

148. While the use of torque tubes appears to offer a potentially acceptable means of increasing leaf stiffness for miter gates, only actual fabrication and construction, combined with an extended period of operation, will determine if the method will, in reality, be beneficial. There may be side effects, other than possible weld cracking and loss of ability to deflect into an acceptable miter position, that would be unacceptable. It is, therefore, recommended that the utilization of horizontal and/or vertical torque tubes, be approached carefully. The selection of these systems for individual gates should be made only after prudent consideration of all factors, including but not limited to, structural integrity, fabrication cost, and maintenance. This selection should also give due consideration to possible future leaf modifications to alleviate problems and return the gate to a more conventional status, should side effects be too detrimental. Detailed records of all aspects of design, fabrication, construction, maintenance, repair, and performance must be accurately documented for a proper system evaluation.

149. It is too soon to recommend a method of increasing stiffness that could apply to all miter gates as a part of normal and standard design procedure. The FE method of analysis, while valuable and worthwhile, must be compared with and supported by known facts. This can only be accomplished by designing, fabricating, instrumenting, and operating a miter gate of alternate configuration.

REFERENCES

American Institute of Steel Construction. 1978 (Nov). "Specification for the Design, Fabrication, and Erection of Structural Steel for Building," 8th ed., American Institute of Steel Construction.

Blodgett, O. W. 1976. "Design of Welded Structures," The James F. Lincoln Arc Welding Foundation, Cleveland, Oh.

Cherng, M. D., Phang, M. K., and Chang, C. H. 1983 (Oct). "Miter-Type Navigation Lock Gates," Journal, Structural Engineering, American Society of Civil Engineers, Vol 109, No. 10.

Emkin, L. Z., Goodno, B. J., and Will, K. M. "Finite Element Studies of a Horizontally Framed Miter Gate; Initial and Refined Finite Element Models (Phases A, B, C)," Technical Report ITL-87-4, Report 1 (in preparation), Georgia Institute of Technology, Atlanta, Ga., and US Army Engineer Waterways Experiment Station, Vicksburg, Miss.

_____. "Finite Element Studies of a Horizontally Framed Miter Gate; Simplified Frame Model (Phase D)," Technical Report ITL-87-4, Report 2 (in preparation), Georgia Institute of Technology, Atlanta, Ga., and US Army Engineer Waterways Experiment Station, Vicksburg, Miss.

_____. "Finite Element Studies of a Horizontally Framed Miter Gate; Alternate Configuration Miter Gate Finite Element Studies--Open Sections," Technical Report ITL-87-4, Report 3 (in preparation), Georgia Institute of Technology, Atlanta, Ga., and US Army Engineer Waterways Experiment Station, Vicksburg, Miss.

_____. "Finite Element Studies of a Horizontally Framed Miter Gate; Alternate Configuration Miter Gate Finite Element Studies--Closed Sections," Technical Report ITL-87-4, Report 4 (in preparation), Georgia Institute of Technology, Atlanta, Ga., and US Army Engineer Waterways Experiment Station, Vicksburg, Miss.

_____. "Finite Element Studies of a Horizontally Framed Miter Gate; Alternate Configuration Miter Gate Finite Element Studies--Additional Closed Sections," Technical Report ITL-87-4, Report 5 (in preparation), Georgia Institute of Technology, Atlanta, Ga., and US Army Engineer Waterways Experiment Station, Vicksburg, Miss.

_____. "Finite Element Studies of a Horizontally Framed Miter Gate; Elastic Buckling of Girders in Horizontally Framed Miter Gates," Technical Report ITL-87-4, Report 6 (in preparation), Georgia Institute of Technology, Atlanta, Ga., and US Army Engineer Waterways Experiment Station, Vicksburg, Miss.

Headquarters, Department of the Army, Office of the Chief of Engineers. 1984. "Lock Gates and Operating Equipment," Engineer Manual 1110-2-2703, Washington, DC.

APPENDIX A: SUMMARIES-FINITE ELEMENT STUDIES OF A HORIZONTALLY FRAMED METER GATE

		Page
PART I:	GENERAL OVERVIEW	A-2
PART II:	SUMMARY OF REPORT 1, "INITIAL AND REFINED FINITE ELEMENT MODELS (PHASES A, B, C)"	A-3
PART III:	SUMMARY OF REPORT 2, "SIMPLIFIED FRAME MODEL (PHASE D)"	A-14
PART IV:	SUMMARY OF REPORT 3, "ALTERNATE CONFIGURATION MITER GATE FINITE ELEMENT STUDIES -- OPEN SECTIONS"	A-17
PART V:	SUMMARY OF REPORT 4, "ALTERNATE CONFIGURATION MITER GATE FINITE ELEMENT STUDIES -- CLOSED SECTIONS"	A-21
PART VI:	SUMMARY OF REPORT 5, "ALTERNATE CONFIGURATION MITER GATE FINITE ELEMENT STUDIES -- ADDITIONAL CLOSED SECTIONS"	A-26
PART VII:	SUMMARY OF REPORT 6, "ELASTIC BUCKLING OF GIRDERS IN HORIZONTALLY FRAMED MITER GATES"	A-31

PART I: GENERAL OVERVIEW

1. The appendix to this report includes information from the introductions, summaries, and conclusions of the six separate miter gate finite element studies (in preparation) of the John Hollis Bankhead Lower Miter Gate, Black Warrior River, Ala., listed and numbered for cross referencing in the preface to this report. These reports were prepared by Drs. L. Z. Emkin, K. M. Will, and B. J. Goodno of the Georgia Institute of Technology under the direction of the Computer-Aided Structural Engineering (CASE) Project managed by the Information Technology Laboratory, US Army Engineer Waterways Experiment Station.

2. A summary of the separate finite element studies and how they interrelate is also included in the preface.

PART II: SUMMARY OF REPORT 1, "INITIAL AND REFINED FINITE ELEMENT MODELS (PHASES A, B, C)"

Scope

3. Report 1 describes Phases A, B, and C of the study series as investigations with both member and plate finite elements used to represent one gate leaf. This summary of Report 1 focuses on the different phase studies and how they relate and are involved.

Phase A Study

Objective

4. The primary objective of the Phase A study was to develop a gross mesh finite element (FE) model of one leaf of the miter gate and to investigate its deformational behavior for a variety of construction and operational loadings.

5. The original plan of the Phase A study called for a gate model having as few degrees of freedom as practicable. Skin and thrust plates were to be represented by planar FE's, while the horizontal girders, vertical diaphragms, and intermediate stiffener members were to be added as one-dimensional member elements.

6. After study of the displaced shape of the model for gravity loads, it became apparent that the model was too flexible and did not properly account for torsional stiffness properties of the horizontal girders and vertical diaphragms. After several iterations and test runs were made of a member of modeling refinements including finite size of framed joints and member eccentricities, it became apparent that a better FE model was needed.

Approach

7. The final model in Phase A of this study employs member elements to represent the horizontal girder and vertical diaphragm flanges, intercostal angles, and web stiffener plates. The same model functioned with prestressing diagonals and plate FE's to represent the girder webs, vertical diaphragm plates, and quoin and miter region thrust and connecting plates. The static analysis of a single leaf was performed for gravity, temperature, and hydraulic loadings for several different sets of gate support conditions. The

sequence of diagonal prestressing operations (before, during, and after application of prestressing forces) was considered in the analysis using a superposition procedure.

Summary

8. A variety of member and FE representations of the overall leaf model were developed and analyzed for self-weight loadings to calibrate the computer models. In each instance, however, the computer models were found to be much too flexible in that computed displacements for gravity loads were several times larger than values observed in the field. Successive refinements were made to the model so as to include all possible sources of stiffness in the leaf structure; diagonal connection plates and finite size of framing joints were found to be the principal contributors to this added stiffness. A series of computer experiments involving a two-girder model showed that mesh refinement alone was not sufficient to explain the discrepancy between observed and computed gate performance; however, the refined mesh model would be required for stress computations in follow-up studies. In the final analysis, a coarse mesh (CM) model of the entire leaf, employing member elements for girder and diaphragm flanges, intercostals, web plate stiffener bars, and prestressing diagonals, was assumed to be a sufficiently accurate model of the structure for the Phase A study. This final model was analyzed for temperature and hydraulic loadings, and a special superposition analysis sequence was developed to properly account for construction jacking operations and their effects on diagonal member forces.

Conclusions and Recommendations

9. It is clear from the Phase A study that the CM model which employed member elements to represent vertical diaphragms and horizontal girders is totally inadequate for use in predicting gate leaf deformational behavior. For the dead load analysis in the Phase A study, it was necessary to use the CM FE model of the gate in which FE's are used to define vertical diaphragm and horizontal girder webs. While the more refined model proved entirely adequate for study of the gate leaf in a fully mitered configuration, it did not yield reasonable displacement response values (compared with reported field displacements) for the unprestressed gate leaf acted upon by gravity loads only; in addition, the stress distribution obtained during prestressing operations is inconsistent and will require further study with this model. In essence, it appears that the twisting stiffness of the gate leaf is not well

represented by the Phase A CM FE model. Additional study and, perhaps, field verification of properties, diagonal prestressing operations, etc. may be required before satisfactory behavior is finally achieved.

10. It does appear that the Phase A study resulted in the development of a sequential analysis procedure which accurately represents the actual field prestressing operation and its resulting effects on the diagonals. In addition, the jacking force was accurately predicted by the model.

11. An attempt was made to give an overall sense of the stress levels produced in certain regions of the gate for selected loadings. While some of the stresses were high and most were well below allowable values, it must be noted that an accurate determination of element stresses in the model will require mesh refinement in selected regions of the structure. Determination of element stresses in vertical diaphragms near the bottom of the gate, in diagonal connector (gusset) plates, and in horizontal girder web and thrust plates near quoin and miter ends are strongly recommended for follow-up studies, once model twisting stiffness has been properly accounted for. Until the model is capable of predicting accurate element stresses for all applied loadings, it is a meaningless, albeit simple, exercise to compare present stress values with results of hand computations provided by the US Army Engineer District, Mobile. This was not done in the Phase A study, but should be a high priority task for the subsequent studies.

12. The principal task for follow-up studies must be the continuation of parameter studies initiated with the two-girder model studies, which are used to identify all factors influencing gate leaf twisting stiffness. The two-girder models have shown that finite size of framing joints is an important modeling refinement which cannot be neglected, whereas mesh refinement alone as well as the torsional stiffness of horizontal girder flanges do not significantly affect gate twisting stiffness under gravity load. It is recommended that these parameter studies be continued to identify all factors contributing to dead load response of the gate leaf.

13. With a proper description of gate leaf stiffness properties, it will be possible to consider such additional and important loadings as the effect of wedging of an obstruction at the quoin or under one leaf while opening or closing the gate, or the effect of one diagonal breaking during leaf opening or closing as originally proposed in the scope of work for the Phase B

analysis. Successive refinement of the present model is of fundamental importance to these additional studies.

Phase B Study

Objectives

14. The objective of the Phase B study can be summarized as follows:

a. Develop a fine-mesh verification model for comparison with Phase A model II.

b. Check the torsional stiffness of the gate leaf model with diagonals prestressed to actual field-measured values; also compare torsional stiffness with hand-calculated values from US Army Engineer (USAE) District, Mobile. Work in this area resulted in new prestressing and analysis procedures. However, based on discussions with Mr. James D. Gibson of Q-values and related hand-calculation procedures used by the USAE District, Mobile, a direct comparison of torsional stiffness values using computer and hand-based computational approaches may not be possible at this time because vastly different approaches are used.

c. Compare hand-calculation and model stress results for horizontal girder 10 at the center line of the leaf and at the end diaphragm for normal hydrostatic loading. The hand calculation results were to be obtained from the USAE District, Mobile.

d. Check distribution of forces in the gudgeon pin, pintle, strut-arm connection, and diagonal gusset plate regions of the structure. The free-body diagrams of portions of the gate leaf and procedures used to obtain section nodal forces are described. Force distribution results for specific loadings and analysis conditions are detailed.

e. The final task in the overall scope of work for the Phase B study involved the following set of prioritized analysis conditions:

(1) Find the distribution of dead load and jacking and diagonal prestressing loads to skin plate, diaphragms, girders, and gusset plates.

(2) Determine the distribution of forces in the strut-arm connection area for temporal head loading.

(3) Find gate leaf stresses and deformations due to temperature loads and high pool/low pool loading on a mitered gate.

(4) Discuss the distribution of forces and stresses in vertical diaphragms during prestressing, normal hydrostatic, and temporal head loading conditions.

15. The work conducted under Phase B of the overall investigation of the structural performance of miter gates is organized into two principal

parts. First, the fine mesh model and model verification procedures are described. Then, organized into separate sections according to analysis conditions used, the results of specific analysis are presented. Finally, a summary of the principal findings of the Phase B study, a statement of major conclusions, and recommendations for further work are presented.

Summary and Conclusions

16. The following conclusions are based on the Phase B results:

a. The Phase B fine mesh analysis, as was the case of the Phase A coarse mesh, was unable to accurately predict the out-of-plane warping of the gate leaf due to dead load alone with no prestressing diagonals in place. Therefore, it is the opinion of the authors that:

(1) There may be certain behavioral characteristics that have not been adequately modeled, and/or

(2) There may be certain in situ conditions which were not known and not modeled, and/or

(3) There may be certain construction sequences which affected the behavior, but which were not modeled.

b. Comparisons between the fine and coarse mesh indicated that the coarse mesh produced the same overall behavior with similar values of joint displacements, support reactions, and stress contours in the skin plate. The comparison also indicated that the stress distributions were vastly different in the horizontal girder webs and in the interior vertical diaphragms. This was due to the element type and mesh size differences in these regions. However, since the CM produced the same overall displacement behavior, and was less expensive to analyze, and also since it was believed that the resultant nodal force distributions were very similar between the coarse and fine meshes (even though some stress distributions were not), it was decided that the coarse mesh should be used in this study.

c. The Phase B prestressing superposition procedure that was formulated to produce diagonal prestressing forces which matched the field-measured values also produced miter end displacements which were not plumb. This was expected since matching prestressing forces was the goal, rather than producing a plumb miter end.

d. The stress levels throughout the gate are low for the dead load case alone (LOAD 11).

e. During prestressing, the critical stresses occur when the jacking force is applied with the negative diagonal in place. This is expected.

f. The flow of the force in the gate leaf due to the temporal loading for gate closing is primarily through horizontal

girders 1, 2, 16, 17, and 18 (i.e., the top two girders and the bottom three girders). In addition, in this case, the positive diagonal picks up 82.6^k in tension, while the negative diagonal picks up 140.1^k in compression.

g. Gravity loads were observed to be distributed largely through the skin plate into the quoin post region, and then down to the pintle support. This was expected.

h. Flow of forces due to hydrostatic loads is primarily horizontal through the horizontal girders. This confirms the assumptions used to perform the design of the horizontal girders by hand. However, computer computed stresses could not be used to verify girder stresses computed by hand. This is due to the fact that hand-calculation procedures for girder stresses use effective widths, while the FE model used the full skin plate to resist applied loads.

i. The temperature loading used in this study did not produce significant reactions or stresses in the gate. However, a more accurate representation of the temperature distribution in the gate is needed before temperature can be ruled out as causing adverse effects.

j. Force flow due to the prestressing procedure appeared consistent with the twisting and bending actions of the gate under the application of the jacking force.

k. Diaphragm stresses were noted to be highest during application of jacking in the prestressing procedure.

Recommendations

17. The following recommendations are made:

a. Field measurements should be made of the Bankhead miter gate in its in situ state to determine if there are physical conditions not considered by the computer model.

b. A new miter gate under construction should be selected and carefully monitored as to construction procedures, physical dimensions, etc., and careful measurements made of gate deformations during the various phases of construction. This new gate could then be used to revise the computer modeling procedures used herein.

c. Additional, and possibly more critical, loading conditions should be investigated. These include uneven miter in combination with normal operating loadings, wear of quoin or miter blocks, misalignment of quoin or miter bearings, etc.

d. A more refined model of the connection detail of the prestressing diagonals and the gusset plates should be developed and its influence determined.

e. Displacement, due to temperature effects, of the coarse mesh model of Phase B should be displayed.

Phase C Study

Objectives

18. The objectives of the Phase C work were to:

a. Develop a more refined model of the connection of the prestressing diagonals to the gusset plates. Figure 1 shows the refinement used at the ends of the prestressing diagonals at joints 'DC1', 'DC2', 'DC3', and 'DC4'.

b. Determine the influence of the refined diagonal connections on the prestressing superposition procedure, on the alignment of the miter end, and on the distribution of boundary nodal forces in the free-body near the pintle and in the free-body near the gudgeon pin. Figure 2 shows a view of the free-body used near the pintle, and Figure 3 shows a view of the free-body used near the gudgeon pin.

c. Display the displacements of the CM model of Phase B due to the effects of temperature alone.

Summary

19. The more refined diagonal connection model of the Phase C work caused the following changes of results when compared with the original CM Phase B model:

a. The stiffness of the gate with respect to a downstream unit displacement increased 13 percent for the intermediate jacking case (only a negative diagonal in place), and increased 20 percent for the fully prestressed case (both positive and negative diagonal in place).

b. The superposition factors f_1 , f_2 , and f_3 changed a great deal. However, the changes were such that they had a small effect on the final force distribution in the gate.

c. The prestressing jacking force decreased by 16 percent.

d. For the intermediate jacking load case, relatively large changes occurred in the resultant boundary nodal forces in the region of the pintle and gudgeon pin, with a weighted average overall decrease of approximately 18.9 percent. This appears to be consistent with the decrease in jacking force of 16 percent.

e. For the fully prestressed state, relatively small changes occurred in the resultant boundary nodal forces in the region of the pintle and gudgeon pin, with a weighted average overall increase of approximately 0.88 percent.

f. Displacements due to temperature effects alone in the Phase B coarse mesh are less than 0.1 in., and therefore are negligible for the temperature loads considered.

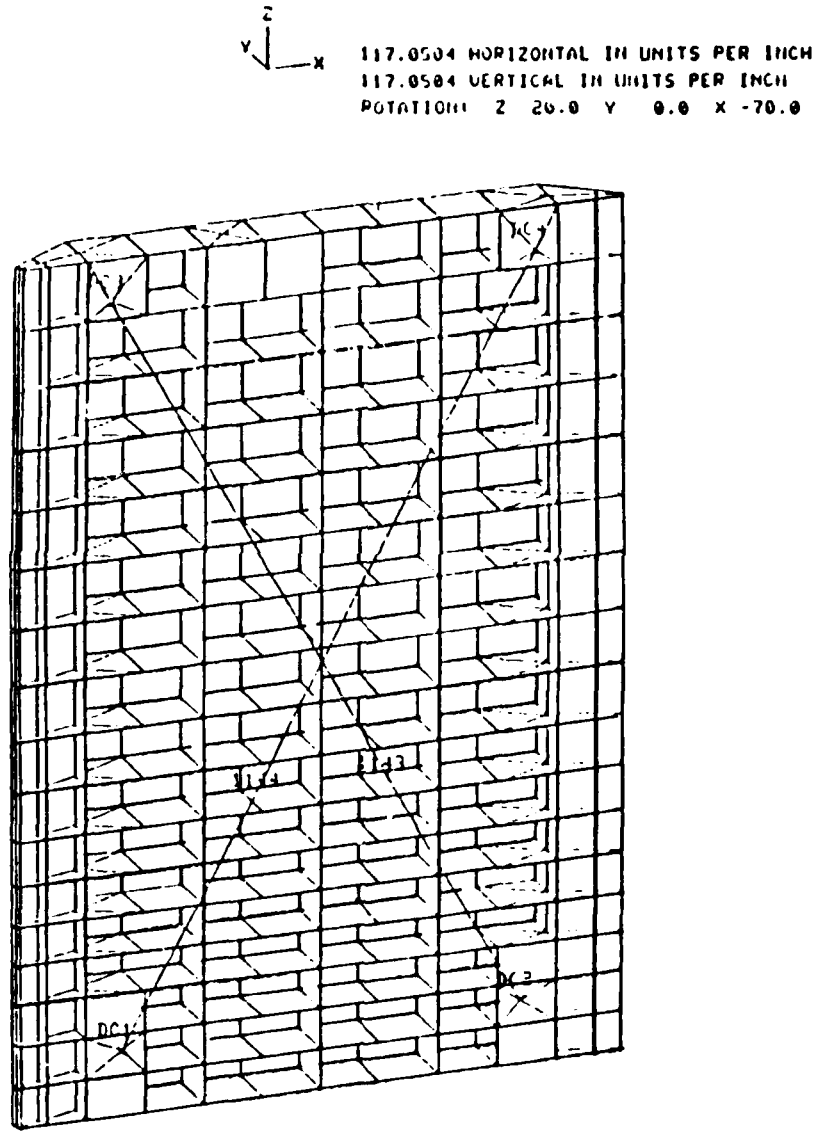

Figure 1. Refined diagonal connection model

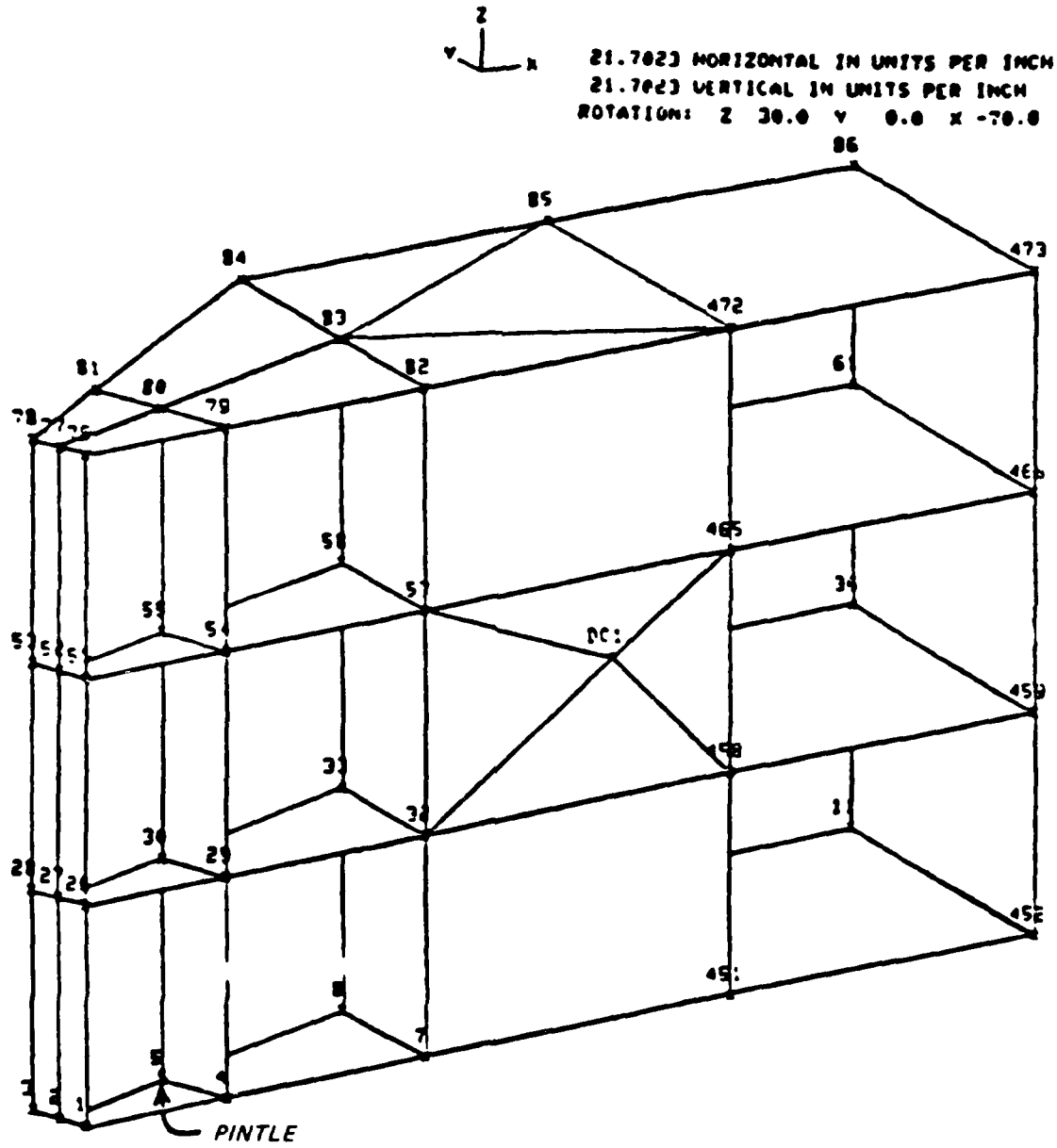

Figure 2. Free-body in region of the pintle

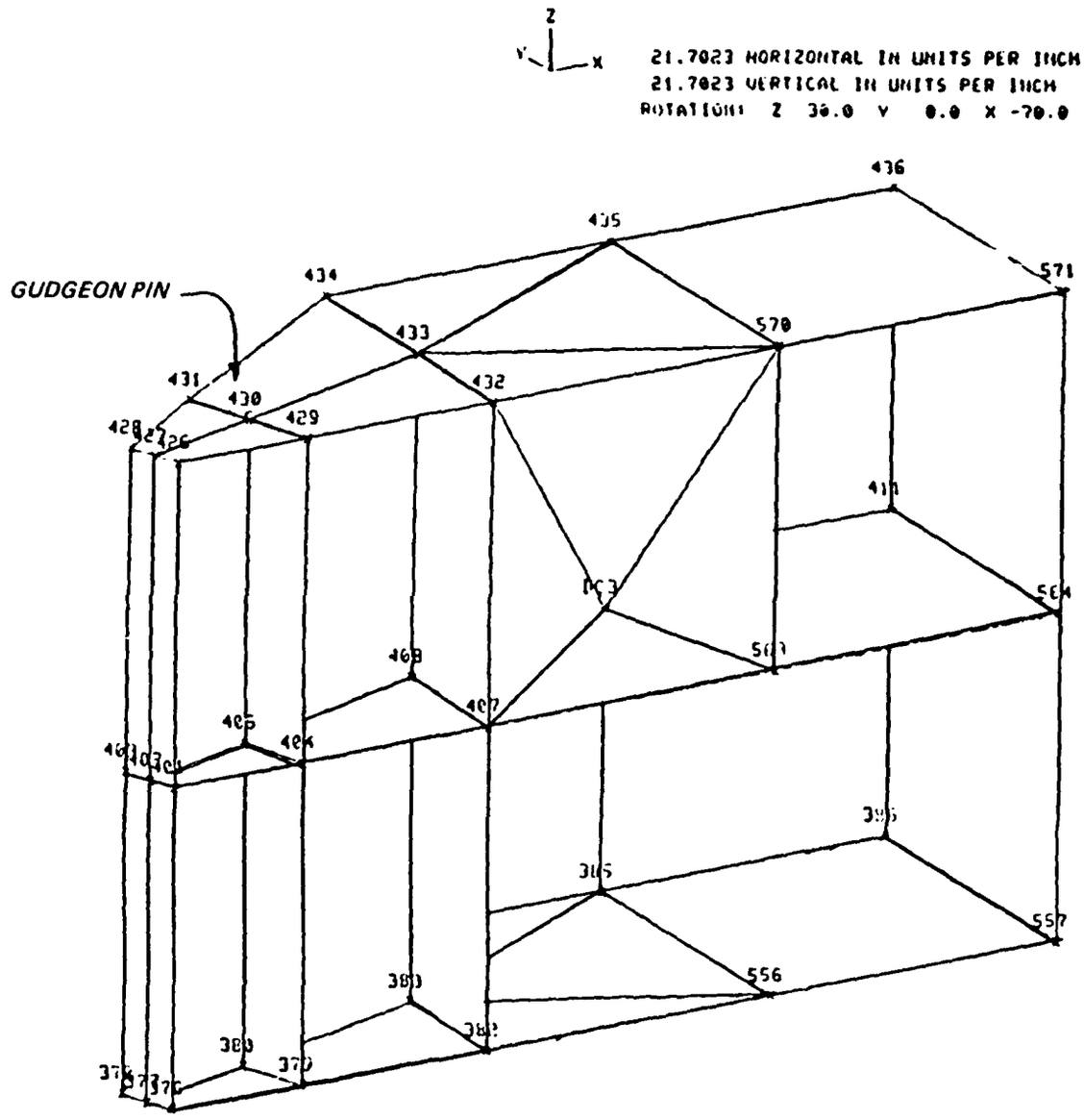

Figure 3. Free-body in region of the gudgeon pin

Conclusions

20. On the basis of the above summary of results, it is concluded that although the more refined mesh diagonal connection model caused somewhat smaller resultant nodal forces, on the average, and a smaller jacking force, the final resultant nodal force distribution for the fully prestressed state is, on the average, essentially the same as that for the Phase B CM model. Therefore, the results from the Phase B study are still considered valid for purposes of evaluating the gate behavior during and after prestressing (although they are somewhat conservative during prestressing).

PART III: SUMMARY OF REPORT 2, "SIMPLIFIED FRAME MODEL (PHASE D)"

Scope

21. Report 2 explains Phase D (Phase B-simplified frame model study of Report 1) and describes simplified frame models S1 and S2. This summary highlights the findings of this study and presents a comparison with the previous report and recommendation for use of simplified models in design.

Problem Description

22. Report 2 contains a continuation of performance studies of the lower miter gate of the John Hollis Bankhead Lock and Dam on the Black Warrior River, Ala. The results reported herein are a direct continuation of the Phase B work detailed in Report 1, and are related to:

- a. The development of alternate configurations (models 4 and 5) of the miter gate wherein a truss system is used on the downstream face of the gate, causing the gate to behave like a torque tube.
- b. The development of a simplified frame model using predominately space frame members to model the entire gate.

23. The alternate configuration model studies are reported in Reports 3 through 5, while the simplified frame model study is reported herein.

Objectives

24. The objective of continuing the Phase B work and study was to:

- a. Develop simplified frame models wherein space frame members are used to model the skin plate, all horizontal girder and vertical diaphragm webs and flanges, all end and intermediate crossing plates, all web stiffeners, and the prestressing diagonals. In addition, a few finite elements (FE) were used to model the strut arm and prestressing diagonal connection points.
- b. Compare gross force distributions between the simplified frame models and the Phase C model of Report 1.
- c. Present recommendations related to the use of simplified frame models.

Summary

25. Simplified frame models S1 and S2 used in place of the Phase C finite element model (FEM) of the gate leaf produced results which, in general, were considerably different from corresponding values for the Phase C FEM. In particular:

a. Model S1 consisted of space frame members only (except at diagonal and strut arm gusset plate attachment points), and without diagonals to represent skin, web, and diaphragm plates. Model S1 was 26 to 46 percent less stiff than the Phase C FEM during prestressing and also produced much larger unprestressed dead load deflections.

b. Model S2 consisted of space frame members and diagonals to represent skin, web, and diaphragm plates. Model S2 was 7 to 42 percent less stiff than the Phase C FEM during prestressing and produced much larger unprestressed dead load deflections. Hence, diagonal space truss members were largely ineffective in providing the needed additional stiffness required to bring simplified frame and CM FEM's into agreement. However, the diagonals did add considerable complexity in the form of a large increase in the number of members to the model but, apparently, the displacement and stiffness results do not justify their use.

c. A comparison of boundary nodal forces for free bodies in the gudgeon and pintle regions of simplified frame models S1 and S2 to the Phase C FEM reveals significant discrepancies in the predicted gross force distributions in these regions. While selected values of force and moment resultants agree at certain nodal points, there is no consistent pattern evident in the force comparisons. This is to be expected, however, in view of the substantial variations in overall gate leaf stiffness between the frame and FEM's.

d. The absolute and normalized (i.e., relative) values of gross resultant forces for the prestressing loads vary by an amount which is sufficiently great. This indicates that the Simplified Frame Model approach is unreliable for the purpose of predicting gross force distributions for cases of prestressing loads.

e. A substantial amount of effort must be expended in preparing the member property data (by hand) for the simplified frame models, when compared with the relatively straight-forward process of recording plate thicknesses for the FEM. These hand computations require that many assumptions be made with regard to effective width of plates, influence of stiffeners, the use of end joint size, and member eccentricity effects in setting up the model. By using simple frame models, it is unclear at this point. What will be the combined effect of these simplifying assumptions on the predicted performance of the gate

leaf? Presumably, the simpler frame models make the task of evaluating the flow of forces throughout the gate an easier one (hence the forces are more directly useful for the designer), but results presented herein suggest that models S1 and S2 do not yield the correct member forces.

Conclusions and Recommendations

26. On the basis of the above summary and if it is assumed that the FEM of the Phase C report is the baseline for comparison, it is concluded that simplified frame models of the type of miter gates considered herein are not suitable for the reliable prediction of gross force distributions for the load cases relating to the prestressing procedures. It appears that the only analysis model which has a reasonable chance to predict such gross force distributions is an FEM similar to the Phase C model. However, the difficulty in predicting the downstream dead load deflections prior to field measured prestressing is still an issue for the FEM. In order to resolve this issue, it is suggested that a special analysis procedure be formulated and executed in an attempt to model a number of heretofore unaddressed influences including:

a. Sequential construction procedures followed in the field to include the layered construction techniques, intermediate tie backs to provide alignment, and others.

b. Initial stress states that may be induced by welding practices.

PART IV: SUMMARY OF REPORT 3, "ALTERNATE CONFIGURATION MITER GATE FINITE ELEMENT STUDIES--OPEN SECTIONS"

Scope

27. This study resulted from recommendations from the CASE Project Task Group on Miter Gates concerning the studies described in Report 1. This summary comments on and highlights specific sections of this report.

Problem

28. Consideration of the conclusions and recommendations of the studies in Report 1 led to a decision to explore ways to increase the torsional stiffness of the gate leaf to reduce twisting due to dead load, Report 3. Finite element model II of the Phase A study was selected as a basis for investigation of alternative configurations. This investigation would explore the advantages which might be associated with using additional diagonal and vertical bracing elements on the downstream face of the horizontally framed miter gate.

Objectives

29. The first alternative model, referred to in Report 3 as model 4, was to contain vertical and diagonal bracing elements over the entire downstream face of the gate (with the new bracing hinged or rigidly connected to each horizontal girder that was intersected). The second model, alternative model 5, contained two panels of x-bracing over the downstream face between horizontal girders 2 to 18 with the new bracing members also hinged or rigidly connected to each horizontal girder that was intersected. It was believed that the new models, alternative configuration models 4 and 5, would not contain any of the disadvantages of the double-skin plate or torque-tube models considered in Report 4, since the downstream face of the gate would contain no closed sections. Therefore, maintenance and inspection of the gate would be only slightly more difficult and expensive than that of a conventional gate due to the added members on the downstream face. In addition, fabrication of the gate leaf should be less expensive than the Report 4 torque-tube or

double-skin plate structures since there are no closed sections in the new alternate configuration models.

Approach

30. The open section alternative configuration study is defined as follows:

a. Modify the conventional gate model (Phase A, model II) to include the new diagonal and/or vertical bracing elements. Generate separate models to evaluate the effect of hinging or rigidly connecting the new bracing members. This step resulted in four new models, models 4, 4R, 5, and 5R, with the R denoting moment releases or hinging at the start and end of the new bracing members.

b. Analyze the model for dead load. Evaluate the torsional stiffness.

c. Determine the jacking force and the resulting forces in the diagonals due to the prestressing procedure by using the procedure from the Phase A studies (Report 1) that ensured a plumb condition of the miter end after prestressing.

d. Evaluate deflections and stress distributions due to hydrostatic, temporal, dead load, and jacking loading conditions.

e. Compare the results for the new models with results for the conventional gate, double-skin plate, and torque-tube model 3 where appropriate.

Summary

31. This study represents the first step in evaluation of the two alternate miter gate configurations proposed by the CASE Miter Gate Task Group. The new models do not have the problems associated with the fabrication, maintenance, or inspection as do the double-skin plate or torque-tube models investigated in previous studies. In addition, the new models provide better overall behavioral characteristics than a conventional gate design.

32. All models, models 4, 4R (a variation on model 4), 5, and 5R (a variation on model 5), were considerably stiffer than the conventional gate model when subjected to dead loading. Models 4 and 4R produced almost the same out-of-plumb deflection as the recommended torque-tube model, model 3 in Report 4. Although models 5 and 5R were more flexible than models 4 and 4R, they still produce out-of-plumb deflections considerably less than the

conventional gate model (1.7 in. versus 8.9 in.). Models 5 and 5R were only slightly heavier than the conventional gate (580 kips versus 572 kips, respectively) while models 4 and 4R were considerably heavier at 619 kips dead weight.

33. The end connections of the new bracing members had a negligible effect on the reactions or displacements of the gate but had a considerable effect on the forces in the bracing members. The high stress due to combined axial force and bending moments in the bracing members of models 4 and 5 for LOADINGS 12 and 13 indicated that rigid connections should not be used for the bracing members. Therefore, models 4 and 5 should not be considered. Although stresses were also high in models 4R and 5R (±30 ksi in magnitude), an iterative analysis and design process should find an acceptable section reducing the high stresses since these stresses are due to axial load only. The original section, the WT5x34, was chosen only as a starting point for the purposes of evaluating the new alternate configurations.

34. Both models 4R and 5R produced acceptable behavior when subjected to the hydrostatic and temporal loadings. The overall behavior due to both of these loadings was very close to that of the conventional gate. Stresses in the new bracing members were found to be much lower for these loadings than for the jacking and prestressing loadings.

35. Further evaluation of models 4R and 5R reveals that model 4R has other negative aspects in addition to the added weight mentioned previously. The fabrication of model 4R could be more expensive and time consuming due to the large number of vertical and horizontal bracing members and the added connections. In addition, model 4R required a jacking force during prestressing of 437.80 kips, while model 5R required only 212 kips.

Recommendations

36. Due to the reasons stated above, model 5R is recommended over model 4R for further evaluation. More detailed studies are warranted to determine if the stresses in the new bracing members due to the jacking and prestressing loading, the sensitivity of the overall behavior due to the sizes of the new bracing elements, or the sensitivity of the overall behavior due to slight alterations in the bracing configuration can be lowered to acceptable values. Should these studies determine that model 5R is still an acceptable

alternate configuration, the next step should be an overall optimization of the gate leaf, considering the complete system rather than taking an existing structure designed by existing techniques and adding the new bracing members. The final step is the development of a methodology for design office engineers--a revision to the engineer manual for miter gates.

PART V: SUMMARY OF REPORT 4, "ALTERNATE CONFIGURATION MITER GATE FINITE ELEMENT STUDIES--CLOSED SECTIONS"

Scope

37. The Report 4 study is an alternative to the open configuration studied in Report 3, and this summary gives an overview by presenting specific sections of the report.

Problem and Objectives

38. Initially, the purpose of this investigation was to explore the potential advantages which may be associated with use of a double-skin plate system rather than the single-skin plate arrangement used in conventional miter gate structures. In particular, the displacement and stress states, the torsional stiffnesses, and the shear center locations of the single- and double-skin plate models were to be compared.

39. Later, the decision was made to study the potential advantages associated with several models having a double-skin plate over only a portion of the gate leaf. These so-called "torque-tube" models would provide zones of greatly increased torsional stiffness in localized regions of the gate, thereby yielding a savings in weight and material as well as improved access to closed cells compared with a full double-skin plate arrangement. Three cases were to be investigated: first, with torque tubes added only at the top and bottom of the leaf; second, with torque tubes positioned at the top, bottom, and sides of the conventional gate leaf; and third, with torque tubes on the sides of the conventional gate leaf model.

40. In addition to determining the dead load stresses and displacements, torsional stiffnesses, and shear center locations, the effect of the jacking and prestressing procedure was studied. Since two of the models used torque tubes on the sides of the conventional gate leaf, the effect of a vertical access hole in the webs of the horizontal girders was investigated. Finally, the performance of two of the torque-tube models, one subjected to hydrostatic loading with the gate in the mitered position and the other subjected to hydrostatic resistance with the gate closing, is presented.

Approach

41. The study is defined in terms of the following tasks:

a. Modify the Phase A FEM by adding a 5/8-in. skin plate full height between end diaphragms on the downstream face of the structure (double-skin plate model). Horizontal girder flange elements covered by the added skin plate are to be removed but flanges in the quoin and miter end regions shall remain. Results included dead load displacements, gross stresses in selected regions of the gate, and required diagonal prestressing and jacking forces.

b. Find the torsional stiffness of the double-skin plate structure without diagonals by introducing a unit displacement loading condition at the bottom of the gate.

c. Estimate and compare the shear center locations for the Phase A and double-skin plate miter gate models. Assume that the shear center can be determined by an analysis in which external jacking forces are applied to the upstream and downstream nodes of the miter end diaphragm to cancel gudgeon pin reactions and to return the gate to plumb position.

d. Modify the double-skin plate model by deleting portions of the downstream skin plate to generate the torque-tube models.

(1) Model 1 - downstream skin plate at the top and bottom.

(2) Model 2 - downstream skin plate at the top, bottom, and both sides.

(3) Model 3 - downstream skin plate on the sides only.

For all torque-tube models, horizontal and vertical flange members on the downstream face were removed when covered by the torque tubes. Results include dead load displacement, gross stresses in selected regions of the gate, as well as torsional stiffness and shear center locations of models 1 and 2.

e. Choose between model 2 and model 3 for further studies. The additional studies are to include the prestressing procedure and the torsional stiffness of the gate with diagonals. Use the prestressing procedure described in Report 1 to insure plumbness of the gate after prestressing the diagonals. A report can be written on the jacking force required for prestressing and the resulting forces in the diagonals due to the prestressing procedure.

f. Repeat Phase 2b for model 1 - the top and bottom torque tubes only.

g. Evaluate the effect on the overall behavior of the gate by adding a vertical access hole measuring 2.5 ft square in the webs of horizontal girders 1 to 17 on the chosen model 2 or 3.

h. Evaluate deflections and stress distributions due to hydrostatic, temporal, dead load, and jacking loading conditions on

the chosen model. Perform this phase with and without the diagonals, where appropriate.

i. Repeat Phase 2e model 1 with prestressing diagonals.

42. The findings of tasks 1 to 4 above are presented with the double-skin plate model and the torque-tube models (models 1, 2, and 3). Static analysis results for dead load are discussed and compared with selected displacements and stresses from the Phase A model. The approximate position of the shear center is described for the double-skin plate model and torque-tube models 1 and 2. The behavior of the various models due to the jacking and prestressing procedure is given and due to hydrostatic and temporal loadings is documented.

Conclusions

43. The analyses indicate that the double-skin plate model is a considerably stiffer structure than the original Bankhead design. The dead load out-of-plumb deflection at the miter end was predicted to be 0.044 in. for the double-skin model as compared with 8.907 in. for model II from the Phase A miter gate report. This large reduction in the deflection is due to the fact that the shear center is much closer to the center of gravity than approximated by the calculations in section 2.4 and also that the torsional stiffness of a gate with closed cross section is much larger than that of the original Bankhead design with open cross sections.

44. The four torque-tube models (models 1, 2, 3, and 3H) have dead load deflection values and torsional stiffnesses which lie in between the conventional and double-skin plate designs. Torque-tube model 1 (with horizontal torque tubes at bottom and top of the gate only) weighs about the same as the conventional design, is slightly less stiff in torsion (without diagonals), and has enough out-of-plumb displacement (3.5 in.) that some prestressing diagonal system would probably be required to plumb the gate leaf. The addition of diagonals approximately doubles the torsional stiffness of model 1. Torque-tube model 2 (with torque tubes at top, bottom, and sides), on the other hand, weighs about 4 percent more than the conventional gate but is approximately 4.5 times as stiff in torsion (without diagonals) and has an out-of-plumb displacement of only 0.45 in. Torque-tube model 3 (with torque tubes on the sides only) also weights about 4 percent more than the

conventional gate. It is approximately 4.02 times as stiff without diagonals and 4.5 times as stiff with diagonals as the conventional gate with diagonals. In addition, the out-of-plumb displacement is just slightly greater (0.51 in.) than the displacement of model 2 (0.45 in.).

45. Although the double-skin plate model is stiffer than the original Bankhead model, there are several disadvantages in using the double-skin plate: (1) increased amount of steel required (approximately 10 percent), (2) the increased cost and/or difficulty in fabricating the closed sections, and (3) the increased maintenance costs and difficulty of inspection of the enclosed regions. The torque-tube models, however, models 2 and 3 in particular, appear to offer promise of increased stiffness and reduced dead load deflection, without the problem of access to enclosed regions associated with a full downstream skin plate. In addition, torque-tube model 3 does not require horizontal access holes to be cut in the webs of the vertical diaphragms between girders 17 and 18 as would be necessary in model 2. For this reason as well as the negligible decrease in stiffness of model 3 when compared with model 2, model 3 was selected for further studies. The further studies included the following:

a. The effect of a 2.5-ft square access hole in the web of girders 1 to 17 in each of the two side torque tubes.

b. The behavior of model 1 with diagonals and model 3 with diagonals during the prestressing procedure.

c. The behavior of model 1 with diagonals and model 3 with and without diagonals due to hydrostatic and temporal loading.

46. The access hole in model 3H produced a negligible difference in the out-of-plumb displacement of model 3 as discussed in section 2.3. In addition, the differences in the behavior due to the hydrostatic loading were also negligible. Therefore, the access holes have little effect on the gross behavior of model 3.

47. The jacking and prestressing procedure produced extremely different behavior between model 1 and model 3. Although model 3 required almost twice the jacking force as model 1 during the prestressing procedure, model 3 yielded significantly lower stresses in the end vertical diaphragm near the miter end. The maximum stresses in the skin plate during jacking were approximately the same but the distribution of stresses was considerably different. The final forces in the diagonals were much lower in model 3 than in

model 2 thereby raising the issue of whether or not diagonals are needed in model 3.

48. The hydrostatic loading with the gate in the mitered position yielded negligible differences in the reactions and skin plate stresses as reported in section 4.2 for model 1 with diagonals, model 3 with and without diagonals, and model 3H with diagonals. The diagonals do not contribute significantly to the behavior of the gate when the gate is fully mitered. The access hole had a negligible effect on the overall behavior of the gate due to the hydrostatic loading.

49. The temporal loading condition presented in section 4.3 also illustrated the advantages of model 3 over model 1 and the conventional gate model. The twist at the miter end for model 3 with and without diagonals was less than one-half the twist of the conventional gate. Again, the diagonals in model 3 contributed little to the overall stiffness of the gate.

50. These studies have shown that torque-tube model 3 offers several advantages over conventional gates as well as the other torque-tube models and the double-skin plate model. A question yet to be answered concerns the need for diagonals and the associated prestressing procedure. The diagonals were found to only slightly alter the torsional stiffness and stress distributions due to hydrostatic and temporal loadings. The effect of the vertical access hole was also found to be negligible on the overall behavior of the gate. Therefore, model 3 appears to offer an excellent alternative to conventional gate design.

PART VI: SUMMARY OF REPORT 5, "ALTERNATE CONFIGURATION MITER GATE FINITE ELEMENT STUDIES--ADDITIONAL CLOSED SECTIONS"

Scope

51. The study stemmed from findings of the CASE Project Task Group on Miter Gates regarding the studies described in Reports 1 and 4. The summary gives the reader insight concerning information that may be obtained in this report.

Problem and Objectives

52. In this Report 5 study, two of the more promising torque-tube models from the Report 4 studies were refined further to determine their behavior under dead load, torsional stiffness, prestressing, and hydrostatic and temporal loading conditions. The first, referred to as model 1L, contains torque tubes along the top and bottom of the gate leaf which span three horizontal girders instead of two as in earlier investigations. In the second model, model 3S, side torque tubes in earlier studies were reduced in size to cover only the region from the end diaphragms to a point midway between the end and first interior diaphragms at both ends of the gate leaf. Then, to form the torque tube, an intermediate vertical diaphragm was added at both locations to form the closed vertical cells. Results of these studies of improved torque-tube models are presented in Report 5.

53. As a final step in the present study, the conventional miter gate leaf model, referred to as model II in the Phase A/B studies (Report 1), was modified to consider the influence of doubling the cross-sectional area of the diagonals on dead load displacements, torsional stiffness, and response to temporal loading. Only the cross-sectional areas of the diagonal members were changed to produce the modified form of Phase A model II used in this investigation. Report 1 should be consulted for a detailed description of this model, but dead load displacements and torsional stiffness values and response to temporal loading are presented in chapters 2 to 4 for comparison with torque-tube model results.

Approach

54. The approach of work for the present study of modified torque-tube models encompasses the following activities:

a. Prepare a refined torque-tube model of the gate leaf which includes torque tubes at top and bottom of the gate covering two cells between the three horizontal girders at each location (model 1L). Use 5/8-in. plate and analyze behavior with and without diagonals. Determine dead load displacements, torsional stiffness, effect of jacking and prestressing, and response to hydrostatic and temporal loadings. Study stress patterns in critical regions of the gate leaf. Compare results with previous values for conventional and closed section alternate configuration studies.

b. Repeat (1) above for a refined torque-tube model containing vertical torque tubes along both ends (quoin, miter) of the gate leaf (model 3S). These side torque tubes are to extend from the end diaphragm to a point midway between end and first interior diaphragms at both locations. The tubes are to be completed by the addition of new vertical diaphragms at the midway points.

c. Reanalyze Phase A model II (of the conventional gate leaf structure) using prestressing diagonals which have twice the cross-sectional area of previous models. Find gate leaf response to dead and temporal loadings, and compare its torsional stiffness with the conventional model. Use a superposition analysis procedure to plumb the gate leaf, not to control the values of the prestressing forces in the diagonals.

In Report 4, a double-skin plate model was assembled in which a full skin plate was added between end diaphragms on the downstream side of the actual gate leaf model. As a result, dead load displacements were reduced by a factor of 200 and torsional stiffness was increased by a factor of 29.5 compared to the conventional gate model without diagonals, but the weight of the gate leaf was increased by approximately 10 percent. When the problems of increased fabrication costs and reduced access to closed cells on the gate were added to possible difficulties in plumbing the structure, the concept of a full double-skin plate was discarded. However, this concept gave rise to a number of "torque-tube" models in which a double-skin plate was used only over a portion of the downstream face of the leaf to provide localized regions of high torsional stiffness. Previous studies considered the performance improvements and associated cost impacts of using torque tubes along the top and bottom only, along the sides only, and along both top, bottom, and sides of the conventional gate leaf. In general, these torque-tube models offered

increased torsional stiffness and reduced dead load displacement compared to the conventional gate design, but the percentage of improvements were not as dramatic as that reported above for the double-skin plate model. At the same time, these torque-tube models were found to be lighter and less costly to fabricate, while offering improved access to closed cells, compared to the double-skin plate arrangement. Detailed results of these investigations of closed section alternate configuration models for miter gates may be found in Report 4. Key results from past studies are summarized in this report, wherever appropriate, for comparison with values generated in the present study of several improved models.

55. For completeness, it should be noted that a number of open-section alternate configuration miter gate leaf models were also studied as described in Report 3. In these open-section models, different arrangements of diagonal bracing were employed on the downstream side in an attempt to achieve the same performance improvements offered by the torque-tube models while, at the same time, to permit ready access to all regions of the gate leaf for inspection purposes. The results of the study showed that gate performance improvements comparable to those of the torque-tube models could be achieved with certain open-section models, but the associated weight increase and fabrication problems made them unacceptable.

Conclusions

56. The analyses of model II Phase A with enlarged diagonals and of torque-tube models 1L and 3S have focused on their performance characteristics, relative to conventional model II and torque-tube models 1 and 3, in the following areas: (1) dead weight and out-of-plumb displacements; (2) torsional stiffness values; (3) jacking and diagonal forces due to prestressing; (4) response to hydrostatic and temporal loadings; (5) and reaction forces and stress states associated with hydrostatic, temporal, and jacking and prestressing loadings. The aforementioned tables present summary data to support the principal findings of the study which are discussed below.

57. First, enlarging the diagonals to twice the cross-sectional area values used for model II Phase A results in generally undesirable changes to the present, or conventional, model of the gate leaf. Its weight is increased by 3 percent which causes a 5 percent increase in dead load deflection. At

the same time, the torsional stiffness of the gate is increased only 15 percent by the larger diagonals yielding a modest 13 percent reduction in twist displacements due to temporal loading. For jacking and prestressing operations, a 24 percent (or 50-kip) increase in jacking force is required for the enlarged diagonal case and the final diagonal forces are increased by 20 to 30 percent over corresponding values for the conventional model II. Overall, model II with doubled diagonals appears to be an uneconomical and largely ineffective (although simple) approach to improve gate performance.

58. A comparison of torque-tube models 1 and 1L reveals that model 1L offers significant improvements over model 1 in that dead load displacements are reduced to one half of model 1 in that dead load displacements are reduced to one half of model 1 values while dead weight of the leaf increases by only 7 kips (1.2 percent) due to the increase in size of horizontal torque tubes. At the same time, model 1L offers a 37 percent improvement in torsional stiffness and a 30 percent reduction in gate twist due to temporal loading compared with model 1. However, models 1 and 1L each produce areas of concentrated stresses in the quoin end diaphragm due to jacking. Finally, model 1L has the requirement for additional horizontal access holes for inspection of the enlarged top and bottom torque tubes.

59. Models 3 and 3S offer a more uniform distribution of stiffness and stress than model 1 or 1L. Model 3 has greatly increased torsional stiffness and, thus, a small dead load deflection value. However, model 3 is 15 kips or more (approximately 3 percent) heavier than models 1, 1L, or 3S and may be too stiff in that the required jacking force for model 3 exceeds that for models 1L and 3S by, roughly, 160 kips. On the other hand, model 3S has the same desirable attribute of uniformity of stress distribution as model 3 but requires approximately the same level of jacking force as conventional model II.

Final Recommendations

60. In summary, model 3S appears to offer the most promise of the torque-tube models studies to date and is recommended as the model worthy of further investigation. In particular, a more refined model should be used in any further investigation to insure that the model is producing a reasonably accurate prediction of the state of stress in the gate leaf and to aid in the

understanding of the flow of force through the gate. Although the stress contour plots used in this study helped pinpoint localized areas of high stress in the end diaphragms, torque tubes, and other components, more definitive design information is needed before any of the torque-tube models can be designed by staff engineers.

PART VII: SUMMARY OF REPORT 6, "ELASTIC BUCKLING OF GIRDERS IN HORIZONTALLY FRAMED MITER GATES"

Scope

61. Elastic buckling of girders in horizontally framed miter gates is the particular concern of study in Report 6. This summary attempts to prepare the reader for the in depth study presented in Report 6.

Objectives

62. The primary objective of this research investigation was to study linear elastic buckling behavior of one horizontal girder in the Bankhead gate and to evaluate current Corps of Engineers design procedures in light of the predicted buckling loads and modal displacement patterns of the FE analysis. Girder G-10 was selected as a representative component for the in-depth study, and a variety of different FEM's of it were developed to study its local buckling (i.e., weak axis) and overall buckling (i.e., strong axis) characteristics for symmetric modes only. Only one half of the girder was modeled in these studies and appropriate symmetry boundary conditions imposed at the girder centerline in the eigenvalue analysis by the stiffness method. Several different FORTRAN computer programs were used to assemble the models in the local and overall buckling analyses, and an iteration scheme was employed in each program to solve for the lowest buckling mode and the associated mode shape.

63. Preliminary findings of the buckling study were presented to the Miter Gate Task Group at its meeting of 22-24 March 1983 in Atlanta, Georgia. Based on the guidance and recommendations of the Task Group members, the study was continued and the results of the overall investigation of girder buckling are summarized in this report. Results presented herein are the final publication.

Approach

64. One half of girder G-10 shown in Figure 4 was selected as typical of the other 17 girders in the gate leaf and FEM's were developed for the half

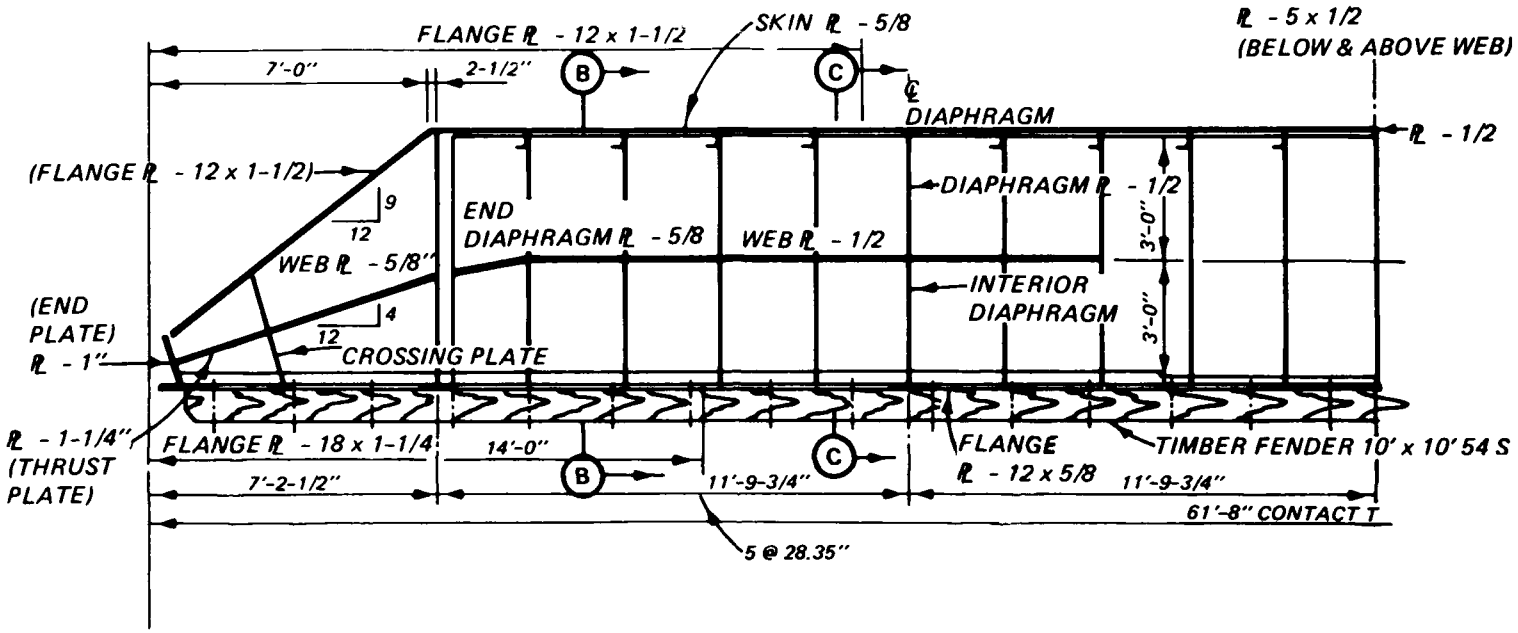

Figure 4. Horizontal girder G-10

girder. The global XY coordinate system was used in all studies. The timber fender and intercostal angles were not included in the models, but all transverse and longitudinal stiffeners were represented in the FEM used in local buckling studies. For the strong axis studies, transverse and longitudinal stiffeners were not modeled explicitly but all other girder components were represented by FE's.

65. All girder components were assumed to be 46-ksi steel and the provisions of the 8th Edition of the American Institute of Steel Construction (AISC) Manual of Steel Construction were assumed to govern in this investigation.

66. Results of the stability evaluation of girder G-10 are organized into two parts: local buckling analysis and overall buckling analysis. Within each chapter of Report 6, the FEM's and appropriate boundary conditions and loadings are described, along with a brief review of relevant theory and the analysis sequence employed. This discussion is then followed by presentation of results in the form of displaced shapes, stress contours, buckled mode shapes, and Lambda (λ) values (i.e., eigenvalues, or the critical stress ratios).

67. The conclusions which follow from an evaluation of FE results, in light of current hand-based procedures, are presented for local and overall buckling.

68. Alternative analysis approaches are presented which could be used to study plastic buckling. The associated computer cost of using commercially available software packages to perform plastic buckling analyses of girder G-10 are estimated.

69. Overall findings of the study are presented, along with hand computations and additional plots.

Summary and Conclusions

70. A number of different FEM's of one half of horizontal girder G-10 in the John Hollis Bankhead lower miter gate were assembled to evaluate its weak and strong axis buckling characteristics for symmetric modes only. The study was restricted to linear elastic buckling only but an overview of several procedures for analysis of inelastic buckling was presented to guide possible future studies. The girder models formulated as part of this

investigation were viewed as separate structures extracted from the overall gate leaf. The restraining effect of the skin plate and vertical diaphragms which tie the whole structure together was accounted for only in the effective width computations which lead up to a determination of member and element properties for each girder component. On the basis of current hand design procedures, propped cantilever boundary conditions were employed throughout much of the study even though girder behavior for these boundary conditions was not entirely consistent with results of Phase A and B studies. As a result, it is not possible to state with complete certainty, on the basis of these studies, that the girder may not exhibit other buckling modes or that the gate leaf as a whole might not possess some overall forms of instability (symmetric or unsymmetric) which were not detected by this investigation.

71. With the above restrictions in mind, it can be stated that the principal finding of this study was that girder buckling behavior is much more localized than current hand-based analysis procedures reflect. Linear elastic buckling models which are consistent with the K, L, and r assumptions of current hand-based procedures were not observed in either the weak or strong axis investigations. Instead, both weak and strong axis buckling models and results point to the effectiveness of transverse and longitudinal web stiffeners in controlling localized web instability. If additional longitudinal web stiffeners are provided in the models, analysis results indicate that critical stress ratios will be correspondingly increased. Eventually, the product of the critical stress ratio and some measure of the applied stress will exceed yield stress levels and an elastic analysis is no longer appropriate. This was the case in the local buckling portion of the study when more than two rows of longitudinal web stiffeners were present in the Phase A coarse mesh model. In the strong axis buckling portion of the study, high localized stresses were observed in the quoin region of the models, while web stresses in other areas were in reasonable agreement with local buckling study results. With the addition of more and more web restraints to simulate the effect of longitudinal web stiffeners in the strong axis study models, girder web instability shifted to the region at which the size of the downstream flange is reduced. The mode shape involved web buckling combined with rotation of the downstream flange at stress levels in the flange and adjacent web which were well below yield for all cases considered. However, the effect of the high quoin stresses, although very localized, is unknown.

72. Finally, it is possible that buckling modes which correspond to the K, L, and r values and other design parameters used in hand-based analyses do exist for horizontal girders in miter gates. It appears likely, however, that such modes are associated with stress levels well in excess of yield which would require an inelastic analysis to properly evaluate.

WATERWAYS EXPERIMENT STATION REPORTS PUBLISHED UNDER THE COMPUTER-AIDED STRUCTURAL ENGINEERING (CASE) PROJECT

(Concluded)

	Title	Date
Instruction Report K-83-1	User's Guide: Computer Program With Interactive Graphics for Analysis of Plane Frame Structures (CFRAME)	Jan 1983
Instruction Report K-83-2	User's Guide: Computer Program for Generation of Engineering Geometry (SKETCH)	Jun 1983
Instruction Report K-83-5	User's Guide: Computer Program to Calculate Shear, Moment and Thrust (CSMT) from Stress Results of a Two-Dimensional Finite Element Analysis	Jul 1983
Technical Report K-83-1	Basic Pile Group Behavior	Sep 1983
Technical Report K-83-3	Reference Manual: Computer Graphics Program for Generation of Engineering Geometry (SKETCH)	Sep 1983
Technical Report K-83-4	Case Study of Six Major General-Purpose Finite Element Programs	Oct 1983
Instruction Report K-84-2	User's Guide: Computer Program for Optimum Dynamic Design of Nonlinear Metal Plates Under Blast Loading (CSDOOR)	Jan 1984
Instruction Report K-84-7	User's Guide: Computer Program for Determining Induced Stresses and Consolidation Settlements (CSETT)	Aug 1984
Instruction Report K-84-8	Seepage Analysis of Confined Flow Problems by the Method of Fragments (CFRAG)	Sep 1984
Instruction Report K-84-11	User's Guide for Computer Program CGFAG, Concrete General Flexure Analysis with Graphics	Sep 1984
Technical Report K-84-3	Computer-Aided Drafting and Design for Corps Structural Engineers	Oct 1984
Technical Report ATC-86-5	Decision Logic Table Formulation of ACI 318-77, Building Code Requirements for Reinforced Concrete for Automated Constraint Processing, Volumes I and II	Jun 1986
Technical Report ITL-87-2	A Case Committee Study of Finite Element Analysis of Concrete Flat Slabs	Jan 1987
Instruction Report ITL-87-1	User's Guide: Computer Program for Two-Dimensional Analysis of U-Frame Structures (CUFRAM)	Apr 1987
Instruction Report ITL-87-2	User's Guide: For Concrete Strength Investigation and Design (CASTR) in Accordance with ACI 318-83	May 1987
Technical Report ITL-87-6	Finite Element Method Package for Solving Steady-State Seepage Problems	May 1987
Instruction Report ITL-87-3	User's Guide: A Three-Dimensional Stability Analysis Design Program (3D-SAD), Report 1, Revision 1, General Geometry Module	[illegible]
Instruction Report ITL-87-4	User's Guide: 2-D Frame Analysis [illegible] Program [illegible]	[illegible]
Technical Report ITL-87-1	Finite Element Studies of a Horizontally Framed Miter Gate Report 1: Initial and Refined Finite Element Models (Phases A, B, and C), Volumes I and II Report 2: Simplified Frame Model (Phase D) Report 3: Alternate Configuration Miter Gate Finite Element Studies (Open Section) Report 4: Alternate Configuration Miter Gate Finite Element Studies (Closed Section)	[illegible]

(Continued)

WATERWAYS EXPERIMENT STATION REPORTS PUBLISHED UNDER THE COMPUTER-AIDED STRUCTURAL ENGINEERING (CASE) PROJECT

(Concluded)

	Title	Date
Technical Report ITL-87-4	Finite Element Studies of a Horizontally Framed Miter Gate	Aug 1987
	Report 5: Alternate Configuration Miter Gate Finite Element Studies—Additional Closed Sections	
	Report 6: Elastic Buckling of Girders in Horizontally Framed Miter Gates	
	Report 7: Application and Summary	

END

12-87

DTIC